frontiers | Research Topics

Environmental threats to the state of Florida—climate change and beyond, volume II

Edited by
Frank S. Gilliam, Michael C. Murrell and Marcus W. Beck

Published in
Frontiers in Ecology and Evolution

ISSN 1664-8714
ISBN 978-2-8325-3278-2
DOI 10.3389/978-2-8325-3278-2

About Frontiers

Frontiers is more than just an open access publisher of scholarly articles: it is a pioneering approach to the world of academia, radically improving the way scholarly research is managed. The grand vision of Frontiers is a world where all people have an equal opportunity to seek, share and generate knowledge. Frontiers provides immediate and permanent online open access to all its publications, but this alone is not enough to realize our grand goals.

Frontiers journal series

The Frontiers journal series is a multi-tier and interdisciplinary set of open-access, online journals, promising a paradigm shift from the current review, selection and dissemination processes in academic publishing. All Frontiers journals are driven by researchers for researchers; therefore, they constitute a service to the scholarly community. At the same time, the *Frontiers journal series* operates on a revolutionary invention, the tiered publishing system, initially addressing specific communities of scholars, and gradually climbing up to broader public understanding, thus serving the interests of the lay society, too.

Dedication to quality

Each Frontiers article is a landmark of the highest quality, thanks to genuinely collaborative interactions between authors and review editors, who include some of the world's best academicians. Research must be certified by peers before entering a stream of knowledge that may eventually reach the public - and shape society; therefore, Frontiers only applies the most rigorous and unbiased reviews. Frontiers revolutionizes research publishing by freely delivering the most outstanding research, evaluated with no bias from both the academic and social point of view. By applying the most advanced information technologies, Frontiers is catapulting scholarly publishing into a new generation.

What are Frontiers Research Topics?

Frontiers Research Topics are very popular trademarks of the *Frontiers journals series*: they are collections of at least ten articles, all centered on a particular subject. With their unique mix of varied contributions from Original Research to Review Articles, Frontiers Research Topics unify the most influential researchers, the latest key findings and historical advances in a hot research area.

Find out more on how to host your own Frontiers Research Topic or contribute to one as an author by contacting the Frontiers editorial office: frontiersin.org/about/contact

Environmental threats to the state of Florida—climate change and beyond, volume II

Topic editors

Frank S. Gilliam — University of West Florida, United States
Michael C. Murrell — University of West Florida, United States
Marcus W. Beck — Tampa Bay Estuary Program, United States

Citation

Gilliam, F. S., Murrell, M. C., Beck, M. W., eds. (2023). *Environmental threats to the state of Florida—climate change and beyond, volume II*. Lausanne: Frontiers Media SA. doi: 10.3389/978-2-8325-3278-2

Table of contents

frontiers | Frontiers in Ecology and Evolution

TYPE Editorial
PUBLISHED 04 August 2023
DOI 10.3389/fevo.2023.1258317

OPEN ACCESS

EDITED AND REVIEWED BY
Peter Convey,
British Antarctic Survey (BAS),
United Kingdom

*CORRESPONDENCE
Frank S. Gilliam
fgilliam@uwf.edu

RECEIVED 13 July 2023
ACCEPTED 26 July 2023
PUBLISHED 04 August 2023

CITATION
Gilliam FS, Murrell MC and Beck MW (2023) Editorial: Environmental threats to the state of Florida—climate change and beyond: volume II.
Front. Ecol. Evol. 11:1258317.
doi: 10.3389/fevo.2023.1258317

Editorial: Environmental threats to the state of Florida—climate change and beyond: volume II

Frank S. Gilliam[1]*, Michael C. Murrell[1] and Marcus W. Beck[2]

[1]Department of Biology, University of West Florida, Pensacola, FL, United States, [2]Tampa Bay Estuary Program, Saint Petersburg, FL, United States

KEYWORDS

climate change, global warming, environmental threats, marine ecosystems, Florida

Editorial on the Research Topic

Environmental threats to the state of Florida—climate change and beyond: volume II

As discussed in the editorial to Volume I of this series on environmental impacts on the State of Florida, global-scale human alteration of natural ecosystems has an ancient legacy (Gilliam, 2021). Especially in the temperate zone, evidence is widespread of anthropogenic change in natural ecosystems going back several millennia, often with effects persisting even to the present time (Gilliam, 2016). Human occupation by indigenous people of what is now Florida extends back to >12,000 years BCE (Hine, 2013; Milanich, 2017), yet anthropogenic activities in the past two centuries, and their environmental consequences (e.g., climate change, large scale hydrologic alteration), dwarf these ancient land-use legacies, in spite of their long-lived nature.

Also discussed in the Volume I editorial were numerous facets of the unique susceptibility of Florida to the effects of climate change. Superimposed on all of these is a large and rapidly growing human population with a heavy reliance on both marine and terrestrial ecosystems, all increasingly vulnerable to effects of climate change. These challenges are not unique to Florida, as many ecosystems worldwide are exposed to the cumulative effects of multiple stressors that degrade the resources and services provided by natural environments (Crain et al., 2008; Zimmerman et al., 2008). As of the U.S. Census Bureau's Vintage 2022 population estimates, Florida—the third populous in the U.S. as it is—has the highest population growth rate (nearly 2%) in the country. The last time that happened (in 1957) was due to the intersection of technology and societal change, including the 1950's nascent wide-spread use of air conditioning, along with the population growth peak following World War II known as the Baby Boom. From 1900 to the present, Florida's population growth has been exponential (Figure 1). The current rate of 1.9% suggests that the state's population of 22.2 million persons may double within ~40 yr.

Volume II of this Research Topic addresses widely-varied issues with direct or indirect links to climate change and all serious threats to aquatic and terrestrial ecosystems of great importance to Florida. These include urbanization of estuaries leading to critical habitat destruction, phytoplankton dynamics of inner continental shelf waters potentially affected by terrestrial nutrients, saltwater intrusion effects on species of palms, effects of oil spills on marine microbes, release of nutrients from legacy mining, alteration in seagrass and oyster

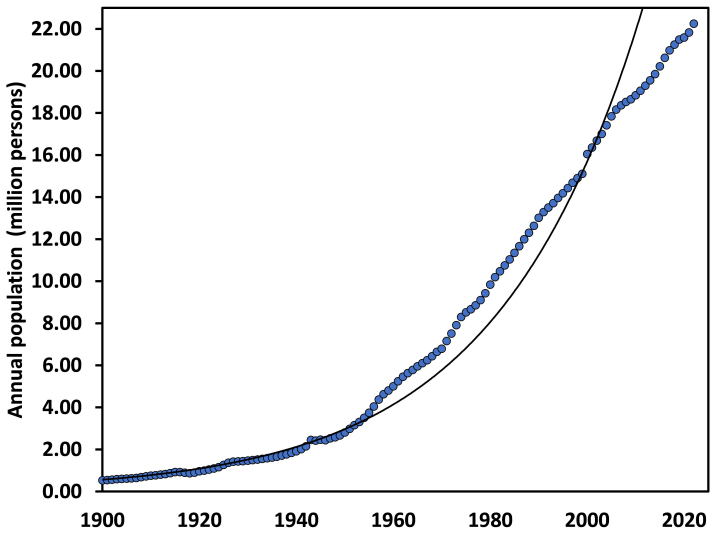

FIGURE 1
Annual population of Florida, 1900—2022. Curve is an exponential fit, r^2 =0.99. Data taken from www.census.gov.

habitat, and the increasingly ubiquitous nature of microplastics in marine and estuarine ecosystems.

In many cases, anthropogenic alterations of natural ecosystems call for attempts to restore them. Beck et al. established both short-term targets and long-term goals for restoration in an urban estuary within the Tampa Bay watershed. Although results have been inconsistent, they appropriately developed a novel approach for restoration that accommodates sea-level rise, climate change, and watershed development. Phytoplankton comprise the essential autotrophs of aquatic ecosystems, and are highly sensitive to cultural eutrophication. Stelling et al. examined biomass/composition of phytoplankton of waters of the inner continental shelf off Cape Canaveral on the Atlantic coast of Florida. They found notable seasonal dynamics, with chlorophyll *a* increasing 4-fold from summer to fall, which was ascribed to seasonal changes in wind patterns. With climate change-driven sea level rise, saltwater intrusion becomes an increasing threat to terrestrial ecosystems. Khoddamzadeh et al. used a factorial design to quantify the effect of saltwater intrusion on four species of palms. Although all species exhibited declines in health indicators (e.g., growth and nitrogen uptake) with increasing salinity, there was notable interspecific variation. Although oil spills are not a new phenomenon, the 2010 Deepwater Horizon oil spill in the Gulf of Mexico was the largest on record. Brock et al. examined temporal dynamics of marine microbes with nearshore samples taken from Pensacola Beach, FL, and subjected to a standard oil exposure protocol. They found pronounced temporal variability, much of which was related to temperature. Aware that chemical composition—and related photoreactivity—varies among different sources of crude oil, Headrick et al. examined the effects of oils of contrasting composition on marine microbes. They found that microbial responses in Florida waters to oil spills were highly dependent on the source of the oil and solar conditions on the surface at the time and location of the spill, ultimately affecting the potential for bioremediation. The results from both Brock et al. and Headrick et al. have implications for understanding the dynamics of oil spills on surface waters that originated from spills in deep waters. A regrettably unavoidable consequence of phosphorus mining in Florida is the creation of reservoirs for the retention of mining waste slurries. Morrison et al. investigated the effects of the April 2021 infrastructure failure at Piney Point, a retired reservoir that released phosphorus-laden water into Tampa Bay, and the potential risk such a release has in exacerbating blooms of red tide organisms, such as the dinoflagellate, *Karenia brevis*. This study also demonstrated that the spatial extent of the wastewater release was much farther than expected, with Piney Point water identified by stable isotope analysis at a control site over 48 kilometers outside of Tampa Bay. Croteau et al. used historical data (1985—2020) to assess climate change mediated alteration in seagrass and oyster habitats. They reported patterns of increased temperature and decreased streamflow across sites in the eastern Gulf Coastal Plain. Such results have important implications for restoration and management of seagrass and oyster habitat and underscore the importance of understanding climatic and hydrologic dynamics. A topic of increasing popular interest, is the ubiquitous nature of plastics in marine and estuarine ecosystems. Gowans and Suida conducted the first-ever study on the ingestion of plastics by manatees within the order *Sirenia*, a large marine mammal commonly found in Tampa Bay, FL. Necropsies performed of 26 manatees found macro-and micro-plastic ingestion in 26.9% and 73.1% of individuals, respectively, indicating that plastic consumption by manatees is common. In sharp size contrast, Fibbe et al. studied microplastic ingestion by copepods, an important primary consumer in marine and estuarine ecosystems.

The two-year study comprised 14 sampling dates at seven sites within Tampa Bay examining gut contents of *Acartia tonsa*. Although there were no clear spatial or temporal trends, ingestion of microplastics by copepods was commonly observed.

What should be clear from the articles in Volume II of this Research Topic is the wide diversity in environmental threats. Although some may be unique to Florida, most are globally relevant. Based on the various impacts discussed in this volume, ecosystem restoration is warranted in many cases (see Beck et al.). A challenge implicit in any restoration project, however, is to determine a desirable endpoint that constitutes success, and climate change creates an ecological 'moving target.' This reminds us of the venerable quote from plant ecologist, Henry Chandler Cowles (Cowles, 1899), that ecological change is "… a variable approaching a variable, not a constant." The collective empirical evidence provided by these studies could not be clearer as a clarion call for action to reverse the trends of all factors driving climate change, especially through the further and wide-spread development of non-fossil fuel sources of energy. Use of fossil fuels is an undeniable legacy of our past, and we must do what we can to keep it thus—a part of our past, but not our future.

Author contributions

FG: Writing – original draft, Writing – review & editing. MM: Writing – review & editing. MB: Writing – review & editing.

Acknowledgments

We would like to thank the editorial staff of *Frontiers in Ecology and Evolution* for their time and effort with this Research Topic. Tampa Bay Estuary Program (TBEP) funding for this work stems from EPA Section 320 Grant Funds, and the TBEP's local government partners (Hillsborough, Manatee, Pasco, and Pinellas Counties; the Cities of Clearwater, St. Petersburg, and Tampa; Tampa Bay Water; and the Southwest Florida Water Management District) through contributions to the operating budget.

Conflict of interest

The authors declare that the research was conducted in the absence of any commercial or financial relationships that could be construed as a potential conflict of interest.

Publisher's note

References

Cowles, H. C. (1899). The ecological relations of the vegetation on the sand dunes of Lake Michigan. *Bot. Gazette.* 27, 95–117, 167–202, 281–308, 361–391.

Crain, C. M., Kroeker, K., and Halpern, B. S. (2008). Interactive and cumulative effects of multiple human stressors in marine systems. *Ecol. Lett.* 11, 1304–1315. doi: 10.1111/j.1461-0248.2008.01253.x

Gilliam, F. S. (2016). Forest ecosystems of temperate climatic regions: from ancient use to climate change. *New Phytol.* 212, 871–887. doi: 10.1111/nph.14255

Gilliam, F. S. (2021). Editorial: Environmental threats to the State of Florida—climate change and beyond. *Front. Ecol. Evol.* 9, 799590. doi: 10.3389/fevo.2021.799590

Hine, A. C. (2013). *Geologic history of Florida: major events that formed the Sunshine State* (Gainesville, FL: University Press of Florida).

Milanich, J. T. (2017). *Archaeology of Precolumbian Florida* (Gainesville, FL: University Press of Florida).

Zimmerman, J. B., Mihelcic, J. R., and Smith, J. (2008). Global stressors on water quality and quantity. *Env. Sci. Tech.* 42, 4247–4254. doi: 10.1021/es0871457

frontiers | Frontiers in Ecology and Evolution

TYPE Original Research
PUBLISHED 25 January 2023
DOI 10.3389/fevo.2023.1070266

OPEN ACCESS

EDITED BY
Thomas George Bornman,
South African Environmental Observation Network (SAEON), South Africa

REVIEWED BY
Tian Xie,
Beijing Normal University, China
Jacqueline Raw,
Nelson Mandela University, South Africa

*CORRESPONDENCE
Marcus W. Beck
✉ mbeck@tbep.org

SPECIALTY SECTION
This article was submitted to Biogeography and Macroecology, a section of the journal Frontiers in Ecology and Evolution

RECEIVED 14 October 2022
ACCEPTED 10 January 2023
PUBLISHED 25 January 2023

CITATION
Beck MW, Robison DE, Raulerson GE, Burke MC, Saarinen J, Sciarrino C, Sherwood ET and Tomasko DA (2023) Addressing climate change and development pressures in an urban estuary through habitat restoration planning.
Front. Ecol. Evol. 11:1070266.
doi: 10.3389/fevo.2023.1070266

Addressing climate change and development pressures in an urban estuary through habitat restoration planning

Marcus W. Beck[1]*, Douglas E. Robison[2], Gary E. Raulerson, Maya C. Burke[1], Justin Saarinen[2], Christine Sciarrino[2], Edward T. Sherwood[1] and David A. Tomasko[3]

[1]Tampa Bay Estuary Program, St. Petersburg, FL, United States, [2]Environmental Science Associates, Tampa, FL, United States, [3]Sarasota Bay Estuary Program, Sarasota, FL, United States

Native habitats in Florida face dual pressures at the land-sea interface from urban development and sea-level rise. To address these pressures, restoration practitioners require robust tools that identify reasonable goals given historical land use trends, current status of native habitats, and anticipated future impacts from coastal stressors. A restoration framework for native habitats was created for the Tampa Bay watershed that identifies current opportunities and establishes short-term (2030) targets and long-term (2050) goals. The approach was informed through a three-decade habitat change analysis and over 40years of habitat restoration projects in the region. Although significant gains in subtidal habitats have been observed, expansion of mangroves into salt marshes and loss of native upland habitats to development highlights the need to target these locations for restoration. The long-term loss of potentially restorable lands to both coastal and upland development further underscores the diminishing restoration opportunities in the watershed. The established targets and goals identified habitats to maintain at their present level (e.g., mangroves) and those that require additional progress (e.g., oyster bars) based on past trends and an expected level of effort given the restoration history of the region. The new approach also accounts for the future effects of sea-level rise, climate change, and watershed development by prioritizing native coastal habitats relative to subtidal or upland areas. Maps were created to identify the restoration opportunities where practitioners could focus efforts to achieve the targets and goals, with methods for repeatable analyses also available using an open source workflow.

KEYWORDS

Florida, land use change, sea-level rise, Tampa Bay, urbanization, habitat loss

1. Introduction

The health of estuarine systems and coastal habitats is tightly linked to land use and management of the watershed (Yoskowitz and Russell, 2015). Coastal habitats provide multiple ecosystem services, including wildlife shelter and migratory corridors (Yoskowitz and Russell, 2015), fisheries production (Houde and Rutherford, 1993), water quality improvement (Kushlan, 1990; Sprandel et al., 2000; Ávila-García et al., 2020), erosion and flood attenuation (Calil et al., 2015; Menéndez et al., 2018), carbon sequestration (Dontis et al., 2020) and recreation (Chung et al., 2018). Anthropogenic stressors can negatively impact the services provided by coastal habitats and restoration practitioners must consider the anticipated effects of these stressors during planning (Elliott et al., 2007;

White and Kaplan, 2017). The combined effects of land development and climate change are especially problematic for prioritizing habitat restoration activities in coastal environments. Habitat changes in response to climate change include landward migration of mangroves into salt marshes, upstream migration of salt marshes within tidal tributaries, and upland forest migration (Brinson et al., 1995; Vogelmann et al., 2012; Cavanaugh et al., 2019). Landward migration of critical habitats in response to sea-level rise may not be possible due to anthropogenic barriers in the watershed. Sea-level rise can occur quicker than landward migration of salt marshes and the upland slope may already be lost to urban development and hardening (Titus et al., 2009). Given projected habitat losses and the limited resources available, appropriate and realistic sites for restoration need to be identified that account for future stressors and past trends.

Past approaches for guiding restoration planning have been successfully used in other contexts, but they do not fully balance competing needs among public and private sectors, nor do they fully account for anticipated effects of multiple stressors. For example, an integrated watershed approach (Environmental Protection Agency, 1996) has been utilized since the early 1990s to diagnose and manage water quantity and quality problems by addressing issues within hydrologically-defined geographic areas. Additionally, the habitat mosaic approach (Henningsen, 2005) of including multiple habitat types within restoration projects has been recognized as an effective means of allowing ecosystem state changes in response to different environmental pressures (Duarte et al., 2009; Palmer, 2009). Adaptive management (Holling, 1978; Gregory et al., 2006) components have also been used to address challenges of sea-level rise, climate change, and development stressors, including monitoring to identify critical restoration decision points and needed intervention with contingency plans. Elements of each of these approaches could be combined to create a more holistic approach to guide restoration and conservation activities for coastal habitats in urban settings.

The Tampa Bay watershed (Florida, United States) is a valuable case study for developing a habitat restoration plan that addresses pervasive coastal stressors. Compared to other estuaries, the ratio of watershed to estuary area is small and the area is heavily developed with 42% of land use classified as urban and suburban residential (Southwest Florida Water Management District, 2018). A retrospective approach to setting habitat protection and restoration targets in Tampa Bay was previously used (Lewis and Robison, 1996; Robison, 2010; Cicchetti and Greening, 2011; Russell and Greening, 2015). Priority was given to restoration activities focused on habitat types that were important for a suite of estuarine faunal guilds disproportionately lost or degraded compared to a *circa* 1950 benchmark period considered as pre-development. Criticisms of this approach included lack of consideration for future sea-level rise and other climate change factors (Yoskowitz and Russell, 2015), use of expanded and different habitats outside the Tampa Bay watershed (Robison, 2010), lack of attention to upland or freshwater wetland habitats, and little recognition of land development trends or actual available space for restoration efforts. These challenges are shared by restoration practitioners in other coastal environments and an approach that accommodates these challenges for planning would be highly transferable.

In this paper, we describe an approach for habitat restoration and conservation planning that addresses the above challenges by considering the whole watershed, addressing historical changes, focusing on trajectories that have occurred during contemporary time periods, and considering both current and future stressors – particularly land development and sea-level rise. Current and historical data are available for most Tampa Bay habitats, representing a time period when federal, state and local regulations were in effect and regional impacts from climate change have been documented (Raabe et al., 2012; Cavanaugh et al., 2014). The approach establishes a framework that can guide both watershed-level habitat planning and site-level restoration activities and incorporates applicable elements of other habitat restoration paradigms discussed above (Palmer, 2009). The general approach includes (1) designation of habitat types by strata relative to the aquatic-terrestrial gradient, (2) quantification of historical trends by habitat types to identify appropriate future targets in coverage, and (3) identification of opportunity areas that could be used by practitioners to achieve restoration goals based on habitat type and past trajectories. These opportunity areas provide a first assessment of where restoration could occur and where on the ground assessments could be pursued to further quantify restoration potential. The outcomes of the approach are also spatially specific by providing maps to identity opportunity areas and reproducible using an open science workflow (Lowndes et al., 2017) that allows regular updates as new data become available.

2. Methods

2.1. Study area

Tampa Bay is a large open water estuary (surface area approximately 983 km^2) on the west-central coast of Florida (Figure 1). The watershed covers approximately 5,872 km^2, for a total combined area of approximately 6,855 km^2. The climate is subtropical and within the 2020 ecotone for mangrove and salt marsh habitats. Native habitats in the watershed include pine flatwoods, forested freshwater wetlands and non-forested vegetated wetlands. The watershed is heavily developed with an estimated population of 3.3 million people in the four major counties (Rayer and Wang, 2020). Numerous anthropogenic changes have altered the natural habitats of Tampa Bay, including direct removal of habitat (e.g., dredge and fill of bay bottom, mining activities), alteration of hydrology, and destruction and fragmentation of habitat from development.

2.2. Habitats of Tampa Bay

The major habitat types of Tampa Bay were stratified by tidal influence and location in the watershed to define broad categories for restoration planning. Subtidal habitats included those that are submerged all or most of the time, intertidal habitats included emergent tidal wetlands that are submerged during high tides but exposed during low tides, and supratidal habitats included those that occur above the high tide line (i.e., the remainder of the watershed).

Subtidal habitats included hard bottom (Jaap and Hallock, 1990; Ash and Runnels, 2005; Kaufman, 2017; CSA Ocean Sciences, 2019), artificial reefs (Dupont, 2008), tidal flats (Moore et al., 1968; Eisma, 1998), seagrasses (Heck et al., 2003; Sherwood et al., 2017), and oyster reefs (Coen et al., 2007; Ermgassen et al., 2013). Intertidal habitats (or emergent tidal wetlands) included mangroves (Odum and McIvor, 1990), salt marshes (Comeaux et al., 2012; Raabe et al., 2012), salt barrens (Bertness, 1985; Hsieh, 2004), tidal tributaries (Sherwood, 2008; Wessel et al., 2022), and living shorelines (National Oceanic and Atmospheric Administration, 2015; Restore America's Estuaries, 2015; Smith et al., 2018). Supratidal habitats included non-developed uplands (Meyers and Ewel,

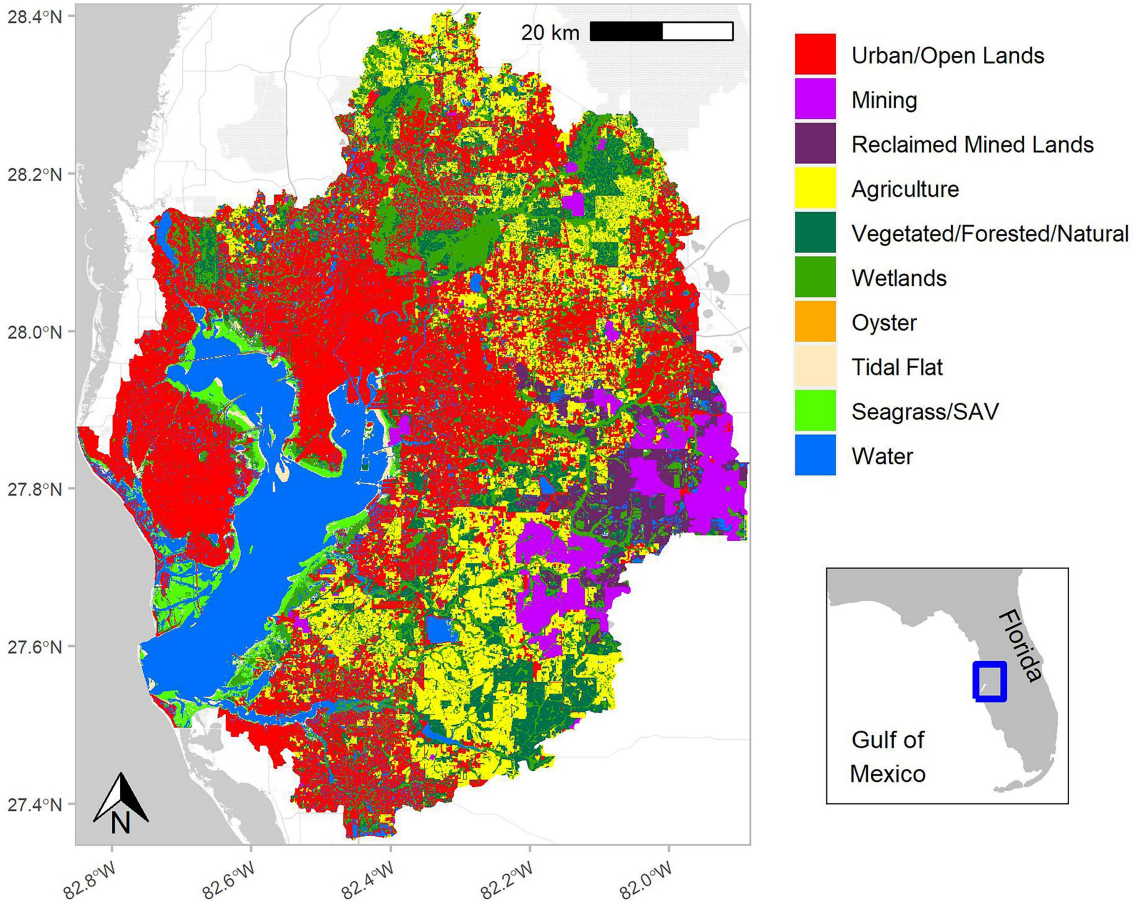

FIGURE 1
Land use, cover, and subtidal habitats for the Tampa Bay watershed, Florida, United States. The watershed includes the natural hydrologic boundary with minor modifications to include partners working with the Tampa Bay Estuary Program. Categories are based on the Florida Land Use Cover and Forms Classification System (Florida Department of Transportation, 1999; Southwest Florida Water Management District, 2014; Kawula and Redner, 2018) with relevant codes combined for presentation in the figure.

1990), freshwater forested wetlands (Conner et al., 2007), and freshwater non-forested wetlands (Kushlan, 1990). Data sources are described below and in Supplementary Table S1. Uplands were further sub-divided into coastal and non-coastal uplands based on location relative to the 5-foot contour (~1.5 m elevation) that covers an area of land from the local Mean Lower Low Water (MLLW) elevation landward to an elevation 5 feet above Mean Sea Level. This 5-foot contour or coastal stratum is an area of intense urban development and is expected to be affected by sea-level rise based on current estimates (Burke et al., 2019). Since 1946, the St. Petersburg tidal gauge (NOAA gauge 872,650) has documented a nearly 20 cm increase in mean tidal height to present day. Projections from the year 2000 to 2,100 suggest sea levels can increase between 58 and 259 cm in the region (Burke et al., 2019). The coastal stratum within the 5-foot contour is used to better identify and prioritize coastal habitats at risk of landward migration and coastal development given that it includes the area of land within the sea level rise projections.

2.3. Approach

Coverage targets for habitat types and opportunity areas for restoration were identified by integrating multiple datasets available for the region. First, habitat status and historical trends were quantified using land use/land cover and subtidal datasets to understand relative changes that have occurred over time. Second, historic habitat restoration efforts conducted in the watershed were synthesized to inform on a practical and feasible level of effort that could be conducted by restoration practitioners in the future. The first two steps were used to identify short-term (2030) targets and long-term (2050) goals for native habitat coverage (hectares). The short-term targets provided an interim set of native habitat coverages to attain within a reasonable planning horizon, after which progress in attaining the long-term goals will be re-assessed. Finally, remaining restoration opportunities were spatially identified by combining current coverages with existing or proposed protected areas and areas anticipated to be affected by sea-level rise. As such, the approach identifies reasonable goals and targets based on past trends and provides spatially explicit information that identifies where restoration practitioners could prioritize projects based on opportunities within their respective jurisdictions.

2.4. Habitat status and trends

For the majority of subtidal, intertidal and supratidal habitats, coverages were quantified from two routine spatial assessment programs conducted by the Southwest Florida Water Management District

(SWFWMD). For subtidal habitats, 2018 data were used to estimate current coverage of seagrasses, tidal flats, and oysters (Southwest Florida Water Management District, 2019). These data include vector polygon coverages of the major subtidal habitats in Tampa Bay, as interpreted from 1:24,000 scale natural color aerial photographs flown in winter 2018 under cloud free conditions. Accuracy assessments of the photo-interpreted map included field verification by random sample points, with a requirement of 90% accuracy for the seagrass categories. The minimum mapping unit for seagrass polygons is reported as 0.25 acres (~0.1 ha). Historical datasets for subtidal habitats using identical methods began in 1988 with updates occurring on an approximate biennial basis (Sherwood et al., 2017; Tomasko et al., 2020). Oyster bed coverage has been routinely estimated in these data products beginning in 2014.

Current intertidal and supratidal habitat coverages were estimated using the 2017 SWFWMD Land Use Land Cover (LULC) maps (Southwest Florida Water Management District, 2018). Land use and cover types (natural and developed) are classified following the Florida Land Use Cover and Forms Classification System (FLUCCS; Florida Department of Transportation, 1999; Southwest Florida Water Management District, 2014; Kawula and Redner, 2018). Similar methods as the subtidal habitats described above are used for the intertidal and supratidal coverage maps, although at a slightly higher spatial resolution (1:12,000). Mangroves, salt barrens, and salt marshes were reported individually. While the photointerpretation of specific freshwater wetland types is often difficult, forested wetlands and non-forested wetlands can be distinguished with these data. Therefore, all applicable FLUCCS codes representing natural freshwater wetlands were combined for these classifications. Native upland habitats were also combined in one classification. Historical estimates for all intertidal and supratidal habitats were also quantified starting with the earliest database in 1990 and occurring every 2 to 3 years until the current estimate in 2017.

To address data gaps for habitats not included in the routine SWFWMD datasets, results from special studies were compiled to obtain current estimates. These included hard bottom subtidal habitats, artificial reefs, tidal creeks, and living shorelines (Robison et al., 2020). No information on historical trends is available for these habitats.

Finally, a habitat coverage change analysis between the terminal years of data (1988 to 2018 for subtidal, 1990 to 2017 for intertidal and supratidal) was conducted to understand how habitats were changing between types. This required an intersection of the data layers to quantify if habitat types were unchanged or changed for any given location and identifying the type of change (e.g., seagrass to tidal flats). Specifically, the spatial datasets were unionized and the total areal change of the polygons for each habitat type was quantified by calculating the difference between the two terminal years. For example, the area that remained as native uplands between the 1990 and 2017 intertidal and supratidal layers was quantified, whereas the area that changed from native uplands to another habitat category was also quantified. This process was repeated for all native habitats, including developed and restorable lands (described below). The results were summarized as Alluvial diagrams showing relative proportions of habitat change by type and between years (Allaire et al., 2017).

2.5. Restoration and enhancement projects

Restoration and enhancement projects conducted over the past 40 years were quantified for each of the major habitat types to inform expectations for setting short-term targets and long-term goals. Here and throughout, restoration describes the process of assisting the recovery of an ecosystem that has been degraded, damaged, or destroyed (Gann et al., 2019). Restoration projects in the database were also those that involved earthwork to reshape the land or the addition of structural elements (e.g., rock). This distinct categorization is useful for restoration practitioners familiar with the projects in the region. Enhancement was defined as any activity not including earthwork that improved the environment (e.g., planting native vegetation, invasive species or debris removal, prescribed burns, etc.). Data were gathered from the SWFWMD Surface Water Improvement and Management Program, Federal Government Performance and Results Act reporting, the Tampa Bay Water Atlas,[1] Tampa Bay Watch, and the Technical Advisory Committee of the Tampa Bay Estuary Program. The collected data included project name, year, description, size (area or length), and location (latitude and longitude). Data gaps were supplemented by archival research, site visits, contacting entities, and expert knowledge from local professionals. The synthesized dataset is available.[2]

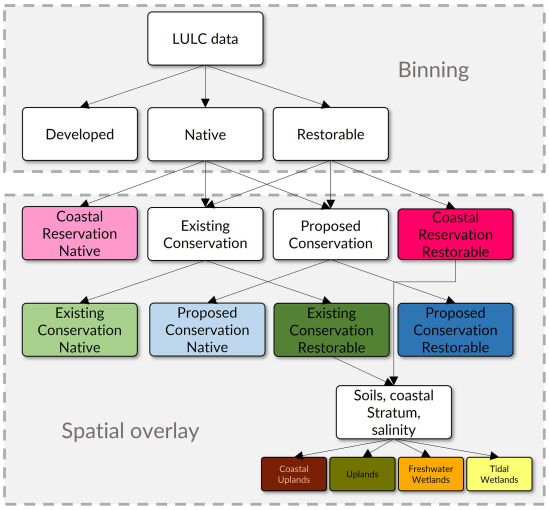

FIGURE 2
Spatial analysis workflow used to identify opportunity areas (existing conservation native, proposed conservation native, existing conservation restorable, proposed conservation restorable, reservation native, reservation restorable) and restoration potential (coastal uplands, uplands, freshwater wetlands, tidal wetlands) in the Tampa Bay watershed. Workflows are divided into binning of land use/land cover categories into relevant habitat types and spatial overlay of datasets to identify the opportunity areas and restoration potential. The approach was applied to both the intertidal and supratidal strata of the watershed.

2.6. Opportunity areas and restoration potential

Spatially explicit estimates of the opportunity areas and their restoration potential in the Tampa Bay watershed were obtained using a spatial analysis shown in Figure 2. The two main processes included

1 https://www.tampabay.wateratlas.usf.edu/
2 https://www.tampabay.wateratlas.usf.edu/restoration/

(1) binning existing datasets into relevant categories and (2) overlaying multiple datasets to identify opportunities. Opportunity areas were defined as locations where habitat protection and restoration activities are possible and where they could occur to attain the targets and goals described above. Identifying opportunity areas is necessary to quantify the restoration potential for a particular habitat type, which is a measure of what is actually possible given underlying soil conditions, expected land use change, and sea-level rise. The identification of these areas on a broad spatial scale serves as a planning tool for restoration practitioners, where follow-up assessments are expected to more fully quantify restoration potential at selected sites.

The Land Use Land Cover 2017 dataset from SWFWMD was used for binning existing coverages into the relevant habitat types in the intertidal and subtidal strata. All FLUCCS classification codes were placed into one of three categories. First, native habitats were those that included the full range of natural plant communities and other habitats that are endemic to the watershed. Second, restorable habitats included existing altered but non-hardened and pervious FLUCCS codes that could potentially support native habitats through restoration. Third, existing development included developed land FLUCCS codes that are hardened and impervious (e.g., structures and pavement) and not suitable for habitat restoration.

After binning, the native and restorable lands were overlaid with additional layers to identify (1) coastal reservation native and coastal reservation restorable areas, and (2) existing and proposed native and restorable areas. Collectively, each of these unique products are considered the opportunity areas in the Tampa Bay watershed (Table 1). The coastal reservation native and coastal reservation restorable areas are native and restorable habitats, respectively, that occur in the 5-foot contour or coastal stratum and do not occur in existing or proposed conservation areas (described in the following paragraph). Native habitats in this stratum were identified as those to be reserved, whereas restorable habitats were identified as those where tidal wetlands or coastal uplands could be restored.

The existing and proposed native and restorable areas were those that occurred in public lands that are currently acquired or proposed for acquisition. To identify these areas, native and restorable lands were intersected with data created from the Florida Natural Areas Inventory (FNAI) and permit databases of conservation and drainage easements (Florida Natural Areas Inventory, 2020). The FNAI data are Florida Managed Areas as vector polygons of public and some private lands identified as having natural resource value and that are being managed at least partially for conservation. The source data for this layer are provided to FNAI directly from the managing agency in digital format or as paper maps that are digitized using appropriate topographic quadrangles, ortho-imagery, and property appraiser parcel data at a minimum spatial resolution of 1:5,000. Intersecting the native and restorable lands in these areas produced four unique opportunity areas: existing conservation native, proposed conservation native, existing conservation restorable, and proposed conservation restorable. This workflow created the existing conservation and proposed conservation layers in Figure 2.

TABLE 1 Description of the opportunity areas in the Tampa Bay watershed identified through spatial analysis.

Opportunity area	Description
Existing conservation native	Native habitats currently within existing conservation lands
Existing conservation restorable	Restorable areas currently within existing conservation lands
Proposed conservation native	Native habits within proposed conservation lands
Proposed conservation restorable	Restorable areas within proposed conservations lands
Coastal reservation native	Native habitats within the coastal stratum
Coastal reservation restorable	Restorable areas within the coastal stratum

Native habitats include those in the watershed not considered developed or restorable (e.g., freshwater wetlands, forested uplands, etc.). Restorable areas are altered but non-hardened and pervious lands that could potentially support native habitats through restoration. Existing and proposed conservation areas are those that are publicly owned or on conservation easements that currently exist or are proposed for acquisition, respectively, as identified primarily in the Florida Natural Areas Inventory. Coastal reservation areas occur within the coastal stratum identified from the bay shoreline to the 5-foot elevation contour.

All opportunity areas identified as restorable included coastal reservation restorable, existing conservation restorable, and proposed conservation restorable. To identify discrete habitat types that could be the goal of future restoration projects, restorable lands in the coastal stratum and on existing conservation areas (coastal reservation native and existing conservation restorable) were further grouped into their restoration potential by underlying soil types. Proposed conservation areas were excluded from the analysis to provide a more confident assessment of restoration potential in areas that have already been acquired (i.e., existing conservation) or are immediately threatened by sea-level rise and/or coastal development (i.e., the coastal stratum).

Compared to vegetation communities, soil characteristics typically change slowly (e.g., decades to centuries) in response to hydrologic impacts, unless physically disturbed (Osland et al., 2012; Stockmann et al., 2014). Therefore, soil distributions can be used to estimate historical habitat distribution and restoration potential. A soils suitability layer was used for the Tampa Bay watershed (Ries and Scheda, 2014) that classified soils as xeric, mesic, or hydric. The mesic and hydric categories were combined to represent wetland restoration potential and the xeric category was used to represent upland restoration potential. A distinction was made between tidal and freshwater wetland restoration potential by intersecting the mesic and hydric soils with the coastal stratum. Mesic or hydric soils that occur below the 5-foot contour were assigned a restoration potential for tidal wetlands, whereas mesic or hydric soils above the 5-foot contour were assigned a restoration potential for freshwater wetlands. This distinction explicitly accounts for potential salinity changes to soil properties as a function of sea-level rise based on regional projections in the time period for establishing the targets and goals.

Two distinct mapping products were created from the above analysis. The first was an opportunities map that showed areas in the watershed identified as existing conservation native, existing conservation restorable, proposed conservation native, proposed conservation restorable, coastal reservation native, and coastal reservation restorable. The second was a map that identified the restorable lands (either existing or coastal reservation) based on their restoration potential as coastal uplands, freshwater wetlands, native uplands, or tidal wetlands. All spatial analyses described above and as outlined in Figure 2 were conducted using the R statistical programming language (R Core Team, 2022), specifically leveraging functions from the tidyverse package for data wrangling (Wickham et al., 2019) and the simple features (sf) package for geospatial analysis (e.g., the *st_intersection* and *st_union* functions for intersect and union operations, Pebesma, 2018). All spatial data were transformed to the NAD83(2011) / Florida West (ftUS) projection prior to analysis. The workflows and

data are provided in an open-access repository available on GitHub[3] (Beck et al., 2022).

3. Results

3.1. Habitat status and trends

Current estimates and trend information on subtidal habitats were available for seagrasses, tidal flats, and oyster bars (Table 2). Oyster bars were estimated at 67 ha in 2018 (Table 2), showing a 29% increase since mapping began in 2014. The increase in oyster bars may represent improved ground-truthing and photointerpretation. Tidal flats have generally increased from 1988 to the mid−2000s, followed by a decrease to present. The current estimate for tidal flats is 6,569 hectares, showing a 24% decline compared to the 1988 estimate of 8,700 hectares. Seagrasses have increased by 75% (6,986 ha) since 1988 to a current estimate of 16,293 ha. The change analysis comparing 1988 to 2018 for subtidal habitats (Figure 3) confirmed trends in Table 2 and showed that the seagrass increases were primarily associated with the colonization of non-vegetated areas of tidal flats, as well as unclassified areas of open water. Current estimates for subtidal habitats without historical trend information included 171 ha for hard bottom habitat and 67 hectares for artificial reefs.

Total intertidal habitat (mangroves, salt barrens, and salt marshes) increased by 12% to 8,340 ha from 1990 to 2017 (Table 3). Mangroves increased by 15% to 6,276 ha, salt barrens increased by 7% to 203 ha, and salt marshes increased by 3% to 1,861 ha. Despite a net increase in salt marsh habitat, the change analysis showed that 153 ha were replaced by mangroves (Figure 4). The current extent of tidal tributary length is 622 km (no trend information is available).

Trend assessments for supratidal habitats showed the effects of increasing land development and loss of restorable habitats in the Tampa Bay watershed (Table 3). Developed lands increased by 44% to 217,047 ha from 1990 to 2017. Coastal uplands decreased by 30% to 1,446 ha, native uplands decreased by 38% to 57,836 ha, and restorable lands decreased by 18% to 189,512 ha. Non-forested freshwater wetlands increased by 24% to 27,358 ha, whereas forested freshwater wetlands decreased by 5% to 61,667 ha. The change analysis (Figure 4) showed that a majority of conversion to developed lands came from restorable areas (21,292 ha) and native uplands (7,184 ha), with smaller proportions converted from forested freshwater wetlands (1,407 ha) and coastal uplands (193 ha). Habitats converted to restorable areas primarily included native uplands (8,304 ha), forested freshwater wetlands (1,700 ha), and developed lands (2,794 ha). The increase in non-forested freshwater wetlands was primarily from restorable lands (2,759 ha).

3.2. Habitat restoration and enhancement

A total of 460 restoration projects were documented in Tampa Bay and its watershed between 1971 and 2019. These projects were divided among habitat types that included estuarine ($n=228$), freshwater ($n=53$), uplands ($n=119$), and a mix of all three ($n=60$). A total of 1,978 ha have been restored, whereas 12,930 ha and 42.8 km (as shoreline or tributaries) were enhanced. Forty partners were responsible for these projects, although

TABLE 2 Change over time in hectares for subtidal habitats in Tampa Bay.

Habitat type	1988	1990	1992	1994	1996	1999	2001	2004	2006	2008	2010	2012	2014	2016	2018	1988 to 2018	% change
Seagrasses	9,307	10,086	10,299	10,609	10,758	9,920	10,417	10,795	11,309	11,862	13,171	13,874	16,153	16,701	16,293	6,986	75
Tidal flats	8,700	8,207	8,272	8,117	8,199	10,878	10,300	11,601	11,387	10,878	9,617	8,714	5,976	5,557	6,569	-2,130	−24
Oyster bars	-	-	-	-	-	-	-	-	-	-	-	-	52	65	67	-	-

Columns show years with available data and the final two columns show the change and percent change from 1988 to 2018. Oyster bars were not meaningfully quantified prior to 2014.

3 https://github.com/tbep-tech/hmpu-workflow

some were from departments within the same agency. Eighty-nine living shoreline projects, seawall enhancements, and oyster reef installations were documented, totaling 18.2 km. Although projects were documented for the whole period of record, few projects were completed prior to 1990.

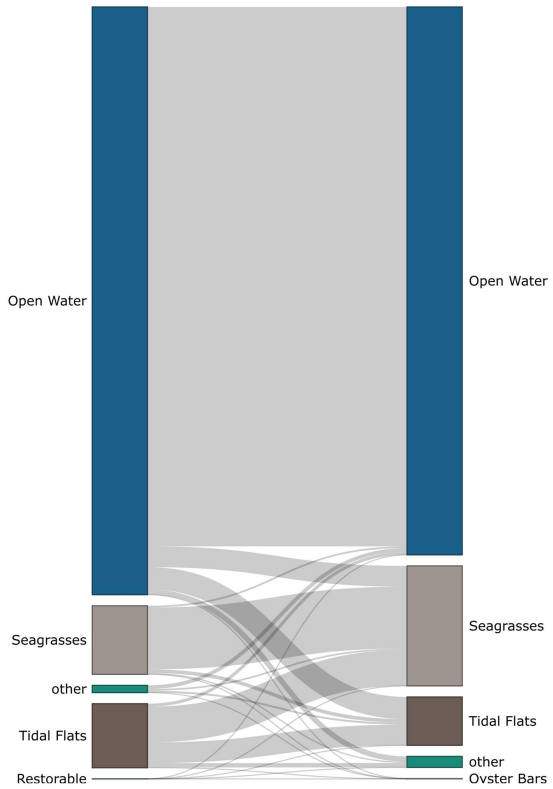

FIGURE 3
Change analysis of habitat categories in the subtidal strata of the Tampa Bay watershed. The left column shows relative areas in 1988 and the right column shows relative areas in 2018 for each habitat category, where the bar heights are proportional to extents in each year. The grey lines show the proportional change in area of each habitat category between the years.

From 1990 to 2010 and from 2010 to 2019, an annual mean of 68 ha/yr. and 81 ha/yr. of habitat was restored, respectively. These means were used to define appropriate expectations for future restoration, described below.

3.3. Summary of opportunity areas and restoration potential

The current extent of each habitat type is shown in Table 4 as summaries for the opportunity areas and restoration potential. The extent of each habitat in existing conservation lands and proposed conservation lands is shown. Summaries of the restoration potential under existing and proposed conservation lands is also shown. Most restoration opportunities on existing conservation lands are for native uplands and freshwater wetlands. Less opportunities exist for intertidal wetlands (mangrove forests, salt barrens, and salt marshes). These summaries are also shown spatially in Figures 5, 6.

The map of the remaining opportunity areas provided a spatial summary of where practitioners could target future restoration projects (Figure 5). Native habitats currently protected (existing conservation native), proposed for protection (proposed conservation native), or in the coastal stratum (coastal reservation native) totaled 119,410 ha (20.3% of the watershed above MLLW). Similarly, restorable lands currently protected (existing conservation restorable), proposed for protection (proposed conservation restorable), or in the coastal stratum (coastal reservation restorable) totaled 83,423 ha (14.2% of the watershed). Understandably, most of the native and restorable lands occurred in undeveloped areas in northern and southeastern areas of the watershed (Figure 6). Existing conservation lands (existing conservation native, existing conservation restorable) totaled 79,396 ha (13.5% of the watershed) and proposed conservation lands (proposed conservation native, proposed conservation restorable) totaled 123,437 ha (21% of the watershed). Reservation areas in the coastal stratum (coastal reservation native, coastal reservation restorable) totaled 6,498 ha (1.1% of the watershed).

Combining the restorable lands on existing conservation areas and in the coastal stratum with soils data provided a spatial summary of the restoration potential grouped by habitat type (Figure 6). A total of 17,205 ha (2.9% of the watershed) of potentially restorable lands on

TABLE 3 Change over time in hectares for intertidal and supratidal land cover in Tampa Bay.

Stratum	Land cover category	1990	1995	1999	2004	2007	2011	2014	2017	1990 to 2017	% change
Intertidal											
	Mangrove forests	5,472	5,808	5,793	6,318	6,300	6,299	6,266	6,276	804	15
	Salt barrens	189	194	199	197	185	203	199	203	14	7
	Salt marshes	1,814	1,795	1,798	1,877	1,874	1,863	1,939	1,861	47	3
Supratidal											
	Coastal uplands	2,055	2,122	2,014	1,672	1,515	1,498	1,999	1,446	−609	−30
	Developed	150,724	159,180	171,066	193,986	203,438	209,081	214,710	217,047	66,324	44
	Forested freshwater wetlands	64,573	63,766	62,726	63,109	62,258	62,081	63,562	61,667	−2,906	−5
	Native uplands	93,076	83,850	75,313	64,482	61,277	60,319	62,794	57,836	−35,239	−38
	Non-forested freshwater wetlands	22,037	20,831	20,710	23,662	26,363	27,893	27,972	27,358	5,320	24
	Restorable	231,288	232,195	228,531	212,549	201,609	195,529	184,342	189,512	−41,777	−18

Columns show years with available data and the final two columns show the change and percent change from 1990 to 2017.

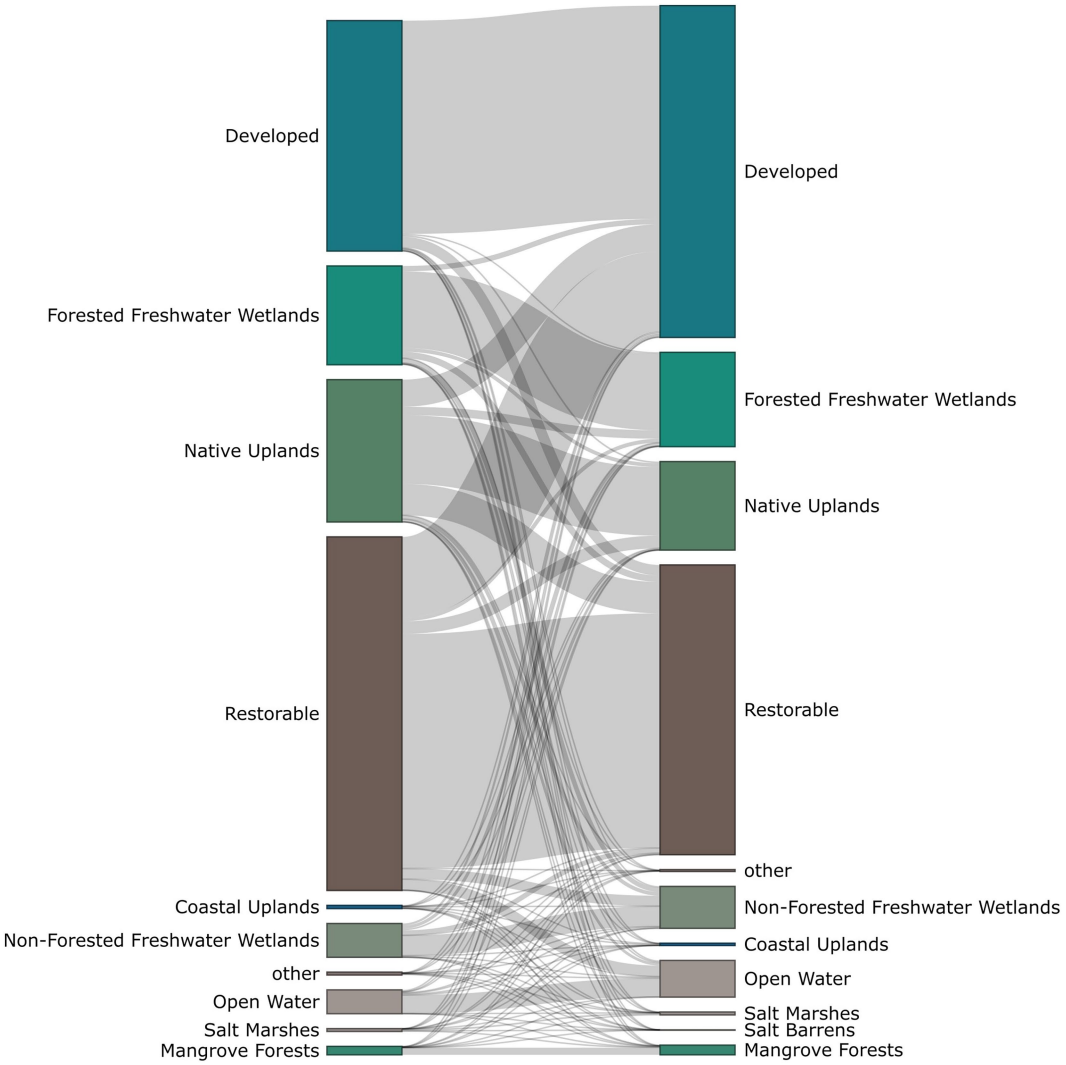

FIGURE 4
Change analysis of habitat categories in the intertidal and supratidal strata of the Tampa Bay watershed. The left column shows relative areas in 1990 and the right column shows relative areas in 2017 for each habitat category, where the bar heights are proportional to extents in each year. The grey lines show the proportional change in area of each habitat category between the years.

existing conservation areas were identified, further partitioned as coastal uplands (128 ha, < 0.1% of the watershed), freshwater wetlands (11,034 ha, 1.9% of the watershed), native uplands (5,419 ha, 0.9% of the watershed), or tidal wetlands (624 ha, 0.1% of the watershed).

3.4. Establishment of targets and goals

Identifying short-term (2030) targets and long-term (2050) goals for the restoration extent of native habitats in Tampa Bay was informed by the assessment of current extents, past trends, and relative effort for past restoration and enhancement projects. These targets and goals do not consider an explicit projection of how habitats are expected to change as a result of climate change and anticipated development because no such estimates are available. However, the methods implicitly account for these anticipated changes by differentiating the watershed by strata and setting the targets and goals based on past trends that are affected both by climate change and development trajectories. The methods herein provide the best estimate of what restoration is likely to be achieved over the next few decades.

Table 5 shows the targets and goals identified through this analysis and the associated rationale. For example, the targets and goals are established based on the current extent and informed by the restoration potential. If restoration potential exists and coverage restored from past projects suggests a reasonable level of effort, the targets and goals reflect the current extent relative to the restoration opportunity, past trends, and anticipated effort. Conversely, other habitats with no identified restoration opportunity, or with sufficient current extents (e.g., mangrove forests), were assigned targets and goals similar to the current extent, i.e., these habitats should be protected and further restoration will only increase resilience. The proposed targets and goals do not represent the current extent plus restoration potential for these reasons. Implicit in the targets and the goals is recurring re-assessment over time to evaluate progress and adjust expectations as appropriate.

TABLE 4 Summary of habitat restoration opportunities in the Tampa Bay watershed.

		Native habitats			Restorable habitats		
Stratum	Habitat type	Current extent	Existing conservation lands	Proposed conservation lands	Total restoration opportunity	Existing conservation lands restoration opportunity	Proposed conservation lands restoration opportunity
Subtidal							
	Hard bottom	171 ha	171 ha	N/A	N/A	N/A	N/A
	Artificial reefs	88 ha	88 ha	N/A	N/A	N/A	N/A
	Tidal flats	6,569 ha	6,569 ha	N/A	I/D	I/D	N/A
	Seagrasses	16,293 ha	16,293 ha	N/A	5,719 ha	5,719 ha	N/A
	Oyster bars	67 ha	67 ha	N/A	I/D	I/D	N/A
Intertidal							
	Living shorelines	18 km	N/A	N/A	N/A	N/A	N/A
	Mangrove forests	6,276 ha	4,516 ha	1,604 ha	1,043 ha	521 ha	522 ha
	Salt barrens	203 ha	177 ha	25 ha			
	Salt marshes	1,861 ha	881 ha	917 ha	526 ha	102 ha	424 ha
	Tidal tributaries	622 km	N/A	N/A	N/A	N/A	N/A
Supratidal							
	Coastal uplands	1,446 ha	722 ha	664 ha	513 ha	128 ha	385 ha
	Non-forested freshwater wetlands	27,358 ha	4,761 ha	10,353 ha	63,705 ha	11,034 ha	52,671 ha
	Forested freshwater wetlands	61,667 ha	24,052 ha	22,399 ha			
	Native uplands	57,836 ha	27,083 ha	21,256 ha	17,636 ha	5,419 ha	12,217 ha

Summaries are based on 2017 land use data, 2018 subtidal data, best estimates for habitat types not in existing GIS layers, and current extent of existing and proposed conservation lands. Proposed conservation lands are those identified for acquisition. Current extent is the sum of existing and proposed conservation lands, plus those not in conservation. Total restoration opportunity does not account for lands currently existing or proposed for conservation. N/A: not applicable, I/D: insufficient data.

4. Discussion

Priorities for comprehensive, watershed-wide habitat restoration should be informed by current assessments and what is possible to achieve in the future. These priorities are necessary given anticipated impacts of land development and climate change, while also considering competing societal interests for use of the environment and limited resources for land acquisition and restoration. Our approach balances these tradeoffs by identifying targets and goals that are informed by current extent, past trends, and realistic effort from past projects. Further, spatially explicit locations are identified where these targets and goals could be achieved based on existing opportunities for restorable habitats, including areas anticipated to be impacted by coastal stressors (i.e., sea-level rise and land development). This approach departs from previous restoration paradigms by identifying what is possible rather than attempting to recreate an ideal historical baseline. Methods are also provided using open source tools (Beck et al., 2022) that (1) allow for the most current datasets to be synthesized to assess progress, and (2) can be used in other locations with similar needs for identifying restoration priorities.

4.1. Habitat trends

Identifying appropriate targets and goals would not have been possible without a detailed assessment of current extent and past trends over 30 years of native habitats in Tampa Bay and its watershed. The most notable trends included (1) an increase of seagrasses by 75%, (2) an increase of emergent tidal wetlands (12%) and freshwater wetlands (24%), and (3) a loss of native uplands (38%).

Seagrass recovery in Tampa Bay is a well-known success story that demonstrated how public-private partnerships can effectively reduce total nitrogen loads into Tampa Bay (Greening et al., 2014; Sherwood et al., 2017). The nutrient reductions, primarily from point-source controls and advanced wastewater treatment, contributed to improvements in water quality and light environments that were favorable for seagrass growth. Reducing nitrogen inputs into Tampa Bay remains the primary strategy for maintaining water quality conditions. However, the most recent (2020) coverage estimate showed a seagrass loss of 18% baywide since peak coverages in 2016, falling below the target defined herein. These data were unavailable at the time this habitat restoration workflow was initially developed and trends informed by the new restoration paradigm have prompted bay managers to assess barriers in achieving the seagrass restoration goal. In particular, much of the seagrass losses have occurred in Old Tampa Bay (northwest segment of Tampa Bay), where recurring algal blooms of *Pyrodinium bahamense* have contributed to water quality decline (Lopez et al., 2019). The greatest percent loss of seagrass in 2020 was observed in Hillsborough Bay (northeast segment of Tampa Bay), which does not experience *P. bahamense* blooms. Ongoing research to understand mechanisms for mitigating blooms that negatively affect water quality, in addition to identifying potential regional stressors, will be critical for restoring seagrass in Tampa Bay.

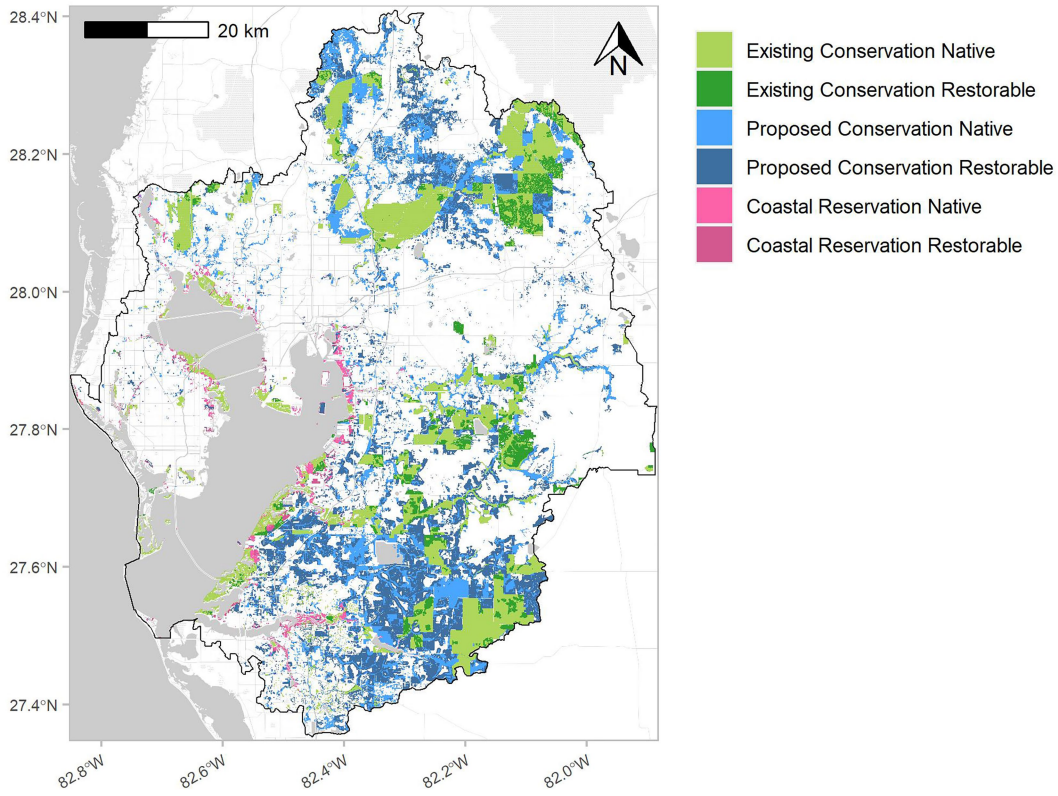

FIGURE 5
Opportunity areas for habitat restoration in the Tampa Bay watershed. Green indicates existing conservation, blue indicates proposed conservation, and pink indicates reservation opportunities. Each category is also grouped into native and restorable habitats. The outline is the Tampa Bay watershed.

Emergent tidal and freshwater wetlands in Tampa Bay have also experienced dramatic changes over the last three decades. Dual pressures from sea-level rise and changes in the length of the freeze-free season have affected tidal wetlands, such that mangrove forests are outcompeting salt marshes and salt barrens for available niche space. Mangrove expansion as a result of climate change has been observed throughout the Gulf of Mexico (Comeaux et al., 2012; Osland et al., 2022). Anthropogenic water withdrawals have also reduced freshwater flows reaching tidal marshes, contributing to reductions in coverage of key species (e.g., *Juncus roemerianus*) that have favored mangroves (Raabe et al., 2012). As such, the identified targets and goals for mangroves indicate protection of these habitats, without the need for additional restoration. However, mangroves are expected to continue colonization of the intertidal zone, contributing to additional losses of salt marshes and salt barrens. The reservation areas identified in Figure 5 represent critical remaining areas in the intertidal zone that could be protected to prevent additional losses of tidal wetlands. Likewise, gains in non-forested freshwater wetlands are a reflection of (1) constructed stormwater ponds required by state and federal regulatory programs, and (2) the cumulative gains from publicly-funded habitat restoration projects. Creative restoration approaches (e.g., habitat acquisition and optimal management of freshwater flows) that address the likely expansion of mangroves at the expense of salt marshes and salt barrens will be required to meet the targets and goals for these habitats.

The decrease in native uplands is the result of continued development in the Tampa Bay watershed (Figure 4) and lack of regulatory protection of these habitats. Attaining the target and goal will require restoration of upland habitats on existing conservation lands (i.e., restoration potential in Figure 6) and new conservation lands to offset the continued loss of these habitats to development. The long-term conversion of restorable areas to developed lands (Figure 4) presents additional challenges for restoration of native uplands. Additional education about best practices in land development, market-based incentives, and amendments to existing planning, zoning, and land development regulations will be needed to address these issues. Although federal and state regulations for endangered species provide some protection to rare habitats, such as scrub jay (*Aphelocoma coerulescens*) habitat, common and historically abundant native habitats are largely unprotected (e.g., pine flatwoods). Voluntary approaches to low impact urban or suburban development may also gain traction among developers as more viable methods for land conversion that minimize impacts to natural resources while increasing quality of life (Jones et al., 2009). Education and outreach activities that target land developers to raise awareness of the benefits of alternative practices are critical in this effort. Market-based approaches to mitigating urban sprawl may also be practical (e.g., conservation subdivisions; Mohamed, 2006) given the estimated economic gains relative to conventional approaches. Regardless, reductions in native uplands will likely continue in the short-term unless local governments improve regulatory protections, such as strengthening language within comprehensive plans and development regulations to maintain a defined extent of these habitats within a rapidly urbanizing coastal watershed.

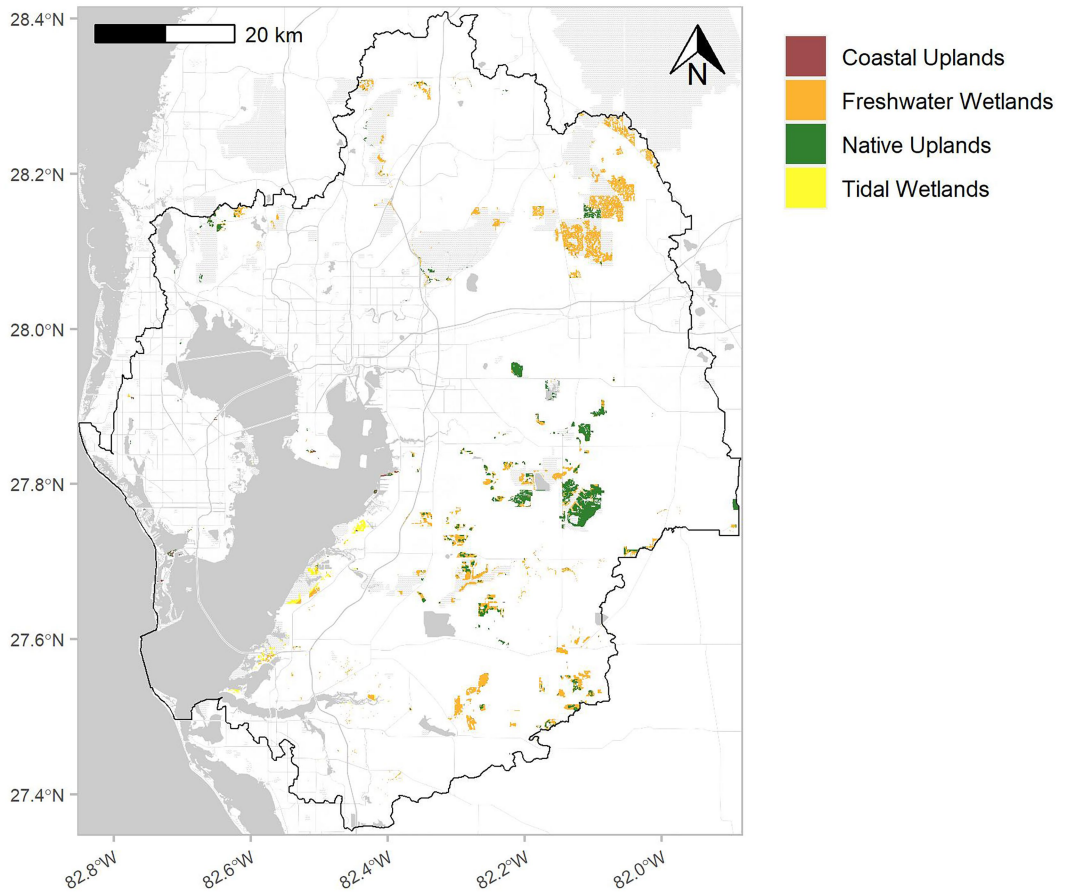

FIGURE 6
Habitat restoration potential in the Tampa Bay watershed. Areas are identified as those where habitat restoration could target the four identified categories as coastal uplands, freshwater wetlands, native uplands, or tidal wetlands. Categories are based on the opportunity areas, soil types, and coastal boundaries. The outline is the Tampa Bay watershed.

4.2. Achieving restoration targets and goals

Achieving the defined targets and goals will require diverse approaches for habitat restoration and management. Focusing efforts on publicly-owned conservation lands is expected to have long-term benefits and will be most cost-effective given the level of restoration effort compared to habitats that have already been impacted by anthropogenic activities. As such, public acquisition of remaining critical lands (e.g., coastal uplands) is a high priority given current development trends in the watershed. Other restoration targets (e.g., salt marshes) will not be obtained without additional public acquisition or initiating novel public-private partnerships as a mechanism for doing so (Holl and Howarth, 2001; Benson et al., 2018). Therefore, varied approaches to leverage resources for restoration are needed and could include pursuing traditional grants, matching funds from multiple partners, or voluntary initiatives that incentivize habitat restoration (e.g., Blue Carbon investments; Sheehan et al., 2019). Recent gains in tidal and freshwater wetlands are primarily due to publicly-funded habitat restoration projects, state and federal wetland regulatory programs, and to a lesser extent, regulatory mitigation. Restoration activities for habitats without similar regulatory frameworks should pursue the options above to achieve the defined targets and goals.

Other restoration activities could be pursued for the opportunity areas. Substantial opportunities exist for upland restoration on reclaimed mined lands within the watershed (Figures 1, 5). For estuarine habitats, opportunity areas could include dredged holes or spoil disposal areas, either for enhancing existing subtidal habitats or creating areas that could be colonized by seagrasses. Some opportunities also exist on developed lands primarily through enhancement projects, although these have not been explicitly identified in the products herein. Examples include the construction of living shorelines in place of hardened seawalls, placement of submerged habitat modules along urban shorelines (e.g., artificial oyster reefs), and creation of backyard habitats. Tidal tributary restoration could also include removal of salinity barriers and filling of dredged channel sections. Overall, restoration practitioners must consider several options and choose those that are most feasible given the available resources and likelihood of success. Further, finer-scale land cover classification datasets are currently being investigated to refine identification of opportunity areas within the urbanized, developed landscape of the watershed.

Creative approaches may be required in areas affected by sea-level rise if land acquisition is not possible. These approaches are necessary to accommodate future landward migration of tidal wetlands or the protection of coastal uplands, while also reducing risks to build infrastructure that, when inappropriately sited, can inhibit landward habitat shifts. Coastal setbacks, buffers, or public easements are traditionally used to restrict development within a given distance from the shoreline. However, rolling easements may be an alternative approach whereby

TABLE 5 Recommended 2030 targets and 2050 goals for habitat restoration and protection in the Tampa Bay watershed.

Stratum	Habitat type	Current extent	Total restoration opportunity	2030 Target	2050 Goal	Target narrative and restoration and protection rationale
Subtidal						
	Hard bottom	171 ha	N/A	>171 ha	>171 ha	Protect existing hard bottom; continue to identify new hard bottom area through mapping
	Artificial reefs	88 ha	N/A	>88 ha	>88 ha	Protect existing artificial reefs; enhance habitat complexity where feasible; expand reef area to promote fish and wildlife benefits
	Tidal flats	6,569 ha	I/D	6,564 ha	6,564 ha	Identify and protect existing tidal flats; assess restoration potential of other non-vegetated subtidal areas
	Seagrasses	16,293 ha	5,719 ha	>16,188 ha	>16,188 ha	Protect existing seagrasses; assess restoration potential of non-vegetated subtidal areas
	Oyster bars	67 ha	I/D	87 ha	189 ha	2030: Protect existing oysters and restore 20 hectares; increase target by 20 hectares each decade
Intertidal						
	Living shorelines	18 km	N/A	34 km	90 km	2030: Construct 1.6 kilometers each year; better define opportunity areas; increase target to 2.4 and 3.2 kilometers per year for each decade
	Total intertidal	**8,340 ha**	**1,570 ha**	**8,745 ha**	**9,737 ha**	**2030: Protect existing intertidal mosaic and restore 405 hectares; increase target by 61 hectares each decade; includes the mosaic of mangrove, salt barren, and salt marsh habitats**
	Mangrove forests	6,276 ha	1,044 ha	>6,276 ha	>6,276 ha	Protect existing mangrove forests; restore opportunistically within the intertidal mosaic
	Salt barrens	203 ha		223 ha	324 ha	2030: Protect existing salt barrens and restore 20 hectares; increase target by 20 hectares each decade
	Salt marshes	1,861 ha	527 ha	1,962 ha	2,225 ha	2030: Protect existing low salinity salt marshes and restore 101 hectares; increase target by 20 hectares each decade
	Tidal tributaries	622 km	I/D	628 km	651 km	Inventory mapped tidal tributaries and identify restoration potential; restore 6.4 kilometers of urban tidal creek habitat where feasible; increase target by 3.2 kilometers each decade
Supratidal						
	Coastal uplands	1,446 ha	513 ha	1,507 ha	1,689 ha	2030: Protect existing coastal uplands and restore 61 hectares; increase target by 20 hectares each decade
	Non-forested freshwater wetlands	27,358 ha	63,705 ha	27,904 ha	29,058 ha	2030: Protect existing non-forested freshwater wetlands and restore 546 hectares; increase target by 20 hectares each decade
	Forested freshwater wetlands	61,667 ha		61,728 ha	61,910 ha	2030: Protect existing forested freshwater wetlands and restore 61 hectares; increase target by 20 hectares each decade
	Native uplands	57,836 ha	17,637 ha	58,018 ha	58,443 ha	2030: Protect existing native uplands and restore 182 hectares; increase target by 20 hectares each decade; focus on pine flatwoods and protect current extent

Targets and goals are based on 2017 land use data, 2018 subtidal data, best estimates for habitat types not in existing GIS layers, and current extent of existing and proposed conservation lands. Total restoration opportunity does not account for lands currently existing or proposed for conservation. N/A: not applicable, I/D: insufficient data.

protected areas are allowed to "roll" landward with expected changes in sea-level rise. Rolling easements could disincentivize more intense urban development of low-lying coastal uplands in less developed agricultural or recreational land uses. Landowners could maintain current economic uses with a rolling easement, while reserving such lands to accommodate future landward habitat migration. These approaches also offer risk-reduction to build infrastructure by offering increased protection from potential affects of sea-level rise and other coastal stressors (e.g., storm surge).

Finally, wetland impacts and associated compensatory mitigation projects authorized under wetland regulatory programs could serve as more directed restoration mechanisms to help achieve watershed-wide goals. Mitigation activities have historically been conducted independent of watershed-level planning and monitoring processes. This disconnect has contributed to fragmented implementation, marginal habitat function, and inconsistent compliance monitoring of mitigation projects, including historically poor documentation of wetland losses and gains in the Tampa Bay watershed. However, if properly focused and coordinated, compensatory mitigation activities could significantly contribute to the attainment of restoration targets and goals for the region.

4.3. Limitations of the approach

Identifying restoration priorities was data intensive and would not have been possible without the resources available for the region. The workflow for identifying priorities required detailed and spatially explicit datasets specific to the Tampa Bay watershed. Long-term datasets describing land use and cover and the extent of subtidal habitats were necessary to categorize current extent and past trends. Similarly, supporting datasets included those that described existing and proposed conservation areas, soils, past restoration activities, and relevant spatial boundaries (i.e., watershed and coastline). Many of these datasets are available outside of Tampa Bay, although temporal and spatial resolutions may limit application to other areas. Despite the region's data richness, limitations still exist in classifying restoration opportunities based on the spatial-scale of the LULC datasets. Additional refinements within the classified developed lands and coastal reservation space are currently being explored with 1-m scale national land cover datasets, which could expose additional opportunities in urban or suburban areas (e.g., improving stormwater infrastructure) or differential changes within native habitat classes (e.g., interspecific differences in mangrove colonization). Additionally, considerable effort was made in working with regional partners to identify and fill knowledge gaps for relevant habitat types. For example, inventories of hard bottom habitats, living shorelines, tidal tributaries, and artificial reefs were created through special studies or were available only as current estimates from regional entities. Tracking progress towards these habitat targets and goals is heavily reliant on regular updates to these datasets, as well as routine land use and cover map updates.

An additional assumption of the workflow, particularly for tracking progress, is that implemented restoration projects reported by partners will ultimately manifest into a classification within the map products. Specifically, restoration effort by regional partners is cataloged in the available restoration database, which not only depends on voluntary reporting, but also represents a source of information on restoration extent that is separate from land cover maps. An expectation is that the reported coverage restored by a partner will ultimately be shown as a change in land use and cover on regional maps. The temporal lag between an actual project and how it may be reflected in a GIS product is unknown, which may create a disconnect between the updates in achieving targets and goals as new data layers are released and the effort reported by partners becomes represented within the data layers. The spatial resolution of mapping products may also be insufficient to detect habitat changes as reported in the restoration database. For these reasons, projects reported by partners are currently summarized separately from the assessments above that depend on GIS layers. Additional work is needed to reconcile these datasets for more streamlined reporting.

5. Conclusion

The establishment of targets and goals that account for climate change, development trajectories, land availability, and past restoration effort expands the restoration opportunities to a more comprehensive list of habitats for the entire watershed. Land acquisition is critical for attaining the defined targets and goals and will also provide new opportunities for outdoor access to the broader community. Successful restoration is also contingent on engaging multiple partners, non-governmental organizations, and private citizens. The products created herein will guide these efforts for the next 30 years by providing a continuously updated assessment of where the opportunities exist and if targets and goals are expected to be met. The Tampa Bay region is not unique in the challenges resource managers face to protect and restore native habitats, and the approach described herein is readily transferable to other locations where restoration priorities are needed in response to pervasive coastal stressors.

Data availability statement

The datasets presented in this study can be found in online repositories. The names of the repository/repositories and accession number(s) can be found at: https://github.com/tbep-tech/hmpu-workflow, https://github.com/tbep-tech/hmpu-manu.

Author contributions

DR, JS, and CS contributed to original conception and design of the study, with guidance from all authors. MWB and JS performed the analyses. MWB and GR wrote the first draft of the manuscript with contributions from ES, MCB, and DT. MWB created the open source content. All authors contributed to the article and approved the submitted version.

Acknowledgments

The Technical Advisory Committee of the Tampa Bay Estuary Program reviewed drafts of the original reports that are the basis of this paper and their comments are immensely appreciated. We also recognize the extensive efforts of regional partners, of which there are too many to mention, for past restoration efforts in the Tampa Bay region that have contributed to native habitats. These efforts will be critical for continued success of restoration in the future. Substantial efforts by partners in creating and curating routine datasets for the region, especially by the Southwest Florida Water Management District and the Florida Natural Areas Inventory, are also gratefully recognized.

Conflict of interest

The authors declare that the research was conducted in the absence of any commercial or financial relationships that could be construed as a potential conflict of interest.

Publisher's note

Supplementary material

The Supplementary material for this article can be found online at: https://www.frontiersin.org/articles/10.3389/fevo.2023.1070266/full#supplementary-material

References

Allaire, J. J., Gandrud, C., Russell, K., and Yetman, C. (2017). networkD3: D3 JavaScript network graphs from R. Available at: https://CRAN.R-project.org/package=networkD3.

Ash, T., and Runnels, R. (2005). Hard bottom habitats: an overview of mapping and monitoring needs on epibenthic communities in Tampa Bay, Florida. in *Proceedings of the Tampa Bay Area Scientific Information Symposium (BASIS 4)*, ed. S. F. Treat (St. Petersburg, Florida: Tampa Bay Estuary Program), 179–182.

Ávila-García, D., Morató, J., Pérez-Maussán, A. I., Santillán-Carvantes, P., and Alvarado, J. (2020). Impacts of alternative land-use policies on water ecosystem services in the Rio Grande de Comitan-Lagos de Montebello watershed, Mexico. *Ecosyst. Serv.* 45:101179. doi: 10.1016/j.ecoser.2020.101179

Beck, M. W., Raulerson, G. E., and Sherwood, E. T. (2022). Tbep-tech/hmpu-workflow: v1.2.0. Zenodo. doi: 10.5281/zenodo.7032909

Benson, C. E., Carberry, B., and Langen, T. A. (2018). Public-private partnership wetland restoration programs benefit species of greatest conservation need and other wetland-associated wildlife. *Wetl. Ecol. Manag.* 26, 195–211. doi: 10.1007/s11273-017-9565-8

Bertness, M. D. (1985). Fiddler crab regulation of *Spartina alterniflora* production on a New England salt marsh. *Ecology* 66, 1042–1055. doi: 10.2307/1940564

Brinson, M. M., Christian, R. R., and Blum, L. K. (1995). Multiple states in the sea-level induced transition from terrestrial forest to estuary. *Estuaries* 18, 648–659. doi: 10.2307/1352383

Burke, M., Carnahan, L., Hammer-Levy, K., and Mitchum, G. (2019). *Recommended projections of sea level rise for the Tampa Bay region (update)*. Tampa Bay Estuary Program: St. Petersburg, Florida.

Calil, J., Beck, M. W., Gleason, M., Merrifield, M., Klausmeyer, K., and Newkirk, S. (2015). Aligning natural resource conservation and flood hazard mitigation in California. *PLoS One* 10:e0132651. doi: 10.1371/journal.pone.0132651

Cavanaugh, K. C., Dangremond, E. M., Doughty, C. L., Williams, A. P., Parker, J. D., Hayes, M. A., et al. (2019). Climate-driven regime shifts in a mangrove-salt marsh ecotone over the past 250 years. *Proceedings of the National Academy of Sciences* 116, 21602–21608. doi: 10.1073/pnas.1902181116

Cavanaugh, K. C., Kellner, J. R., Forde, A. J., Gruner, D. S., Parker, J. D., Rodriguez, W., et al. (2014). Poleward expansion of mangroves is a threshold response to decreased frequency of extreme cold events. *Proceedings of the National Academy of Sciences* 111, 723–727. doi: 10.1073/pnas.1315800111

Chung, M. G., Dietz, T., and Liu, J. (2018). Global relationships between biodiversity and nature-based tourism in protected areas. *Ecosyst. Serv.* 34, 11–23. doi: 10.1016/j.ecoser.2018.09.004

Cicchetti, G., and Greening, H. (2011). Estuarine biotope mosaics and habitat management goals: an application in Tampa Bay, FL, USA. *Estuar. Coasts* 34, 1278–1292. doi: 10.1007/s12237-011-9408-4

Coen, L. D., Brumbaugh, R. D., Bushek, D., Grizzle, R., Luckenbach, M. W., Posey, M. H., et al. (2007). Ecosystem services related to oyster restoration. *Mar. Ecol. Prog. Ser.* 341, 303–307. doi: 10.3354/meps341303

Comeaux, R. S., Allison, M. A., and Bianchi, T. S. (2012). Mangrove expansion in the Gulf of Mexico with climate change: implications for wetland health and resistance to rising sea levels. *Estuar. Coast. Shelf Sci.* 96, 81–95. doi: 10.1016/j.ecss.2011.10.003

Conner, W. H., Doyle, T. W., and Krauss, K. W. (2007). *Ecology of tidal freshwater forested wetlands of the southeastern United States*. Dordrecht, Netherlands: Springer.

CSA Ocean Sciences. (2019). *Tampa Bay hard bottom mapping project*. Tampa Bay Estuary Program, St. Petersburg, Florida.

Dontis, E. E., Radabaugh, K. R., Chappel, A. R., Russo, C. E., and Moyer, R. P. (2020). Carbon storage increases with site age as created salt marshes transition to mangrove forests in Tampa Bay, Florida (USA). *Estuar. Coasts* 43, 1470–1488. doi: 10.1007/s12237-020-00733-0

Duarte, C. M., Conley, D. J., Carstensen, J., and Sánchez-Camacho, M. (2009). Return to Neverland: shifting baselines affect eutrophication restoration targets. *Estuar. Coasts* 32, 29–36. doi: 10.1007/s12237-008-9111-2

Dupont, J. M. (2008). Artificial reefs as restoration tools: a case study on the West Florida shelf. *Coast. Manag.* 36, 495–507. doi: 10.1080/08920750802395558

Eisma, D. (1998). *Intertidal deposits: River mouths, tidal flats, and coastal lagoons*. London: CRC Press.

Elliott, M., Burdon, D., Hemingway, K. L., and Apitz, S. E. (2007). Estuarine, coastal and marine ecosystem restoration: confusing management and science–a revision of concepts. *Estuar. Coast. Shelf Sci.* 74, 349–366. doi: 10.1016/j.ecss.2007.05.034

Environmental Protection Agency (1996). Watershed approach framework. *Office of Water* 4501F. 15.

Ermgassen, P. S. E., Spalding, M. D., and Grizzle, R. E. (2013). Quantifying the loss of a marine ecosystem service: filtration by the eastern oyster in U.S. estuaries. *Estuar. Coasts* 36, 36–43. doi: 10.1007/s12237-012-9559-y

Florida Department of Transportation. (1999). *Florida land use, cover and forms classification system*. *Third*, Tallahassee, Florida: FDOT Surveying and Mapping Office Geographic Mapping Section.

Florida Natural Areas Inventory. (2020). Florida Conservation Lands (FLMA) GIS Dataset, March 2020. Available at: https://www.fnai.org/publications/gis-data.

Gann, G. D., McDonald, T., Walder, B., Aronson, J., Nelson, C. R., Jonson, J., et al. (2019). International principles and standards for the practice of ecological restoration, 2nd. *Restor. Ecol.* 27, S1–S46. doi: 10.1111/rec.13035

Greening, H., Janicki, A., Sherwood, E., Pribble, R., and Johansson, J. O. R. (2014). Ecosystem responses to long-term nutrient management in an urban estuary: Tampa Bay, Florida, USA. *Estuar. Coast. Shelf Sci.* 151, A1–A16. doi: 10.1016/j.ecss.2014.10.003

Gregory, R., Ohlson, D., and Arvai, J. (2006). Deconstructing adaptive management criteria for applications to environmental management. *Ecol. Appl.* 16, 2411–2425. doi: 10.1890/1051-0761(2006)016[2411:DAMCFA]2.0.CO;2

Heck, K., Hays, G., and Orth, R. (2003). Critical evaluation of the nursery role hypothesis for seagrass meadows. *Mar. Ecol. Prog. Ser.* 253, 123–136. doi: 10.3354/meps253123

Henningsen, B. (2005). The maturation and future of habitat restoration programs for the Tampa Bay estuarine ecosystem. In *proceedings of the Tampa Bay Area scientific information symposium (BASIS 4)*, ed. S. F. Treat (St. Petersburg, FL: Tampa bay Estuary Program), 165–170.

Holl, K. D., and Howarth, R. B. (2001). Paying for restoration. *Restor. Ecol.* 8, 260–267. doi: 10.1046/j.1526-100x.2000.80037.x

Holling, C. S. (1978). *Adaptive environmental assessment and management*. Chichester, UK: John Wiley & Sons.

Houde, E. D., and Rutherford, E. S. (1993). Recent trends in estuarine fisheries: predictions of fish production and yield. *Estuaries* 16, 161–176. doi: 10.2307/1352488

Hsieh, Y. P. (2004). "Dynamics of tidal salt barren formation and the record of present-day sea level change" in *The ecogeomorphology of tidal marshes*. eds. S. Fagherazzi, M. Marani and L. Blum (Washington: American Geophysical Union), 231–245.

Jaap, W. C., and Hallock, P. (1990). "Coral reefs" in *Ecosystems of Florida*. eds. R. L. Myers and J. J. Ewel (Orlando, Florida, USA: University of Central Florida Press), 574–618.

Jones, P. H., Larson, B. C., and Clark, M. W. (2009). Reduced impact development practices at "restoration." in *American Institute of Physics Conference Proceedings* (American Institute of Physics), 151–161.

Kaufman, K. (2017). *Tampa Bay environmental restoration fund final report: Hard bottom mapping and characterization for restoration planning in Tampa Bay*. Tampa Bay Estuary Program, St. Petersburg, Florida.

Kawula, R., and Redner, J. (2018). "Florida land cover classification system," in *Center for Spatial Analysis, fish and Widlife research institute, Florida fish and wildlife conservation commission*. (Tallahassee, Florida: Center for Spatial Analysis, Fish and Widlife Research Institute, Florida Fish and Wildlife Conservation).

Kushlan, J. A. (1990). "Freshwater marshes," in *Ecosystems of Florida*. eds. R. L. Myers and J. J. Ewel (Orlando, Florida: University of Central Florida Press), 324–363.

Lewis, R. R., and Robison, D. E. (1996). *Setting priorities for Tampa Bay habitat protection and restoration: Restoring the balance*. Tampa Bay Estuary Program, St. Petersburg, Florida.

Lopez, C. B., Karim, A., Murasko, S., Marot, M., Smith, C. G., and Corcoran, A. A. (2019). Temperature mediates secondary dormancy in resting cysts of *Pyrodinium bahamense* (Dinophyceae). *J. Phycol.* 55, 924–935. doi: 10.1111/jpy.12883

Lowndes, J. S. S., Best, B. D., Scarborough, C., Afflerbach, J. C., Frazier, M. R., O'Hara, C. C., et al. (2017). Our path to better science in less time using open data science tools. *Nature Ecol. Evol.* 1, 1–7. doi: 10.1038/s41559-017-0160

Menéndez, P., Losada, I. J., Beck, M. W., Torres-Ortega, S., Espejo, A., Narayan, S., et al. (2018). Valuing the protection services of mangroves at national scale: the Philippines. *Ecosyst. Serv.* 34, 24–36. doi: 10.1016/j.ecoser.2018.09.005

Meyers, R. L., and Ewel, J. J. (1990). *Ecosystems of Florida*. Orlando, Florida: University of Central Florida Press.

Mohamed, R. (2006). The economics of conservation subdivisions: Price premiums, improvement costs, and absorption rates. *Urban Aff. Rev.* 41, 376–399. doi: 10.1177/1078087405282183

Moore, H. B., Davies, L. T., Fraser, T. H., Gore, R. H., and López, N. R. (1968). Some biomass figures from a tidal flat in Biscayne Bay, Florida. *Bull. Mar. Sci.* 18, 261–279.

National Oceanic and Atmospheric Administration. (2015). *Guidance for considering the use of living shorelines, final guidance document prepared by the NOAA living shorelines workgroup*. Silver Spring, Maryland: National Oceanic and Atmospheric Administration.

Odum, W. E., and McIvor, C. C. (1990). "Mangroves," in *Ecosystems of Florida*. eds. R. L. Myers and J. J. Ewel (Orlando, Florida: University of Central Florida Press), 517–548.

Osland, M. J., Hughes, A. R., Armitage, A. R., Scyphers, S. B., Cebrian, J., Swinea, S. H., et al. (2022). The impacts of mangrove range expansion on wetland ecosystem services in the southeastern United States: current understanding, knowledge gaps, and emerging research needs. *Glob. Chang. Biol.* 28, 3163–3187. doi: 10.1111/gcb.16111

Osland, M. J., Spivak, A. C., Nestlerode, J. A., Lessmann, J. M., Almario, A. E., Heitmuller, P. T., et al. (2012). Ecosystem development after mangrove wetland creation: plant-soil change across a 20-year chronosequence. *Ecosystems* 15, 848–866. doi: 10.1007/s10021-012-9551-1

Palmer, M. A. (2009). Reforming watershed restoration: science in need of application and applications in need of science. *Estuar. Coasts* 32, 1–17. doi: 10.1007/s12237-008-9129-5

Pebesma, E. (2018). Simple features for R: standardized support for spatial vector data. *R J.* 10, 439–446. doi: 10.32614/RJ-2018-009

R Core Team. (2022). *R: A language and environment for statistical computing*. Vienna, Austria: R Foundation for Statistical Computing.

Raabe, E., Roy, L. C., and McIvor, C. (2012). Tampa Bay coastal wetlands: nineteenth to twentieth century tidal marsh-to-mangrove conversion. *Estuar. Coasts* 35, 1145–1162. doi: 10.1007/s12237-012-9503-1

Rayer, S., and Wang, Y. (2020). Projections of Florida population by county, 2020-2045, with estimates for 2019. *Florida Population Stud.* 53:186.

Restore America's Estuaries. (2015). *Living shorelines: From barriers to opportunities*. Arlington, Virginia: Restore America's Estuaries.

Ries, T., and Scheda, S. (2014). *Master plan for the protection and restoration of freshwater wetlands in the Tampa Bay watershed, Florida*. Tampa Bay Estuary Program, St. Petersburg, Florida.

Robison, D. E. (2010). *Tampa bay Estuary Program habitat master plan update*. Tampa Bay Estuary Program, Saint Petersburg, Florida.

Robison, D., Ries, T., Saarinen, J., Tomasko, D., and Sciarrino, C. (2020). *Tampa bay estuary program: 2020 habitat master plan update*. Tampa Bay Estuary Program, St. Petersburg, Florida.

Russell, M., and Greening, H. (2015). Estimating benefits in a recovering estuary: Tampa Bay, Florida. *Estuar. Coasts* 38, 9–18. doi: 10.1007/s12237-013-9662-8

Sheehan, L., Sherwood, E. T., Moyer, R. P., Radabaugh, K. R., and Simpson, S. (2019). Blue carbon: an additional driver for restoring and preserving ecological services of coastal wetlands in Tampa Bay (Florida, USA). *Wetlands* 39, 1317–1328. doi: 10.1007/s13157-019-01137-y

Sherwood, E. (2008). *Tampa Bay tidal tributary habitat initiative: Integrated summary document, Tampa Bay Estuary Program tidal tributaries project team*. Tampa Bay Estuary Program, St. Petersburg, Florida.

Sherwood, E., Greening, H., Johansson, J. O. R., Kaufman, K., and Raulerson, G. (2017). Tampa Bay (Florida, USA): documenting seagrass recovery since the 1980's and reviewing the benefits. *Southeast. Geogr.* 57, 294–319. doi: 10.1353/sgo.2017.0026

Smith, C. S., Puckett, B., Gittman, R. K., and Peterson, C. H. (2018). Living shorelines enhanced the resilience of saltmarshes to hurricane Matthew (2016). *Ecol. Appl.* 28, 871–877. doi: 10.1002/eap.1722

Southwest Florida Water Management District. (2014). Photo interpretation key for land use classification. Available at: https://www31.swfwmd.state.fl.us/Documents/Photo_Interpretation_Key_2014.pdf.

Southwest Florida Water Management District. (2018). Land use land cover data. c1990-2017. Available at: https://data-swfwmd.opendata.arcgis.com/.

Southwest Florida Water Management District. (2019). Seagrass in 2018. Available at: https://data-swfwmd.opendata.arcgis.com/datasets/seagrass-in-2018.

Sprandel, J. A., Gore, D., and Cobb, T. (2000). Distribution of wintering shorebirds in coastal Florida. *J. Field Ornithol.* 71, 708–720. doi: 10.1648/0273-8570-71.4.708

Stockmann, U., Minasny, B., and McBratney, A. B. (2014). How fast does soil grow? *Geoderma* 216, 48–61. doi: 10.1016/j.geoderma.2013.10.007

Titus, J. G., Hudgens, D. E., Trescott, D. L., Craghan, M., Nuckols, W. H., Hershner, C. H., et al. (2009). State and local governments plan for development of most land vulnerable to rising sea level along the US Atlantic coast. *Environ. Res. Lett.* 4:044008. doi: 10.1088/1748-9326/4/4/044008

Tomasko, D., Alderson, M., Burnes, R., Hecker, J., Iadevaia, N., Leverone, J., et al. (2020). The effects of hurricane Irma on seagrass meadows in previously eutrophic estuaries in Southwest Florida (USA). *Mar. Pollut. Bull.* 156:111247. doi: 10.1016/j.marpolbul.2020.111247

Vogelmann, J. E., Xian, G., Homera, C., and Tolk, B. (2012). Monitoring gradual ecosystem change using Landsat time series analyses: case studies in selected forest and rangeland ecosystems. *Remote Sens. Environ.* 122, 92–105. doi: 10.1016/j.rse.2011.06.027

Wessel, M. R., Leverone, J. R., Beck, M. W., Sherwood, E. T., Hecker, J., West, S., et al. (2022). Developing a water quality assessment framework for Southwest Florida tidal creeks. *Estuar. Coasts* 45, 17–37. doi: 10.1007/s12237-021-00974-7

White, E., and Kaplan, D. (2017). Restore or retreat? Saltwater intrusion and water management in coastal wetlands. *Ecosystem Health Sustain.* 3:e01258. doi: 10.1002/ehs2.1258

Wickham, H., Averick, M., Bryan, J., Chang, W., McGowan, L. D., François, R., et al. (2019). Welcome to the tidyverse. *J. Open Source Software* 4:1686. doi: 10.21105/joss.01686

Yoskowitz, D., and Russell, M. (2015). Human dimensions of our estuaries and coasts. *Estuar. Coasts* 38, 1–8. doi: 10.1007/s12237-014-9926-y

frontiers | Frontiers in Ecology and Evolution

TYPE Original Research
PUBLISHED 13 February 2023
DOI 10.3389/fevo.2023.1096880

OPEN ACCESS

EDITED BY
Marcus W. Beck,
Tampa Bay Estuary Program, United States

REVIEWED BY
Laura Bretherton,
Dalhousie University, Canada
Colin J. Brislawn,
Contamination Source Identification,
United States

*CORRESPONDENCE
Wade H. Jeffrey
✉ wjeffrey@uwf.edu

†PRESENT ADDRESS
Melissa L. Brock,
Department of Ecology and Evolutionary Biology, University of California, Irvine, Irvine, CA, United States
Melissa Ederington-Hagy,
Department of Earth and Environment, Boston University, Boston, MA, United States
Lisa Nigro,
Microbial Analysis, Resources and Services, Center for Open Research Resources and Equipment, University of Connecticut, Storrs, CT, United States

SPECIALTY SECTION
This article was submitted to Biogeography and Macroecology, a section of the journal Frontiers in Ecology and Evolution

RECEIVED 12 November 2022
ACCEPTED 23 January 2023
PUBLISHED 13 February 2023

CITATION
Brock ML, Richardson R, Ederington-Hagy M, Nigro L, Snyder RA and Jeffrey WH (2023) Temporal variability of microbial response to crude oil exposure in the northern Gulf of Mexico.
Front. Ecol. Evol. 11:1096880.
doi: 10.3389/fevo.2023.1096880

Temporal variability of microbial response to crude oil exposure in the northern Gulf of Mexico

Melissa L. Brock[1†], Rachel Richardson[1], Melissa Ederington-Hagy[1†], Lisa Nigro[1†], Richard A. Snyder[2] and Wade H. Jeffrey[1*]

[1]Center for Environmental Diagnostics and Bioremediation, University of West Florida, Pensacola, FL, United States, [2]Virginia Institute of Marine Science Eastern Shore Laboratory, College of William & Mary, Wachapreague, VA, United States

Oil spills are common occurrences in the United States and can result in extensive ecological damage. The 2010 *Deepwater Horizon* oil spill in the Gulf of Mexico was the largest accidental spill recorded. Many studies were performed in deep water habitats to understand the microbial response to the released crude oil. However, much less is known about how planktonic coastal communities respond to oil spills and whether that response might vary over the course of the year. Understanding this temporal variability would lend additional insight into how coastal Florida habitats may have responded to the *Deepwater Horizon* oil spill. To assess this, the temporal response of planktonic coastal microbial communities to acute crude oil exposure was examined from September 2015 to September 2016 using seawater samples collected from Pensacola Beach, Florida, at 2-week intervals. A standard oil exposure protocol was performed using water accommodated fractions made from MC252 surrogate oil under photo-oxidizing conditions. Dose response curves for bacterial production and primary production were constructed from ^{3}H-leucine incorporation and ^{14}C-bicarbonate fixation, respectively. To assess drivers of temporal patterns in inhibition, a suite of biological and environmental parameters was measured including bacterial counts, chlorophyll *a*, temperature, salinity, and nutrients. Additionally, 16S rRNA sequencing was performed on unamended seawater to determine if temporal variation in the *in situ* bacterial community contributed to differences in inhibition. We observed that there is temporal variation in the inhibition of primary and bacterial production due to acute crude oil exposure. We also identified significant relationships of inhibition with environmental and biological parameters that quantitatively demonstrated that exposure to water-soluble crude oil constituents was most detrimental to planktonic microbial communities when temperature was high, when there were low inputs of total Kjeldahl nitrogen, and when there was low bacterial diversity or low phytoplankton biomass.

KEYWORDS

oil spill, coastal environment, marine microbes, temporal response, primary production, secondary production

1. Introduction

Oil spills are common occurrences in waterways of the United States. From 2000 to 2019, an average of 3,871 spills occurred each year resulting in an average of 1,233,863 gallons of oil released per year (Ramseur and Resources, Science, and Industry Division, 2017). Depending on the location and severity of the spill, extensive economic and ecological destruction may result. The 2010 *Deepwater Horizon* (*DWH*) oil spill in the Gulf of Mexico is the largest accidental oil spill recorded. The *DWH* oil platform suffered a catastrophic blowout on 20 April 2010 that began releasing crude oil at a subsurface depth of 1,500 m until the well was capped 84 days later on 15 July 2010 (McNutt et al., 2012). The *DWH* spill released 4.9 million barrels of crude oil ∼80 km offshore (McNutt et al., 2012). An estimated 60% of the subsurface oil reached the sea surface where hydrodynamic forces then affected its distribution (Ziervogel et al., 2012). A portion of the *DWH* oil (<15%) reached the shoreline (Beyer et al., 2016) where it contaminated 1,773 km of shoreline with 847 km of shoreline oiling persisting after 1 year (Michel et al., 2013).

Coastal habitats are environmentally and economically critical for the region (Mendelssohn et al., 2012; Wiesenburg et al., 2021), yet the impact of the *DWH* spill on planktonic microbial communities in coastal waters was not studied nearly as extensively as coastal sediments (Kostka et al., 2011; Bik et al., 2012; King et al., 2015; Huettel et al., 2018) and offshore environments (Joye et al., 2014). It has been hypothesized that natural oil seeps in the Gulf of Mexico "pre-primed" microbial communities for oil degradation (Atlas and Hazen, 2011; Hazen et al., 2016; Liu et al., 2017), but the toxic effects of these seeps are spatially limited as opposed to a massive spill. Exposure to crude oil released by *DWH* reduced microbial diversity and altered community structure from the surface ocean to the seafloor in offshore environments (Hazen et al., 2010; Valentine et al., 2010; Kessler et al., 2011). However, the impact of *DWH* oil on planktonic coastal microbial communities may be more complex due to the variable extent of weathering that the crude oil underwent before reaching coastal environments. As crude oil was transported, its physical and chemical properties changed due to evaporation, emulsification, dissolution, photo-oxidation, and microbial degradation (Mendelssohn et al., 2012; Farrington et al., 2021). Dissolution of crude oil releases highly toxic compounds such as low-molecular-weight aliphatic compounds, aromatic hydrocarbons, and PAHs into the surrounding seawater (Abbriano et al., 2011). This solution of water-soluble petroleum compounds is termed the water accommodated fraction (WAF). Compounds in the WAF have variable effects on phytoplankton growth with low PAH concentrations (1 mg L^{-1}) observed to stimulate growth while high PAH concentrations (100 mg L^{-1}) inhibited growth (Harrison et al., 1986). Additionally, photo-oxidation of crude oil degrades large, aromatic hydrocarbons, and produces water-soluble oxidized species which facilitate biodegradation but may also increase the toxicity of the surrounding seawater (King et al., 2015; Beyer et al., 2016). Thus, weathered crude oil is a dynamic substance which may have variable impacts on planktonic coastal microbes.

Weathering of crude oil is also influenced by nutrient availability and by physicochemical parameters, such as temperature, indicating that the location (e.g., eutrophic versus oligotrophic waters) and the timing (e.g., winter versus summer) of an oil spill plays a large role on its impact. Nutrient availability, specifically N and P, controls the rate of hydrocarbon degradation in the environment (Atlas and Bartha, 1972; Head et al., 2006). Because WAFs have high C content, their mineralization results in little regenerated nitrogen or phosphorus which hinders further microbial production (Mendelssohn et al., 2012). This effect may be more severe in environments with low inorganic nutrient concentrations, such as oligotrophic waters. Additionally, high temperature has consistently been shown to influence crude oil physicochemical properties by reducing viscosity which increases bioavailability and degradation rates (Wright et al., 1997; Coulon et al., 2007; King et al., 2015). Higher temperatures (24°C) increased the bioavailability of water-soluble components and increased the degradation of total petroleum hydrocarbons compared to lower temperatures (4°C) (Coulon et al., 2007). Following the *DWH* spill, temperature was suggested to be a significant determinant in structuring microbial communities and in selecting for oil degraders within deep waters, surface waters, and oil mousses (Redmond and Valentine, 2012; Liu and Liu, 2013). However, crude oil is highly toxic to many members within these microbial communities (Parsons et al., 2015; Doyle et al., 2018; Kamalanathan et al., 2021). In microcosm and mesocosm experiments, exposure to crude oil drastically changed the community structure (Doyle et al., 2018) and reduced the relative abundance of bacteria that were initially abundant (Doyle et al., 2018; Kamalanathan et al., 2021). Additionally, in an incubation experiment, Cyanobacteria initially dominated the *in situ* surface community (60.4% relative abundance). After incubation with crude oil, there was a large reduction in Cyanobacteria abundance (10–30% relative abundance) at low temperature (4°C), and under high temperature (24°C) Cyanobacteria were almost eliminated (Liu et al., 2017). Therefore, under low nutrient availability and high temperature conditions, an oil spill may reduce microbial growth. It remains unknown how weathered crude oil components (i.e., WAF), temperature, and nutrients interact across seasons and how those interactions affect microbial growth.

Here, we ask the following questions: (1) Is there a temporal response of planktonic coastal microbes to WAF? and; (2) What are the environmental drivers of this temporal response? We hypothesized that there is a temporal response that is primarily driven by variations in temperature and inorganic nutrient availability. Thus, we expected highest inhibition of primary production and bacterial production under high temperatures and low inorganic nutrient concentrations. To test these hypotheses, we developed a standard WAF exposure assay and measured inhibition of primary and bacterial production in bi-weekly seawater samples collected over a year from coastal Northwest Florida waters. Understanding temporal variability in the microbial response to crude oil contamination will provide additional insight into the ecological response to *DWH* within Florida waters.

2. Materials and methods

2.1. Sample overview

Surface seawater samples were collected bi-weekly for 1 year (09/2015 to 09/2016; $n = 26$) from the end of the Pensacola Beach pier (30° 19.640′ N, 87° 08.514′W) which extends approximately 0.3 km into the Northwestern Gulf of Mexico. Samples were transported at *in situ* temperatures in the dark to the laboratory. Samples were classified into seasons based on the astronomical calendar as follows:

fall was defined as September 23rd – December 20th, winter was defined as December 21st – March 18th, spring was defined as March 19th – June 19th, and summer was defined as June 20th – September 21st.

2.2. Analytics and laboratory techniques

In situ seawater temperature, salinity, NO_3^- + NO_2^- concentrations, NH_3 concentrations, total Kjeldahl nitrogen (TKN) concentrations, orthophosphate concentrations, and total phosphorus (TP) concentrations were measured for each water sample (**Table 1**). NO_3^- + NO_2^- and orthophosphate concentrations were measured on a Lachat QuickChem 8500 using EPA standard method 353.2 (1993) for NO_3^- + NO_2^- concentrations and 365.1 (Kopp, 1979) for orthophosphate concentrations. NH_3, TKN, and TP concentrations were measured using EPA standard method 350.1 (1993), EPA standard method 351.2 (1993), and EPA standard method 365.4 (1974), respectively.

Samples for bacterial counts were preserved with 0.2 μm filtered, buffered formalin. Preserved samples were stained with 4′,6-diamidino-2-phenylindole, dihydrochloride (DAPI) using the method of Porter and Feig (1980) and counted using an epifluorescence microscope. Samples for chlorophyll *a* concentrations were filtered (200 mL) onto 25 mm GF/F filters in triplicate, extracted in 90% acetone overnight, and measured fluorometrically (Turner Trilogy Laboratory Fluorometer) using a standard curve (Welschmeyer, 1994).

Aged Gulf of Mexico seawater (collected ∼40 km offshore Pensacola, FL and >3 years old) was filtered using a 0.2 μm pore-size polycarbonate filter (Millipore). Twenty-five milliliter of filtered seawater was aliquoted into 35 mL Teflon bottles (Nalgene FEP). Bottles containing filtered seawater were pasteurized at 70°C for 2–4 h. Once cooled, pasteurized seawater was amended with surrogate crude oil (Pelz et al., 2011) to contain a final volume of 2% crude oil. Bottles were incubated in a 20°C temperature-controlled water table (Fisherbrand, Isotemp 4100) under full solar exposure for 5 days during the summer on the roof of the Environmental Sciences building at the University of West Florida (Vaughan et al., 2016). Bottles were shaken twice per day and returned to the water table. Samples were pooled into a separatory funnel, and the aqueous fraction (i.e., the WAF) was collected and transferred to 20 mL scintillation vials in 10 mL aliquots and stored frozen at −20°C. Here, we make the assumption that because we used filtered, pasteurized aged seawater, any organic carbons in the seawater were dissolved hydrocarbons. Therefore, total organic carbon (TOC) was used as a proxy for hydrocarbon concentrations. TOC concentrations of the WAF were determined as non-purgeable organic carbon with a Shimadzu TPC-VVSN Analyzer using standard method 5310 (2018). WAFs contained an average TOC concentration of 68.9 ppm (SD = 1.1, n = 4). Fractions were thawed prior to each sensitivity assay. In this way, each bi-weekly water sample was exposed to the same WAF for the duration of the project.

Bacterial production was estimated through incorporation of ^{3}H-leucine. The standard WAF exposure consisted of a dose response curve of 0, 0.5, 1, 2.5, 5, and 10% v/v WAF (final concentration amended to the seawater sample) for each time point. WAF was aliquoted into 4 replicate 5 mL polystyrene snap-cap tubes for each treatment. Four replicate controls received 100 μL of filtered seawater (0.2 μm pore size syringe filter). Seawater was amended with ^{3}H-leucine (52.9 Ci mmol^{-1} PerkinElmer, Bridgeport, CT, USA) to a final concentration of 10 nM; 3.1 mL of labeled seawater was added to each tube. Samples were capped, mixed, and incubated in the dark at *in situ* temperature for 4 h. To terminate leucine incorporation, triplicate 1.0 mL subsamples were removed from each snap cap tube and placed into 2 mL microfuge tubes containing 50 μL of 100% trichloroacetic acid. Samples were processed following the procedure of Smith and Azam (1992). Liquid scintillation counting using a Packard Tri-Carb 2900 was performed to determine ^{3}H-leucine incorporation in samples.

Primary production was determined through the fixation of ^{14}C-bicarbonate under increasing light exposures (PI curves) (Matrai et al., 1995) using a modified photosynthetron. Triplicate dose response curves of 0, 0.5, 1, 2.5, 5, and 10% WAF treatment were generated for each time point. WAF and 33 mL of seawater were aliquoted into 50 mL conical centrifuge tubes for each treatment which were then amended with ^{14}C-bicarbonate (2 μCi/mL). Triplicate controls received 1 mL of filtered seawater (0.2 μm pore size syringe filter) and 33 mL of seawater that were then amended with ^{14}C-bicarbonate. Each treatment was aliquoted into eight, 4 mL snap cap tubes that were incubated at *in situ* temperature for 4 h in a photosynthesis irradiance incubator. The photosynthetically active radiation of each position was measured with a quantum scalar laboratory radiometer (Biospherical Instruments Inc.) and recorded. Irradiances for the eight positions were ∼180, 90, 50, 30, 20, 15, 10, and 7 μE cm^{-2} for each treatment and time point. Lower irradiances were used to maximize the number of points within the linear part of the curve for calculating inhibition of primary production (see below). Fixed ^{14}C was determined after overnight acidification of the samples *via* liquid scintillation counting using a Packard Tri-Carb 2900. Photosynthetic efficiency was determined as described by Matrai et al. (1995).

Bacterial production inhibition and primary production inhibition were determined using dose response curves (0, 0.5, 1, 2.5, 5, and 10% WAF). For bacterial production inhibition, the average disintegrations per minute (DPM) of each treatment replicate were expressed as a percent of the average DPM of the control (0% WAF). The percent control was log-transformed, and a linear regression of the log-transformed percent of the control versus percent WAF concentration was performed in Excel. The positive slope of the regression for each experiment was then used as a quantitative value for degree of inhibition and is referred to as "bacterial production inhibition" throughout. For primary production inhibition, PI curves were constructed for each control and each treatment replicate. Linear regressions were performed on the linear part of the curve in Kaleidagraph. The slope of each treatment replicate was expressed as a percent of the average slope of the control. The percent control was log-transformed, and a linear regression of the log-transformed percent of the control versus percent WAF concentration was performed in Excel. The positive slope of the regression for each experiment was then used as a quantitative value for degree of inhibition and is referred to as "primary production inhibition" throughout. The standard error of the regression slopes was obtained from Kaleidagraph and was used to assess the uncertainty in bacterial production inhibition and

primary production inhibition. Raw data and example calculations are available on GitHub.[1]

2.3. DNA extraction and 16S rRNA amplicon sequencing

To determine how temporal variation in the background bacterial community contributed to temporal changes in the inhibition of bacterial production, samples for DNA extraction were collected bi-weekly. Samples were collected by filtering 2 L of seawater through three 0.22 μm GPWP (MilliporeSigma) filters. Samples were stored at −80°C until further processing. Half of each previously frozen filter and 250 μL of extraction buffer (Milli-Q water, 5 mM EDTA, 25 mM Tris, and 50 mM glucose) were added to tubes containing a mixture of 0.1 mm silica and 0.5 mm glass beads. Filters were ground using a sterile plastic pestle and were homogenized for two 1-min cycles at 2,000 rpm. Samples were cooled to −80°C, heated to 80°C for 10 min, cooled to −80°C again, and then brought to room temperature. Lysozyme (final concentration = 1.5 mg mL^{-1}) was added to each sample, and samples were incubated for 90 min at 37°C. Proteinase K (final concentration = 3 mg mL^{-1}) was added to each sample, and samples were incubated for 90 min at 50°C. Sodium chloride (final concentration = 0.5 M) and M1 buffer from the Omega E.Z.N.A. Mollusc DNA Kit were added to each sample. The Omega E.Z.N.A. Mollusc DNA Kit was used to wash and collect purified DNA. Extracted DNA was quantified using a NanoDrop spectrophotometer and were stored at −20°C. DNA extracts were sent to the University of Illinois at Chicago's Sequencing Core for amplification and sequencing. The V4–V5 region of the 16S rRNA gene was amplified using the 515F/926R universal primers (Needham and Fuhrman, 2016). Amplicons were pair-end sequenced (2 ×300) with the MiSeq Illumina platform. Sequence files are available at the NCBI Sequence Read Archive under BioProject ID: PRJNA894536. Accession numbers for each sample are reported in **Supplementary Table 1**.

2.4. Data analysis and statistics

Forward and reverse primers were removed using cutadapt (Martin, 2011) in QIIME2 (Bolyen et al., 2019). Forward and reverse reads were quality filtered with fastq-mcf (Aronesty, 2013). A window-size of 10 was used to calculate mean quality score. Reads were truncated when the mean quality score was less than 20. After trimming, reads that were shorter than the minimum length threshold of 150 bp were removed. Reads that contained N-calls were also removed. Forward and reverse reads were merged based on a minimum overlap threshold of 10 bp, minimum merge length threshold of 350 bp, and number of maximum differences of 5 bp allowed in the overlapping region using usearch (Edgar, 2010). Final trimming, quality filtering, clustering of amplicons, and removal of chimeras was performed using DADA2 (Callahan et al., 2016) in QIIME2. The merged reads were trimmed to a length threshold of 365 bp to maintain alignment. Reads that matched to the PhiX genome or that contained more than 3 expected errors were removed. The error model was trained using a minimum of 800,000 reads. Samples were then dereplicated, reads were clustered into amplicon sequence variants (ASVs), and chimeric ASVs were removed using a consensus procedure. QIIME2 artifacts generated from this bioinformatics workflow are available on GitHub[2] and the contents of each artifact are described in **Supplementary Table 2**.

Taxonomic, diversity, and statistical analyses were performed in R (version 3.5.1) (R Core Team, 2018). All R code is available on GitHub.[3] All colors used in figures were checked for accessibility using Adobe Color's "Color Blind Safe" Accessibility Tool. Taxonomy was assigned ("assignTaxonomy" function; dada2 package; Callahan et al., 2016) using RDP's Naïve Bayesian classifier (Wang et al., 2007) and the SILVA 138 reference database (Quast et al., 2012). ASVs matching to eukaryotes, archaea, or that were unassigned at the bacterial Kingdom or Phylum level were removed from subsequent taxonomy and diversity analyses. Temporal trends in the 25 most abundant genera were examined across the time series. Counts of all genera in each sample are available in **Supplementary Table 3**.

For alpha-diversity analyses, sequencing depth was normalized by rarefying each sample to 16000 sequences ("rrarefy" function; vegan package; Oksanen et al., 2022). Alpha-diversity was calculated using the Shannon index ("diversity" function; vegan package) which is a composite metric of richness and evenness. Therefore, alpha-diversity was also calculated as richness (i.e., the number of ASVs in each sample; "richness" function; microbiome package) and evenness using Pielou's index. Pielou's index was calculated as H/log(S) where H is the Shannon index and S is richness. A one-way analysis of variance (ANOVA) was performed to determine if the three metrics of alpha-diversity varied by season. Prior to performing ANOVAs, assumptions of normality and homogeneity were checked using the Shapiro–Wilk test and Levene's test, respectively. Tukey's HSD was then performed to identify differences in alpha-diversity between seasons. To visualize similarities and differences in ASV composition by season, a Euler diagram was constructed using the rarefied ASV count table ("ps_euler" function; MicEco package; Russel, 2021). Additionally, the nestedness and turnover of ASVs between seasons were calculated ("beta.temp" function; betapart package; Baselga et al., 2022) to better understand ecological succession throughout the year. Lastly, correlation analysis of the three metrics of alpha-diversity with temperature and TKN were performed ("cor.test" function, method = "pearson").

For beta-diversity analyses, sequences were normalized using the variance stabilizing transformation ("varianceStabilizingTransformation" function; DESeq2 package; Love et al., 2014). Principal component analysis (PCA) was conducted on the normalized ASV table to visualize differences in microbial community structure by season ("ordinate" function; phyloseq package; McMurdie and Holmes, 2013). PC1 was extracted and correlation tests of temperature and TKN with PC1 were conducted ("cor.test" function; method = "pearson"). A PCA was also conducted on the environmental variables ("rda" function; vegan package), loadings were extracted, and the environmental loadings were overlaid as vectors onto the community ordination plot to create a biplot. Permutational ANOVA was performed to determine if community structure varied by season ("adonis"

1 https://github.com/melissa-brock/temporal-response-oil-exposure/tree/main/Production%20Inhibition

2 https://github.com/melissa-brock/temporal-response-oil-exposure/tree/main/QIIME2%20artifacts

3 https://github.com/melissa-brock/temporal-response-oil-exposure/tree/main/R%20Code

function; vegan package). Prior to performing the permutational ANOVA, the assumption of homogeneity of dispersion among groups was checked ("betadisper" function; vegan package). To identify which seasons significantly differed in their community structures, pairwise permutation multivariate ANOVA was performed ("pairwise.perm.manova" function; RVAideMemoire package; Hervé, 2020). To prevent inflation of Type I error rate due to multiple comparisons, the Hochberg method was applied to calculate adjusted *p*-values.

To determine if changes in the inhibition of primary and bacterial production varied by season, ANOVAs were performed, as described above. Simple linear regressions were performed to identify significant linear relationships between inhibition and biological/environmental variables. A mantel test was performed to determine if variation in the inhibition of bacterial production was correlated with changes in microbial community structure ("mantel" function; vegan package). The mantel test was performed using 10,000 permutations on two normalized dissimilarity matrices: (1) a Euclidean distance matrix of inhibition of bacterial production and (2) a Bray–Curtis distance matrix constructed from the rarefied ASV count table ("vegdist" function; vegan package).

3. Results

3.1. Environmental conditions

Surface coastal waters exhibited a strong temporal temperature trend but lacked temporal variability in salinity and nutrient concentrations (**Figure 1** and **Table 1**). Sea surface temperatures during the summer were significantly higher than all other seasons ($p < 0.05$) with a maximum value of 28.2°C, while temperatures during the winter were significantly colder than all other seasons ($p < 0.01$) with a minimum value of 13.6°C (**Figure 1A**). Salinity ranged from 27 to 37 with no significant differences between seasons but with higher variability observed at the end of spring and during summer due to increased rainfall (**Figure 1B**). NH_3 and TP concentrations were below the minimum detection limits (MDL). NO_3^- + NO_2^-, TKN, and orthophosphate concentrations were above the MDL but exhibited minimal variation and had no temporal trends ($p > 0.05$) (**Figures 1C-E**).

3.2. Bacterial diversity, community structure, and composition

Patterns in bacterial diversity, community structure, and taxonomic composition were examined by sequencing the V4–V5 region of the 16S rRNA gene. Alpha-diversity was calculated using three different metrics: the Shannon index, ASV richness, and Pielou's evenness index (**Supplementary Table 1**). The Shannon index and ASV richness did not exhibit any temporal trends (**Supplementary Figures 1A, B**), but evenness did significantly vary between winter and summer with winter having higher evenness than summer ($p < 0.05$) (**Figure 2A** and **Supplementary Figure 1C**). While alpha-diversity varied minimally across seasons, there were significant differences in community structure by season. Although PCA indicates that there is some overlap in community structure (**Figure 2B**), PERMANOVA confirmed that they are statistically distinct from each other according to season ($p < 0.05$). Partitioning beta-diversity into turnover and nestedness components revealed that the differences in community structure are largely due to turnover, with the turnover component accounting for 84–93% of the dissimilarity between seasons. This analysis is supported by a Euler diagram which shows that there are larger proportions of ASVs unique to each season compared to the proportion of ASVs shared between subsequent seasons (**Figure 2C**). There are also noticeable transitions between seasons in community composition. *Candidatus* Actinomarina, SAR11 clade Ia, HIMB11, NS2b marine group, NS4 marine group, NS5 marine group, OM60 (NOR5) clade, and *Synechococcus* dominated the bacterial community throughout the year (>1% average relative abundance) (**Figure 3A**), but their relative abundances shifted across seasons (**Figure 3B**). Within each season, particular genera became dominant (>1% average relative abundance). During the spring, *Blastopirellula, Candidatus* Aquiluna, and *Cyanobium* were dominant genera, while during the summer, *Balneola* and *Cyanobium* were dominant. The largest shifts in dominant genera occurred during the fall and winter with *Cyanobium, Formosa,* MB11C04 marine group, and SAR11 clade Ib becoming dominant in the fall, and *Ascidiaceihabitans, Blastopirellula, Formosa,* and the OM43 clade being dominant in the winter. Thus, we observed that these bacterial communities have distinct structures and compositional shifts according to season.

3.3. Inhibition of primary and bacterial production

To determine the temporal effect that exposure to water-soluble crude oil components had on the inhibition of primary and bacterial production, triplicate dose response curves (0, 0.5, 1, 2.5, 5, and 10% WAFs) were generated bi-weekly for 1 year. Exposure to WAFs led to inhibition of primary production across all seasons (**Figure 4A**). Inhibition of primary production was significantly lower during the winter compared to the spring and summer ($p < 0.05$) (**Figure 4A**). Inhibition of primary production exhibited strong negative relationships with chlorophyll *a* concentrations ($p < 0.0001$; Adj. $R^2 = 0.765$) (**Figure 4B**). Additionally, inhibition of primary production had a positive relationship with temperature ($p = 0.0002$; Adj. $R^2 = 0.444$) (**Figure 4C**) but no relationship with NO_3^- + NO_2^- concentrations ($p = 0.08$) or with orthophosphate concentrations ($p = 0.51$). However, inhibition of primary production had a negative relationship with TKN ($p = 0.002$; Adj. $R^2 = 0.332$) (**Figure 4D**). These results indicate that water soluble crude oil constituents have the strongest inhibitory effect on primary production when surface coastal waters are warm, when TKN concentrations are low, or when phytoplankton abundance is low.

Exposure to WAFs also led to inhibition of bacterial production across all seasons. Inhibition of bacterial production was significantly lower during winter compared to all other seasons ($p < 0.05$) (**Figure 5A**). There was no relationship of the inhibition of bacterial production with absolute bacterial abundance ($p = 0.34$), but there were weak, negative relationships of bacterial production inhibition with bacterial alpha-diversity (Shannon index: $p = 0.028$, Adj. $R^2 = 0.152$; Pielou's evenness index: $p = 0.012$, Adj. $R^2 = 0.205$) (**Figure 5B**). Additionally, there was a weak, positive correlation of bacterial production inhibition with bacterial community structure ($p = 0.002$; mantel $r = 0.28$), indicating that the severity of

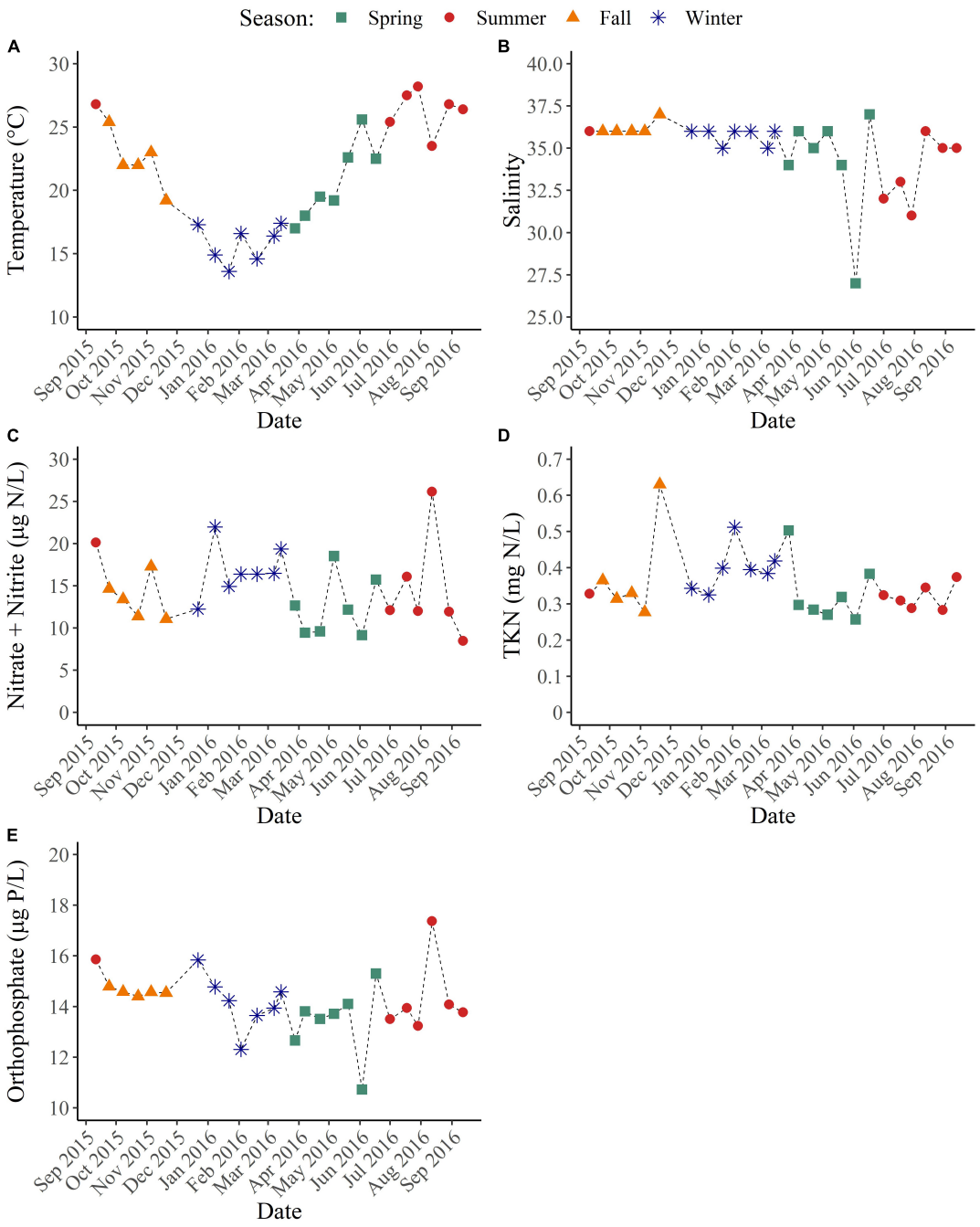

FIGURE 1
Environmental conditions of coastal Pensacola Beach waters from 09/2015 to 09/2016. **(A)** Temperature (°C). **(B)** Salinity. **(C)** NO_3^- + NO_2^- (µg N/L). **(D)** Total Kjeldahl nitrogen (mg N/L). **(E)** Orthophosphate (µg P/L).

inhibition is partially dependent on the background bacterial community. Although inhibition of bacterial production had no relationship with inorganic nutrient concentrations (NO_3^- + NO_2^- and orthophosphate) ($p > 0.10$), it did have a weak, negative relationship with TKN ($p = 0.032$; Adj. $R^2 = 0.143$) (Figure 5D) as well as a strong, positive relationship with temperature ($p < 0.0001$; Adj. $R^2 = 0.64$) (Figure 5C). These results are similar to what was seen for inhibition of primary production and indicate that water soluble crude oil constituents are most inhibitory to bacterial production when temperatures are high, when TKN concentrations are low, or when alpha-diversity is low.

Additionally, there were strong relationships between environmental conditions and the bacterial community which corresponded to the degree of bacterial production inhibition. Temperature had a strong positive correlation with PC1 ($p < 0.0001$, $r = 0.756$) (Figure 2B), a moderate negative correlation with the Shannon index ($p = 0.028$, r = −0.431), and a moderate negative correlation with Pielou's evenness index ($p = 0.01$, $r = -0.498$), while TKN had a moderate negative correlation with PC1 ($p = 0.025$, $r = -0.438$), a moderate positive correlation with the Shannon index ($p = 0.048$, $r = 0.392$), and a moderate positive correlation with ASV richness ($p = 0.035$, $r = 0.415$). Also, winter, which was the season

TABLE 1 Environmental parameters for each sample.

Sample date and season		Physical conditions		Nutrient concentrations				
Date (D/M/Y)	Season	Salinity	Temperature (°C)	Nitrate + nitrite (μg N/L)	NH_3 (μg N/L)	Total Kjeldahl nitrogen (mg N/L)	Orthophosphate (μg P/L)	Total phosphorus (μg P/L)
11/9/2015	Summer	36	26.8	20.110	Below MDL	0.328	15.86	Below MDL
24/9/2015	Fall	36	25.4	14.650	Below MDL	0.365	14.79	Below MDL
8/10/2015	Fall	36	22.0	13.400	Below MDL	0.314	14.58	Below MDL
23/10/2015	Fall	36	22.0	11.390	Below MDL	0.330	14.40	Below MDL
5/11/2015	Fall	36	23.0	17.280	Below MDL	0.277	14.57	Below MDL
20/11/2015	Fall	37	19.2	11.070	Below MDL	0.630	14.54	Below MDL
22/12/2015	Winter	36	17.3	12.240	Below MDL	0.343	15.84	Below MDL
8/1/2016	Winter	36	14.9	21.970	Below MDL	0.325	14.78	Below MDL
22/1/2016	Winter	35	13.6	14.930	Below MDL	0.399	14.23	Below MDL
3/2/2016	Winter	36	16.6	16.390	Below MDL	0.512	12.31	Below MDL
19/2/2016	Winter	36	14.6	16.390	Below MDL	0.395	13.65	Below MDL
7/3/2016	Winter	35	16.4	16.480	Below MDL	0.384	13.94	Below MDL
14/3/2016	Winter	36	17.4	19.360	Below MDL	0.419	14.58	Below MDL
28/3/2016	Spring	34	17.0	12.660	Below MDL	0.503	12.66	Below MDL
7/4/2016	Spring	36	18.0	9.438	Below MDL	0.297	13.81	Below MDL
22/4/2016	Spring	35	19.5	9.598	Below MDL	0.284	13.51	Below MDL
6/5/2016	Spring	36	19.2	18.520	Below MDL	0.270	13.71	Below MDL
20/5/2016	Spring	34	22.6	12.170	Below MDL	0.319	14.10	Below MDL
3/6/2016	Spring	27	25.6	9.148	Below MDL	0.257	10.72	Below MDL
17/6/2016	Spring	37	22.5	15.730	Below MDL	0.383	15.30	Below MDL
1/7/2016	Summer	32	25.4	12.090	Below MDL	0.324	13.50	Below MDL
18/7/2016	Summer	33	27.5	16.060	Below MDL	0.309	13.94	Below MDL
29/7/2016	Summer	31	28.2	11.990	Below MDL	0.288	13.23	Below MDL
12/8/2016	Summer	36	23.5	26.130	Below MDL	0.345	17.37	Below MDL
29/8/2016	Summer	35	26.8	11.930	Below MDL	0.283	14.08	Below MDL
12/9/2016	Summer	35	26.4	8.460	Below MDL	0.374	13.77	Below MDL

10.3389/fevo.2023.1096880

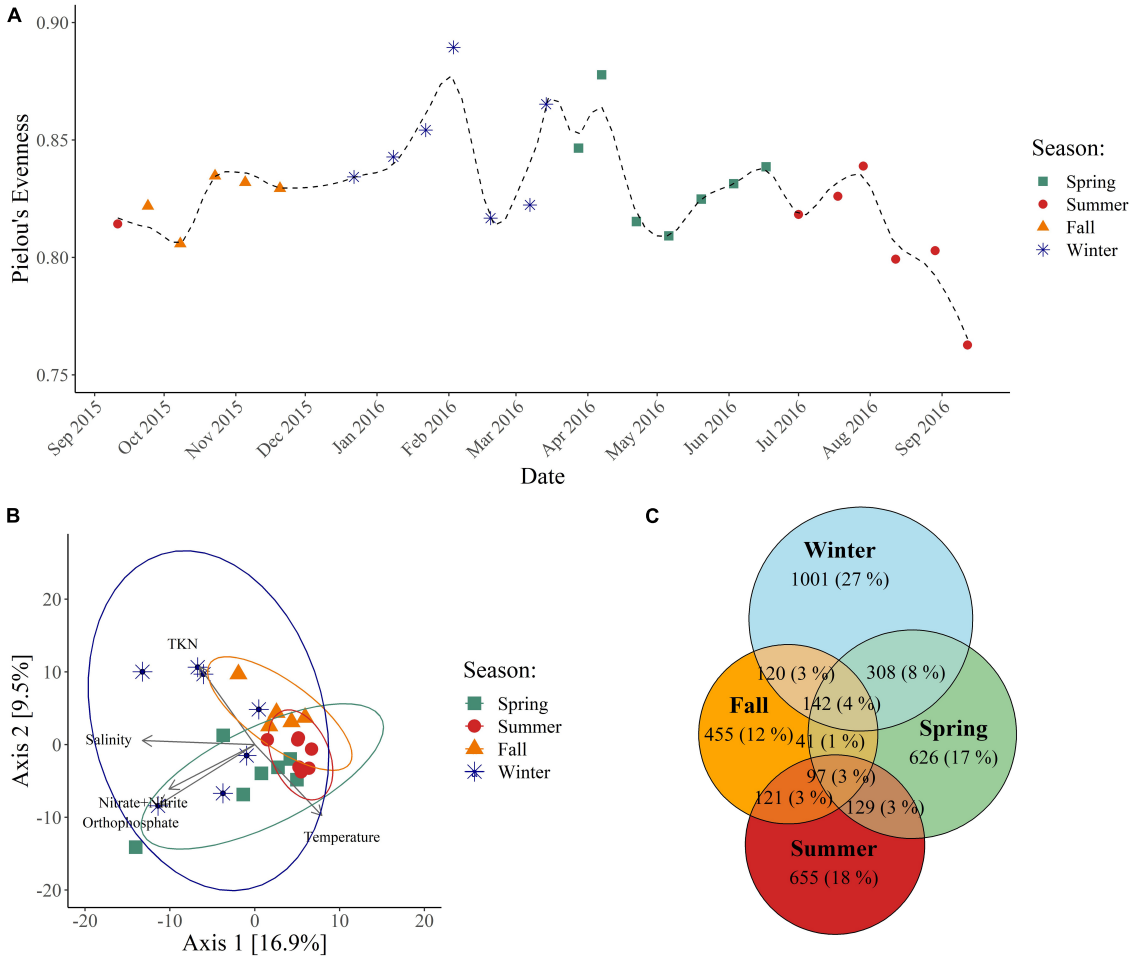

FIGURE 2
Bacterial alpha-diversity and community structure. **(A)** Alpha-diversity calculated from the rarefied ASV count table using Pielou's evenness index. **(B)** PCA constructed from the variance stabilizing transformed ASV count table. Ellipses represent the 95% confidence interval. **(C)** Euler diagram constructed from the rarefied ASV count table.

with the coldest temperatures, had more unique ASVs compared to warmer seasons (Figure 2C). This demonstrates that changes in temperature strongly corresponded with changes in bacterial community structure and with variability in alpha-diversity through changes in evenness, while TKN had a weaker correspondence with bacterial community structure and with variability in alpha-diversity through changes in richness. Combined, the data showed that lower temperatures corresponded to a bacterial community with more unique ASVs, higher evenness, and less inhibition of bacterial production, while higher concentrations of TKN corresponded to a bacterial community with higher richness and lower inhibition of bacterial production.

These results partially supported our hypothesis that there is a temporal response in inhibition due to acute exposure to water-soluble components of crude oil and that this response would be primarily driven by high temperature and low inorganic nutrient availability. We observed that exposure led to inhibition of primary and bacterial production across all seasons. The impact of exposure was found to be highest during warm months. Interestingly, we did not observe any effects of inorganic nutrient concentrations (NO_3^- + NO_2^- and orthophosphate), likely because there was low variability throughout the year. Surprisingly, there was a negative relationship between inhibition and TKN concentrations for both primary and bacterial production. This relationship may suggest links between human inputs of nitrogen, microbial community response, and the inhibition of production due to water soluble crude oil constituents. TKN primarily comes from human inputs and is a composite measurement of organic nitrogen, ammonia, and ammonium. When TKN concentrations increase in coastal waters, some heterotrophs and phytoplankton can use these compounds for their growth. Thus, increases in TKN may alter the community and buffer the impacts of water-soluble crude oil components. This is further supported by the relationships we observed between TKN, microbial community structure, and microbial community diversity. Additionally, we observed that changes in temperature strongly corresponded with changes in the bacterial community which then corresponded to the severity of bacterial production inhibition. For example, we observed that the impact of exposure to WAF was partially dependent on the background phytoplankton and bacterial communities as seen through the positive relationship of primary production inhibition with chlorophyll *a* concentrations (i.e., phytoplankton abundance), the negative relationship of bacterial production inhibition with alpha-diversity, and the positive relationship of bacterial production inhibition with bacterial community structure. Therefore, it appears that there are tight linkages between environmental factors, the

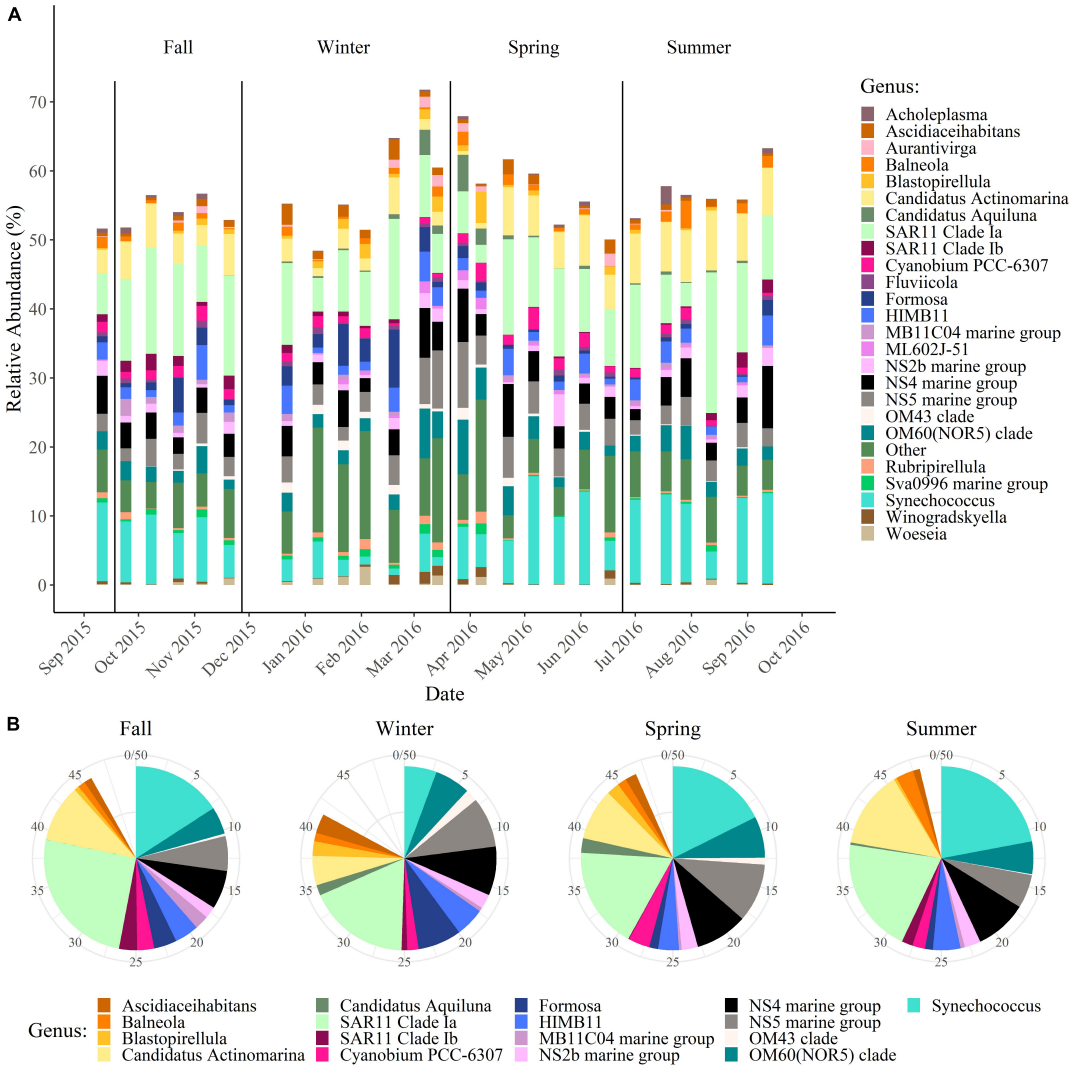

FIGURE 3
Shifts in the most abundant bacterial genera. Taxonomy was assigned using RDP's Naïve Bayesian classifier and the SILVA138 reference database. **(A)** Changes in the top 25 most abundant genera by date. **(B)** Changes in the dominant genera (>1% average relative abundance) between seasons.

microbial community, and the response to WAF. Combined, these results suggest that changes in environmental factors, such as temperature and TKN, corresponded with changes in the microbial community, which thus resulted in varying degrees of production inhibition when exposed to WAF.

4. Discussion

In this study, we exposed *in situ* planktonic coastal microbial communities to water-soluble components of crude oil and assessed the temporal response in the inhibition of primary and bacterial production. Temporal variability in inhibition was observed across seasons with temperature having a strong influence on inhibition. Temperature has been hypothesized to be a significant factor in structuring microbial responses to the *DWH* oil spill (Redmond and Valentine, 2012; Liu and Liu, 2013). Additionally, it has been demonstrated that oil biodegrades more rapidly at higher temperatures (Venosa and Holder, 2007) and that higher temperatures increase oil toxicity to sensitive microbes (Liu et al., 2017). This suggests that the interaction between temperature and oil exposure should most severely impact microbes at high temperatures. Our results quantitatively demonstrate that exposure to the water-soluble components of MC252 surrogate crude oil most severely inhibited production during the warmest months of the year.

We hypothesized that inorganic nutrient concentrations would be a key environmental driver of inhibition under crude oil exposure, but this relationship was not observed. The impact of inorganic nutrient concentrations on microbial communities in oiled environments is variable. Many studies have observed that the addition of inorganic nutrients to oiled polar and subtropical environments increases microbial hydrocarbon degradation rates (Head et al., 2006; Atlas and Hazen, 2011; Sun and Kostka, 2019) as well as increases heterotrophic abundance and biomass (Edwards et al., 2011). However, this response is not observed in nutrient-rich systems. In a Louisiana marsh, nutrient additions had little effect on crude oil biodegradation due to high background pore water ammonium concentrations (Tate et al., 2012), and in temperate estuarine waters, nutrient additions to oiled seawater

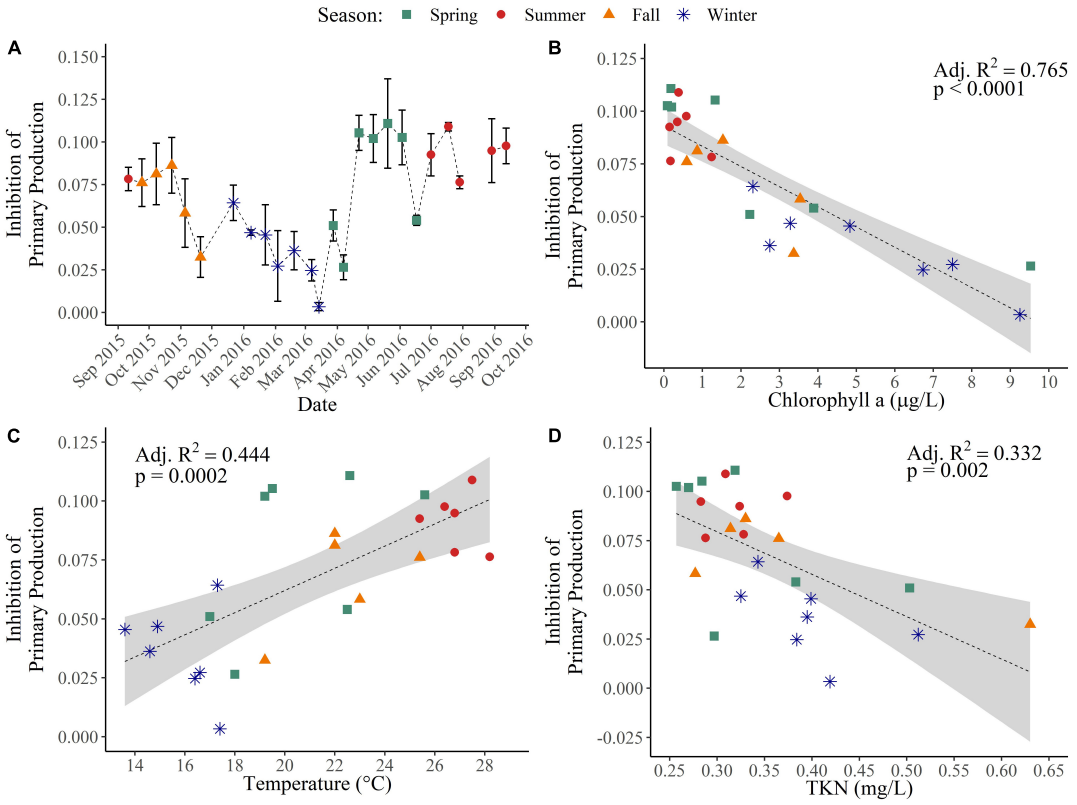

FIGURE 4
Inhibition of primary production across seasons and environmental drivers. **(A)** Inhibition of primary production was determined through the fixation of ^{14}C-bicarbonate along triplicate dose response curves of 0, 0.5, 1, 2.5, 5, and 10% WAF treatment. Linear regressions of the inhibition of primary production with **(B)** chlorophyll *a* concentrations (µg/L), **(C)** with temperature (°C), and **(D)** with total Kjeldahl nitrogen (mg N/L).

did not alter microbial community structure as observed in oligotrophic environments (Coulon et al., 2007). In our study, we used *in situ* coastal Gulf of Mexico waters with no nutrient additions. NO_3^- + NO_2^- and orthophosphate concentrations varied minimally throughout the year with a maximum difference of 17.67 µg N/L NO_3^- + NO_2^- and 6.65 µg P/L orthophosphate. Therefore, because nutrient concentrations exhibited small fluctuations, they were not a main factor influencing production. Thus, fluctuations in nutrient concentrations may not have a strong influence on microbes in oiled environments that experience small temporal fluctuations in nutrient concentrations or in oiled environments that are nutrient-rich year-round.

In this study, the background bacterial community structure played a role in the severity of inhibition due to oil exposure. A general pattern in bacterial succession is expected after marine oil spills. Accordingly, clear patterns of bacterial succession within the deep-sea hydrocarbon plume of *DWH* were observed (Dubinsky et al., 2013) which began with a community dominated by *Oceanospirillales* (Hazen et al., 2010; Redmond and Valentine, 2012) to a community dominated by *Colwellia* and *Cycloclasticus* (Valentine et al., 2010; Redmond and Valentine, 2012) and then to a community dominated by methylotrophic bacteria (Kessler et al., 2011). However, less is known about succession in surface water microbial communities and how responses to crude oil contamination varies based on the background microbial community. Our finding that the background bacterial community structure correlated with the severity of inhibition aligns with results from microcosms and incubation experiments. In a microcosm study, microcosms were seeded with surface water from polar, subtropical, and tropical sites (Sun and Kostka, 2019). The source waters each had a distinct initial microbial structure which resulted in different hydrocarbon-degrading microbial communities developing and ultimately resulted in different hydrocarbon degradation rates by site. Additionally, in an incubation experiment using surface waters from the Gulf of Mexico, initial community structure was a key driver in the development of bacterial communities following oil exposure (Liu et al., 2017). Therefore, the background bacterial community may be an important factor in the microbial response to marine oil spills.

Temperature can interact with WAF and the microbial community in a variety of ways that may have influenced production inhibition. Specifically, there are three ways in which temperature could have impacted production inhibition. The first way is that temperature can have a direct effect on WAF composition (Faksness et al., 2008; Bilbao et al., 2022), which could cause variability in production inhibition. However, since the same WAF was used throughout the experiment, we can eliminate this as a possibility. The second way is that temperature can have a direct effect on microbial physiology (Brown et al., 2004). However, to observe these effects, large differences in temperature are typically needed. For example, bacterial growth of planktonic communities from a eutrophic lake was measured at 2, 4, 8, 16, 20, and 30°C (Felip et al., 1996). Bacterial growth was significantly lower at the lowest temperatures of 2, 4, and 8°C compared to higher temperatures of 16, 20, and 30°C, but bacterial growth did not significantly vary within

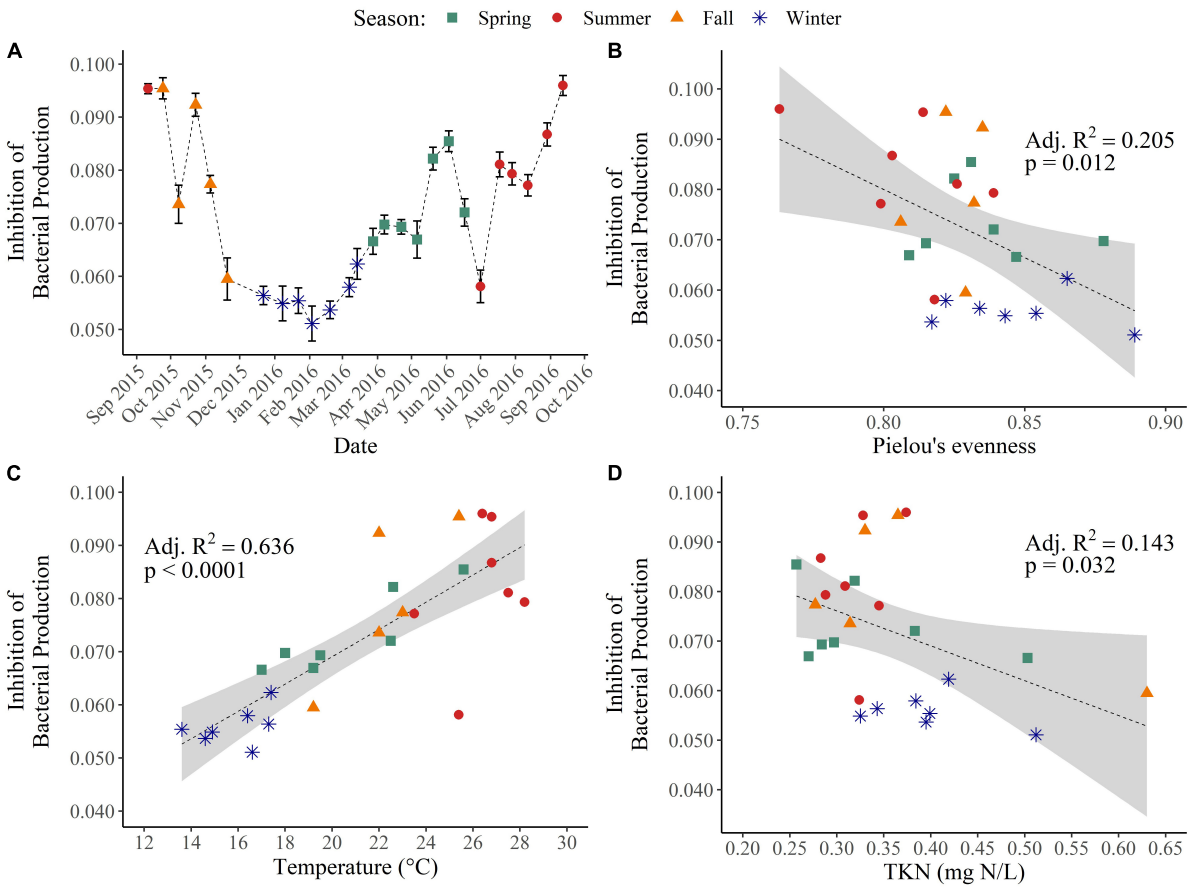

FIGURE 5
Inhibition of bacterial production across seasons and environmental drivers. **(A)** Inhibition of bacterial production was determined through the incorporation of ^{3}H-leucine along triplicate dose response curves of 0, 0.5, 1, 2.5, 5, and 10% WAF treatment. Linear regression of the inhibition of bacterial production **(B)** with alpha-diversity, **(C)** with temperature (°C), and **(D)** with total Kjeldahl nitrogen (mg N/L).

the higher temperature treatments. Additionally, measurements of bacterial production from a 2-year time-series in a temperate estuary showed that bacterial production at temperatures ranging from 10 to 30°C exhibited an upward trend until 25°C but were not statistically distinct (Apple et al., 2006). Our bi-weekly production inhibition experiments were conducted at *in situ* temperatures, which varied from 13.6 to 28.2°C, and we observed that there was no relationship of bacterial production inhibition with absolute bacterial abundance even though abundance varied throughout the year. The third way is that temperature may exert a strong influence on microbial diversity, resulting in variability in the community level response to WAF exposure. Planktonic microbial communities are influenced by temporal variability in environmental conditions. For example, a 5-year time-series in Ofunato Bay, Japan, found that changes in bacterial communities corresponded with changes in temperature, salinity, and dissolved oxygen (Kobiyama et al., 2021). Additionally, a 2-year time-series in the North Pacific Subtropical Gyre found that changes in alpha-diversity correlated most strongly with average wind speed (Bryant et al., 2016), while a 6-year coastal time-series in the English Channel found that variability in alpha-diversity was best explained by change in day length (Gilbert et al., 2012). Here, we observed that changes in temperature most strongly corresponded with changes in bacterial community structure and with variability in alpha-diversity and that changes in temperature strongly corresponded with changes in production inhibition. Our results therefore suggest that temperature had a strong influence on bacterial diversity and that these changes in the community affected the overall response to WAF exposure.

5. Conclusion

In conclusion, we observed that temperature was a key driver of the inhibition of primary and bacterial production under acute exposure to water-soluble components of MC252 surrogate crude oil. Inorganic nutrient concentrations had no significant effect on the inhibition of primary or bacterial production, perhaps because concentrations varied minimally throughout the year. Additionally, we observed that the background bacterial community structure and diversity correlated with changes in the inhibition of bacterial production, indicating that certain communities are more susceptible to exposure than others. Lastly, we observed that temperature strongly corresponded with changes in the microbial community, providing linkages between environmental conditions, the microbial community, and the community level response to oil exposure. Combined, these observations indicate that there is no universal response to oil spills and that in coastal, surface waters crude oil exposure has the highest inhibitory effect on phytoplankton and bacterial communities during warm months.

Data availability statement

Environmental data collected during this study are available in **Supplementary Table 1**. Raw data from dose response curves, example calculations for determining production inhibition from the raw data, QIIME2 artifacts, and R code are available on GitHub at https://github.com/melissa-brock/temporal-response-oil-exposure. The 16S rRNA sequences generated for this study can be found in the NCBI Sequence Read Archive under BioProject: PRJNA894536.

Author contributions

MB performed the laboratory experiments, conducted the bioinformatics and statistical analysis, generated the figures, and wrote the manuscript. RR performed the laboratory experiments. ME-H performed the laboratory experiments and oversaw the sample analysis. LN extracted the DNA, conducted the bioinformatics analysis, and edited the manuscript. RS contributed to conceptualization and edited the manuscript. WJ conceptualized the project, developed the experimental methodology, acquired the funding, and edited the manuscript. All authors contributed to the article and approved the submitted version.

Funding

This research was made possible in part by a grant from BP/The Gulf of Mexico Research Initiative as part of the C-IMAGE II Consortium and the University of West Florida Office of Undergraduate Research.

Acknowledgments

We thank Jane Caffrey, Elba de la Torre, Nine Henriksson, Gary Baine, Sigrid Solgard, Claire Quina, Emily Marshall, and Adelyn Benz for their contributions to this work. We thank Brandi Kiel Reese of the Dauphin Island Sea Lab for carbon analysis of WAFs.

Conflict of interest

The authors declare that the research was conducted in the absence of any commercial or financial relationships that could be construed as a potential conflict of interest.

Publisher's note

All claims expressed in this article are solely those of the authors and do not necessarily represent those of their affiliated organizations, or those of the publisher, the editors and the reviewers. Any product that may be evaluated in this article, or claim that may be made by its manufacturer, is not guaranteed or endorsed by the publisher.

Supplementary material

The Supplementary Material for this article can be found online at: https://www.frontiersin.org/articles/10.3389/fevo.2023.1096880/full#supplementary-material

References

Abbriano, R. M., Carranza, M. M., Hogle, S. L., Levin, R. A., Netburn, A. N., Seto, K. L., et al. (2011). Deepwater Horizon oil spill: A review of the planktonic response. *Oceanography* 24, 294–301. doi: 10.5670/oceanog.2011.80

Apple, J., del Giorgio, P., and Kemp, W. (2006). Temperature regulation of bacterial production, respiration, and growth efficiency in a temperate salt-marsh estuary. *Aquat. Microb. Ecol.* 43, 243–254. doi: 10.3354/ame043243

Aronesty, E. (2013). Comparison of sequencing utility programs. *Open Bioinform. J.* 7, 1–8. doi: 10.2174/1875036201307010001

Atlas, R. M., and Bartha, R. (1972). Degradation and mineralization of petroleum in sea water: Limitation by nitrogen and phosphorous. *Biotechnol. Bioeng.* 14, 309–318. doi: 10.1002/bit.260140304

Atlas, R. M., and Hazen, T. C. (2011). Oil biodegradation and bioremediation: A tale of the two worst spills in U.S. history. *Environ. Sci. Technol.* 45, 6709–6715.

Baselga, A., Orme, D., Villeger, S., De Bortoli, J., Leprieur, F., and Logez, M. (2022). *Betapart: partitioning beta diversity into turnover and nestedness components.* R package version 1.5.6. Available online at: https://CRAN.R-project.org/package=betapart

Beyer, J., Trannum, H. C., Bakke, T., Hodson, P. V., and Collier, T. K. (2016). Environmental effects of the Deepwater Horizon oil spill: A review. *Mar. Pollut. Bull.* 110, 28–51. doi: 10.1016/j.marpolbul.2016.06.027

Bik, H. M., Halanych, K. M., Sharma, J., and Thomas, W. K. (2012). Dramatic shifts in benthic microbial eukaryote communities following the Deepwater Horizon oil spill. *PLoS One* 7:e38550. doi: 10.1371/journal.pone.0038550

Bilbao, D., De Miguel-Jiménez, L., Igartua, A., Olivares, M., Izagirre, U., Prieto, A., et al. (2022). Chemical characterization of oil and water accommodated fraction (WAF) at different temperatures. *Results Eng.* 14:100433. doi: 10.1016/j.rineng.2022.100433

Bolyen, E., Rideout, J. R., Dillon, M. R., Bokulich, N., Abnet, C., and Al-Ghalith, G. (2019). Reproducible, interactive, scalable and extensible microbiome data science using QIIME 2. *Nat. Biotechnol.* 37, 852–857. doi: 10.1038/s41587-019-0209-9

Brown, J. H., Gillooly, J. F., Allen, A. P., Savage, V. M., and West, G. B. (2004). Toward a metabolic theory of ecology. *Ecology* 85, 1771–1789. doi: 10.1890/03-9000

Bryant, J. A., Aylward, F. O., Eppley, J. M., Karl, D. M., Church, M. J., and DeLong, E. F. (2016). Wind and sunlight shape microbial diversity in surface waters of the North Pacific Subtropical Gyre. *ISME J.* 10, 1308–1322. doi: 10.1038/ismej.2015.221

Callahan, B. J., McMurdie, P. J., Rosen, M. J., Han, A. W., Johnson, A. J. A., and Holmes, S. P. (2016). DADA2: High-resolution sample inference from Illumina amplicon data. *Nat. Methods* 13, 581–583. doi: 10.1038/nmeth.3869

Coulon, F., McKew, B. A., Osborn, A. M., McGenity, T. J., and Timmis, K. N. (2007). Effects of temperature and biostimulation on oil-degrading microbial communities in temperate estuarine waters. *Environ. Microbiol.* 9, 177–186. doi: 10.1111/j.1462-2920.2006.01126.x

Doyle, S. M., Whitaker, E. A., De Pascuale, V., Wade, T. L., Knap, A. H., Santschi, P. H., et al. (2018). Rapid formation of microbe-oil aggregates and changes in community composition in coastal surface water following exposure to oil and the dispersant Corexit. *Front. Microbiol.* 9:689. doi: 10.3389/fmicb.2018.00689

Dubinsky, E., Conrad, M., Chakraborty, R., Bill, M., Borglin, S., Hollibaugh, J., et al. (2013). Succession of hydrocarbon-degrading bacteria in the aftermath of the Deepwater Horizon oil spill in the Gulf of Mexico. *Environ. Sci. Technol.* 47, 10860–10867. doi: 10.1021/es401676y

Edgar, R. C. (2010). Search and clustering orders of magnitude faster than BLAST. *Bioinformatics* 26, 2460–2461. doi: 10.1093/bioinformatics/btq461

Edwards, B. R., Reddy, C. M., Camilli, R., Carmichael, C. A., Longnecker, K., and Van Mooy, B. A. S. (2011). Rapid microbial respiration of oil from the Deepwater Horizon spill in offshore surface waters of the Gulf of Mexico. *Environ. Res. Lett.* 6:035301. doi: 10.1088/1748-9326/6/3/035301

EPA standard method 350.1. (1993). "Determination of ammonia nitrogen by semi-automated colorimetry. Revision 2.0," in *Selected analytical methods for environmental remediation and recovery (SAM)*.

EPA standard method 351.2. (1993). "Determination of total kjeldahl nitrogen by semi-automated colorimetry. Revision 2.0," in *Methods for the chemical analysis of water and wastes, (MCAWW) (EPA/600/4-79/020)*.

EPA standard method 353.2. (1993). "Determination of nitrate-nitrite nitrogen by automated colorimetry. Revision 2.0," in *Methods for the determination of inorganic substances in environmental samples, (EPA/600/R-93/100)*.

EPA standard method 365.4. (1974). "Phosphorus, total (colorimetric, automated, block digestor AA II)," in *Methods for the chemical analysis of water and wastes, (MCAWW) (EPA/600/4-79/020)*.

Faksness, L.-G., Brandvik, P. J., and Sydnes, L. K. (2008). Composition of the water accommodated fractions as a function of exposure times and temperatures. *Mar. Pollut. Bull.* 56, 1746–1754. doi: 10.1016/j.marpolbul.2008.07.001

Farrington, J. W., Overton, E. B., and Passow, U. (2021). Biogeochemical processes affecting the fate of discharged Deepwater Horizon gas and oil new insights and remaining gaps in our understanding. *Oceanography* 34, 76–97.

Felip, M., Pace, M. L., and Cole, J. J. (1996). Regulation of planktonic bacterial growth rates: The effects of temperature and resources. *Microb. Ecol.* 31, 15–28. doi: 10.1007/BF00175072

Gilbert, J. A., Steele, J. A., Caporaso, J. G., Steinbrück, L., Reeder, J., and Temperton, B. (2012). Defining seasonal marine microbial community dynamics. *ISME J.* 6, 298–308. doi: 10.1038/ismej.2011.107

Harrison, P. J., Cochlan, W. P., Acreman, J. C., Parsons, T. R., Thompson, P. A., Dovey, H. M., et al. (1986). The effects of crude oil and Corexit 9527 on marine phytoplankton in an experimental enclosure. *Mar. Environ. Res.* 18, 93–109. doi: 10.1016/0141-1136(86)90002-4

Hazen, T. C., Dubinsky, E. A., DeSantis, T. Z., Andersen, G., Piceno, Y., Singh, N., et al. (2010). Deep-sea oil plume enriches indigenous oil-degrading bacteria. *Science* 330, 204–208. doi: 10.1126/science.1195979

Hazen, T. C., Prince, R. C., and Mahmoudi, N. (2016). Marine oil biodegradation. *Environ. Sci. Technol.* 50, 2121–2129. doi: 10.1021/acs.est.5b03333

Head, I. M., Jones, D. M., and Röling, W. F. M. (2006). Marine microorganisms make a meal of oil. *Nat. Rev. Microbiol.* 4, 173–182. doi: 10.1038/nrmicro1348

Hervé, M. (2020). *RVAideMemoire: Testing and plotting procedures for biostatistics. R package version 0.9-81-2*. Available online at: https://CRAN.R-project.org/package=RVAideMemoire

Huettel, M., Overholt, W. A., Kostka, J. E., Hagan, C., Kaba, J., Wells, W. B., et al. (2018). Degradation of Deepwater Horizon oil buried in a Florida beach influenced by tidal pumping. *Mar. Pollut. Bull.* 126, 488–500. doi: 10.1016/j.marpolbul.2017.10.061

Joye, S. B., Teske, A. P., and Kostka, J. E. (2014). Microbial dynamics following the Macondo oil well blowout across Gulf of Mexico environments. *Bioscience* 64, 766–777. doi: 10.1093/biosci/biu121

Kamalanathan, M., Schwehr, K. A., Labonté, J. M., Taylor, C., Bergen, C., Patterson, N., et al. (2021). The interplay of phototrophic and heterotrophic microbes under oil exposure: A microcosm study. *Front. Microbiol.* 12:675328. doi: 10.3389/fmicb.2021.675328

Kessler, J. D., Valentine, D. L., Redmond, M. C., Du, M., Chan, E., Mendes, S., et al. (2011). A persistent oxygen anomaly reveals the fate of spilled methane in the deep Gulf of Mexico. *Science* 331, 312–315. doi: 10.1126/science.1199697

King, G. M., Kostka, J. E., Hazen, T. C., and Sobecky, P. A. (2015). Microbial responses to the Deepwater Horizon oil spill: From coastal wetlands to the deep sea. *Ann. Rev. Mar. Sci.* 7, 377–401. doi: 10.1146/annurev-marine-010814-015543

Kobiyama, A., Rashid, J., Reza, M. S., Ikeda, Y., Yamada, Y., Kudo, T., et al. (2021). Seasonal and annual changes in the microbial communities of Ofunato Bay, Japan, based on metagenomics. *Sci. Rep.* 11:17277. doi: 10.1038/s41598-021-96641-9

Kopp, J. F. (1979). *Methods for chemical analysis of water and wastes. 1978*. Cincinnati, OH: Environmental Monitoring and Support Laboratory, Office of Research and Development, US Environmental Protection Agency.

Kostka, J. E., Prakash, O., Overholt, W. A., Green, S., Freyer, G., Canion, A., et al. (2011). Hydrocarbon-degrading bacteria and the bacterial community response in Gulf of Mexico beach sands impacted by the Deepwater Horizon oil spill. *Appl. Environ. Microbiol.* 77, 7962–7974. doi: 10.1128/AEM.05402-11

Liu, J., Bacosa, H. P., and Liu, Z. (2017). Potential environmental factors affecting oil-degrading bacterial populations in deep and surface waters of the northern Gulf of Mexico. *Front. Microbiol.* 7:2131. doi: 10.3389/fmicb.2016.02131

Liu, Z., and Liu, J. (2013). Evaluating bacterial community structures in oil collected from the sea surface and sediment in the northern Gulf of Mexico after the Deepwater Horizon oil spill. *Microbiologyopen* 2, 492–504. doi: 10.1002/mbo3.89

Love, M. I., Huber, W., and Anders, S. (2014). Moderated estimation of fold change and dispersion for RNA-seq data with DESeq2. *Genome Biol.* 15:550. doi: 10.1186/s13059-014-0550-8

Martin, M. (2011). Cutadapt removes adapter sequences from high-throughput sequencing reads. *EMBnet J.* 17:10. doi: 10.14806/ej.17.1.200

Matrai, P. A., Vernet, M., Hood, R., Jennings, A., Brody, E., and Saemundsdóttir, S. (1995). Light-dependence of carbon and sulfur production by polar clones of the genus Phaeocystis. *Mar. Biol.* 124, 157–167. doi: 10.1007/BF00349157

McMurdie, P. J., and Holmes, S. (2013). phyloseq: An R package for reproducible interactive analysis and graphics of microbiome census data M. Watson [ed.]. *PLoS One* 8:e61217. doi: 10.1371/journal.pone.0061217

McNutt, M. K., Camilli, R., Crone, T. J., Guthrie, G. D., Hsieh, P. A., Ryerson, T. B., et al. (2012). Review of flow rate estimates of the Deepwater Horizon oil spill. *Proc. Natl. Acad. Sci. U.S.A.* 109, 20260–20267. doi: 10.1073/pnas.1112139108

Mendelssohn, I. A., Andersen, G. L., Baltz, D. M., Caffey, R., Carman, K., Fleeger, J., et al. (2012). Oil impacts on coastal wetlands: Implications for the Mississippi River Delta ecosystem after the Deepwater Horizon oil spill. *Bioscience* 62, 562–574. doi: 10.1525/bio.2012.62.6.7

Michel, J., Owens, E. H., Zengel, S., Graham, A., Nixon, Z., Allard, T., et al. (2013). Extent and degree of shoreline oiling: Deepwater Horizon oil spill, Gulf of Mexico, USA. *PLoS One* 8:e65087. doi: 10.1371/journal.pone.0065087

Needham, D. M., and Fuhrman, J. A. (2016). Pronounced daily succession of phytoplankton, archaea and bacteria following a spring bloom. *Nat. Microbiol.* 1:16005. doi: 10.1038/nmicrobiol.2016.5

Oksanen, J., Simpson, G., Blanchet, F., Kindt, R., Legendre, P., Minchin, P., et al. (2022). *Vegan: community ecology package. R package version 2.6-4*. Available online at: https://CRAN.R-project.org/package=vegan

Parsons, M. L., Morrison, W., Rabalais, N. N., Turner, R. E., and Tyre, K. N. (2015). Phytoplankton and the Macondo oil spill: A comparison of the 2010 phytoplankton assemblage to baseline conditions on the Louisiana shelf. *Environ. Pollut.* 207, 152–160. doi: 10.1016/j.envpol.2015.09.019

Pelz, O., Brown, J., Huddleston, M., Rand, G., Gardinali, P., Stubblefield, W., et al. (2011). "Selection of a surrogate MC252 oil as a reference material for future aquatic toxicity tests and other studies," in *Proceedings of the SETAC 2011 meeting*, Boston, MA.

Porter, K. G., and Feig, Y. S. (1980). The use of DAPI for identifying and counting aquatic microflora. *Limnol. Oceanogr.* 25, 943–948. doi: 10.4319/lo.1980.25.5.0943

Quast, C., Pruesse, E., Yilmaz, P., Gerken, J., Schweer, T., Yarza, P., et al. (2012). The SILVA ribosomal RNA gene database project: Improved data processing and web-based tools. *Nucleic Acids Res.* 41, D590–D596. doi: 10.1093/nar/gks1219

R Core Team (2018). *R: A language and environment for statistical computing*. Vienna: R Foundation for Statistical Computing.

Ramseur, J. L., and Resources, Science, and Industry Division (2017). *Oil spills: background and governance (United States environmental protection agency)*. Washington, DC: Library of Congress, Congressional Research Service.

Redmond, M. C., and Valentine, D. L. (2012). Natural gas and temperature structured a microbial community response to the Deepwater Horizon oil spill. *Proc. Natl. Acad. Sci. U.S.A.* 109, 20292–20297. doi: 10.1073/pnas.1108756108

Russel, J. (2021). *MicEco: Various functions for microbial community data*. San Francisco, CA: GitHub.

Smith, D. C., and Azam, F. (1992). A simple, economical method for measuring bacterial protein synthesis rates in seawater using 3H-leucine. *Mar. Microb. Food Webs.* 6, 107–114.

standard method 5310 (2018). *Standard methods for the examination of water and wastewater*, eds W. Lipps, T. Baxter, and E. Braun-Howland (Washington, DC: APHA Press).

Sun, X., and Kostka, J. E. (2019). Hydrocarbon-degrading microbial communities are site specific, and their activity is limited by synergies in temperature and nutrient availability in surface ocean waters. *Appl. Environ. Microbiol.* 85, e00443–19. doi: 10.1128/AEM.00443-19

Tate, P. T., Shin, W. S., Pardue, J. H., and Jackson, W. A. (2012). Bioremediation of an experimental oil spill in a coastal Louisiana salt marsh. *Water Air Soil Pollut.* 223, 1115–1123. doi: 10.1007/s11270-011-0929-z

Valentine, D. L., Kessler, J. D., Redmond, M. C., Mendes, S., Heintz, M., Farwell, C., et al. (2010). Propane respiration jump-starts microbial response to a deep oil spill. *Science* 330, 208–211. doi: 10.1126/science.1196830

Vaughan, P. P., Wilson, T., Kamerman, R., Hagy, M. E., McKenna, A., Chen, H., et al. (2016). Photochemical changes in water accommodated fractions of MC252 and surrogate oil created during solar exposure as determined by FT-ICR MS. *Mar. Pollut. Bull.* 104, 262–268. doi: 10.1016/j.marpolbul.2016.01.012

Venosa, A. D., and Holder, E. L. (2007). Biodegradability of dispersed crude oil at two different temperatures. *Mar. Pollut. Bull.* 54, 545–553. doi: 10.1016/j.marpolbul.2006.12.013

Wang, Q., Garrity, G. M., Tiedje, J. M., and Cole, J. R. (2007). Naïve Bayesian classifier for rapid assignment of rRNA sequences into the new bacterial taxonomy. *Appl. Environ. Microbiol.* 73, 5261–5267. doi: 10.1128/AEM.00062-07

Welschmeyer, N. A. (1994). Fluorometric analysis of chlorophyll a in the presence of chlorophyll b and pheopigments. *Limnol. Oceanogr.* 39, 1985–1992. doi: 10.4319/lo.1994.39.8.1985

Wiesenburg, D., Shipp, B., Fodrie, J., Powers, S., Lartigue, J., Darnell, K. M., et al. (2021). Prospects for gulf of mexico environmental recovery and restoration. *Oceanography* 34, 164–173. doi: 10.5670/oceanog.2021.124

Wright, A. L., Weaver, R. W., and Webb, J. W. (1997). Oil bioremediation in salt marsh mesocosms as influenced by N and P fertilization, flooding, and season. *Water. Air. Soil Pollut.* 95, 179–191. doi: 10.1007/BF02406164

Ziervogel, K., McKay, L., Rhodes, B., Osburn, C. L., Dickson-Brown, J., Arnosti, C., et al. (2012). Microbial activities and dissolved organic matter dynamics in oil-contaminated surface seawater from the Deepwater Horizon oil spill site. *PLoS One* 7:e34816. doi: 10.1371/journal.pone.0034816

frontiers | Frontiers in Ecology and Evolution

TYPE Original Research
PUBLISHED 01 March 2023
DOI 10.3389/fevo.2023.1134069

OPEN ACCESS

EDITED BY
Michael C. Murrell,
University of West Florida,
United States

REVIEWED BY
Sarat Chandra Tripathy,
National Centre for Polar and Ocean Research,
India
Marcos Mateus,
University of Lisbon,
Portugal
Sarah Tominack,
University of West Florida,
United States

*CORRESPONDENCE
Edward Phlips
✉ phlips@ufl.edu

SPECIALTY SECTION
This article was submitted to Biogeography and Macroecology, a section of the journal Frontiers in Ecology and Evolution

RECEIVED 29 December 2022
ACCEPTED 09 February 2023
PUBLISHED 01 March 2023

CITATION
Stelling B, Phlips E, Badylak S, Landauer L, Tate M and West-Valle A (2023) Seasonality of phytoplankton biomass and composition on the Cape Canaveral shelf of Florida: Role of shifts in climate and coastal watershed influences.
Front. Ecol. Evol. 11:1134069.
doi: 10.3389/fevo.2023.1134069

Seasonality of phytoplankton biomass and composition on the Cape Canaveral shelf of Florida: Role of shifts in climate and coastal watershed influences

Ben Stelling, Edward Phlips*, Susan Badylak, Leslie Landauer, Mary Tate and Anne West-Valle

School of Forest, Fisheries, and Geomatic Sciences, University of Florida, Gainesville, FL, United States

Seasonal patterns of phytoplankton biomass and composition in the inner continental shelf off Cape Canaveral on the east coast of Florida were examined for a 6-year period (2013–2019). *In situ* water samples were collected and analyzed for chlorophyll *a*, phytoplankton biomass and composition, along with water quality parameters. Regional satellite data on chlorophyll *a,* and temperature was also obtained from NASA. Average chlorophyll *a* values over the study period ranged from $0.63 \pm 0.03 \mu g L^{-1}$ in the summer to $2.55 \pm 0.10 \mu g L^{-1}$ in the fall. Phytoplankton community composition also showed seasonal differences, with persistent dominance by picoplanktonic cyanobacteria in the summer, but mixed dominance by picocyanobacteria and dinoflagellates in the fall. Seasonal differences were attributed to a shift in predominant seasonal wind directions, which drive water along the coast from the north in the fall and winter, but from the south in the spring and summer, including eddies and upwelling from the Gulf Stream. Water masses moving along the Florida coast from the north are influenced by nutrient and phytoplankton-enriched inputs from estuaries along the north coast of Florida, explaining the higher phytoplankton biomass levels on the Cape Canaveral shelf in the fall and winter. Seasonal patterns observed in this study demonstrate the importance of allochthonous influences on phytoplankton biomass and composition, and highlight the potential sensitivity of phytoplankton communities to continuing cultural eutrophication and future climate changes, including the frequency and intensity of tropical storms, and alterations in discharges from land.

KEYWORDS

climate, eutrophication, chlorophyll, cyanobacteria, dinoflagellates, South Atlantic Bight, Gulf Stream

Introduction

Coastal shelf habitats are among the most productive regions in the marine environment (Harris et al., 2014). High productivity is in part driven by the proximity to nutrient inputs from land for both planktonic and benthic primary producer communities (Falkowski et al., 1998, Herrmann et al., 2015, Cloern et al., 2014). The shallow nature of shelf environments also accentuates light availability for photosynthesis and access to nutrients in benthic sediments

(Harris et al., 2014). Coastal waters of Florida in the southeastern United States have extensive continental shelf habitats on both the Atlantic Ocean and Gulf of Mexico sides of the peninsula. The shelf on the Gulf side is subject to inputs from several major rivers, including the Mississippi, Apalachicola, Suwannee, and Caloosahatchee Rivers. The Gulf shelf is also subject to frequent and intense toxic red tides (Steidinger, 2009; Vargo, 2009; Heil et al., 2014), which can be disruptive for the health of marine fauna and humans (Hoagland et al., 2014; Grattan et al., 2016). Due in part to the high frequency of red tides, the Gulf of Mexico has been the subject of extensive research on phytoplankton ecology (Heil et al., 2014). By contrast, phytoplankton communities on the Atlantic shelf of Florida have received less attention (Atkinson et al., 1978, 1984; Yoder, 1985; Yoder et al., 1985; Barnard et al., 1997), despite the important fishery and recreational resources located along the entire east coast of the state (Iafrate et al., 2019).

The Atlantic shelf of Florida is subject to inputs from a major river (St. Johns River) and inlets connected to restricted lagoons within the barrier islands spanning the east coast of the state. Rapid human development along the eastern seaboard of Florida since the 1940s has led to accelerated eutrophication of coastal environments (Tillman et al., 2004; Winkler and Ceric, 2004; Badruzzaman et al., 2012; Lapointe et al., 2015; Longley et al., 2019, Herren et al., 2021). The limited understanding of phytoplankton communities on the eastern continental shelf of Florida is reflective of the relative scarcity of extensive studies on sub-tropical and tropical phytoplankton compared to temperate ecosystems (Cloern and Jassby, 2008; Winder and Cloern, 2010; Zingone et al., 2010; Carstensen et al., 2015; Estrada et al., 2016; Liu et al., 2022). However, rapid human development in sub-tropical and tropical regions around the world has increased rates of cultural eutrophication, highlighting the need to better understand the factors that drive phytoplankton composition and dynamics in these coastal regions, especially with the possible exacerbating impacts of climate change (Nixon, 1995; Paerl et al., 2006; Heisler et al., 2008; Glibert and Burkholder, 2020; Griffith and Gobler, 2020; Anderson et al., 2021).

This study focused on the inner shelf environment off the coast of Cape Canaveral, located in the central east coast of Florida (Figure 1), which is part of the southern extent of the South Atlantic Bight (Miles and He, 2010). Studies on phytoplankton biomass on the shelf of the South Atlantic Bight have mainly involved satellite-based investigations of chlorophyll distribution, or short-term transect studies of phytoplankton biomass (Verity et al., 1998; Bontempi and Yoder, 2004; Martins and Pelegrí, 2006; Signorini and McClain, 2007; Miles and He, 2010). To date, there have been no extended *in situ* time-series studies of phytoplankton biomass and composition off the coast of east-central Florida.

The Cape Canaveral shelf (CCS) is bordered on the eastern side by the Gulf Stream, which impacts the region *via* eddies that propagate from the western side of the stream and upwelling of deep Gulf Stream water, particularly during the summer (Atkinson, 1977; Atkinson et al., 1978; Iafrate et al., 2019). The shelf region is also impacted by wind-driven longshore currents along the east coast of Florida (Lee et al., 1985; AlYousif et al., 2021). Longshore currents from the north flow toward the CCS and are subject to influxes of nutrient- and phytoplankton-rich water from rivers and inlets linked to estuaries within the system of barrier islands spanning the east coast of Florida. While currents from the south, including the Florida Current (Gulf Stream), bring in phytoplankton communities of more tropical origin to the CCS.

The goal of this study was to describe temporal trends of phytoplankton biomass and composition using the results of a 6-year *in situ* examination of chlorophyll *a*, phytoplankton composition & biomass, and selected water quality parameters for the CCS. The results were compared to chlorophyll *a* values obtained from NASA's MODIS-Aqua satellite (Justice et al., 1998; Miles and He, 2010; Gorelick et al., 2017). Together, the results provide a view of seasonal shifts in phytoplankton communities, and the environmental conditions associated with the shifts. The bases for the seasonal patterns are discussed within the context of the climatic conditions, hydrodynamic characteristics, and land influences on the continental shelf environment of the east coast of Florida.

Materials and methods

Sampling protocols

Water samples were collected seasonally, from the fall of 2013 through the summer of 2019. One date from the winter, spring, summer and fall of each year for a total of 23 separate sampling dates. The sampling area was located ~5 miles off the coast of Cape Canaveral, FL and 24 sampling sites were divided evenly among four regions: Chester, Bull, North Shoal, and South Shoal (Figure 1). The North and South shoal were part of the same shoal, and Chester and Bull sites represented other shoals north. Sites were split between shallower ridge and deeper swale sites (Figure 1). This was done to ensure that sampling sites occurred inside the ridge and swale portions of the Cape Canaveral shoals.

Surface water column samples and associated field data were collected at all 24 sites using a 3-m water-column, integrating pole sampler. The pole sampler was used to help avoid misrepresentation of surface water phytoplankton abundances due to surface scums or discrete depth chlorophyll maxima. At each site, a minimum of five poles of water taken to yield at least five liters of water, mixed and sub-samples were immediately withdrawn for subsequent analyses of chlorophyll *a* concentrations, phytoplankton composition and biomass, total phosphorus (TP) and total nitrogen (TN) concentrations.

Field parameters

At each sampling site, water temperatures and salinity were recorded using a YSI multi-parameter field probe ~0.5 m from the surface, aliquots of whole water were tested for turbidity using a LaMotte meter (APHA, 2005), and Secchi disk depths were determined to provide data on light attenuation.

Nutrient analyses

Sub-samples of water were frozen immediately after collection, then TN and TP concentrations were determined by the Soil and Water Science Department Wetland Biogeochemistry Laboratory at the University of Florida according to NELAP certification guidelines (1692 McCarty Drive, Room 2181, Building A, Gainesville, FL 32611).

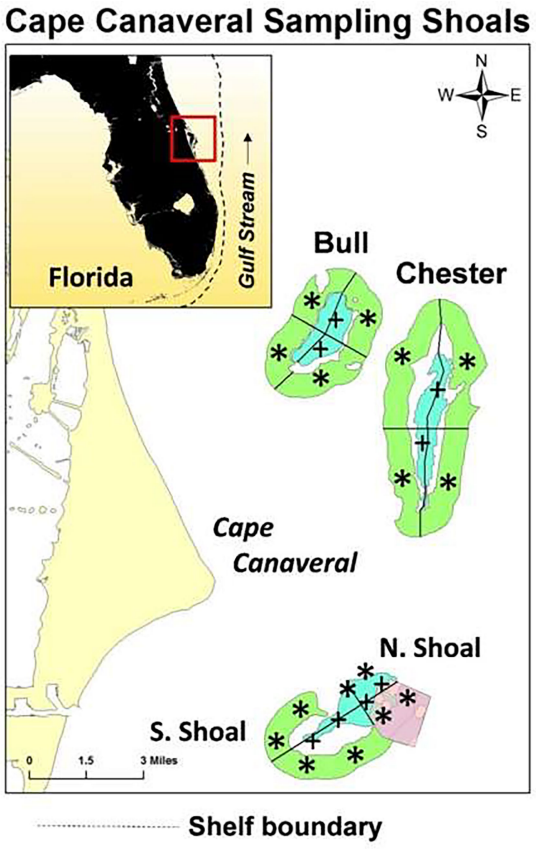

FIGURE 1
East coast of Florida showing the location of the Cape Canaveral Shelf (CCS) sampling region. Four sub-regions include Bull Shoal, Chester Shoal, North Shoal, and South Shoal. Ridge areas are shown in blue and swale areas in green. Sampling locations in each region are marked as "+" for ridge sites and "*" for swale sites. The pink area in North Shoal was the site of dredging activity for beach re-nourishment in the early winter of 2013.The inset shows the location of the study region and the dotted line shows the boundary of the shelf. SJR is outlet of the St. Johns River, SAI is the St. Augustine Inlet, MI is the Matanzas Inlet, and PI is the Ponce de Leon Inlet.

Precipitation and wind

Precipitation and wind data were gathered from the National Oceanic and Atmospheric Administration (NOAA) National Centers for Environmental Information.[1] Monthly precipitation data for weather stations in the Brevard County area were averaged and used to create a precipitation time series to approximate the rainfall and storm conditions that may have affected the study region.

The wind velocities were obtained from the NOAA National Data Buoy Center[2] for the station 41,009 off coast from Cape Canaveral, FL. The wind velocity data had a directional component in degrees. The north–south (vertical) component was extracted to analyze the seasonal shift in north–south wind direction to estimate its effect on surface currents in the study region. The vertical velocity component (north and south) was obtained using the equation below (Equation 1). The wind data were in degree-vector form and the convention where positive wind velocity was in the northern direction was used. v refers to the vertical component of the wind velocity, S refers to the speed, and W is the wind direction in degrees where 360 degrees refers to true north, 180 degrees is true south, east is 90°, and west is 270°.

$$v = S \times \sin\left(W \times \frac{\pi}{180}\right) \quad (1)$$

Chlorophyll *a* analysis of water collected *in situ*

In duplicate, 700-mL of sampled water was filtered through a 0.3-µm Whatman glass fiber filter and stored in a light-protected container at −20°C. Chlorophyll *a* was solvent extracted (Sartory and Grobbelaar, 1984) and measured spectrophotometrically according to Standard Methods (APHA, 2005). Chlorophyll *a* values used for analysis were not pheophytin corrected because pheophytin-corrected chlorophyll *a* values measured spectrophotometrically have shown inconsistent results when compared with HPLC chlorophyll determinations (Stich and Brinker, 2005).

Satellite chlorophyll *a*

Surface chlorophyll concentrations were acquired using the Google Earth Engine (Gorelick et al., 2017) platform and extracting the Ocean Color SMI: Standard Mapped Image from NASA's Moderate Resolution Imaging Spectroradiometer (MODIS; Justice et al., 1998; Gorelick et al., 2017). Images were filtered for those with low cloud cover, and a polygon was drawn to enclose the study region. Chlorophyll values used represent the average of all pixels inside the polygon for each day; then, a mean of all daily chlorophyll values for each month was used for analysis.

For satellite chlorophyll maps, MODIS-Aqua 8-day composite images were obtained from the NOAA/ERDAPP data server version 2.16 (Simons, 2011) to illustrate chlorophyll spatial patterns during a pair of fall and summer sampling dates.

When the satellite chlorophyll values were compared to the seasonal samples collected *in situ* at 24 sites within the same geographic region. The satellite chlorophyll values are a mean of the entire sampling region, and compared to the 24 discrete samples that were averaged together from the same region.

Phytoplankton biomass and composition

Samples for general phytoplankton composition analysis were collected in 125 mL amber glass bottles and preserved with Lugol's during the field collections. Analyses were based on the Utermöhl method (Utermöhl, 1958). Samples were settled in 19-mm diameter cylindrical chambers. Phytoplankton cells were identified and counted at 400× and 100× with a Leica phase contrast inverted microscope. At

1 https://www.ncdc.noaa.gov/
2 https://www.ndbc.noaa.gov/

400×, a minimum of 100 cells of a single taxon and 30 grids were counted. If 100 cells of a single taxon were not counted by 30 grids, grids were counted until 100 cells of a single taxon were reached up to a maximum of 100 grids. At 100×, a total bottom count was completed for taxa >30 µm in size.

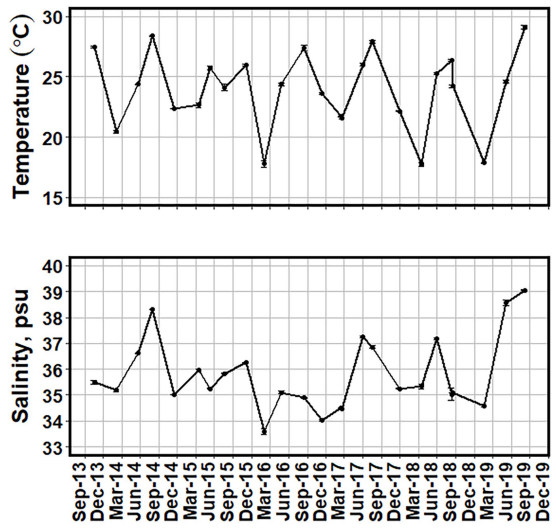

FIGURE 2
Mean surface water temperature (°C) and salinity (psu) from all sites between October 2013 and August 2019. Error bars of one standard error are added to show the variance of the values.

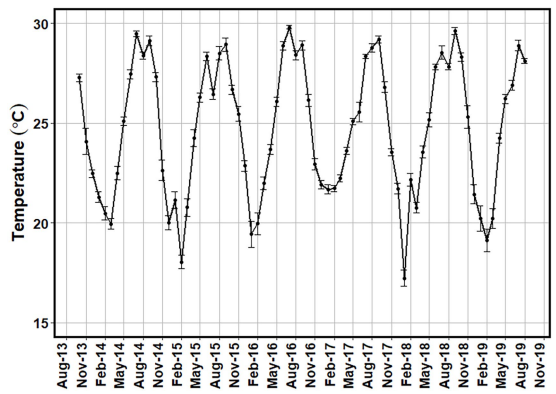

FIGURE 3
Monthly average surface temperature (°C) for the study region from MODIS-Aqua satellite from October 2013 to August 2019.

Samples for picoplankton analyses were collected in 22 mL glass scintillation vials and preserved with buffered glutaraldehyde solution in the field. Fluorescence microscopy was used to enumerate picoplanktonic cyanobacteria (e.g., *Synechococcus* spp., spherical picocyanobacteria spp.) at 1,000× magnification. Subsamples of waterwere filtered onto 0.2 µm Nucleopore filters and mounted between a microscope slide and cover slip with immersion oil (Phlips et al., 1999).

Cell biovolumes (i.e., μm^{-3} mL^{-1}) were estimated by assigning combinations of geometric shapes to fit the characteristics of individual taxa (Smayda, 1978; Sun and Liu, 2003). Specific phytoplankton dimensions were measured for at least 30 randomly selected cells. Species which vary substantially in size, such as many diatom species, were placed into size categories. Phytoplankton biomass as carbon values (i.e., µg carbon mL^{-1}), were estimated by using conversion factors for different taxonomic groups applied to biovolume, as prescribed by Menden-Deuer and Lessard (2000), with adjustments to biovolumes for the effects of Lugol's preservative (Strathmann, 1967; Ahlgren, 1983; Sicko-Goad et al., 1984; Verity et al., 1992; Work et al., 2005).

Statistical analyses

Comparison of seasonal differences in chlorophyll *a*, phytoplankton biomass, and physical/chemical parameters was done by comparison of means using the Games-Howell pairwise comparison (Games and Howell, 1976) using the *posthocTGH* function in the *Rosetta* package in R (Peters, 2018). This comparison was chosen because it does not require the assumptions of homogeneity of variance to be met. When correlation was compared (including pairwise), the Pearson correlation coefficient was used and the significance of this relationship was tested using the *t*-statistic.

Results

Temperature and salinity

Mean surface water temperatures for the *in situ* sampling events ranged from 17.7 ± 0.1°C in the winter of 2015/16 to 29.1 ± 0.2°C in the summer of 2019 (Figure 2). More temporally intensive surface water temperature data from MODIS-Aqua satellite showed a similar range of values (Figure 3).

Mean surface salinities ranged from 33.58 ± 0.10 psu in the winter of 2015/16 to 39.06 ± 0.03 psu in the summer of 2019 (Figure 2). Fall and winter sampling periods had lower salinity than spring and summer ($p < 0.05$; Table 1).

TABLE 1 Mean seasonal values for physical and chemical variables for different seasons with the standard error in paratheses.

Season	SAL (psu)	TP (mgL^{-1})	TN (mgL^{-1})	Secchi (m)	Turb (ntu)
Spring	36.68 (0.06) A	0.016 (0.001) A	0.15 (0.01) A	5.2 (0.2) C	1.18 (0.08) B
Summer	36.43 (0.09) A	0.016 (0.001) A	0.13 (0.01) A	7.1 (0.2) D	0.70 (0.05) A
Fall	35.26 (0.05) B	0.017 (0.001) A	0.20 (0.01) B	2.6 (0.1) A	2.65 (0.12) D
Winter	34.84 (0.08) C	0.018 (0.001) A	0.15 (0.00) A	3.7 (0.1) B	1.86 (0.13) C

The letters are the results of the Games-Howell pairwise comparison post-hoc test. Groups sharing the same letter are not significantly different from each other ($p > 0.05$).

Turbidity and Secchi disk depth

Mean Secchi depths ranged from 1.9 m in the winter of 2017/18 to 8.1 m in the summer of 2015 Mean turbidites ranged from 0.7 ntu in the summer of 2018 to 9.0 ntu in the winter of 2018/19 winter season (Figure 4). Turbidity and Secchi disk depths showed similar trends, with higher Secchi depths and lower turbidity in the summer, and higher turbidity and lower Secchi depths in the winter and fall seasons (Figure 4, Table 1).

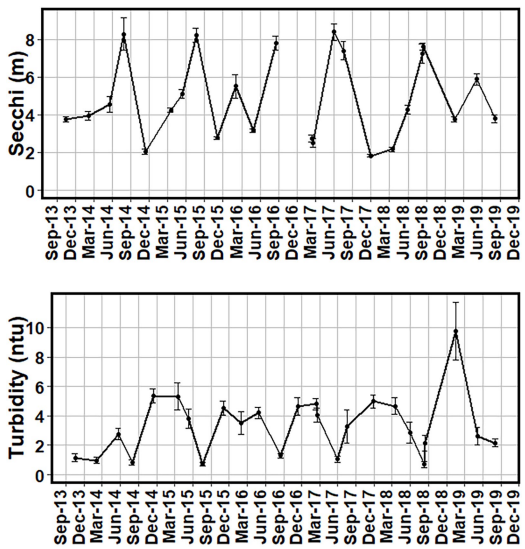

FIGURE 4
Mean Secchi disk depths in meters (m) and turbidity (ntu) from all sites between October 2013 and August 2019. The missing point is from November 2016 for the Secchi figure. Error bars of one standard error are added to show the variance of the values.

Precipitation and wind

Mean monthly rainfall totals in Brevard County ranged from 8.0 ± 0.7 mm in February of 2018 to 343.3 ± 26.4 mm in September of 2017 (Figure 5). Precipitation patterns reflect a warm rainy season (May–October), followed by a cooler, dry season (November–April), which is characteristic of the sub-tropical environment of central Florida (Irizarry-Ortiz et al., 2013). The region was also directly affected by three tropical systems in August of 2016 and September of 2016–2017 (Figure 5). The lowest monthly rainfall was in February of 2018 where 8 mm of rain was collected. The spring and summer seasons were characterized by heavier rain with the maximum monthly rainfall of 343 mm occurring in September of 2017, coinciding with Hurricane Irma (Figure 5).

The north/south component of wind velocities were taken for each season to examine changes between seasons in the origin of water effecting the sampling region. The first three sampling dates for the spring showed little prevailing north/south wind direction, while the last three dates showed consistent northward wind velocities for just over 70% of days. This southerly wind trend was much stronger in the summer with over 80% of days leading up to the summer sampling dates had a net northern component with velocities ranging from 2.0 m/s to 3.6 m/s (Figure 6). The fall season shows a reversal in wind direction showing a northerly prevailing wind direction for over 74% of days leading up to each sampling date and had a net southern component with velocities ranging from −1.4 m/s to −3.1 m/s. The winter sampling dates did not show a consistent wind direction with only the winter of 2016 having 68% of days showing a northerly wind direction for that sampling date (Figure 6). Consistent wind directions were seen in the fall and summer, while the winter and spring had less consistent directionality.

Total nitrogen and phosphorus

Mean TN concentrations of the study ranged from >0.04 ± 0.01 mg L^{-1} in the summer of 2014 to 0.35 ± 0.05 mg L^{-1} in the

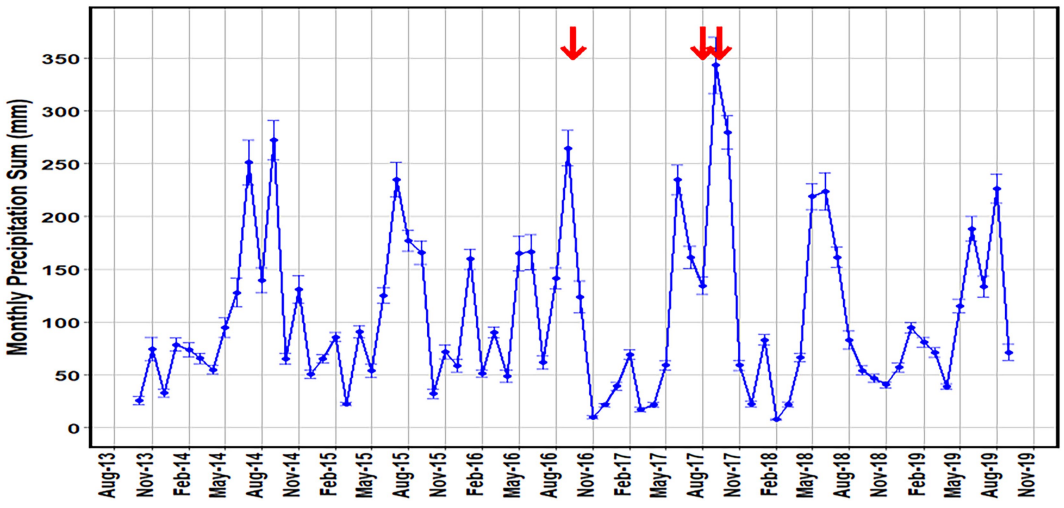

FIGURE 5
Mean monthly precipitation sum (mm) for land stations in Brevard County, Florida (NOAA). Error bars of one standard error are added to show the variance of the values. Red arrows indicate tropical systems that passed over or near the sampling sites during the sampling period.

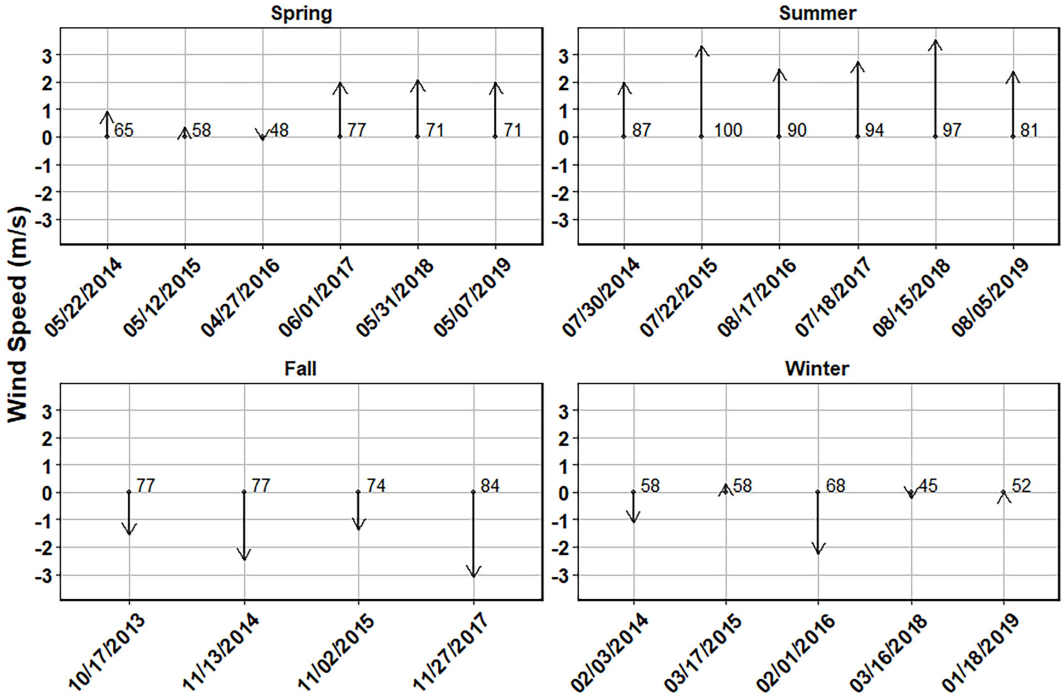

FIGURE 6
Average vertical wind speed (m/s) over a 30-day period prior to the sampling date for each season. Positive values represent wind traveling from south to north. Numbers to the right of the vector arrows represent the percentage of days where the average wind was traveling in the direction of the arrow.

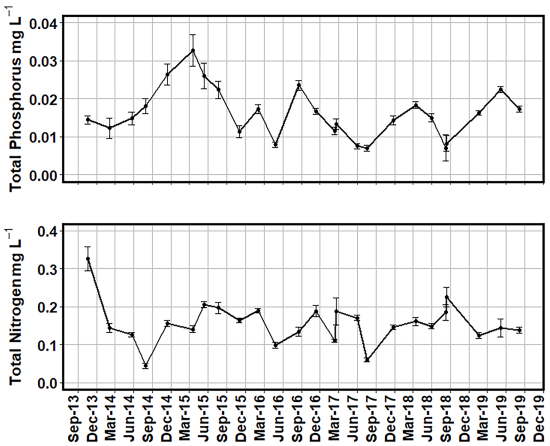

FIGURE 7
Mean surface total nitrogen and total phosphorus concentration (mgL^{-1}) for all sites from October 2013 to August 2019. Error bars of one standard error are added to show the variance of the values.

fall of 2013 (Figure 7). Mean TN levels often remained between 0.1–0.25 mg L^{-1}. Notably, the high levels of TN in the fall of 2013 coincided with a bloom of the nitrogen-fixing cyanobacterium *Trichodesmium erythraeum* (Tate et al., 2020).

Mean total phosphorus concentrations ranged from 0.007 ± 0.001 mg L^{-1} to 0.033 ± 0.004 mg L^{-1} in summer 2018 and in spring 2015, respectively, (Figure 7). Besides the maximum in 2015, TP never exceeded 0.03 mg L^{-1} during the sampling period. No significant correlation was seen between TP and TN values.

TABLE 2 Mean chlorophyll concentrations (μgL^{-1}) at different seasons, site topographies, and depths with the standard error in paratheses.

Season	Chl a	*Post-hoc*
Spring	0.66 (0.03)	A
Summer	0.63 (0.03)	A
Fall	2.55 (0.10)	C
Winter	1.31 (0.06)	B

The letters are the results of the Games-Howell pairwise comparison post-hoc test. Groups sharing the same letter are not significantly different from each other ($p > 0.05$).

Seasonality of physical/chemical variables

Mean TN was highest in the fall at 0.20 ± 0.01 mg L^{-1}, significantly higher than TN during the other three seasons ($p < 0.01$; Table 1). The fall season also coincided with the highest mean chlorophyll (Table 2) and turbidity (Table 1) values and the lowest Secchi depths ($p < 0.01$; Table 1). Mean TP values showed no significant difference among seasons (Table 1). Secchi depth/turbidity showed a significant difference ($p < 0.01$) among all seasons, with the summer showing the lowest surface turbidity and deepest Secchi depth (Table 1).

In situ chlorophyll *a*

Variability in chlorophyll *a* concentrations were examined using medians and interquartile ranges for each sampling date to compare the interannual variability (Figure 8). Spring chlorophyll *a* median values ranged from 0.16 μg L^{-1} in 2017 to 1.11 μg L^{-1} in 2016 (Figure 8).

10.3389/fevo.2023.1134069

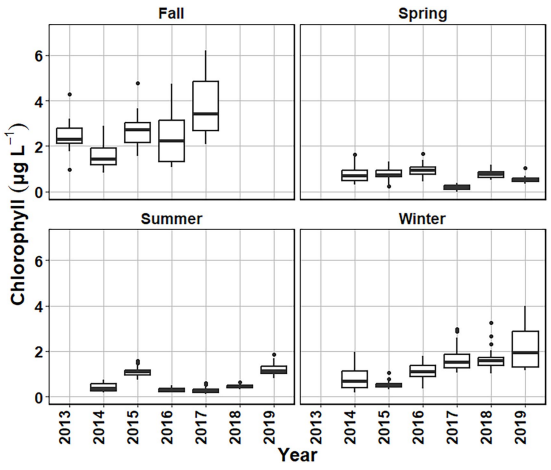

FIGURE 8
Surface chlorophyll (µgL^{-1}) boxplots for each sampling date arranged by season and year from October 2013 to August 2019.

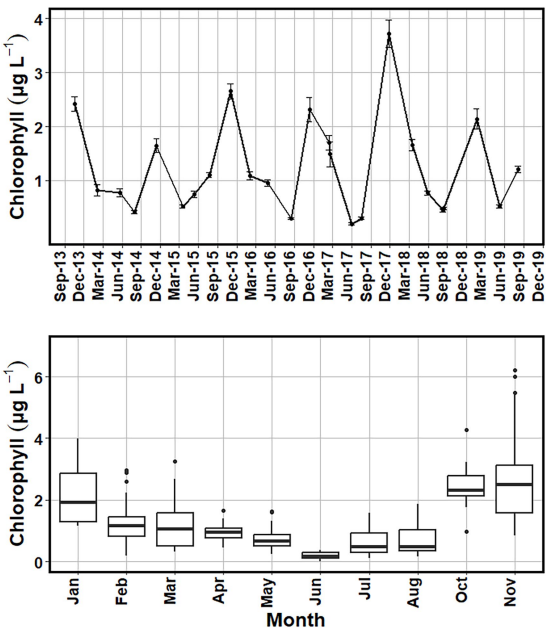

FIGURE 9
Average surface chlorophyll (µgL^{-1}) (top) with error bars of one standard error added to show the variance of the values. Boxplots of surface chlorophyll (µgL^{-1}) (bottom) showing the range of chlorophyll values obtained for sampling dates within each month from October 2013 to August 2019.

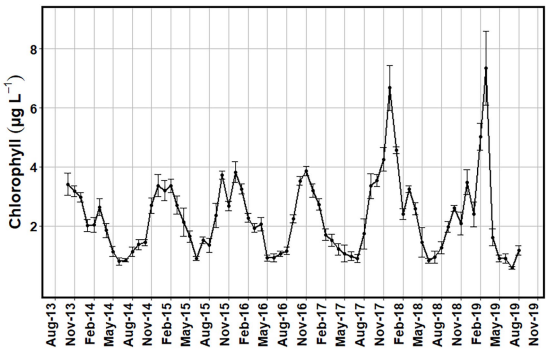

FIGURE 10
Monthly average surface chlorophyll (µgL^{-1}) values for the study region obtained from MODIS-Aqua satellite images with low cloud cover from October 2013 to August 2019. Error bars of one standard error were added to show the variance of the values.

Summer chlorophyll *a* median concentrations ranged from 0.27 µg L^{-1} in 2016 and 2017 to 1.35 µg L^{-1} for 2019. Fall had the highest median chlorophyll *a* concentrations among the four seasons and had a higher associated variance. Fall median chlorophyll *a* values ranged from 1.35 µg L^{-1} in 2015 to 3.66 µg L^{-1} for 2017. Winter chlorophyll *a* median values ranged from 0.49 µg L^{-1} in 2015 to 2.03 µg L^{-1} for 2017 (Figure 8). While the winter season did have a higher median chlorophyll *a* concentration than the spring or summer seasons, there were periods early in the investigation (2014–2015) when chlorophyll *a* values were comparable to the spring and summer (Figure 8). Separating the sampling dates by month, November had the highest median chlorophyll *a* 2.73 µg L^{-1} and June had the lowest median chlorophyll *a* 0.19 µg L^{-1} for the *in situ* sampling (Figure 9).

Summer and spring *in situ* mean chlorophyll *a* concentrations for the study period did not differ significantly, with means of 0.63 and 0.66 µg L^{-1} (Table 2). Winter chlorophyll *a* mean concentration was 1.31 ± 0.06 µg L^{-1}, which differed significantly ($p < 0.001$) from all other seasonal means. Fall mean chlorophyll *a* concentration was 2.55 ± 0.10 µg L^{-1}, significantly higher than all other seasonal means (Table 2).

Comparison of *in situ* and satellite chlorophyll *a*

Surface chlorophyll *a* concentrations from both satellite and *in situ* collections showed a similar seasonal pattern, with higher levels in the fall and winter months (Figures 8–10). When comparing the two methods, the satellite data revealed higher concentrations of chlorophyll *a*, with values exceeding 6 µg L^{-1} in December of 2017 and March of 2019 (Figures 6, 8). *In situ* collected chlorophyll *a* concentrations also peaked during these periods, but monthly mean chlorophyll *a* concentrations did not exceed 4 µg L^{-1} (Figure 9). Also, while the satellite data showed similar chlorophyll seasonality to *in situ* data, the chlorophyll maxima for the satellite imagery alternated between fall and winter dates, while the *in situ* data consistently showed peak chlorophyll values during the fall in October and November (Figure 9). Investigating some of the satellite imagery, there is a distinct enhancement of chlorophyll on the Atlantic shelf during the fall season compared to the summer season (Figure 11).

In situ chlorophyll values and satellite chlorophyll values were compared on dates where both satellite and *in situ* data were available. Overall, the values showed a linear relationship but deviated from the 1:1 line with satellite chlorophyll tending to have higher chlorophyll values on the same dates (Figure 12). Linear modeled satellite chlorophyll concentrations were higher than the *in situ* chlorophyll values by 60%.

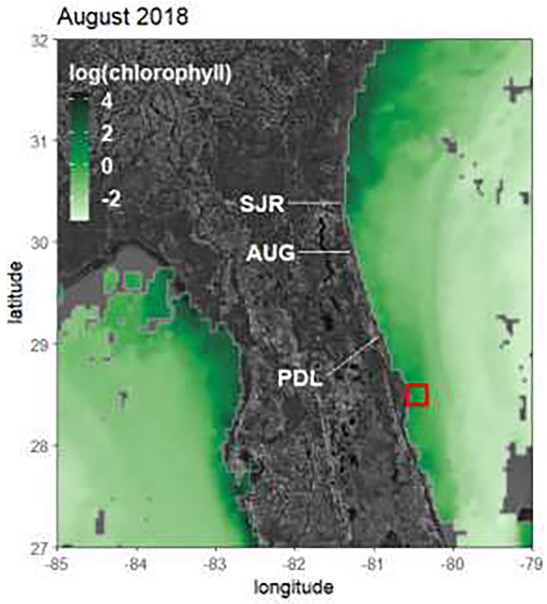

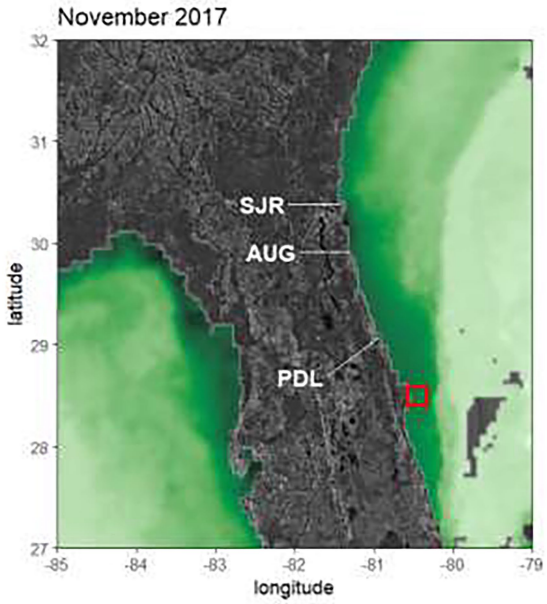

FIGURE 11
Natural log of chlorophyll concentrations (mgm^{-3}) measured by MODIS-Aqua satellite for an 8-day composite for November 2017 and August 2018. The red square denotes the sampling region. SJR, St. John's River Estuary; AUG, St. Augustine Inlet; PDL, Ponce de Leon Inlet.

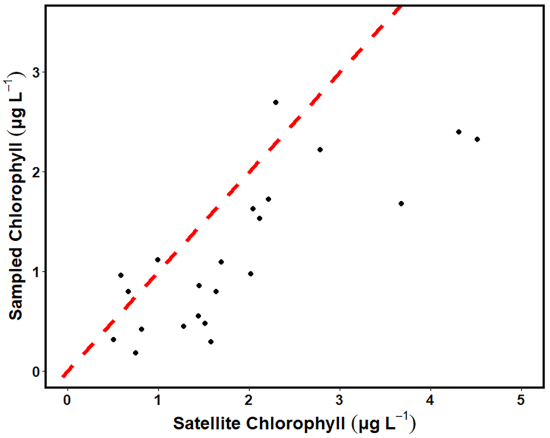

FIGURE 12
Correlation between the mean of sampled surface chlorophyll (µgL^{-1}) and the satellite chlorophyll estimate for the region (µgL^{-1}). The dashed red line represents the 1:1 ratio.

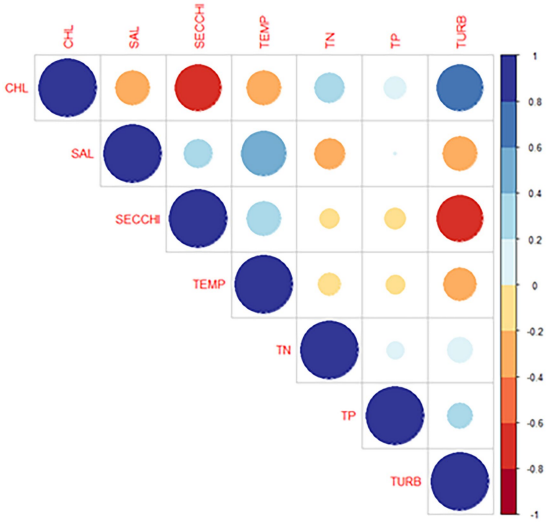

FIGURE 13
Pairwise correlation between physical/chemical variables and chlorophyll concentration during sampling period. Scale is in Pearson's correlation coefficient.

Correlation of chlorophyll *a* with physical/chemical variables

In situ chlorophyll *a* showed a strong positive correlation with turbidity, a positive correlation with TN, and a weaker positive correlation with TP (Figure 13). Surface chlorophyll *a* showed a negative correlation for parameters associated with the summer season including higher temperature and higher salinity (Figure 13). All correlations mentioned were statistically significant ($p < 0.05$).

Phytoplankton biomass and composition

Mean total phytoplankton biomass per sampling event, in terms of estimated carbon, ranged from 50 µg carbon L^{-1} in Spring 2016 to 340 µg carbon L^{-1} in fall of 2013 (Figure 14). Over the study period there were significant seasonal differences in mean total biomass over the study period (Table 3). The highest mean value was in the fall, followed by winter, summer, and lowest in spring. In order to examine the relative contribution of different taxonomic groups to total biomass, phytoplankton were subdivided into four groups: cyanobacteria, dinoflagellates, diatoms and "other" (i.e., all other taxa). The fall season had the highest mean biomass for all four groups (Table 3). However, for

diatoms winter mean biomass was statistically similar to fall, and for cyanobacteria summer mean biomass was similar to fall. In terms of each season, cyanobacteria had the highest mean biomass in the spring, summer and winter (Table 3). In fall, dinoflagellates and cyanobacteria had higher mean biomass than diatoms or "Other" taxa.

In addition to mean biomass patterns for the four groups of taxa, there were also noteworthy differences in the dominant individual taxa by season. The seasonal differences are illustrated by a comparison of the frequency of occurrence of taxa in the Top-200 list of highest biomass values observed for individual taxa in the summer and fall seasons (Table 4). Cyanobacteria were major elements of the Top-200 list in both the summer and fall. In summer, picoplanktonic cyanobacteria (i.e., spherical forms and *Synechococcus* spp.) represented 90% of the Top-200 entries (Table 4). In fall, picoplanktonic cyanobacteria were only 48% of the Top-200 entries. In addition, the filamentous nitrogen-fixing cyanobacteria *Trichodesmium erythraeum* appeared four times on the list, principally in 2013. *T. erythraeum* also registered the highest single biomass observation in the Top-200 list in either list. *T. erythraeum* is considered a Harmful Algal Bloom (HAB) species with potential for toxin production (Lundholm et al., 2009; Lassus et al., 2016).

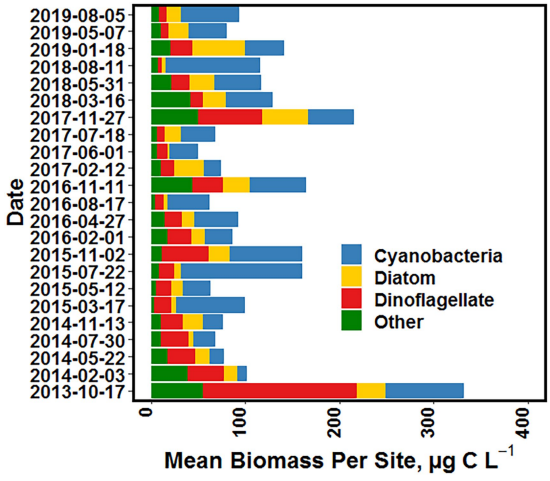

FIGURE 14
Mean surface water phytoplankton biomass (µg carbon L^{-1}) for each sampling date, sub-divided into four major groups, i.e., cyanobacteria, diatoms, dinoflagellates and all "other" (i.e., all other taxa) groups, from October 2013 to August 2019.

The second most prominent group in the Top-200 list of both the summer and fall was dinoflagellates (Table 4). In the summer, the most prominent of the four species on the list was the known toxin producer *Azadinium caudatum* (Lassus et al., 2016). The other three dinoflagellates on the summer Top-200 list were two mixotrophs, *Scrippsiella* sp., and *Torodinium robustum*, and the heterotroph *Gyrodinium spirale*. In the fall, there were 15 dinoflagellate taxa on the Top-200 list (Table 4). The HAB species *Margalefidinium polykrikoides* had the highest frequency of occurrence on the Top-200, and had the highest single biomass observation, 92 µg carbon L^{-1}. The next dinoflagellates most frequently on the list were three heterotrophic species, including *Protoperidinium* sp., *Gyrodinium* sp., and *Gyrodinium spirale*. Seven other dinoflagellates were on the Top-200 list multiple times, including three HAB species, including *Prorocentrum micans*, *Prorocentrum triestinum*, and *Karlodinium veneficum*.

Overall, diatoms showed lower biomass levels in the summer than fall (Table 3).

In the summer, two diatom species were present on the Top-200 list, *Leptocylindrus danicus*, with four entries, and *Dactyliosolen fragilissimus,* with one entry (Table 4). Both species are cosmopolitan in distribution (Hoppenrath et al., 2009). In the fall, there were five diatom taxa that appear on the Top-200 list, including *Guinardia delicatula, Paralia Sulcata, Brockmaniella brockmannii, Bellerochea horologicalis*, and an undefined centric diatom. *B. brockmannii* had the highest observed biomass at 76 µg carbon L^{-1}.

Within the "Other" category of taxa, prasinophytes (Chlorophyta) had the highest frequency of occurrence in the Top-200 list in both the summer and fall (Table 4). They were often among the numerically abundant taxa in many samples

TABLE 3 Comparison of mean phytoplankton biomass (µg carbon L^{-1}) by functional group between the four seasons with standard errors shown in parentheses.

Group	Spring	Summer	Fall	Winter
Diatom	15 (1.1) B	9.0 (0.8) A	30.2 (2.1) C	24.3 (1.8) C
	a	a	a	a
Dinoflagellate	16.9 (1.5) AB	12.6 (1.3) A	66.7 (6.0) C	22.1 (0.9) B
	a	b	b	a
Cyanobacteria	35.1 (1.7) A	65.7 (4.1) B	58.1 (4.0) B	36.6 (2.4) A
	b	c	b	b
Other*	12.8 (1.2) B	7.5 (0.6) A	34.1 (3.3) D	22.0 (2.5) C
	a	a	a	a
Total	79.8 (3.2) A	94.8 (4.1) B	189.1 (9.8) D	105.0 (3.8) C

Results of Games-Howell post-hoc pairwise comparison of means are shown with capital letters comparing the functional group across different seasons (horizontally) and lower-case letters comparing different functional groups in a single season (vertically). Mean values which share letter designations are not significantly different (p of 0.05).
*Other group included all other phytoplankton taxa (mostly nanoflagellate).

TABLE 4 Top-200 list of highest biomass of individual taxonomic groups for the summer and fall.

Top-200: Summer				
Species	Group	Freq. in Top-200	Highest Biomass μg carbon L^{-1}	Highest Density 10^3 cells L^{-1}
Spherical Picocyano spp.	Cyanobacteria	141	219	957,918
Synechococcus spp.		39	85	194,550
Azadinium caudatum	Dinoflagellate	**5**	**60**	**50**
Scrippsiella sp.^{M}		2	21	14
Torodinium robustum^{M}		1	17	18
Gyrodinium spirale^{H}		1	15	2
Leptocylindrus danicus	Diatom	4	23	113
Dactyliosolen fragilissimus		1	27	72
Prasinophyte spp.	Other	6	63	9,612
Top-200: Fall				
Species	Group	Freq. in Top-200	Highest Biomass μg carbon L^{-1}	Highest Density 10^3 cells L^{-1}
Spherical Picocyano spp.	Cyanobacteria	95	140	612,862
Trichodesmium erythraeum		**4**	**286**	**44**
Synechococcus spp.		1	33	75,965
Margelefidium polykrikoides^{M}	Dinoflagellate	11	92	20
Protoperidinium sp.^{H}		7	78	32
Gyrodinium sp.$^{M, H}$		7	54	713
Gyrodinium spirale^{H}		5	47	6
Scrippsiella sp.^{M}		4	76	50
Prorocentrum micans^{M}		**4**	**28**	**7**
Prorocentrum triestinum^{M}		**3**	**92**	**81**
Gymnoid spp. (UD)		3	62	831
Torodinium robustum^{M}		3	43	45
Kapelodinium vestifici		2	53	181
Karlodinium veneficum^{M}		**2**	**45**	**182**
Amphidinium sp.^{M}		1	45	54
Protoperidinium bipes^{H}		1	41	60
Protoperidinium steinii^{H}		1	26	26
Tripos hircus^{M}		1	25	8
Centric diatom sp.	Diatom	3	25	1
Guinardia delicatula		3	25	91
Paralia sulcata		2	32	131
Brockmanniella brockmannii		1	76	770
Bellerochea horologicalis		1	31	12
Prasinophyte spp.	Other	14	102	15,525
Eukaryotic nanoplankton (UD)		12	97	10,328
Spherical flagellate spp. (UD)		9	170	14,691

Table shows the frequency of occurrence of each taxa in the Top-200, the highest biomass and cell abundance of each taxa during each season. "^{M}" refers to taxa that are known to be mixotrophic through the ability to engage in phagotrophy, "^{H}" refers to heterotrophic species that do not contain plastids. "UD" refers to taxonomic group where species are not defined. Taxa in red lettering are known Harmful Algal Bloom (HAB) species (Lundholm et al., 2009; Lassus et al., 2016; Anderson et al., 2021).

next to picoplanktonic cyanobacteria, and in fall reached the fourth highest individual biomass observation on the Top-200 list, at 102 μg carbon L^{-1}. In the fall, other nanoplanktonic (i.e., >2–20 μm) taxa were in the Top-200 list, including undefined eukaryotic taxa and spherical flagellates.

Discussion

Phytoplankton biomass trends

The results of this study of the Cape Canaveral shelf (CCS) reveal distinct seasonal patterns in phytoplankton biomass and composition, and identify key environmental drivers. Using mean chlorophyll *a* as the measure of phytoplankton biomass, mean concentrations were higher in the fall and winter than in the spring or summer. A similar seasonal pattern has been reported in previous remote sensing studies of chlorophyll *a* in several other near-shore regions of the South Atlantic Bight along the east coast of the United States (Badylak and Phlips, 2004; Martins and Pelegrí, 2006; Signorini and McClain, 2007). The range of *in situ* chlorophyll *a* values is similar to the range of values for satellite studies of the broader South Atlantic Bight, i.e., 0.1–10 $\mu g\,L^{-1}$ (Yoder et al., 1993, 2001, 2002; Barnard et al., 1997). This range is also in line with chlorophyll *a* values reported for many other subtropical coastal regions across the globe (Gregg et al., 2005; Xiao et al., 2018).

Although seasonal trends in chlorophyll *a* in the CCS were similar using *in situ* and satellite data, satellite-derived values were proportionally higher by around 60% of the *in situ* values. Similar disparities have been reported for coastal zone color scanner (CZCS) data for the continental shelf of the Southeast United States, where chlorophyll concentrations from satellites were ~50% higher than chlorophyll concentrations of *in situ* collected samples (Martins and María, 1998, Martins and Pelegrí, 2006). Much of the disparity appears to arise from the MODIS chlorophyll *a* algorithm, which uses the OC3/OC4 band ratio (Hu et al., 2012) and is intended for clear, case-1 waters. Shallow continental shelf water has higher turbidity than open ocean waters, as a result surface reflectance in these regions can be mistaken as an increase in chlorophyll concentration. To combat this overestimation, some researchers have used regional remote sensing algorithms for chlorophyll estimates in shallow near-shore environments (Brewin et al., 2013; Vazyulya et al., 2014). The differences between *in situ* and satellite chlorophyll *a* concentrations may also been influenced by uneven vertical distribution of phytoplankton in the portion of the water column captured by the two methods.

Estimates of phytoplankton biomass in terms of carbon obtained from microscopic analyses of water samples collected *in situ* in the CCS, yielded similar seasonal patterns obtained using chlorophyll *a* data. The highest mean carbon values were observed in the fall, followed by winter, then summer, and the lowest in the spring. The fall peak in mean phytoplankton biomass contrasts with the more typical observation of peaks in the spring reported for many temperate environments (Yamada et al., 2004; Harding et al., 2005; Cloern and Jassby, 2008; Winder and Cloern, 2010; Carstensen et al., 2015). The factors that drive the seasonal pattern of phytoplankton biomass in the CCS can be viewed within the context of two related questions: (1) what conditions promote the potential for elevated phytoplankton biomass in the fall and winter, and (2) what explains the comparatively low average biomass in the spring and summer? Three features of the Cape Canaveral shelf provide insights into the potential for elevated fall and winter biomass: the shallow depth of the nearshore shelf as it relates to light availability in the mixed layer, subtropical climatic conditions in the region as it relates to temperature and light intensity optima for algal growth, and seasonal shifts in nearshore circulation patterns which help to define the origins of water masses flowing across the CCS.

The shallow CCS is generally characterized by polymictic conditions with the euphotic zone often extending to the seafloor. In deeper temperate coastal regions, increases in solar irradiance, temperature and water column stratification in the spring provide conditions that drive elevated phytoplankton production (Sverdrup, 1953; Ianson et al., 2001). In addition, the central east coast of Florida is within the sub-tropical zone between the tropical waters of the Florida Keys and temperate waters north of Florida, providing higher fall and winter incident light and temperature than at higher latitudes. For example, maximum daily incident irradiance at Cape Canaveral is ~420 Langley's day^{-1} in December, compared to only 250 Langley's day^{-1} in December on the shores of Long Island in New York (Oswald, 1988). The seasonal range of water temperatures in the CCS fluctuates between winter low temperatures near 20°C to summer high temperatures near 30°C, well within the range to support strong phytoplankton growth throughout the year (Karentz and Smayda, 1984; Andersson et al., 1994; Boyd et al., 2013). While these features help to explain the potential for high phytoplankton biomass in the fall and winter, they do not explain the comparatively low phytoplankton biomass in the spring and summer when light and temperature conditions should be favorable.

Another important feature of the east coast of Florida is seasonal shifts in the prevailing longshore wind direction (Signorini and McClain, 2007; AlYousif et al., 2021), with a predominance of winds from the north in the fall and winter, and the reverse in the spring and summer. Longshore winds have a strong influence on the direction of currents along the inner shelf of Florida (Signorini and McClain, 2007; Miles and He, 2010; AlYousif et al., 2021). Seasonal changes in these wind patterns change the origin of water masses entering the CCS, which play a role in defining phytoplankton biomass and composition in the region. In other words, the character of the phytoplankton community is partially determined by the history of water masses introduced to the CCS from the north, south or east by longshore currents, eddies from the Gulf Stream, or upwelling of deep water from off the shelf (Atkinson et al., 1978, 1984; Lee et al., 1985).

During the peak phytoplankton biomass seasons of fall and winter, the predominant wind and surface current direction along the east coast of north Florida is from the north (Signorini and McClain, 2007, AlYousif et al., 2021). Nearshore water masses moving southward along the Florida peninsula toward the CCS interact with a number of major inputs from the peninsula, including the St. Johns River (one of Florida's largest rivers) and three inlets to the intracoastal waterway: St. Augustine, Matanzas, and Ponce de Leon (Figure 1). The St. Johns River, and the inner barrier island estuaries linked to the three inlets, are associated with watersheds subject to significant cultural eutrophication and periodic major algal blooms (Scholl et al., 1980; Hendrickson et al., 2002; Phlips et al., 2007, 2015, 2021; Dix et al., 2013; Srifa et al., 2016; Herren et al., 2021). The St Johns River provides the highest riverine discharges to the eastern coast of Florida (Nordlie, 1990), with the fall demonstrating highest mean discharges within the annual cycle (Srifa et al., 2016). Watershed inputs of nutrients to the river yield high levels of nitrogen and phosphorus in the downstream reaches of the river, which are transformed into elevated levels of NH_4^+, NO_x^-, and dissolved inorganic phosphorus in the estuary (Wang and Zhang, 2020). Short water residence times in the saline reaches of the river diminish the potential for major marine

phytoplankton blooms in the estuary, but elevated levels of phytoplankton have been detected in the river plume in the Atlantic shelf (Wang and Zhang, 2020).

Similar to the St. Johns River, the estuaries associated with the St. Augustine, Matanzas, and Ponce de Leon inlets are subject to significant cultural eutrophication, and are characterized by high nutrient levels compared to coastal waters (Dix et al., 2013; Phlips et al., 2010, 2021). Taken together, these observations indicate that inputs from estuaries along the northeast coast of Florida enhance nutrient and algal loads to the coast, which can be the basis for increases in phytoplankton biomass extending from the outflow of the St. Johns River down to the CCS – as illustrated by satellite images of nearshore chlorophyll *a* levels (e.g., Figure 11). Nutrient loads are heightened due to increased discharges during the fall because of high rainfall levels in the late summer and early fall, in part due to tropical storm activity during the peak of the hurricane season (i.e., August–October; Srifa et al., 2016; Phlips et al., 2020).

In contrast to fall and winter, there are two major components of water movement from the south during the spring and summer: (1) nearshore currents that move up the coast from the south, and (2) the Florida Current (Gulf Stream), which passes ~60 miles off the shore of Cape Canaveral, and is subject to eddies which propagate off the current toward the coast. A satellite image from August 2018 (Figure 11) illustrates the effect of northerly nearshore water movement on chlorophyll *a* levels in the summer, with elevated levels of chlorophyll *a* north of the outflow of the St. Johns River. This image indicates that nutrient and algal inputs from the river and other tributaries in Georgia (e.g., St. Mary's River) and the Carolinas have a positive effect on phytoplankton biomass on the nearshore shelf. The Florida Current can influence the CCS directly when eddies periodically come off the western side of the Current (Yoder et al., 1981; Lee and Atkinson, 1983) driving water of tropical origin with comparatively low phytoplankton biomass and nutrient levels onto the shelf. Winds from the south in the summer can also drive upwelling of deep water from off the continental shelf into nearshore regions (Atkinson, 1977; Atkinson et al., 1978; Yoder et al., 1985; Miles and He, 2010). Deep cold-water intrusion onto the shelf likely has a depressing effect on phytoplankton biomass since it is low in phytoplankton abundance. While deep-water can contain elevated nutrient levels, the infrequency and limited magnitude of the events, and the limited residence time of the deep-water on the inner shelf, minimize the potential for significant impacts of autochthonous phytoplankton production from the upwelling on inner shelf biomass.

Seasonal differences in phytoplankton composition

The hypothesis that seasonal differences in phytoplankton biomass are in part linked to changes in the sources of water masses passing through the CCS is further supported by seasonal differences observed in the character of phytoplankton communities. These differences are illustrated by a comparison of the species composition in the Top-200 list of highest biomass of individual taxonomic groups for the summer and fall. In the summer, the list is dominated by picoplanktonic cyanobacteria, which likely reflects a strong influence of Gulf Stream water. The latter observation coincides with previous studies that show the prominence of this group in open ocean ecosystems around the world (Jochem, 2003; Vaulot et al., 2008; Flombaum et al., 2013; Caroppo, 2015; Linacre et al., 2019). Picocyanobacteria have been shown to account for up to 80% of the total primary production in the tropical Eastern Pacific, and for ~60% in the tropical Western Atlantic (Blanchot et al., 1992). The peak densities for picocyanobacteria in this study (10^9 cells L^{-1}) were generally higher than typically found in the open ocean (Flombaum et al., 2013), but similar to values observed in some other nearshore habitats where upwelled nutrients or terrestrial nutrient inputs provide the potential for higher biomass levels (Paerl et al., 2010; Scanlon, 2012, Caroppo, 2015).

In the fall, while picoplanktonic cyanobacteria are still well represented on the Top-200 list, dinoflagellates and nanoplanktonic eukaryotes are also prominent. Dinoflagellates on the list included a range of obligate autotrophs, mixotrophs and heterotrophs. For example, one of the mixotrophic dinoflagellates most frequently present on the fall Top-200 list is the HAB species *Margelefidinium polykrikoides* (aka *Cochlodinium polykrikoides*). *M. polykrikoides* has been linked to bloom events in other ecosystems subject to elevated levels of NH_4 and dissolved organic nitrogen (DON; Kudela and Gobler, 2012; Qin et al., 2021). It has been proposed that elevated levels of NH_4^+ and DON provide a competitive advantage for dinoflagellates over diatoms, which favor elevated levels of nitrate as the principal source of nitrogen (Kang and Kang, 2022) and can even be inhibited by high levels of NH_4^+ (Lomas and Glibert, 1999; Berg et al., 2003). By contrast, many dinoflagellates and cyanobacteria are efficient users of NH_4^+ and dissolved organic forms of nitrogen, such as urea (Glibert et al., 2006; Hattenrath-Lehmann and Gobler, 2015; Huang et al., 2020; Ivey et al., 2020), and many mixotrophic/heterotrophic dinoflagellates, like *M. polykrikoides*, can also take advantage of particulate carbon and nitrogen through phagotrophy (Jeong et al., 2004).

The major sources of water inflows into the northeast coast of Florida emanate from estuaries that have experienced significant anthropogenic eutrophication over the past century, including the St. Johns River, St. Augustine Inlet, Matanzas Inlet, and the Ponce de Leon Inlet. Many of the dinoflagellate species most prominently represented on the Top-200 list for fall are also commonly observed in the aforementioned estuaries (Hart et al., 2015; Phlips et al., 2011, 2021). In addition, the strong representation of nanoplanktonic species (i.e., prasinophytes and other undefined nanoplanktonic eukaryote) in the Top-200 list for the fall is a feature shared by the aforementioned northeast coastal estuaries and the CCS, and may in part reflect elevated levels of inorganic and organic forms of nutrients. Taken together, these observations support the hypothesis that inputs from estuaries along the Northeast coast of Florida strongly influence not only nutrient levels along the coast, but also the composition and biomass of phytoplankton communities in water masses moving southward toward the CCS in the fall and winter.

Top-down control and other issues

Top-down processes may also contribute to the seasonal pattern of phytoplankton biomass in the CCS. While there are little data on zooplankton grazing rates in the CCS, a recent contemporaneous study of regional zooplankton composition may provide some insights (Phlips et al., 2022). The study showed that ciliates on average represent over a third of total zooplankton biomass. The same study also showed that pico- and nano-phytoplankton taxa represented on average over 50% of total phytoplankton biomass (Tate et al., 2020). Since ciliates are known to be a

major grazer of pico- and nanoplankton (Pierce and Turner, 1992; Calbet and Landry, 2004), they likely play a role in top-down control of phytoplankton biomass. This observation highlights the importance of microbial loop processes (Pomeroy et al., 2007; Fenchel, 2008) in the CCS. The role of the zooplankton community on top-down control of phytoplankton biomass warrants further investigation, as does the role of other key microbial interactions, such as the impacts of marine viruses, which affect the dynamics of phytoplankton populations and nutrients within the water column (Lehahn et al., 2014; Weitz et al., 2015; Knowles et al., 2020).

Conclusion

The atypical pattern of fall/winter peaks of phytoplankton biomass in the Cape Canaveral shelf (CCS) are strongly influenced by allochthonous inputs. Although the CCS is not directly impacted by major river discharge, the origins of water masses moving through the region help to explain the observed seasonality of phytoplankton biomass. In the fall and winter, wind-driven southerly movement of water masses along the coast of northern Florida are exposed to inputs from nutrient- and phytoplankton-rich rivers and inlets to barrier island estuaries. The inputs enhance phytoplankton biomass potential of water masses that ultimately reach CCS. By contrast, persistent south easterly trade winds in the spring and summer enhance the influence of more oligotrophic Gulf Stream waters on the CCS, resulting in lower seasonal average phytoplankton biomass. The seasonal patterns observed highlight the potential sensitivity of coastal phytoplankton communities to continuing cultural eutrophication and future climate changes, such as higher temperatures, frequency and intensity of tropical storms, and alterations in the character and quantity of discharges from land.

Data availability statement

The raw data supporting the conclusions of this article will be made available by the authors, without undue reservation.

Author contributions

BS primary author of the manuscript. EP corresponding author, and contributing author of the manuscript. SB primary taxonomist on research. LL field research leader. MT assistant taxonomist on research. AW-V co-leader of field research. All authors contributed to the article and approved the submitted version.

Funding

This study was funded by U.S. Department of Interior, CFDA no. 15.424, agreement number M13AC00012.

Acknowledgments

We thank the U.S. Department of Interior, Bureau of Ocean Energy Management (BOEM), who funded this project (CFDA No. 15.424, Agreement Number M13AC00012). EP and SB are supported by the USDA National Institute of Food and Agriculture, Hatch Project 1017098. Special thanks to Debra Murie for leading and coordinating the overall BOEM project.

Conflict of interest

The authors declare that the research was conducted in the absence of any commercial or financial relationships that could be construed as a potential conflict of interest.

Publisher's note

All claims expressed in this article are solely those of the authors and do not necessarily represent those of their affiliated organizations, or those of the publisher, the editors and the reviewers. Any product that may be evaluated in this article, or claim that may be made by its manufacturer, is not guaranteed or endorsed by the publisher.

References

Ahlgren, G. (1983). Comparison of methods for estimation of phytoplankton carbon. *Arch Hydrobiologia* 98, 489–508.

AlYousif, A., Laurel-Castillo, J. A., So, S., Parra, S. M., Adams, P., and Valle-Levinson, A. (2021). Subinertial hydrodynamics around a cape influenced by a western boundary current. *Estuar. Coast. Shelf Sci.* 251:107199. doi: 10.1016/j.ecss.2021.107199

Anderson, D., Fensin, E., Gobler, C., Hoeglund, A., Hubbard, K., Kulis, D., et al. (2021). Marine harmful algal blooms (HABs) in the United States: history, current status and future trends. *Harmful Algae* 102:101975. doi: 10.1016/j.hal.2021.101975

Andersson, A., Haecky, P., and Hagström, Å. (1994). Effect of temperature and light on the growth of micro- nano- and pico-plankton: impact on algal succession. *Mar. Biol.* 120, 511–520. doi: 10.1007/BF00350071

APHA (2005). *Standard methods, 21st ed.*. American Public Health Association, Baltimore, Maryland.

Atkinson, L. P. (1977). Modes of gulf stream intrusion into the South Atlantic bight shelf waters. *Geophys. Res. Lett.* 4, 583–586. doi: 10.1029/GL004i012p00583

Atkinson, L. P., O'Malley, P. G., Yoder, J. A., and Paffenhöfer, G. A. (1984). The effect of summertime shelf break upwelling on nutrient flux in southeastern United States continental shelf waters. *J. Mar. Res.* 42, 969–993. doi: 10.1357/002224084788520756

Atkinson, L., Paffenhöfer, G.-A., and Dunstan, W. (1978). The chemical and biological effect of a gulf stream intrusion off St. Augustine, Florida. *Bull. Mar. Sci.* 28, 667–679.

Badruzzaman, M., Pinzon, J., Oppenheimer, J., and Jacangelo, J. G. (2012). Sources of nutrients impacting surface waters in Florida: a review. *J. Environ. Manag.* 109, 80–92. doi: 10.1016/j.jenvman.2012.04.040

Badylak, S., and Phlips, E. J. (2004). Spatial and temporal patterns of phytoplankton composition in a subtropical lagoon, the Indian River lagoon, Florida, USA. *J. Plankton Res.* 26, 1229–1247. doi: 10.1093/plankt/fbh114

Barnard, A. H., Stegmann, P. M., and Yoder, J. A. (1997). Seasonal surface ocean variability in the South Atlantic bight derived from CZCS and AVHRR imagery. *Cont. Shelf Res.* 17, 1181–1206. doi: 10.1016/S0278-4343(97)00002-2

Berg, G. M., Balode, M., Purina, I., Bekere, S., Bechemin, C., and Maestrini, S. Y. (2003). Plankton community composition in relation to availability and uptake of oxidized and reduced nitrogen. *Aquat. Microb. Ecol.* 30, 263–274. doi: 10.3354/ame030263

Blanchot, J., Rodier, M., and Bouteiller, L. (1992). Effect of El Niño southern oscillation events on the distribution and abundance of phytoplankton in the western Pacific tropical ocean along the 165°E. *J. Plankton Res.* 14, 137–156. doi: 10.1093/plankt/14.1.137

Bontempi, P. S., and Yoder, J. A. (2004). Spatial variability in SeaWiFS imagery of the South Atlantic bight as evidenced by gradients (fronts) in chlorophyll *a*, and water-

leaving radiance. *Deep-Sea Res. II Top. Stud. Oceanogr.* 51, 1019–1032. doi: 10.1016/S0967-0645(04)00098-0

Boyd, P. W., Rynearson, T. A., Armstrong, E. A., Fu, F., Hayashi, K., Hu, Z., et al. (2013). Marine phytoplankton temperature versus growth responses from polar to tropical waters – outcome of a scientific community-wide study. *PLoS One* 8:e63091. doi: 10.1371/journal.pone.0063091

Brewin, R. J. W., Raitsos, D. E., Pradhan, Y., and Hoteit, I. (2013). Comparison of chlorophyll in the Red Sea derived from MODIS-aqua and in vivo fluorescence. *Remote Sens. Environ.* 136, 218–224. doi: 10.1016/j.rse.2013.04.018

Calbet, A., and Landry, M. R. (2004). Phytoplankton growth, microzooplankton grazing, and carbon cycling in marine systems. *Limnol. Oceanogr.* 49, 51–57. doi: 10.4319/lo.2004.49.1.0051

Caroppo, C. (2015). Ecology and biodiversity of picoplanktonic cyanobacteria in coastal and brackish environments. *Biodivers. Conserv.* 24, 949–971. doi: 10.1007/s10531-015-0891-y

Carstensen, J., Klais, R., and Cloern, J. E. (2015). Phytoplankton blooms in estuarine and coastal waters: seasonal patterns and key species. *Estuar. Coast. Shelf Sci.* 162, 98–109. doi: 10.1016/j.ecss.2015.05.005

Cloern, J. E., Foster, S. Q., and Kleckner, A. E. (2014). Phytoplankton primary production in the world's estuarine-coastal ecosystems. *Biogeosciences* 11, 2477–2501. doi: 10.5194/bg-11-2477-2014

Cloern, J. E., and Jassby, A. D. (2008). Complex seasonal patterns of primary producers at the land–sea interface. *Ecol. Lett.* 11, 1294–1303. doi: 10.1111/j.1461-0248.2008.01244.x

Dix, N., Phlips, E. J., and Suscy, P. (2013). Factors controlling phytoplankton biomass in a subtropical coastal lagoon: relative scales of influence. *Estuar. Coasts* 36, 981–996. doi: 10.1007/s12237-013-9613-4

Estrada, M., Delgado, M., Blasco, D., Latasa, M., Cabello, A. M., Benítez-Barrios, V., et al. (2016). Phytoplankton across tropical and subtropical regions of the Atlantic, Indian and Pacific oceans. *PLoS One* 11:e0151699. doi: 10.1371/journal.pone.0151699

Falkowski, P. G., Barber, R. T., and Smetacek, V. (1998). Biogeochemical controls and feedbacks on ocean primary production. *Science* 281, 200–206. doi: 10.1126/science.281.5374.200

Fenchel, T. (2008). The microbial loop – 25 years later. *J. Exp. Mar. Biol. Ecol.* 366, 99–103. doi: 10.1016/j.jembe.2008.07.013

Flombaum, P., Gallegos, J. L., Gordillo, R. A., Rincón, J., Zabala, L. L., Jiao, N., et al. (2013). Present and future global distributions of the marine cyanobacteria *Prochlorococcus* and *Synechococcus*. *Proc. Natl. Acad. Sci. U. S. A.* 110, 9824–9829. doi: 10.1073/pnas.1307701110

Games, P. A., and Howell, J. F. (1976). Pairwise multiple comparison procedures with unequal N's and/or variances: a Monte Carlo study. *J. Educ. Stat.* 1, 113–125.

Glibert, P. M., and Burkholder, J. A. M. (2020). Harmful algae at the complex nexus of eutrophication and climate change. *Harmful Algae* 29, 724–738. doi: 10.1007/s00343-011-0502-z

Glibert, P. M., Harrison, J., Heil, C., and Seitzinger, S. (2006). Escalating worldwide use of urea – a global change contributing to coastal eutrophication. *Biogeochemistry* 77, 441–463. doi: 10.1007/s10533-005-3070-5

Gorelick, N., Hancher, M., Dixon, M., Ilyushchenko, S., Thau, D., and Moore, R. (2017). Google earth engine: planetary-scale geospatial analysis for everyone. *Remote Sens. Environ.* 202, 18–27. doi: 10.1016/j.rse.2017.06.031

Grattan, L. M., Holobaugh, S., and Morris, J. G. (2016). Harmful algal blooms and public health. *Harmful Algae* 57, 2–8. doi: 10.1016/j.hal.2016.05.003

Gregg, W. W., Casey, N. W., and McClain, C. R. (2005). Recent trends in global ocean chlorophyll. *Geophys. Res. Lett.* 32:L03606. doi: 10.1029/2004GL021808

Griffith, A. W., and Gobler, C. J. (2020). Harmful algal blooms: a climate change co-stressor in marine and freshwater ecosystems. *Harmful Alga* 91:101590. doi: 10.1016/j.hal.2019.03.008

Harding, L. W., Magnuson, A., and Mallonee, M. E. (2005). SeaWiFS retrievals of chlorophyll in Chesapeake Bay and the mid-Atlantic bight. *Estuar. Coast. Shelf Sci.* 62, 75–94. doi: 10.1016/j.ecss.2004.08.011

Harris, P. T., Macmillan-Lawler, M., Rupp, J., and Baker, E. K. (2014). Geomorphology of the oceans. *Mar. Geol.* 352, 4–24. doi: 10.1016/j.margeo.2014.01.011

Hart, J. A., Phlips, E. J., Badylak, S., Dix, N., Petrinec, K., Mathews, A. L., et al. (2015). Phytoplankton biomass and composition in a well-flushed sub-tropical estuary: the contrasting effects of hydrology, nutrient loads and allochthonous influences. *Mar. Environ. Res.* 112, 9–20. doi: 10.1016/j.marenvres.2015.08.010

Hattenrath-Lehmann, T., and Gobler, C. J. (2015). The contribution of inorganic and organic nutrients to the growth of a north American isolate of the mixotrophic dinoflagellate, *Dinophysis acuminata*. *Limnol. Oceanogr.* 60, 1588–1603. doi: 10.1002/lno.10119

Heil, C. A., Dixon, L. K., Hall, E., Garrett, M., Lenes, J. M., O'Neil, J. M., et al. (2014). Blooms of Karenia brevis (Davis) G. Hansen & Ø. Moestrup on the West Florida shelf: nutrient sources and potential management strategies based on a multi-year regional study. *Harmful Algae* 38, 127–140. doi: 10.1016/j.hal.2014.07.016

Heisler, J. P., Glibert, P. M., Burkholder, J. A., Anderson, D. M., Cochlan, W., Dennison, W., et al. (2008). Eutrophication and harmful algal blooms: a scientific consensus. *Harmful Algae* 8, 3–13. doi: 10.1016/j.hal.2008.08.006

Hendrickson, J., Trahan, E., Stecker, E., and Ouyang, Y. (2002). *TMDL, and PLRG modeling for the lower St. Johns River: calculation of the external load. Technical memorandum*, 109. St. Johns River Water Management District, Palatka, Florida.

Herren, L. W., Brewton, R. A., Wilking, L. E., Tarnowski, M. E., Vogel, M. A., and Lapointe, B. E. (2021). Septic systems drive nutrient enrichment of groundwaters and eutrophication in the urbanized Indian River lagoon, Florida. *Mar. Pollut. Bull.* 172:112928. doi: 10.1016/j.marpolbul.2021.112928

Herrmann, M., Najjar, R. G., Kemp, W. M., Alexander, R. B., Boyer, E. W., Cai, W., et al. (2015). Net ecosystem production and organic carbon balance of U.S. east coast estuaries: a synthesis approach. *Glob. Biogeochem. Cycles* 29, 96–111. doi: 10.1002/2013GB004736

Hoagland, P., Jin, D., Beet, A., Kirkpatrick, B., Reich, A., Ullmann, S., et al. (2014). The human health effects of Florida red tide (FRT) blooms: an expanded analysis. *Environ. Int.* 68, 144–153. doi: 10.1016/j.envint.2014.03.016

Hoppenrath, M., Elbrächter, M., and Drebes, G. (2009). Marine Phytoplankton. Kleine Senckenberg-Reihe 49. (Stuttgart, Germany: E. Schweizerbart'sche Verlagsbuchhandlung).

Hu, C., Lee, Z., and Franz, B. (2012). Chlorophyll algorithms for oligotrophic oceans: a novel approach based on three-band reflectance difference. *J. Geophys. Res. Oceans* 117:117. doi: 10.1029/2011JC007395

Huang, K., Feng, Q., Zhang, Y., Ou, L., Cen, J., Lu, S., et al. (2020). Comparative uptake and assimilation of nitrate, ammonium, and urea by dinoflagellate *Karenia mikimotoi* and diatom *Skeletonema costatum* in the coastal waters of the East China Sea. *Mar. Pollut. Bull.* 155:111200. doi: 10.1016/j.marpolbul.2020.111200

Iafrate, J., Watwood, J. S., Reyier, E., Ahr, B. J., Scheidt, D. M., Holloway-Adkins, K. G., et al. (2019). Behavior, Seasonality, and Habitat Preferences of Mobile Fishes and Sea Turtles within a Large Sand Shoal Complex: Insights from Traditional Sampling and Emerging Technologies. Report to US Dept. of Interior, Bureau of Ocean Energy Mgmt. OCS Study BOEM 43.

Ianson, D., Pond, S., and Parsons, T. (2001). The spring phytoplankton bloom in the coastal Temperate Ocean: growth criteria and seeding from shallow Embayments. *J. Oceanogr.* 57, 723–734. doi: 10.1023/A:1021288510407

Irizarry-Ortiz, M. M., Obeysekera, J., Park, J., Trimble, P., Barnes, J., Park-Said, W., et al. (2013). Historical trends in Florida temperature and precipitation. *Hydrol. Process.* 27, 2225–2246. doi: 10.1002/hyp.8259

Ivey, J. E., Wolny, J. L., Heil, C. A., Murasko, S. M., Brame, J. A., and Parks, A. A. (2020). Urea inputs drive picoplankton blooms in Sarasota Bay, Florida, USA. *Water* 12:2755. doi: 10.3390/w12102755

Jeong, H. J., Yoo, Y. D., Kim, J. S., Kim, T. H., Kim, J. H., Kang, N. S., et al. (2004). Mixotrophy in the phototrophic harmful alga *Cochlodinium polykrikoides* (Dinophycean): prey species, the effects of prey concentration, and grazing impact. *J. Eukaryot. Microbiol.* 51, 563–569. doi: 10.1111/j.1550-7408.2004.tb00292.x

Jochem, F. J. (2003). Photo- and heterotrophic pico- and nanoplankton in the Mississippi River plume: distribution and grazing activity. *J. Plankton Res.* 25, 1201–1214. doi: 10.1093/plankt/fbg087

Justice, C. O., Vermote, E., Townshend, J. R. G., Defries, R., Roy, D. P., Hall, D. K., et al. (1998). The moderate resolution imaging Spectroradiometer (MODIS): land remote sensing for global change research. *IEEE Trans. Geosci. Remote Sens.* 36, 1228–1249. doi: 10.1109/36.701075

Kang, Y., and Kang, C. (2022). Reduced forms of nitrogen control the spatial distribution of phytoplankton communities: the functional winner, dinoflagellates in an anthropogenically polluted estuary. *Mar. Pollut. Bull.* 177:113528. doi: 10.1016/j.marpolbul.2022.113528

Karentz, D., and Smayda, T. (1984). Temperature and seasonal occurrence patterns of 30 dominant phytoplankton species in Narragansett Bay over a 22-year period (1959-1980). *Mar. Ecol. Prog. Ser.* 18, 277–293. doi: 10.3354/meps018277

Knowles, B., Bonachela, J., Behrenfeld, M., Bondoc, K., Cael, B., Carlson, C., et al. (2020). Temperate infection in a virus–host system previously known for virulent dynamics. *Nat. Commun.* 11:4626. doi: 10.1038/s41467-020-18078-4

Kudela, R., and Gobler, C. J. (2012). Harmful dinoflagellate blooms caused by *Cochlodinium* sp.: global expansion and ecological strategies facilitating bloom formation. *Harmful Algae* 14, 71–86. doi: 10.1016/j.hal.2011.10.015

Lapointe, B. E., Herren, L. W., Debortoli, D. D., and Vogel, M. A. (2015). Evidence of sewage-driven eutrophication and harmful algal blooms in Florida's Indian River Lagoon. *Harmful Algae*. 43, 82–101.

Lassus, P., Chomérat, N., Hess, P., and Nézan, E. (2016). Toxic and Harmful Microalgae of the World Ocean in Manuals and Guides 68. (Copenhagen, Denmark: International Society for the Study of Harmful Algae, International Oceanographic Committee, UNESCO).

Lee, T. N., and Atkinson, L. P. (1983). Low-frequency current and temperature variability from gulf stream frontal eddies and atmospheric forcing along the southeast U.S. outer continental shelf. *J. Geophys. Res. Oceans* 88, 4541–4567. doi: 10.1029/JC088iC08p04541

Lee, T. N., Kourafalou, V., Wang, J. D., Ho, W. J., Blanton, J. O., Atkinson, L. P., et al (1985) "Shelf Circulation from Cape Canaveral to Cape Fear during Winter," in *Oceanography of the Southeastern US Continental Shelf*, eds. L. P. Atkinson, D. W. Menzel and K. A. Bush (Washington, D.C.: American Geophysical Union (AGU)) 2, 33–62.

Lehahn, Y., Koren, I., Schatz, D., Frada, M., Sheyn, U., Boss, E., et al. (2014). Decoupling physical from biological processes to assess the impact of viruses on a mesoscale algal bloom. *Curr. Biol.* 24, 2041–2046. doi: 10.1016/j.cub.2014.07.046

Linacre, L., Durazo, R., Camancho-Ibar, V., Selph, K., Lara-Lara, J., Mirabal-Gómez, U., et al. (2019). Picoplankton carbon biomass assessments and distribution of Prochlorococcus ecotype linked to loop current eddies during summer in the southern Gulf of Mexico. *J. Geophys. Res. Oceans* 124, 8342–8359. doi: 10.1029/2019JC015103

Liu, M., Lei, X., Zhou, Y., Gao, J., Zhou, Y., Wang, L., et al. (2022). Save reservoirs of humid subtropical cities from eutrophication threat. *Environ. Sci. Pollut. Res.* 29, 949–962. doi: 10.1007/s11356-021-15560-4

Lomas, M., and Glibert, P. (1999). Interactions between NH4+ and NO3- uptake and assimilation: comparison of diatoms and dinoflagellates at several growth temperatures. *Mar. Biol.* 133, 541–551. doi: 10.1007/s002270050494

Longley, K. R., Huang, W., Clark, C., and Johnson, E. (2019). Effects of nutrient load from St. Jones river on water quality and eutrophication in Lake George, Florida. *Limnologica* 77:125687. doi: 10.1016/j.limno.2019.125687

Lundholm, N., Churro, C., Fraga, S., Hoppenrath, M., Iwataki, M., Larsen, J., et al (Eds). (2009). IOC-UNESCO Taxonomic Reference List of Harmful Micro Algae. Available at: https://www.marinespecies.org/hab

Martins, F. D. S. F., and María, A. (1998). Winter variability of CZCS – derived pigment distributions on the southeastern U.S. continental shelf from 1978 to 1986. PhD thesis. Universidad de Las Palmas de Gran Canaria.

Martins, A. M., and Pelegrí, J. L. (2006). CZCS chlorophyll patterns in the South Atlantic bight during low vertical stratification conditions. *Cont. Shelf Res.* 26, 429–457. doi: 10.1016/j.csr.2005.11.012

Menden-Deuer, S., and Lessard, E. J. (2000). Carbon to volume relationships for dinoflagellates, diatoms and other protist plankton. *Limnol. Oceanogr.* 45, 569–579. doi: 10.4319/lo.2000.45.3.0569

Miles, T. N., and He, R. (2010). Temporal and spatial variability of Chl-a and SST on the South Atlantic bight: revisiting with cloud-free reconstructions of MODIS satellite imagery. *Cont. Shelf Res.* 30, 1951–1962. doi: 10.1016/j.csr.2010.08.016

Nixon, S. W. (1995). Coastal marine eutrophication. A definition, social consequences and future concerns. *Ophelia* 41, 199–219. doi: 10.1080/00785236.1995.10422044

Nordlie, F. (1990). "Rivers and springs" in *Ecosystems of Florida*. eds. R. Myers and J. Ewel (Orlando, FL., USA: University of Central Florida).

Oswald, W. J. (1988). "Micro-algae and wastewater treatment," in *Microalgal Biotechnology*, eds. M. Borowitzka and L. Borowitzka (Cambridge, UK: Cambridge University Press), 305–328.

Paerl, H. W., Rossignol, K. L., Hall, S. N., Peierls, B. L., and Wetz, M. S. (2010). Phytoplankton community indicators of short- and long-term ecological change in the anthropogenically and climatically impacted Neuse River Estuary, North Carolina, USA. *Estuaries Coasts* 33, 485–497.

Paerl, H., Valdes, L. M., Peierls, B. L., Adolf, J. E., and Harding, L. W. (2006). Anthropogenic and climatic influences on the eutrophication of large estuarine systems. *Limnol. Oceanogr.* 51, 448–462. doi: 10.4319/lo.2006.51.1_part_2.0448

Peters, G-J. Y. (2018). Userfriendlyscience: Quantitative Analysis Made Accessible. doi: 10.17605/osf.io/txequ

Phlips, E. J., Badylak, S., Christman, M. C., and Lasi, M. A. (2010). Climatic trends and temporal patterns of phytoplankton composition, abundance and succession in the Indian River Lagoon, Florida, USA. Estuaries Coasts 33, 498–512.

Phlips, E. J., Badylak, S., Christman, M., Wolny, J., Garland, J., Hall, L., et al. (2011). Scales of temporal and spatial variability of harmful algae blooms in the Indian River, Florida, USA. Harmful Algae. 10, 277–290.

Phlips, E. J., Badylak, S., Landauer, L., West-Valle, A., and Stelling, B. (2022). "Chapter 9. Zooplankton," in *Ecological function and recovery of biological communities within dredged ridge-swale habitats in the South-Atlantic bight*. Murie D. J., Smith G. H. Eds. U.S. Department of Interior, Bureau of Ocean Energy Management. Final report for agreement number M13AC00012.

Phlips, E. J., Badylak, S., Lasi, M. A., Chamberlain, R., Green, W. C., Hall, L. M., et al. (2015). From red tides to Green and Brown tides: bloom dynamics in a restricted subtropical lagoon under shifting climatic conditions. *Estuar. Coasts* 38, 886–904. doi: 10.1007/s12237-014-9874-6

Phlips, E. J., Badylak, S., and Lynch, T. L. (1999). Blooms of the picoplanktonic cyanobacterium *Synechococcus* in Florida bay. *Limnol. Oceanogr.* 44, 1166–1175. doi: 10.4319/lo.1999.44.4.1166

Phlips, E. J., Badylak, S., Nelson, N., Hall, L., Jacoby, C., Lasi, M., et al. (2021). Cyclical patterns and a regime shift in the character of phytoplankton blooms in a restricted sub-tropical lagoon, Indian River lagoon, Florida, USA. *Front. Mar. Sci.* 8:730934. doi: 10.3389/fmars.2021.730934

Phlips, E. J., Badylak, S., Nelson, N., and Havens, K. (2020). Hurricanes, El Niño and harmful algal blooms in two sub-tropical Florida estuaries: direct and indirect impacts. *Sci. Rep.* 10:1910. doi: 10.1038/s41598-020-58771-4

Phlips, E. J., Hendrickson, J., Quinlan, E. L., and Cichra, M. (2007). Meteorological influences on algal bloom potential in a nutrient-rich Blackwater river. *Freshw. Biol.* 52, 2141–2155. doi: 10.1111/j.1365-2427.2007.01844.x

Pierce, R. W., and Turner, J. T. (1992). Ecology of planktonic ciliates in marine food webs. *Rev. Aquat. Sci.* 6, 139–181.

Pomeroy, L. R., Williams, P. J., Azam, F., and Hobbie, J. E. (2007). The microbial loop. *Oceanography* 20, 28–33. doi: 10.5670/oceanog.2007.45

Qin, Q., Shen, J., Reece, K., and Mulholland, M. (2021). Developing a 3D mechanistic model for examining factors contributing to harmful blooms of *Margelefidinium polykrikoides* in a temperate estuary. *Harmful Algae* 105:102055. doi: 10.1016/j.hal.2021.102055

Sartory, D. P., and Grobbelaar, J. U. (1984). Extraction of chlorophyll a from freshwater phytoplankton for spectrophotometric analysis. *Hydrobiologia* 114, 177–187. doi: 10.1007/BF00031869

Scanlon, D. J. (2012). "Marine picocyanobacteria" in *Ecology of Cyanobacteria II: Their Diversity in Space and Time*. ed. B. A. Whitton (Dordrecht: Springer Netherlands), 503–533.

Scholl, J., Heaney, J., and Huber, W. (1980). Water quality analysis of the Halifax River, Florida. *Water Resour. Bull.* 16, 285–293. doi: 10.1111/j.1752-1688.1980.tb02392.x

Sicko-Goad, L. M., Schelske, C. L., and Stoermer, E. F. (1984). Estimation of intracellular carbon and silica content of diatoms from natural assemblages using morphometric techniques. *Limnol. Oceanogr.* 29, 1170–1178. doi: 10.4319/lo.1984.29.6.1170

Signorini, S. R., and McClain, C. R. (2007). Large-Scale Forcing Impact on Biomass Variability in the South Atlantic Bight. *Geophys. Res. Lett.* 21, 1–6. doi: 10.1029/2007GL031121

Simons, R. A. (2011). ERDDAP. Monterey, CA: NOAA/NMFS/SWFSC/ERD. Available at: https://coastwatch.pfeg.noaa.gov/erddap

Smayda, T. J. (1978). "From phytoplankters to biomass" in *Phytoplankton manual*. ed. A. Sournia (Paris: UNESCO), 273–279.

Srifa, A., Phlips, E. J., and Hendrickson, J. (2016). How many seasons are there in a sub-tropical lake? A multivariate statistical approach to determine seasonality and its application to phytoplankton dynamics. *Limnologica* 60, 39–50. doi: 10.1016/j.limno.2016.05.011

Steidinger, K. A. (2009). Historical perspective on Karenia brevis red tide research in the Gulf of Mexico. *Harmful Algae* 8, 549–561. doi: 10.1016/j.hal.2008.11.009

Stich, H., and Brinker, A. (2005). Less is better: uncorrected versus pheopigment-corrected photometric chlorophyll-a estimation. *Archiv für Hydrobiologia* 162, 111–120. doi: 10.1127/0003-9136/2005/0162-0111

Strathmann, R. R. (1967). Estimating the organic carbon content of phytoplankton from cell volume or plasma volume. *Limnol. Oceanogr.* 12, 411–418. doi: 10.4319/lo.1967.12.3.0411

Sun, J., and Liu, D. (2003). Geometric models for calculating cell biovolume and surface area for phytoplankton. *J. Plankton Res.* 25, 1331–1346.

Sverdrup, H. (1953). On conditions for the vernal blooming of phytoplankton. *J. Cons. Int. Explor. Mer* 18, 287–295. doi: 10.1093/icesjms/18.3.287

Tate, M. C., Phlips, E. J., Stelling, B., Badylak, S., Landauer, L., West-Valle, A., et al. (2020). Phytoplankton composition in the sub-tropical shelf environment of Cape Canaveral, Florida. *Bull. Mar. Sci.* 96, 593–616. doi: 10.5343/bms.2019.0079

Tillman, D. H., Cerco, C. F., Noel, M. R., Martin, J. L., and Hamrick, J. (2004). *Three-dimensional eutrophication model of the lower St. John River, Florida*. Engineer Research and Development Center, Environmental Laboratory, Vicksburg, MS.

Utermöhl, H. (1958). Zur Vervollkommnung der quantitativen phytoplankton-methodik. *Mitt Int Ver Theor Angew Limnol* 9, 1–38. doi: 10.1080/05384680.1958.11904091

Vargo, G. A. (2009). A brief summary of the physiology and ecology of Karenia brevis (Davis) Hansen and Moestrup red tides on the West Florida shelf and of hypotheses posed for their initiation, growth, maintenance, and termination. *Harmful Algae* 8, 573–584. doi: 10.1016/j.hal.2008.11.002

Vaulot, D., Eikrem, W., and Viprey, M. H. (2008). The diversity of small eukaryotic phytoplankton ($\leq$ 3 µm) in marine ecosystems. *FEMS Microbiol. Rev.* 32, 795–820. doi: 10.1111/j.1574-6976.2008.00121.x

Vazyulya, S., Khrapko, A., Kopelevich, O., Burenkov, V., Eremina, T., and Isaev, A. (2014). Regional algorithms for the estimation of chlorophyll and suspended matter concentration in the Gulf of Finland from MODIS-aqua satellite data. *Oceanologia* 56, 737–756. doi: 10.5697/oc.56-4.737

Verity, P. G., Blanton, J. O., Amft, J., Barans, C., Knott, D., Stender, B., et al. (1998). Influences of physical oceanographic processes on chlorophyll distributions in coastal and estuarine waters of the South Atlantic bight. *J. Mar. Res.* 56, 681–711. doi: 10.1357/002224098765213630

Verity, P., Robertson, C. Y., Tronzo, C. R., Andrews, M. G., Nelson, J. R., and Stieracki, M. E. (1992). Relationships between cell volume and the carbon and nitrogen content of marine photosynthetic nanoplankton. *Limnol. Oceanogr.* 37, 1434–1446. doi: 10.4319/lo.1992.37.7.1434

Wang, J., and Zhang, Z. (2020). Phytoplankton, dissolved oxygen and nutrient patterns along a eutrophic river-estuary continuum: observation and modeling. *J. Environ. Manag.* 261:110233. doi: 10.1016/j.jenvman.2020.110233

Weitz, J., Stock, C., Wilhelm, S., Bourouiba, L., Coleman, M., Buchan, A., et al. (2015). A multitrophic model to quantify the effects of marine viruses on microbial food webs and ecosystem processes. *ISME J.* 9, 1352–1364. doi: 10.1038/ismej.2014.220

Winder, M., and Cloern, J. E. (2010). The annual cycles of phytoplankton biomass. *Philos. Trans. R. Soc. B: Biol. Sci.* 365, 3215–3226. doi: 10.1098/rstb.2010.0125

Winkler, S., and Ceric, A. (2004). *Status and trends in water quality at selected sites in SJRWMD*. Technical Publication SJ2004-3, St Johns River Water Management District, Palatka, FL.

Work, K., Havens, K., Sharfstein, B., and East, T. (2005). How important is carbon to planktonic grazers in a turbid, subtropical lake? *J. Plankton Res.* 27, 357–372. doi: 10.1093/plankt/fbi013

Xiao, Y., Zhang, J., Cui, T., and Sun, L. (2018). A new merged dataset of global ocean chlorophyll a concentration with higher spatial and temporal coverage. *Acta Oceanol. Sineca* 37, 118–130. doi: 10.1007/s13131-018-1249-6

Yamada, K., Ishizaka, J., Yoo, S., Kim, H., and Chiba, S. (2004). Seasonal and interannual variability of sea surface chlorophyll a concentration in the Japan/East Sea (JES). *Prog. Oceanogr.* 61, 193–211. doi: 10.1016/j.pocean.2004.06.001

Yoder, J. A. (1985). "Environmental control of phytoplankton production on the southeastern U.S. continental shelf," in *Oceanography of the southeastern U.S. continental shelf*, eds. L. P. Atkinson, D. W. Menzel and K. A. Bush (Washington, D.C.: American Geophysical Union (AGU)), 93–103.

Yoder, J. A., Atkinson, L. P., Lee, T. N., Kim, H. H., and McClain, C. R. (1981). Role of gulf stream frontal eddies in forming phytoplankton patches on the outer southeastern shelf1. *Limnol. Oceanogr.* 26, 1103–1110. doi: 10.4319/lo.1981.26.6.1103

Yoder, J. A., Atkinson, L. P., Stephen Bishop, S., Blanton, J. O., Lee, T. N., and Pietrafesa, L. J. (1985). Phytoplankton dynamics within gulf stream intrusions on the southeastern United States continental shelf during summer 1981. *Cont. Shelf Res.* 4, 611–635. doi: 10.1016/0278-4343(85)90033-0

Yoder, J. A., O'Reilly, J. E., Barnard, A. H., Moore, T. S., and Ruhsam, C. M. (2001). Variability in coastal zone color scanner (CZCS) chlorophyll imagery of ocean margin waters off the US East Coast. *Cont. Shelf Res.* 21, 1191–1218. doi: 10.1016/S0278-4343(01)00009-7

Yoder, J. A., Schollaert, S. E., and O'Reilly, J. E. (2002). Climatological phytoplankton chlorophyll and sea surface temperature patterns in continental shelf and slope waters off the northeast U.S. coast. *Limnol. Oceanogr.* 47, 672–682. doi: 10.4319/lo.2002.47.3.0672

Yoder, J. A., Verity, P. G., Bishop, S. S., and Hoge, F. E. (1993). Phytoplankton Chl a, primary production and nutrient distributions across a coastal frontal zone off Georgia, U.S.A. *Cont. Shelf Res.* 13, 131–141. doi: 10.1016/0278-4343(93)90102-4

Zingone, A., Phlips, E. J., and Harrison, P. J. (2010). Multiscale variability of twenty-two coastal phytoplankton time series: a global scale comparison. *Estuar. Coasts* 33, 224–229. doi: 10.1007/s12237-009-9261-x

frontiers | Frontiers in Ecology and Evolution

TYPE Original Research
PUBLISHED 06 April 2023
DOI 10.3389/fevo.2023.1113899

OPEN ACCESS

EDITED BY
Marcus W. Beck,
Tampa Bay Estuary Program, United States

REVIEWED BY
Andrew Decker Steen,
The University of Tennessee, Knoxville, United States
William Ross Hunter,
Queen's University Belfast, United Kingdom

*CORRESPONDENCE
Wade H. Jeffrey
✉ wjeffrey@uwf.edu

†PRESENT ADDRESSES
Erika L. Headrick,
Bionano Genomics, Inc., San Diego, CA, United States
Lisa M. Nigro,
Institute for Systems Genomics, University of Connecticut, Storrs, CT, United States
Melissa Ederington-Hagy,
Department of Earth and Environment, Boston University, Boston, MA, United States
Arianna L. Simmering,
Q^2 Solutions, Marietta, GA, United States
Richard A. Snyder,
Virginia Institute of Marine Science Eastern Shore Laboratory, Wachapreague, VA, United States

SPECIALTY SECTION
This article was submitted to Biogeography and Macroecology, a section of the journal Frontiers in Ecology and Evolution

RECEIVED 01 December 2022
ACCEPTED 15 March 2023
PUBLISHED 06 April 2023

CITATION
Headrick EL, Nigro LM, Waidner LA, Ederington-Hagy M, Simmering AL, Snyder RA and Jeffrey WH (2023) Acute inhibition of bacterial growth in coastal seawater amended with crude oils with varied photoreactivities. *Front. Ecol. Evol.* 11:1113899. doi: 10.3389/fevo.2023.1113899

Acute inhibition of bacterial growth in coastal seawater amended with crude oils with varied photoreactivities

Erika L. Headrick†, Lisa M. Nigro†, Lisa A. Waidner, Melissa Ederington-Hagy†, Arianna L. Simmering†, Richard A. Snyder† and Wade H. Jeffrey*

Center for Environmental Diagnostics and Bioremediation, University of West Florida, Pensacola, FL, United States

The increased potential for contamination of seawater by crude oils requires studies of bacterial biodegradation potential, but little is known of the differential negative impacts of oils on bacterial growth. No two wells generate chemically identical oils; and importantly, solar exposure of crude oil may differentially affect the bacterial response. Elucidating the role that sunlight plays on the potential toxicity of spilled crude oils is imperative to understanding how oil spills might affect microbes in the tropical and subtropical waters of Florida. This study examined light exposure of six different crude oils, and subsequent microbial responses to altered oils. Marine bacterioplankton heterotrophic activities were measured *via* ^{3}H-leucine incorporation after the addition of oils' water accommodated fractions (WAFs) that were created under varied solar conditions. Inhibition of production increased with higher concentrations of WAFs, but dose-response trends varied among the oils. Increased solar exposure during WAF preparation generally led to more inhibition, but trends varied among oils. WAFs were also prepared under different parts of the solar spectrum. Solar-irradiated WAFs resulted in significant but variable acute toxicity vs. dark counterparts. Solar-induced toxicity was primarily a result of visible and not ultraviolet light exposure. Results indicate responses to oil spills are highly dependent on the source of the oil and solar conditions at the time and location of the spill. The data presented here demonstrate the importance of photochemical changes and oil source in modulating microbial activity and bioremediation potential.

KEYWORDS

oil spill, bacterioplankton, photoreactivity, photooxidation, crude oil, Gulf of Mexico, solar exposure

1. Introduction

The accidental release of crude oil into marine environments by anthropogenic means often results in higher-than-background discharge rates and is not uncommon (Pampanin and Sydnes, 2013). While 914 persistent crude oil seeps have been identified in the Gulf of Mexico, the total background input of crude oil from these is estimated at 0.25 to 1 × 10^4 m^3

year^{-1} (MacDonald et al., 2015). In contrast, flow rates following the 2010 Deepwater Horizon (DWH) explosion were estimated at roughly 1×10^4 m^3 day^{-1} over 87 days for a total input of 7.95×10^5 m^3 before accounting for containment efforts (McNutt et al., 2012). The DWH explosion released crude oil into the northeast quadrant of the Gulf of Mexico (GOM), where only 7% of the total input from GOM natural seeps is expected (MacDonald et al., 2015).

Local assemblages of hydrocarbon-degrading microorganisms exist in Gulf of Mexico waters due to input of crude oil from natural seeps (Head et al., 2006; Peng et al., 2008; Pampanin and Sydnes, 2013; Prince and Atlas, 2018). It is widely known that crude oil is a complex mixture of hydrocarbons and there is variation between crude oils from different wells (Juyal et al., 2011; Pampanin and Sydnes, 2013; MacDonald et al., 2015). These differences may contribute to differences in responses by bacterioplankton.

Parameters affecting bacterial production when oil is present can also include specific capacities of bacterial taxa to degrade various hydrocarbon species (Head et al., 2006; Vergeynst et al., 2019; Bacosa et al., 2020a), microbial production of biosurfactants that facilitate bioavailability of petroleum molecules (Matvyeyeva et al., 2014), the relative abundance of nitrate-reducers among microbial community members (Melkonian et al., 2021), and the trophic state of the seawater upon oil introduction (Haule and Freda, 2021). Water temperature, nutrient availability, solar exposure, and oxygen affect microbial activity (Scofield et al., 2015; Hutchins and Fu, 2017; Cavicchioli et al., 2019; Robinson, 2019) altering the microbial degradation of crude oil components (Atlas and Hazen, 2011; Gregson et al., 2021).

Physical considerations include evaporation (Gjesteland et al., 2019), photodegradation (Guipeng et al., 2006; Saeed et al., 2013; Jing et al., 2014), or various means of solubilization, emulsification, or degradation of oil constituents (Riazi and Roomi, 2008; Gros et al., 2014; Boehm et al., 2016) upon introduction to seawater. Irradiance of the oil-seawater mixture can result in photo-transformation or photooxidation of the oil constituents (Nicodem et al., 2001; Snyder et al., 2021) and changes to the natural microbial community (Bacosa et al., 2015a). Typical surface water conditions seem to have little to no effect on photodegradation rates in the absence of an inoculum (Saeed et al., 2011), while solar irradiation does.

Biodegradation and/or physical degradation of oil constituents may differ with respect to the characteristics of the crude oils introduced to the aquatic environment. Lighter crude oils with higher American Petroleum Institute (API) gravity are typically degraded more efficiently (Prince, 1993; Sugiura et al., 1997; Hazen et al., 2016). The mixture of hydrocarbons within crude oils. Generally, N-alkanes are degraded most readily by diverse microbial consortia followed by slower degradation of more complex compounds (e.g., PAHs) by a more limited number of microbial species (Sugiura et al., 1997; Hazen et al., 2010; Atlas and Hazen, 2011; Dubinsky et al., 2013; Gutierrez et al., 2013; Kimes et al., 2014). Lower-ring-number PAHs are typically more bioavailable for more rapid biodegradation than higher-ring-number hydrocarbons (Peng et al., 2008; Bacosa et al., 2020b). Macondo well 252 oil from the DWH spill in the GOM (MC-252) and the surrogate oil (described by Pelz et al., 2011) supplied to researchers are oxidized at different rates in seawater mesocosms, but the reasons (biodegradation or photodegradation) for the relative differences in rates observed are not well known (Wozniak et al., 2019). MC-252 and the surrogate were found to oxidize differently in both photosynthetically active radiation (PAR) and full sun exposure (Vaughan et al., 2016).

Predictions of the microbial response to crude oil are further complicated by the potential influence of solar exposure to the oil in seawater. Considerations include both the relative intensity of the irradiance and the wavelengths of light reaching the oil molecules. While PAHs in crude oil with fewer aromatic rings are more easily degraded, alkylated PAHs with higher numbers of aromatic rings are photo-transformed at faster rates (Bacosa et al., 2015b). While MC-252 and surrogate oil water accommodated fractions (WAFs) had different photochemical responses to sunlight, the inhibition of microbial growth was similar for the two oils (Vaughan et al., 2016). Several studies have indicated that the microbial response following a spill may be dependent on the type of oil and its photo-reactivity (Santas et al., 1999; Saeed et al., 2011; Griffiths et al., 2014; Passow and Stout, 2020). Additionally, the effects of various wavelengths of light, including ultraviolet (UV) and photosynthetically active radiation (PAR) on the rates of physical-and/or biodegradation of oil constituents must be considered (Genuino et al., 2012) owing to the wavelength dependency of light attenuation in water when predicting *in situ* exposures.

The standard methods for producing crude oil WAFs were first detailed in Aurand and Coelho (2005) and call for the preparation of WAFs in the dark. These methods have been challenged and defended overtime and the importance of a standardized protocol for comparative research has been stressed (Coelho et al., 2013). However, WAFs produced in the dark vastly underrepresent crude oil dynamics and toxicity in the natural environment. Solar irradiation of crude oil compounds increases solubility in seawater (Lee, 2003; Benigni et al., 2017), which increases the bioavailability and potential toxicity of irradiated compounds relative to parent compounds (Dutta and Harayama, 2000; Maki et al., 2001; Griffiths et al., 2014; Bacosa et al., 2015b). In the DWH disaster, it is estimated that 50% of the crude oil volume reached the ocean surface (McNutt et al., 2012). Environmental conditions at the ocean surface are thus important to account for the potential impact of crude oil on biota, including the bacterioplankton responsible for degradation and transfer of organic matter to higher trophic levels.

Few studies have isolated the photochemical treatment of crude oils during WAF preparation from bacterial degradation (Yang et al., 2016; Cao and Tarr, 2017; Vergeynst et al., 2019; Snyder et al., 2021), and fewer have directly compared multiple crude oil sources (Viggor et al., 2013; Passow and Stout, 2020). To our knowledge, no studies have compared a wide spectrum of geochemically different crude oils exposed to a range of irradiance conditions and the subsequent effects on heterotrophic bacteria. Herein, we compared the acute effects on bacterioplankton growth of the water accommodated fractions (WAFs) produced from six different crude oils. In particular we focused on how the exposure to sunlight during WAF production altered the response to the individual oils. Our primary objective was to determine whether all crude oils produced a similar response as a function of the concentration of added WAF and how that response was dependent on the duration and part of the solar spectrum to which samples were exposed.

2. Materials and methods

2.1. Crude oils

A series of unique crude oils were made available by the National High Magnetic Field laboratory at Florida State University (FSU).[1] The FSU-provided oils were observed alongside crude oils in our collection at the University of West Florida (UWF). In order to maximize replication within the study, only five FSU-provided oils and one UWF-provided oil were selected for further analysis on the basis of density, color, and preliminary assessments of bacterial inhibition (data not shown); the oils were selected to test the widest variety of responses available.

The FSU-provided oils were assigned a number for the duration of the project to conceal the location-identity of the oils until the project's conclusion to avoid biases. The MC-252 surrogate crude oil was the UWF-provided oil (Table 1). Samples of each of the crude oils were sent to Midwest Laboratories (MWL)[2] for measurement of API gravity (ASTM D 4052-15), and contents of carbon (MWL WC PROC 55), nitrogen (MWL WC PROC 55),

1 https://nationalmaglab.org/

2 https://midwestlabs.com/

TABLE 1 Physical and chemical characteristics of crude oil samples, *x:* API gravity >31.1° denotes a light crude oil and API gravity 22.3–31.1° denotes a medium crude oil, *y:* % mass, *z:* crude oils with >0.5% sulfur content are considered sour, while <0.5% sulfur are considered sweet, GOM: samples collected in the Gulf of Mexico.

Crude oil	Location	API gravity^{x}	C (%)^{y}	N (%)^{y}	H (%)^{y}	S (%)^{yz}	Color
1	Undisclosed GOM	27.0°	73.6	0.34	10.8	1.550	Brown/Black
3	Independence Hub GOM	34.6°	56.2	0.23	9.2	0.480	Golden
4	Oxbow well Thompson, Wyoming	30.8°	63.8	0.24	9.7	0.838	Brown/Black
6	Undisclosed GOM	23.8°	76.5	0.47	10.2	1.490	Brown/Black
8	Independence Hub GOM	30.8°	59.4	0.23	9.1	0.652	Red/Brown
S	Marlin Platform GOM	34.2°	64.1	0.19	10.4	0.239	Brown/Black

TABLE 2 Daily light exposures during WAF formation.

	305 nm (J cm^{-2})	320 nm (J cm^{-2})	340 nm (J cm^{-2})	380 nm (J cm^{-2})	PAR (μE cm^{-2})
I. Dose response					
May 9, 2017	0.092	0.678	1.572	1.982	5237
May 10, 2017	0.098	0.686	1.577	1.983	5251
May 11, 2017	0.092	0.593	1.344	1.671	4338
May 12, 2017	0.040	0.344	0.827	1.049	2772
May 13, 2017	0.082	0.643	1.500	1.848	4673
May 14, 2017	0.097	0.711	1.651	2.076	5456
May 15, 2017	0.096	0.670	1.532	1.890	4796
May 16, 2017	0.104	0.718	1.652	2.067	5403
Daily average	0.088	0.630	1.457	1.821	4741
Total	0.701	5.043	11.655	14.566	37926
	305 nm (J cm^{-2})	320 nm (J cm^{-2})	340 nm (J cm^{-2})	380 nm (J cm^{-2})	PAR (μE cm^{-2})
II. Spectral dependency					
May 22, 2017	0.058	0.425	0.977	1.196	2982
May 23, 2017	0.059	0.447	1.035	1.261	3091
May 24, 2017	0.077	0.589	1.370	1.656	4035
May 25, 2017	0.108	0.725	1.664	2.067	5315
May 26, 2017	0.116	0.724	1.646	2.052	5302
May 27, 2017	0.095	0.575	1.299	1.596	4015
May 28, 2017	0.070	0.478	1.102	1.361	3467
May 29, 2017	0.086	0.521	1.178	1.450	3727
Daily average	0.083	0.561	1.284	1.580	3992
Total	0.668	4.484	10.270	12.637	31935

hydrogen (MWL WC PROC 55), and sulfur (ASTM D 5453-19) each expressed as a percent of total mass. MWL WC PROC 55 is a proprietary method used by MWL that is based on method AOAC 993.13. Samples were loaded into an elemental analyzer to be burned in the presence of oxygen releasing gases which were identified, quantified, and reported as a percent of the total oil mass.

2.2. General WAF preparation

Crude oils were added to sterile seawater in a manner similar to the CROSERF protocol (Aurand and Coelho, 2005) in individual Teflon bottles at a concentration of 1% oil: water (v/v) to produce oil-in-water mixtures leading to WAFs. Aged (>3 years) seawater from the central Gulf of Mexico was used to produce WAFs to ensure there were no other labile organic carbon sources to which the bacteria might respond. The aged seawater was filtered through a 47 mm, 0.2 μm pore-size polycarbonate filter by gentle vacuum (<0.3 atm) and 25 mL was added to each 30 mL Teflon bottle (minimum 86% UV transmittance; Vaughan et al., 2016), leaving approximately 5 mL headspace. Seawater was pasteurized in the Teflon bottles at 70°C for a minimum of 2 h and cooled to room temperature before crude oil was added (1% v/v).

Three light regimes were used in WAF production. Oil-in-water mixtures were incubated in Teflon bottles that were (i) uncovered for full-sun exposure (FS), (ii) covered in aluminum foil (Dark), and (iii) covered in Court guard, a broadband cut-off filter (PAR). Court guard transmits photosynthetically active radiation (PAR; 95% of 400–800 nm wavelengths) and blocks ultraviolet radiation (0% of UV-B and 9% of UV-A transmittance) (Fischer et al., 2006; Vaughan et al., 2016). WAFs were incubated in covered and uncovered bottles in a water bath held constant at 20°C directly under natural sunlight. Solar irradiance was measured during exposures using a Biospherical Instruments (San Diego, CA, USA) GUV511 solar radiometer. Full irradiance data during WAF production are presented in **Tables 2**, **4**. All bottles were shaken three times each day for 5 s. At the conclusion of the exposure period, bottles were returned to the lab to settle. The aqueous phases of each mixture containing the oil WAFs were removed, transferred into 20 mL glass scintillation vials maintaining separate WAF stocks, and stored at −20°C until experimental use.

2.3. Coastal seawater inocula

A fresh sample of coastal seawater was collected at sunrise *via* bucket-cast from the end of the Pensacola Beach Pier the day of each experiment (**Supplementary Table 1**). This location is approximately 0.3 km off the coastline (30°19′38″ N, 87° 8′31″ W). Microbes in these seawater samples served as the natural community inoculum in each experiment. Vertical salinity and temperature profiles were measured using a SonTek (San Diego, CA, USA) Castaway conductivity, temperature, and depth meter (CTD). In addition, samples were preserved with sulfuric acid for total Kjeldahl nitrogen (TKN), stored at 4°C, and later analyzed using EPA method 351.2 on a Lachat Quickchem FIA Model autoanalyzer. Sample seawater was also passed through a 25 mm GF/F filter and the filtrate was saved and preserved by freezing at −20°C for eventual analysis of dissolved nutrients. Dissolved inorganic phosphate (DIP) was analyzed as in Parsons et al. (1984), NH_4^+ as in Holmes et al. (1999), and NO_3^- + NO_2^- as in Schnetger and Lehners (2014). The sum of NH_4^+, NO_3^-, and NO_2^- is reported as dissolved inorganic nitrogen (DIN).

2.4. Bacterial production assays

Incorporation of labeled leucine, a proxy for secondary heterotrophic production, was measured by bulk radioactivity measurements of each sample after 4 h of dark incubation. ^{3}H-Leucine (Perkin Elmer; specific activity 50.2 Ci mmol^{-1}) was added to seawater samples to a final concentration of 10 nM. Samples were incubated in 5 mL (12 mm × 75 mm) polystyrene round-bottom (snap-cap) tubes at *in situ* temperature in the dark for 4 h in the presence of oil WAFs. Incorporation reactions were terminated by the addition of trichloroacetic acid (TCA) to a final concentration of 5% (v/v). Samples were transferred from snap-cap tubes into triplicate microcentrifuge tubes and processed by the method established by Kirchman et al. (1985) and amended by Smith and Azam (1992). Briefly, total biomass was precipitated by trichloroacetic acid (TCA) precipitates, and then TCA precipitates were collected by centrifugation, and pellets were washed again with 5% TCA and again with 70% ETOH. Final pellets were resuspended in liquid scintillation cocktail and incorporated leucine was measured using a Tri-Carb 2900TR Liquid Scintillation Analyzer (Perkin Elmer). The same technique was used to determine background or control bacterial production in the sample water from the Pensacola Beach Pier in the absence of WAFs.

2.5. Dose response

Water accommodated fractions were prepared in replicates of four under FS conditions for 8 days using oils 1, 3, 4, 6, 8, and the MC-252 surrogate (S). WAFs were added to snap-cap tubes at final concentrations of 0.5, 1, 2.5, 5, and 10% (v/v) with the seawater inoculum containing ^{3}H-Leucine. Five replicate controls were prepared similarly by the addition of 2.5% (v/v) sterile seawater to the seawater inoculum and ^{3}H-Leucine. Dose-response for each oil WAF was modeled by the natural log of ^{3}H-Leucine incorporation vs. increasing concentration.

2.6. Duration of WAF solar exposure

Twenty replicates of FS-incubated WAFs were prepared for each oil mentioned before and four replicates were removed from solar exposure at time points of 24, 48, 96, 144, and 192 h (**Table 4**). At each time point, replicate WAFs were removed from each bottle, transferred to 20 mL scintillation vials, and stored at −20°C until all bottles were recovered from solar exposure. WAFs were added to snap cap tubes as before at a final concentration 2.5% (v/v) with the seawater inoculum and ^{3}H-Leucine. Controls were prepared as before with sterile seawater (2.5% v/v). Inhibitory effects of increased WAF-preparation solar exposure time were

modeled for each oil by the natural log of ^{3}H-Leucine incorporation vs. increasing UV-exposure times under which the WAFs were prepared.

2.7. Spectral dependency

Water accommodated fractions were prepared in triplicate under FS, PAR, and Dark spectral conditions for 8 days and collected upon return to the lab. WAFs were added to snap cap tubes at final concentration 2.5% (v/v) with the seawater inoculum and ^{3}H-Leucine. Three replicates of controls were prepared with sterile seawater (2.5% v/v). The bacterial production assay was performed, and the ^{3}H-Lecuine incorporation rates were plotted as a percentage of the control.

2.8. WAF fluorescence

Fluorescence signals of FS and DARK WAFs were measured on a Turner Trilogy Fluorometer using the crude oil module (model # 7200-063; excitation: 365 nm, emission: 410–600 nm) as a proxy for total hydrocarbon quantification (Ziervogel et al., 2014). Replicates were pooled prior to measuring fluorescence. Background fluorescence from an un-amended seawater sample was subtracted from WAF fluorescence signals and reported in relative fluorescence units (RFU). This method of analysis was limited by the equipment available in the laboratory and was also performed before carbon contents of the oils were known. Fluorescence data was not used as a direct quantitation method, as additions of crude oil to seawater were on a per-volume basis (i.e., 1% v/v) rather than per-carbon basis. These data were used to differentiate the tendency of various oil constituents to move into the aqueous portion of the oil-in-water mixture during solar exposure. The aqueous fraction was collected as "WAF" and fluorescence was measured. Microbial inhibition corresponding to these WAFs was also measured in triplicate as previously described by ^{3}H-Leucine incorporation before the WAFs were pooled for measurements of fluorescence. The seawater used as the inoculum in this experiment was characterized as mentioned above in section "2.3. Coastal seawater inocula."

2.9. Statistical analyses

Linear models were first constructed for microbial dose response to each oil with increasing WAF concentration as previously described. Slopes and respective error terms for each oil source were estimated in Rv1.3 (R Core Team, 2022). A two-way Analysis of Variance (ANOVA) where concentration and oil source were explanatory variables was performed and a significant interaction term was used to indicate overall heterogeneity of slopes. *Post hoc* pairwise comparisons of dose-response curves for each oil were performed using lstrends in R (Lenth, 2023) and *P*-values were adjusted by the Tukey's method for comparing a family of seven estimates including a control with slope of zero. Additionally, simple effects of WAF oil source were investigated using a one-way ANOVA at each individual concentration.

Similarly, significant differences between oil sources were detected with a linear model estimating microbial response to WAFs prepared under increasing solar exposure time. In this case, time and oil source served as explanatory variables. Simple effects of WAF oil source were investigated using a one-way ANOVA at each individual time point.

Differences were detected (i) between oil sources within each of FS, PAR, and Dark groups, and (ii) between spectral exposures within each oil-source group using one-way ANOVA analyses. Following each ANOVA, pairwise comparisons were made by TukeyHSD. *P*-values reported were determined by the lower limit of each analysis in R and are reported exactly from the corresponding output in the **Supplementary Data Spreadsheet**. The lower limits for reporting *p*-values in each analysis are 2E-16 in an ANOVA, 0.0001 in lstrends and an adjusted *p*-value of zero in TukeyHSD.

Similarities in the elemental composition of the source oils, with respect to percent carbon, hydrogen, nitrogen, and sulfur, as well as API gravity are presented using a resemblance matrix and Bray-Curtis (B-C) similarity hierarchal clustering generated in PRIMER6. The variables included in the similarity clustering analysis included only those with continuous values (API gravity, carbon, hydrogen, nitrogen, and sulfur). As previously described for numerical values of sediment characteristics (Shin and Fong, 1999) and numerical values of water chemistry parameters (Balasubramaniam et al., 2015), we transformed numerical values of oil characteristics and used transformed values in the B-C analysis for this particular type of multivariate analysis. In order to standardize scales between measures of characteristics with continuous values, a min-max transformation was applied within each variable; this transformation standardizes all variables on a scale of 0 to 1 where 0 is the lowest value recorded within the variable and 1 is the highest. Without this transformation, variables on a higher scale contribute more to the clustering of compared oils than variables on a lower scale (i.e., API gravity vs. nitrogen content). The B-C similarity analysis did not include discrete values (color, sour vs. sweet, or location of oils). Those discrete variables are simply included in the dendrogram as follows (from the **Figure 1** legend, circles vs. squares for sour and sweet; open and closed symbols, for light crude and medium crude; and location of oils as leaf label text). Additionally, Pearson correlation coefficient and significance were calculated for microbial inhibition vs. WAF fluorescence using R package ggpubr (Kassambara, 2020).

3. Results

3.1. Crude oil characteristics

Crude oil samples were medium to light oils (**Table 1**) with API gravity that ranged 23.8–34.6°. Oils with API gravity >31.1° were considered light crude oils, while oils with API gravity 22.3–31.1° were considered medium crude oils. In total, two oils were light, four were medium, with Oils 6 and 3 being the heaviest and lightest, respectively. Percent carbon ranged 59.4–76.5%, where oil 8 was the lowest and oil 6 was the highest. Hydrogen content ranged

TABLE 3 Models for dose response of bacterial production inhibition.

Oil	Slope	Intercept	R^2
1	−0.118 ± 0.006	4.551 ± 0.031	0.94
3	−0.155 ± 0.007	4.458 ± 0.035	0.96
4	−0.190 ± 0.009	4.334 ± 0.049	0.95
6	−0.113 ± 0.005	4.543 ± 0.024	0.96
8	−0.065 ± 0.005	4.510 ± 0.025	0.90
S	−2.05 ± 0.006	4.475 ± 0.028	0.98

9.1–10.8%, where oil 8 was the lowest and oil 1 was the highest. Nitrogen content ranged 0.19–0.47% where the surrogate oil was the lowest and oil 6 was the highest. Oils 3 and the surrogate were considered sweet oils with total sulfur <0.5%, while oils 1, 4, 6, and 8 were considered sour with total sulfur >0.5%. Oils 1 and 6 had the highest sulfur content.

Oils 1 and 6 were both medium, sour crude oils that were the most similar, based on Bray-Curtis similarity analysis of chemical composition and API gravity (Figure 1). Oils 3, 4, 8, and the surrogate were in a clade separate from oils 1 and 6. The terrestrially derived oil 4 and oil 8 collected from Independence Hub were also both medium, sour crudes that were similar but clustered separately from the other two medium, sour crude oils. Oils 3 and the Surrogate were the only two light, sweet crude oils and were more similar to oils 4 and 8 than oils 1 and 6 on the basis of variables tested.

3.2. Coastal seawater inocula

Coastal seawater was characterized by temperature, salinity, Total Kjeldahl Nitrogen (TKN), Dissolved Inorganic Nitrogen (DIN), Dissolved Inorganic Phosphate (DIP) and control bacterial production prior to each experiment (Supplementary Table 1). The four experiments (using inocula collected between May 17 and June 19, 2017). were performed to determine dose-response, time course models, spectral dependence, and fluorescence correlation, the results of which are each described below (sections "3.4. Dose response," "3.5. Duration of WAF solar exposure," "3.6. Spectral dependency," and "3.7. WAF fluorescence correlation," respectively). Temperature was relatively consistent in collections for the four experiments performed, ranging from 22.8–24.2°C, while other factors varied slightly (Supplementary Table 1). The seawater collected for the dose response experiment had salinity 27, TKN 0.26 mg L^{-1}, DIN 0.77 μM, DIP 0.02 μM, and control bacterial production of 104 pmol Leu $L^{-1}hr^{-1}$. The seawater collected for the time course experiment had salinity of 30, TKN 0.28 mg L^{-1}, DIN 0.43 μM, DIP 0.02 μM, and the bacterial production rate was 208 pmol Leu L^{-1} hr^{-1}. The inoculum for the spectral dependency experiment had salinity 31, TKN 0.42 mg L^{-1}, DIN 0.97 μM, DIP below detection, and the bacterial production rate was 211 pmol Leu L^{-1} hr^{-1}. The seawater collected for the fluorescence correlation determination had salinity 31, TKN 0.46, DIN 1.00, and DIP was below detection, with a bacterial production rate of 399 pmol Leu L^{-1} hr^{-1}. Overall, water samples were oligotrophic.

3.3. Average solar irradiance

During WAF preparation for dose response experiments total solar ultraviolet radiation exposure at wavelengths 30, 320, 340, and 380 nm were 0.701, 5.043, 11.655, and 14.566 J cm^{-2}, respectively, with photosynthetically active radiation (PAR) exposure of 37,926 μE cm^{-2}. During WAF preparation for spectral dependency experiments total UV exposure at wavelengths 305, 320, 340, and 380 nm were 0.668, 4.484, 10.270, and 12.637 J cm^{-2}, respectively, with PAR exposure of 31,935 μE cm^{-2}. Daily average measurements at each wavelength and for PAR are in Table 2.

3.4. Dose response

Inhibition increased as WAF concentration in seawater increased for all oils assayed (Figure 2) and the linear relationship between increasing dose and inhibition was strong for all oils with R^2 greater than 0.90 (Table 3). The inhibitory dose-response varied overall given significant heterogeneity of slopes ($p < 0.001$) between oils. Inhibition resulting from WAF made with oil 8 increased the least as concentration was increased, while inhibition resulting from WAF made with oil 4 and surrogate increased the most as concentration was increased. Slopes for each dose-response curve are in Table 3. All pairwise comparisons of dose-response slopes were significantly different ($p < 0.01$) except for oils 1 and 6 ($p = 0.9977$) and oil 4 and surrogate ($p = 0.7198$). At a concentration of 0.5% oils 3, 4, 8, and the surrogate demonstrated bacterial production rates significantly different than the control with p-values of 0.00016, < 0.0001, 0.01868, and < 0.0001, respectively, while oils 1 and 6 were not significantly different from the control with p-values of 0.8563 and 0.3552, respectively. At a concentration of 1% WAF to seawater all oils were significantly different from the control ($p < 0.001$). As concentration increased so did the detectability of significant differences in microbial inhibition resulting from each different oil.

TABLE 4 Cumulative solar exposure for each WAF preparation time point in the duration of WAF solar exposure experiment.

Time point	305 nm (J cm^{-2})	320 nm (J cm^{-2})	340 nm (J cm^{-2})	380 nm (J cm^{-2})	PAR (μE cm^{-2})
T24	0.093	0.657	1.523	1.894	4883
T48	0.182	1.307	3.040	3.769	9660
T96	0.376	2.611	6.036	7.453	18865
T144	0.479	3.325	7.663	9.379	23390
T192	0.621	4.237	9.742	11.908	29630

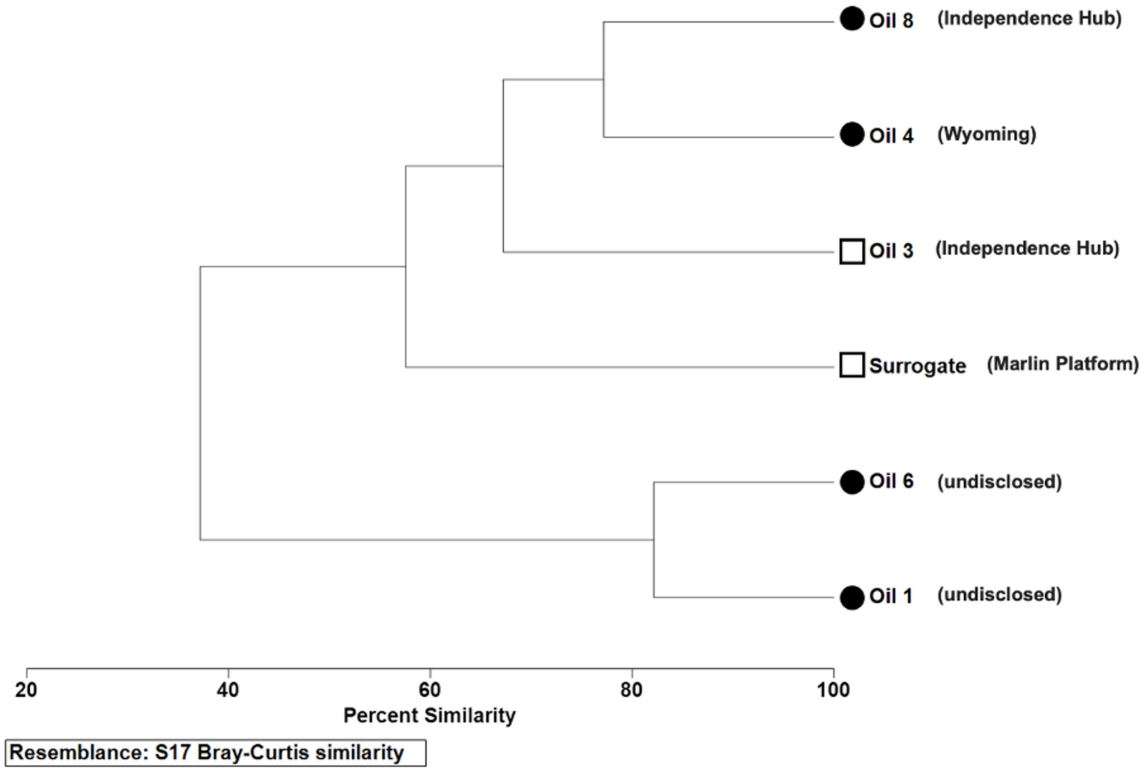

FIGURE 1
Bray-Curtis similarity dendrogram with clustering based on oil chemical characteristics with scales standardized by min-max transformation. Characteristics include physical and chemical characteristics of crude oil samples as outlined in **Table 1**, including sweetness, API gravity, and percent mass of C, N, H, and S. Sweetness ranges were defined as "sweet", for oils with total sulfur <0.5%; "sour", with total sulfur >0.5%. Circles, sour; Squares, sweet. Open symbols, light crude oils (API > 31.1); closed symbols, medium crude (API 22.3–31.1). Location of oils is indicated in parentheses, to the right of the oil name on the leaf.

Complete homogenous subsets at each separate concentration are presented in the (**Supplementary Table 2**) and the (Headrick, 2019; **Supplementary Data Spreadsheet**).

3.5. Duration of WAF solar exposure

Cumulative solar exposure over each period (24–196 h) was calculated during WAF preparation (**Table 4**). WAFs were exposed to a daily average of 0.08 J cm^{-2} of UVB, 0.53 J cm^{-2} of $UVA_{320\ nm}$, 1.22 J cm^{-2} of $UVA_{340\ nm}$, 1.49 J cm^{-2} of $UVA_{380\ nm}$, and 3704 μE cm^{-2} PAR. UV-exposure after just 24 h at wavelengths 305, 320, 340 nm, and 380 nm were, respectively, 0.093, 0.657, 1.523, and 1.894 J cm^{-2}, with PAR exposure of 4883 μE cm^{-2}. After 196 h of solar irradiance, cumulative UV-exposure at wavelengths 305, 320, 340, and 380 nm were, respectively 0.621, 4.237, 9.742, and 11.908, with PAR exposure of 29,630 μE cm^{-2}. Data for remaining time points are in **Table 4**.

The rate by which increased WAF solar exposure affected inhibition varied overall (**Figure 3**) given by significant heterogeneity of slopes ($p < 0.0001$). WAFs, except those made with oils 3 and 8, generally were inhibitory to bacterial growth when prepared under higher amounts of solar exposure. Slopes for all WAF treatments were significantly ($p < 0.0001$) different from a control with a slope of zero, except for Oils 3 ($p = 0.5267$) and 8 ($p = 0.5654$). All pair-wise comparisons of slopes were significantly different ($p < 0.05$) except for oils 1 and 6 ($p = 0.9803$), and oil 4 and the surrogate ($p = 0.116$). Oil 4 was represented by the strongest negative correlation of decreasing bacterial production due to increasing WAF solar exposure time.

Beyond linear models, three distinct patterns between bacterial production and time of WAF solar exposure were observed. Oils 3 and 8 were effectively inhibitory after 24 h and did not change thereafter, oil 1 and the surrogate continuously increased in inhibition as WAF solar exposure time increased, and oils 4 and 6 were represented by higher inhibition at each time point up to 144 h but were relatively unchanged between the time points of 144 h and 192 h.

All oil WAFs solar-exposed for 24 h, resulted in significant inhibition relative to the control ($p < 0.01$) except for oil 1 ($p = 1.00$). While inhibition was greater resulting from oil 1 WAF solar-exposed for 48 h, there was still no significant difference between oil 1 and the control ($p = 0.09$). All oil WAFs solar-exposed for 96 h, including oil 1, resulted in significant inhibition relative to the control ($p < 0.0001$). After the first 24 h, oil 3 was the most inhibitory, however, at the end of the week-long exposure, oils number 4 and the surrogates, which were statistically indistinguishable at the final time point ($p = 0.6677$), were the most inhibitory WAF treatments. Complete homogenous subsets at each separate time point are presented in the (**Supplementary Table 3**), and in the (Headrick, 2019; **Supplementary Data Spreadsheet**).

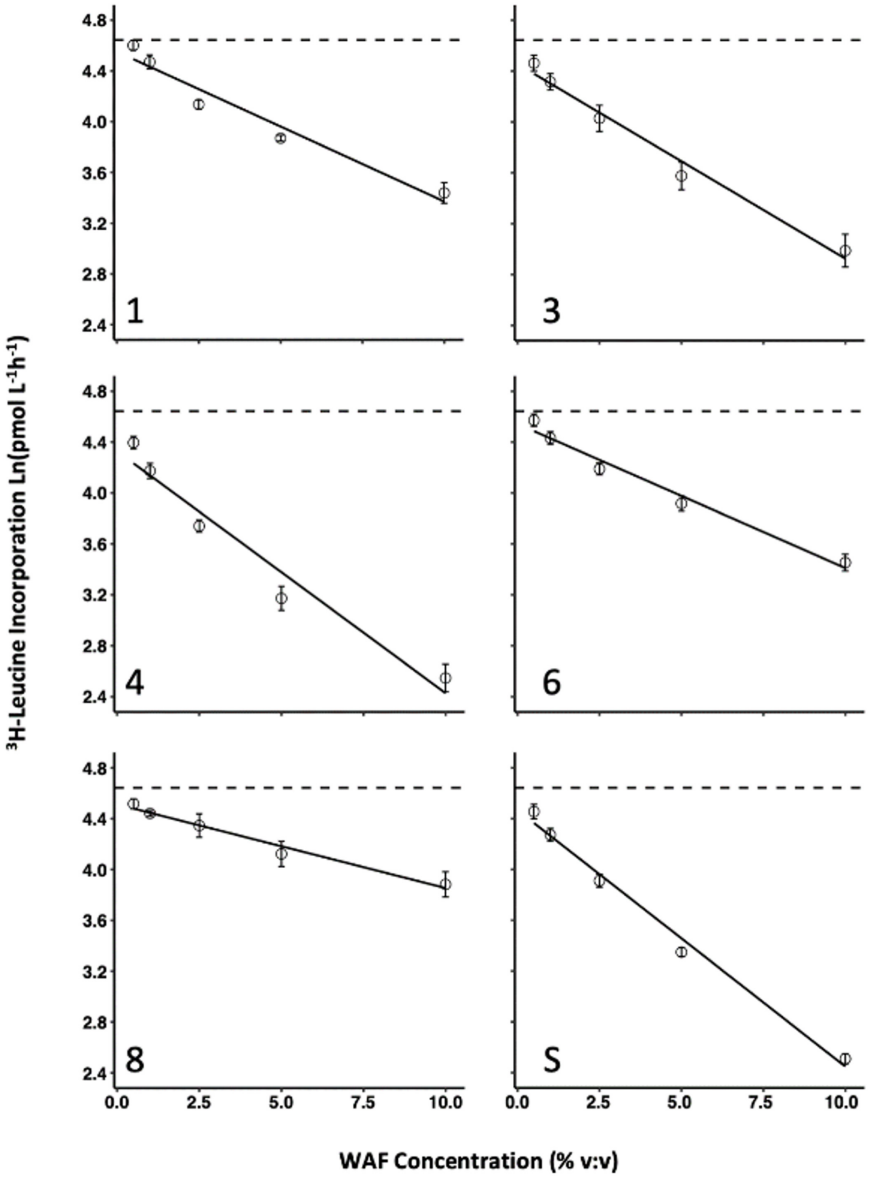

FIGURE 2
Bacterial production response to increasing WAF dose for all 6 oils. WAF dose response of bacterial production (^{3}H-Leucine incorporation) for each of the 6 oils used in this study. Error bars represent the standard deviation of the mean of experimental replicates from the same WAF preparation.

3.6. Spectral dependency

Water accommodated fractions prepared in the dark resulted in little to no inhibition while WAFs prepared in Full Sun or in PAR inhibited bacterial production (**Figure 4**). Counter to the standard pattern, FS WAF from oil 8 was not any more inhibitory than its dark counterpart. WAFs prepared in the dark were found not significantly different from the control, except for oil 8 ($p = 0.024$). However, Oil 8 WAF prepared in the dark was not significantly different from dark WAFs of oils 1, 3, 4, and 6.

For most oils, inhibitions resulting from PAR and FS exposure were similar. Oils 3 and 8 WAFs were far more inhibitory after PAR exposure than FS. WAFs prepared in FS for all oils were different overall, with few that elicited similar inhibition. Oils 1 and 6 in FS were similar ($p = 0.878$), and oils 3 and Surrogate were also similar ($p = 0.824$). WAFs prepared in PAR for all oils were also different overall, with two exceptions. Again, oils 1 and 6 in PAR were similar ($p = 0.159$), and oils 3 and 4 were also similar ($p = 0.946$). PAR WAFs from oils 3 and 4 were the most inhibitory treatments overall. Additional comparisons are in the (**Supplementary Tables 4**, **5**) and the (Headrick, 2019; **Supplementary Data Spreadsheet**).

3.7. WAF fluorescence correlation

Water accommodated fractions fluorescence was higher in FS WAFs vs. Dark counterparts for all oils investigated (**Figure 5A**). Fluorescence was highest in FS WAF from oil 4, followed by FS WAF from the surrogate oil. WAF fluorescence was lowest

in all Dark WAFs. The highest fluorescence in Dark WAFs was from oil 8, followed closely by oil 3. Overall, acute bacterial production inhibition was positively correlated with higher WAF fluorescence (r = 0.856, p = 0.000774, n = 11; **Figure 5B**). FS WAFs assessed separately appeared to be positively correlated with bacterial production inhibition but this relationship was not significant (r = 0.583, p = 0.2247, n = 6). Similarly, Dark WAFs assessed separately appeared to be positively correlated with bacterial production inhibition, but this relationship was not significant (r = 0.415, p = 0.4874, n = 5).

4. Discussion

Inhibition of bacterioplankton activity due to the introduction of different crude oil WAFs was variable, dependent on the oil source, amount of oil to which the organisms were exposed, and the amount and part of the solar spectrum to which the WAFs were exposed. There was no uniform or consistent response. Inhibition of bacterial production was strongly affected by increasing the dose of crude oil FS WAFs for all oil sources tested. Higher doses of WAFs from oil 4 and the surrogate had the strongest effect on inhibition while higher doses of WAF from oil 8 affected inhibition the least. We found that the lowest concentration at which all crude oil sources resulted in significant inhibition relative to a control was with 1% FS WAF per sample, where the WAF was prepared with 1% oil in seawater. At a concentration <1%, some oils (# 1 and # 6) may not result in significant inhibition. At higher concentrations, FS WAFs from the six different oils were statistically more different than at lower concentration. We found some pairwise similarities among oils, with regard to oil characteristics with continuous values (API gravity, carbon, hydrogen, nitrogen, and sulfur) (**Figure 1**). Overall, however, the main consideration of effect of WAF concentration on inhibition of bacterial production suggests that each oil has a distinct inhibitory effect (**Figures 3**, **4**). For instance, all pair-wise comparisons of slopes were significantly different except for oils 1 and 6 and oil 4 and the surrogate. These data in total are supported by similar previous work. In a monoculture growth study, higher concentrations of single crude oil components were found to increasingly inhibit bacterial growth (Ma et al., 2015). Exposure of the culture to increasing concentrations of larger, more complex crude oil compounds resulted in greater inhibition or death when compared to increasing concentrations of less complex crude oil compounds (Ma et al., 2015). Increasing concentration of crude oils overall has also been shown to decrease biodegradation rates, however, this is largely dependent on the chemical makeup of the oil (Balasubramaniam et al., 2015). Higher concentrations of n-Alkanes decreased the biodegradation rate, while higher concentrations of PAHs increased biodegradation rate; yet, again, this is still dependent on the PAHs in the mixture (Balasubramaniam et al., 2015). With the newly reported data in our study on acute bacterial production differences between source oils, it is reasonable to conclude that microbial responses to higher concentrations of crude oil WAFs would greatly depend on the type of oil and the chemical composition of the oil. Further, we hypothesized that as crude oil components are photodegraded, the compounds available in seawater would change, leading to additional differences in microbial response as our results confirm. Complete chemical analyses were beyond the scope of the project and further hindered by the very limited supply of some of the oils.

Inhibition of bacterial production in seawater was shown to be positively correlated with greater solar exposure of MC252 and MC252-surrogate WAFs and both oils resulted in similar amounts of inhibition (Vaughan et al., 2016). Our study has sought to measure the acute direct effect of increasingly irradiated crude oils from varied sources on bacterial production. We found that WAFs exposed to greater doses of solar exposure inhibited bacterial production more, though not at the same rate for all oils tested. This may be attributed to varied concentrations of different PAH species present in the different oils which may respond differently to solar exposure, more so than the n-alkanes in the parent oils (Bacosa et al., 2015b, Balasubramaniam et al., 2015). Increased depletion of PAH concentrations in seawater amended with MC252 crude oil has been linked to higher doses of solar exposure in a sterile mixture (Bacosa et al., 2015b). However, increased solar exposure was shown to have little effect on n-alkanes in a sterile mixture, while a seawater inoculum amended with MC252 crude oil demonstrated that biodegradation was the prominent factor in the depletion of n-alkanes (Bacosa et al., 2015b). The effect of increasing solar exposure is dependent on the source of the oil, and presumably the chemical composition. Consequently, the response to all oils is not the same and complicates the ability to make broad predictions about how spills might affect the environment.

Photodegradation of crude oils has been attributed to ultraviolet (UV) exposure (as reviewed in Lee, 2003), but the use of broad-band cutoff filters has shown the importance of PAR on WAFs (Vaughan et al., 2016; this study). The inhibitory response to most WAFs prepared in FS was indistinguishable from inhibitory responses to WAFs prepared under PAR-only conditions. In contrast, WAFs from oils 3 and 8 were more inhibitory under PAR-only conditions, but the additional UV-radiation in full sun exposure resulted in a reduction of toxicity. This was unexpected and was confirmed by a second trial with similar results (data not shown). Oils 3 and 8 were recovered near Independence Hub, a well in the Gulf of Mexico that contains a compound known as perylene which makes these oils blue in color (Juyal et al., 2011). Perylene is a 5-ring organic PAH that is recognized in industry as a photoredox catalyst when exposed to visible light (He et al., 2018; Gao et al., 2019), which may explain the greater inhibition seen from oils 3 and 8 under PAR-only conditions relative to the FS and dark counterparts. We hypothesize that UV-exposure may affect perylene in a way that quenches photocatalytic properties, however, further investigation is needed. Future analysis on the chemistry of FS WAFs created from these two oils that result in less inhibition as compared to PAR counterparts is necessary to better understand the relationship between hydrocarbons and solar irradiation, and subsequent effects on bacterioplankton.

In addition to varied effects on acute inhibition, WAFs from different oil sources under different solar regimes varied in fluorescence as a result of photochemical changes during WAF production. Fluorescence and inhibition were positively and strongly correlated overall (r = 0.856, p = 0.000774). Fluorescence was used as a proxy for hydrocarbon concentrations dissolved in seawater WAFs (Sørstrøm, 1985; Genders, 1988). Our solar-exposed WAFs had higher fluorescence than dark counterparts (excitation: 365 nm, emission: 410–600 nm, as per Ziervogel et al., 2014). Our WAFs mimicked natural conditions

10.3389/fevo.2023.1113899

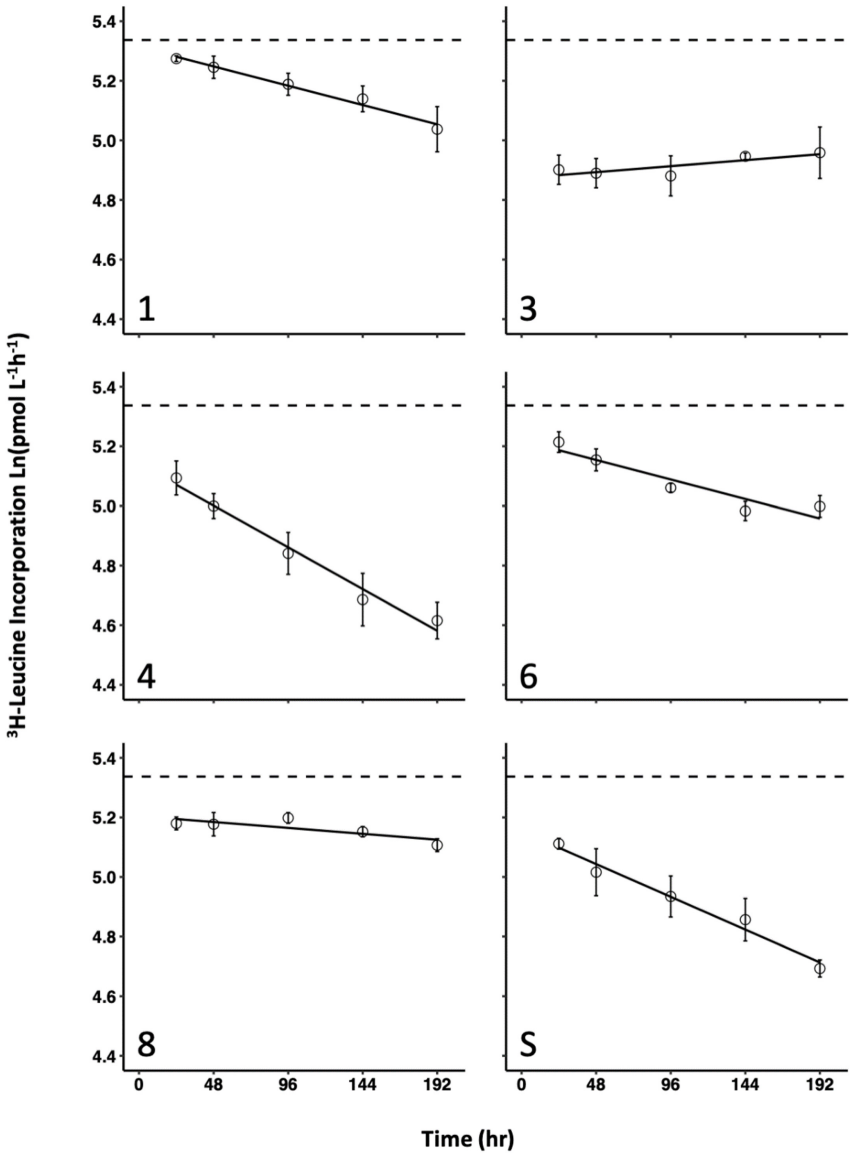

FIGURE 3
Response of bacterial production (^{3}H-Leucine incorporation) with various solar exposure times for each of the 6 oils used in this study. Error bars represent the standard deviation of the mean of experimental replicates from the same WAF preparation.

under which oil and water mix during a spill. WAFs were prepared during solar exposure and were consistently mixed with 1% (v/v) crude oil over the course of 8 days. We subsequently separated the aqueous fraction from the remaining oil layer and measured the fluorescence of the aqueous fraction. Our WAFs were also prepared in sterile seawater, removing any effects of biodegradation on oil components. Our data shows that increased solar exposure during contact of oil and seawater may create fluorescent oil components more miscible with the aqueous fraction.

PAHs are largely responsible for the fluorescence of oil (Owen et al., 1995; Groner et al., 2001; Hou et al., 2019) and are also responsible for most of the toxicity of petroleum (Jiang et al., 2010). Smaller PAHs tend to be more toxic because of bioavailability (miscibility), but toxicity is not always correlated to the number of aromatic rings (Yan et al., 2004; Jajoo et al., 2014). Crude oil PAHs are known to be more toxic when irradiated (Yan et al., 2004; Fu et al., 2012), and can cause cellular DNA damage (Toyooka and Ibuki, 2007). Without knowing PAH concentrations in dark vs. sunlight exposed WAF, we are unable to define what component is leading to greater acute toxicity in our samples, but we do know that the fluorescence of the WAF is strongly and positively correlated with increased inhibition and that PAHs are usually responsible for higher fluorescence in oil treated seawater.

Previous studies suggest that increased solar exposure results in lower fluorescence (Ehrhardt et al., 1992; King et al., 2014; Snyder et al., 2021) although results could be a function of differences in experimental design. For instance, solar-exposure of samples ranged from a simulated 12 days (Ehrhardt et al., 1992; King et al., 2014) up to 67 days (Snyder et al., 2021) and the UV-exposure rate also varied (King et al., 2014). Two of the previous studies were conducted using sterile seawater (King et al., 2014; Snyder et al., 2021), while used non-sterile

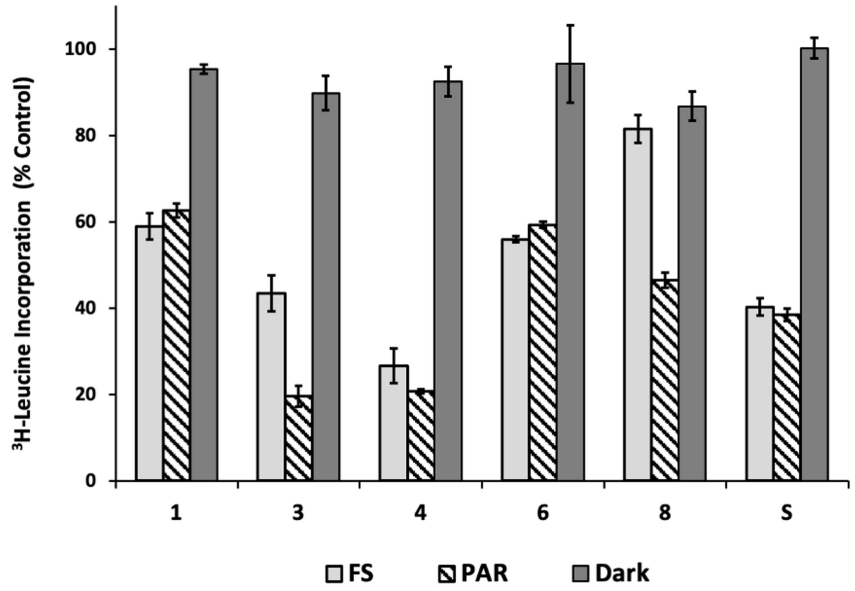

FIGURE 4
Inhibition of bacterial production (^{3}H-Leucine incorporation) as a result of light exposure during WAF preparation. Significance levels of pairwise comparisons (WAF made in FS treatment vs. WAF made in dark, and PAR treatment vs. dark WAF) are indicated (p level indicators here). Inhibition of bacterial production (^{3}H-Leucine incorporation) is expressed as a percent of the control. *P*-values for multiple comparisons within and between oils are in the [Headrick (2019); **Supplementary Data Spreadsheet**].

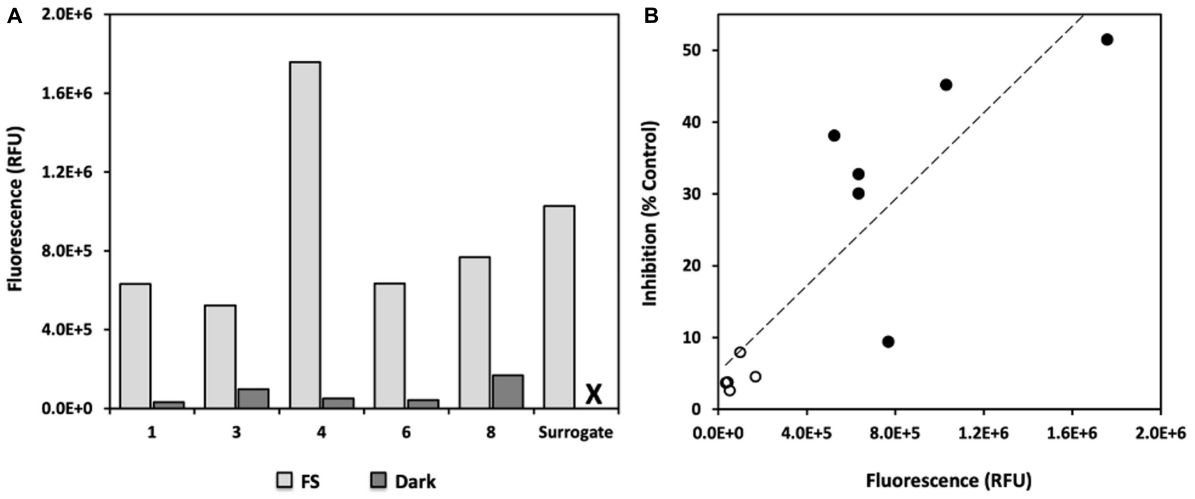

FIGURE 5
Fluorescence of WAFs after exposure of 8 days of sunlight (or dark incubation for 8 days). **(A)** FS (light gray) and dark (dark gray) WAF fluorescence (ex. 365 nm, emiss., 410–600 nm) measured for each pooled WAF preparation and reported as relative fluorescence units (RFU) after subtracting the background fluorescence of the sterile seawater used to prepare WAFs; *X* = no fluorescence data for surrogate WAF prepared in the dark as sample was lost prior to analysis. **(B)** Correlation of bacterial production inhibition with WAF fluorescence. Inhibition of bacterial production (^{3}H-Leucine incorporation) is expressed as a percent of the control; open circles, Dark WAFs; closed circles, FS WAFs.

seawater filtered only to remove large particles (Ehrhardt et al., 1992). Most importantly, the sunlight-exposed fraction and measurements reported varied between studies, whereby some measured changes in fluorescence of solar-exposed WAFs in the absence of oil (Ehrhardt et al., 1992; Snyder et al., 2021), and another measured the fluorescent compounds in the oil fraction extracted from a solar-exposed oil-in-water mixture (King et al., 2014). These studies seem to point toward an expected decrease in fluorescence due to solar exposure, although Snyder et al. (2021) reported results similar to ours. When solar exposure occurs during WAF formation and seawater is constantly in contact with an oil slick, water soluble compounds continue to move from the oil slick into the WAF, confirmed by both increased fluorescence and increased dissolved organic carbon measurements. The duration of solar exposure recorded to yield maximum water-soluble oil compounds is recorded as 96 h of simulated solar exposure (Snyder et al., 2021). Since our WAFs were solar-exposed during WAF-formation, our results indicated

that natural sunlight facilitates the dispersal of fluorescent oil constituents from the oil fraction to the WAF relative to the dark control, likely due to chemical alterations of PAHs that affect hydrophobicity (Yan et al., 2004). Additionally, dispersed oil in WAFs is more bioavailable (Ziervogel et al., 2014) which corresponds to the higher acute (4 h) inhibition observed in FS WAFs vs. dark counterparts.

Water accommodated fractions from different crude oils produced under solar irradiance are prone to differences in photochemical change due to the complexity of crude oil sources, even when oils are geochemically similar (Ray et al., 2014; Vaughan et al., 2016; Benigni et al., 2017). Among the six oils, FS WAF of oil 4 consistently resulted in the highest level of inhibition. The only oil examined that was not recovered from the GOM was Oil 4 and its distinct origin may be responsible for its elevated effect on inhibition of GOM microbes. This implies that greater microbial inhibition may result from a tanker oil spill in which oil from a non-local source is introduced to indigenous microbial communities. Oil 4 is light crude that also resulted in high WAF fluorescence suggesting a high solubility of hydrocarbon constituents and higher toxicity to the microbial inoculum. Oils 1 and 6 were determined to similarly affect bacterial production across all aspects of our study and were also chemically similar medium to heavy sour crude oils (**Figure 1**). On the other hand, oils 4 and 8 were chemically similar with regard to the parameters measured (**Figure 1**), however, elicited very different microbial responses in all parts of this study. Future studies investigating more chemical components of irradiated crude oil WAFs are necessary to fully understand what photochemical changes are affecting bacterial production.

Future investigations should also consider modifying the standard CROSERF WAF preparation methods. In doing so, we can better investigate the dynamic interactions between microorganisms, crude oil, and the natural environment. The current method for WAF production is to mix 1% oil in water and incubate in the dark with moderate mixing for up to 24 h (Aurand and Coelho, 2005). However, the results of this current study demonstrate the diverse response of bacterioplankton to oil WAFs which is largely dependent on exposure to natural sunlight. Irradiated WAFs were consistently represented by greater amounts of acute inhibition of bacterioplankton while WAFs prepared in darkness had minimal effects on microbial inhibition. Since oil spills from tankers occur under direct sunlight and oil well blowouts usually have some portion of oil that reaches the ocean surface, it is important to take this discrepancy between light and dark exposed WAFs into consideration experimentally and ecologically. The vast difference between irradiated and non-irradiated WAFs validates the need for restructuring the standard CROSERF WAF preparation protocol to include a solar exposure component.

We have observed increased inhibition of bacterial production by Surrogate oil WAFs after as little as 2 h solar exposures (data not shown). If a solar component is added to the CROSERF protocol, we recommend that crude oil WAFs be exposed to sunlight for 96 h. By this time, six very different crude oil sources used to generate WAFs all resulted in significant inhibition relative to the control. Previously, WAF composition was documented to change within the first 115 h of exposure to sunlight by photooxidation and irradiance-induced solubilization of hydrocarbon components (Benigni et al., 2017). PAHs are significantly photooxidized after 48 h of exposure (Krylov et al., 1997). In this study, the data demonstrate that in some cases, solar exposure of WAFs results in maximum inhibition within a much shorter time period than previously described as two FS-exposed WAFs (oils 3 and 8) were observed to result in maximum inhibition relative to a control when prepared in only 24 h of natural sunlight. However, the other four WAFs from this study increased in inhibition with increased solar exposure.

In summary, our results indicate that not all oil spills are created equally as different oil spills will elicit different responses. We observed that the response of the bacterioplankton community is dependent on the source oil, the concentration of oil to which the microbes are exposed, and how much and which part of the solar spectrum the oils are exposed. Evidence also suggests the geographic source of the oil as well as seasonal timing of a spill may play important roles. Solar exposure has been shown to be a significant factor in determining how oils will affect microbial communities as the amount of incident solar radiation is a function of seasonality, latitude, water column depth, and water. It is, therefore, important to examine the effects of spills under *in situ* conditions using the same oil as was spilled. These variations demonstrate the complexity of making broad predictions about the effects of oil spills on marine microbes.

Data availability statement

The raw data supporting the conclusions of this article will be made available by the authors, without undue reservation.

Author contributions

EH and WJ: conceptualization and project administration. EH, ME-H, and WJ: methodology. LW and WJ: validation and supervision. EH: formal analysis, data curation, writing—original draft preparation, and visualization. EH, LN, ME-H, AS, and WJ: investigation. WJ: resources. EH, LW, RS, and WJ: writing—review and editing. EH, RS, and WJ: funding acquisition. All authors read and agreed to the published version of the manuscript.

Funding

This research was made possible by a grant from BP/The Gulf of Mexico Research Initiative to the C-IMAGE II and C-IMAGE III consortia to WJ and RS, and by funding from the University of West Florida Hal Marcus College of Science and Engineering (HMCSE Graduate Student Research Grant) to EH.

Acknowledgments

We acknowledge the National High Magnetic Laboratory at Florida State University for providing five of the oils used in this study. We also acknowledge Sarah Zarn for her hands-on assistance in preparing the WAFs.

Conflict of interest

The authors declare that the research was conducted in the absence of any commercial or financial relationships that could be construed as a potential conflict of interest.

Publisher's note

All claims expressed in this article are solely those of the authors and do not necessarily represent those of their affiliated organizations, or those of the publisher, the editors and the reviewers. Any product that may be evaluated in this article, or claim that may be made by its manufacturer, is not guaranteed or endorsed by the publisher.

Supplementary material

The Supplementary Material for this article can be found online at: https://www.frontiersin.org/articles/10.3389/fevo.2023.1113899/full#supplementary-material

References

Atlas, R. M., and Hazen, T. C. (2011). Oil biodegradation and bioremediation: A tale of the two worst spills in U.S. *History Environ. Sci. Technol.* 45, 6709–6715.

Aurand, D., and Coelho, G. (eds) (2005). *Cooperative aquatic toxicity testing of dispersed oil and the "Chemical response to oil spills: Ecological effects research forum (CROSERF),* Technical Report 07-03. Lusby, MD: Ecosystem Management & Associates, Inc.

Bacosa, H. P., Liu, Z., and Erdner, D. L. (2015a). Natural sunlight shapes crude oil-degrading bacterial communities in Northern Gulf of Mexico Surface Waters. *Front. Microbiol.* 6:1325. doi: 10.3389/fmicb.2015.01325

Bacosa, H. P., Erdner, D. L., and Liu, Z. (2015b). Differentiating the roles of photooxidation and biodegradation in the weathering of light louisiana sweet crude oil in surface water from the Deepwater Horizon site. *Mar. Pollut. Bull.* 95, 265–272. doi: 10.1016/j.marpolbul.2015.04.005

Bacosa, H. P., Steichen, J., Kamalanathan, M., Windham, R., Lubguban, A., Labonté, J. M., et al. (2020a). Polycyclic aromatic hydrocarbons (PAHs) and putative PAH-degrading bacteria in Galveston Bay, TX (USA), following Hurricane Harvey (2017). *Environ. Sci. Pollut. Res. Int.* 27, 34987–34999. doi: 10.1007/s11356-020-09754-5

Bacosa, H. P., Kamalanathan, M., Cullen, J., Shi, D., Xu, C., Schwehr, K. A., et al. (2020b). Marine Snow aggregates are enriched in polycyclic aromatic hydrocarbons (PAHs) in Oil contaminated waters: Insights from a Mesocosm study. *J. Mar. Sci. Eng.* 8:781. doi: 10.3390/jmse8100781

Bacosa, H. P., Kang, A., Lu, K., and Liu, Z. (2021). Initial oil concentration affects hydrocarbon biodegradation rates and bacterial community composition in seawater. *Mar. Pollut. Bull.* 162:111867.

Balasubramaniam, A. M., Hall, R. I., Wolfe, B. B., Sweetman, J. N., and Wang, X. (2015). Source water inputs and catchment characteristics regulate limnological conditions of shallow subarctic lakes (Old Crow Flats, Yukon, Canada). *Can. J. Fish. Aquat. Sci.* 72, 1058–1072. doi: 10.1139/cjfas-2014-0340

Benigni, P., Sandoval, K., Thompson, C. J., Ridgeway, M. E., Park, M. A., Gardinali, P., et al. (2017). Analysis of photoirradiated water accommodated fractions of crude oils using tandem TIMS and FT-ICR MS. *Environ. Sci. Technol.* 51, 5978–5988. doi: 10.1021/acs.est.7b00508

Boehm, P. D., Murray, K. J., and Cook, L. L. (2016). Distribution and attenuation of polycyclic aromatic hydrocarbons in Gulf of Mexico seawater from the Deepwater Horizon oil accident. *Environ. Sci. Technol.* 50, 584–592. doi: 10.1021/acs.est.5b03616

Cao, X., and Tarr, M. A. (2017). Aldehyde and Ketone Photoproducts from Solar-Irradiated Crude Oil-Seawater Systems Determined by Electrospray Ionization-Tandem Mass Spectrometry. *Environ. Sci. Technol.* 51, 11858–11866. doi: 10.1021/acs.est.7b01991

Cavicchioli, R., Ripple, W. J., Timmis, K. N., Azam, F., Bakken, L. R., Baylis, M., et al. (2019). Scientists' warning to humanity: Microorganisms and climate change. *Nat. Rev. Microbiol.* 17, 569–586. doi: 10.1038/s41579-019-0222-5

Coelho, G., Clark, J., and Aurand, D. (2013). Toxicity testing of dispersed oil requires adherence to standardized protocols to assess potential real world effects. *Environ. Pollut.* 1987, 185–188. doi: 10.1016/j.envpol.2013.02.004

Dubinsky, E. A., Conrad, M. E., Chakraborty, R., Bill, M., Borglin, S. E., Hollibaugh, J. T., et al. (2013). Succession of hydrocarbon-degrading bacteria in the aftermath of the Deepwater Horizon oil spill in the Gulf of Mexico. *Environ. Sci. Technol.* 47, 10860–10867. doi: 10.1021/es401676y

Dutta, T. K., and Harayama, S. (2000). Fate of crude oil by the combination of photooxidation and biodegradation. *Environ. Sci. Technol.* 34, 1500–1505. doi: 10.1016/j.scitotenv.2019.07.374

Ehrhardt, M. G., Burns, K. A., and Bicego, M. C. (1992). Sunlight-induced compositional alterations in the seawater-soluble fraction of a crude oil. *Mar. Chem.* 37, 53–64. doi: 10.1016/0304-4203(92)90056-G

Fischer, J. M., Nicolai, J. L., Williamson, C. E., Persaud, A. D., and Lockwood, R. S. (2006). Effects of ultraviolet radiation on diel vertical migration of crustacean zooplankton: An in situ mesocosm experiment. *Hydrobiologia* 563, 217–224. doi: 10.1007/s10750-005-0007-x

Fu., P. P., Xia, Q., Sun, X., and Yu, H. (2012). Phototoxicity and environmental transformation of polycyclic aromatic hydrocarbons (PAHs)-light-induced reactive oxygen species, lipid peroxidation, and DNA damage. *J. Environ. Sci. Health C. Environ. Carcinog. Ecotoxicol. Rev.* 30, 1–41. doi: 10.1080/10590501.2012.653887

Gao, Y., Xu, H., Zhang, S., Zhang, Y., Tang, C., and Fan, W. (2019). Visible-light photocatalytic aerobic oxidation of sulfides to sulfoxides with a perylene diimide photocatalyst. *Org. Biomol. Chem.* 7, 7144–7149. doi: 10.1039/c9ob00945k

Genders, S. (1988). In-situ detection and tracking of oil in the water column. *Oil Chem. Pollut.* 4, 113–126. doi: 10.1016/S0269-8579(88)80015-7

Genuino, H. C., Horvath, D. T., King'ondu, C. K., Hoag, G. E., Collins, J. B., and Suib, S. L. (2012). Effects of visible and UV light on the characteristics and properties of crude oil-in-water (O/W) emulsions. *Photochem. Photobiol. Sci.* 11, 692–702. doi: 10.1039/c2pp05275j

Gjesteland, I., Hollund, B. E., Kirkeleit, J., Daling, P. S., Sørheim, K. R., and Bråtveit, M. (2019). Determinants of airborne benzene evaporating from fresh crude oils released into seawater. *Mar. Pollut. Bull.* 140, 395–402. doi: 10.1016/j.marpolbul.2018.12.045

Gregson, B. H., McKew, B. A., Holland, R. D., Nedwed, T. J., Prince, R. C., and McGenity, T. J. (2021). Marine oil snow, a microbial perspective. *Front. Mar. Sci.* 8:619484. doi: 10.3389/fmars.2021.619484

Griffiths, M. T., Da Campo, R., O'Connor, P. B., and Barrow, M. P. (2014). Throwing light on petroleum: Simulated exposure of crude oil to sunlight and characterization using atmospheric pressure photoionization fourier transform ion cyclotron resonance mass spectrometry. *Anal. Chem.* 86, 527–534. doi: 10.1021/ac4025335

Groner, M., Muroski, A. R., and Myrick, M. L. (2001). Identification of major water-soluble fluorescent components of some petrochemicals. *Mar. Pollut. Bull.* 42, 935–941. doi: 10.1016/s0025-326x(01)00052-2

Gros, J., Nabi, D., Würz, B., Wick, L. Y., Brussaard, C. P. D., Huisman, J., et al. (2014). First day of an oil spill on the open sea: Early mass transfers of hydrocarbons to air and water. *Environ. Sci. Technol.* 48, 9400–9411. doi: 10.1021/es502437e

Guipeng, Y., Li, Z., Xiaojing, S., and Weiwen, J. (2006). Photochemical degradation of crude oil in seawater. *Chin. J. Oceanol. Limnol.* 24, 264–269.

Gutierrez, T., Singleton, D. R., Berry, D., Yang, T., Aitken, M. D., and Teske, A. (2013). Hydrocarbon-degrading bacteria enriched by the Deepwater Horizon oil spill identified by cultivation and DNA-SIP. *ISME J.* 7, 2091–2104. doi: 10.1038/ismej.2013.98

Haule, K., and Freda, W. (2021). Remote sensing of dispersed oil pollution in the ocean—The role of chlorophyll concentration. *Sensors* 21:3387. doi: 10.3390/s21103387

Hazen, T. C., Dubinsky, E. A., DeSantis, T. Z., Andersen, G. L., Piceno, Y. M., Singh, N., et al. (2010). Deep-Sea oil plume enriches indigenous oil-degrading bacteria. *Science* 330, 204–208. doi: 10.1126/science.1195979

Hazen, T. C., Prince, R. C., and Mahmoudi, N. (2016). Marine oil biodegradation. *Environ. Sci. Technol.* 50, 2121–2129. doi: 10.1021/acs.est.5b03333

He, B., Lu, M., Yang, C., Liu, Y., Liang, E., and Wang, G. (2018). Perylene as a visible light photoredox catalyst for photoinduced electron transfer-reversible addition-fragmentation chain transfer (PET-RAFT) polymerization of MMA. *J. Macromol. Sci.* 55, 583–587. doi: 10.1080/10601325.2018.1476825

Head, I. M., Jones, D. M., and Röling, W. F. M. (2006). Marine microorganisms make a meal of oil. *Nat. Rev. Microbiol.* 4, 173–182. doi: 10.1038/nrmicro1348

Headrick, (2019). *Comparison of microbial responses to different crude oils with various photoreactivities*. ProQuest Dissertations Publishing.

Holmes, R. M., Aminot, A., Kérouel, R., Hooker, B. A., and Peterson, B. J. (1999). A simple and precise method for measuring ammonium in marine and freshwater ecosystems. *Can. J. Fish. Aquat. Sci.* 56, 1801–1808.

Hou, Y., Li, Y., Liu, Y., Li, G., and Zhang, Z. (2019). Effects of polycyclic aromatic hydrocarbons on the UV-induced fluorescence spectra of crude oil films on the sea surface. *Mar. Pollut. Bull.* 146, 977–984. doi: 10.1016/j.marpolbul.2019.07.058

Hutchins, D. A., and Fu, F. (2017). Microorganisms and ocean global change. *Nat. Microbiol.* 2, 1–11.

Jajoo, A., Mekala, N. R., Tomar, R. S., Grieco, M., Tikkanen, M., and Aro, E.-M. (2014). Inhibitory effects of polycyclic aromatic hydrocarbons (PAHs) on photosynthetic performance are not related to their aromaticity. *J. Photochem. Photobiol. B* 137, 151–155.

Jiang, Z., Huang, Y., Xu, X., Liao, Y., Shou, L., Liu, J., et al. (2010). Advance in the toxic effects of petroleum water accommodated fraction on marine plankton. *Acta Ecol. Sin.* 30, 8–15.

Jing, L., Chen, B., Zhang, B., Zheng, J., and Liu, B. (2014). Naphthalene degradation in seawater by UV irradiation: The effects of fluence rate, salinity, temperature and initial concentration. *Mar. Pollut. Bull.* 81, 149–156.

Juyal, P., McKenna, A. M., Yen, A., Rodgers, R. P., Reddy, C. M., Nelson, R. K., et al. (2011). Analysis and identification of biomarkers and origin of color in a bright blue crude oil. *Energy Fuels* 25, 172–182.

Kassambara, A. (2020). *ggpubr: "ggplot2" Based publication ready plots*.

Kimes, N. E., Callaghan, A. V., Suflita, J. M., and Morris, P. J. (2014). Microbial transformation of the Deepwater Horizon oil spill—past, present, and future perspectives. *Front. Microbiol.* 5:603. doi: 10.3389/fmicb.2014.00603

King, S. M., Leaf, P. A., Olson, A. C., Ray, P. Z., and Tarr, M. A. (2014). Photolytic and photocatalytic degradation of surface oil from the Deepwater Horizon spill. *Chemosphere* 95, 415–422. doi: 10.1016/j.chemosphere.2013.09.060

Kirchman, D., K'nees, E. L., and Hodson, R. (1985). Leucine incorporation and its potential as a measure of protein synthesis by bacteria in natural aquatic systems. *Appl. Environ. Microbiol.* 49, 599–607. doi: 10.1128/aem.49.3.599-607.1985

Krylov, S. N., Huang, X., Zeiler, L. F., Dixon, D. G., and Greenberg, B. M. (1997). Mechanistic quantitative structure-activity relationship model for the photoinduced toxicity of polycyclic aromatic hydrocarbons: I. Physical Model based on chemical kinetics in a two compartment system. *Environ. Toxicol. Chem.* 16, 2283–2295.

Lee, R. F. (2003). Photo-oxidation and photo-toxicity of crude and refined oils. *Spill Sci. Technol. Bull.* 8, 157–162.

Lenth, R. V. (2023). *emmeans: Estimated marginal means, aka least-squares means.* R package version 1.8.5. Available online at: https://CRAN.R-project.org/package=emmeans (accessed February 20, 2023).

Ma, Y.-L., Lu, W., Wan, L.-L., and Luo, N. (2015). Elucidation of fluoranthene degradative characteristics in a newly isolated achromobacter xylosoxidans DN002. *Appl. Biochem. Biotechnol* 175, 1294–1305. doi: 10.1007/s12010-014-1347-7

MacDonald, I. R., Garcia-Pineda, O., Beet, A., Asl, S. D., Feng, L., Graettinger, G., et al. (2015). Natural and unnatural oil slicks in the Gulf of Mexico. *J. Geophys. Res. Oceans* 120, 8364–8380. doi: 10.1002/2015JC011062

Maki, H., Sasaki, T., and Harayama, S. (2001). Photo-oxidation of biodegraded crude oil and toxicity of the photo-oxidized products. *Chemosphere* 44, 1145–1151. doi: 10.1016/s0045-6535(00)00292-7

Matvyeyeva, O. L., Vasylchenko, O. A., and Aliieva, O. R. (2014). Microbial biosurfactants role in oil products biodegradation. *Int. J. Environ. Bioremediat. Biodegrad.* 2, 69–74.

McNutt, M. K., Camilli, R., Crone, T. J., Guthrie, G. D., Hsieh, P. A., Ryerson, T. B., et al. (2012). Review of flow rate estimates of the Deepwater Horizon oil spill. *Proc. Natl. Acad. Sci. U.S.A.* 109, 20260–20267. doi: 10.1073/pnas.1112139108

Melkonian, C., Fillinger, L., Atashgahi, S., da Rocha, U. N., Kuiper, E., Olivier, B., et al. (2021). High biodiversity in a benzene-degrading nitrate-reducing culture is sustained by a few primary consumers. *Commun. Biol.* 4, 1–12.

Nicodem, D. E., Guedes, C. L. B., Conceição, M., Fernandes, Z., Severino, D., Correa, R. J., et al. (2001). Photochemistry of petroleum. *Prog. React. Kinet. Mech.* 26, 219–238.

Owen, C. J., Axler, R. P., Nordman, D. R., Schubauer-Berigan, M., Lodge, K. B., and Schubauer-Berigan, J. P. (1995). Screening for PAHs by fluorescence spectroscopy: A comparison of calibrations. *Chemosphere* 31, 3345–3356.

Pampanin, D. M., and Sydnes, M. O. (2013). *Polycyclic aromatic hydrocarbons a constituent of petroleum: Presence and influence in the aquatic environment*. London: IntechOpen. doi: 10.5772/48176

Parsons, T. R., Maita, Y., and Lalli, C. M. (1984). *A manual of chemical and biological methods for seawater analysis*. Oxford: Pergamon Press.

Passow, U., and Stout, S. A. (2020). Character and sedimentation of "lingering" Macondo oil to the deep-sea after the Deepwater Horizon oil spill. *Mar. Chem.* 218:103733.

Pelz, O., Brown, J., Huddleston, M., Rand, G., Gardinali, P., Stubblefield, W., et al. (2011). "Selection of a surrogate MC252 oil as a reference material for future aquatic toxicity tests and other studies, poster," in *Proceedings of the society of environmental toxicology and chemistry meeting*, (Boston, MA: SETAC).

Peng, R.-H., Xiong, A.-S., Xue, Y., Fu, X.-Y., Gao, F., Zhao, W., et al. (2008). Microbial biodegradation of polyaromatic hydrocarbons. *FEMS Microbiol. Rev.* 32, 927–955.

Prince, R. C. (1993). Petroleum spill bioremediation in marine environments. *Crit. Rev. Microbiol.* 19, 217–242.

Prince, R. C., and Atlas, R. M. (2018). "Bioremediation of marine oil spills," in *Consequences of microbial interactions with hydrocarbons, oils, and lipids: Biodegradation and bioremediation*, ed. R. Steffan (Cham: Springer International Publishing), 1–25.

R Core Team (2022). *R: A language and environment for statistical computing*. R Foundation for Statistical Computing. Vienna: .R Core Team.

Ray, P. Z., Chen, H., Podgorski, D. C., McKenna, A. M., and Tarr, M. A. (2014). Sunlight creates oxygenated species in water-soluble fractions of Deepwater Horizon oil. *J. Haz. Mat.* 280, 636–643. doi: 10.1016/j.jhazmat.2014.08.059

Riazi, M. R., and Roomi, Y. A. (2008). A model to predict rate of dissolution of toxic compounds into seawater from an oil spill. *Int. J. Toxicol.* 27, 379–386. doi: 10.1080/10915810802503578

Robinson, C. (2019). Microbial respiration, the engine of ocean deoxygenation. *Front. Mar. Sci.* 5:533. doi: 10.3389/fmars.2018.00533

Saeed, T., Ali, L. N., Al-Bloushi, A., Al-Hashash, H., Al-Bahloul, M., Al-Khabbaz, A., et al. (2011). Effect of environmental factors on photodegradation of polycyclic aromatic hydrocarbons (PAHs) in the water-soluble fraction of Kuwait crude oil in seawater. *Mar. Environ. Res.* 72, 143–150.

Saeed, T., Ali, L. N., Al-Bloushi, A., Al-Hashash, H., Al-Bahloul, M., Al-Khabbaz, A., et al. (2013). Photodegradation of volatile organic compounds in the water-soluble fraction of Kuwait crude oil in seawater: Effect of environmental factors. *Water. Air. Soil Pollut.* 224:1584.

Santas, R., Häder, D.-P., and Santas, P. (1999). Is crude oil bioremediation affected by changes in ambient ultraviolet radiation? *Mar. Pollut. Bull.* 38, 1022–1025.

Schnetger, B., and Lehners, C. (2014). Determination of nitrate plus nitrite in small volume marine water samples using vanadium (III) chloride as a reduction agent. *Mar. Chem.* 160, 91–98.

Scofield, V., Jacques, S. M. S., Guimarães, J. R. D., and Farjalla, V. F. (2015). Potential changes in bacterial metabolism associated with increased water temperature and nutrient inputs in tropical humic lagoons. *Front. Microbiol.* 6:310. doi: 10.3389/fmicb.2015.00310

Shin, P. K. S., and Fong, K. Y. S. (1999). Multiple discriminant analysis of marine sediment data. *Mar. Poll. Bull.* 39, 285–294.

Smith, D. C., and Azam, F. (1992). A simple, economical method for measuring bacterial protein synthesis rates in seawater using 3H-leucine. *Mar. Microb. Food Webs* 6, 107–114.

Snyder, K., Mladenov, N., Richardot, W., Dodder, N., Nour, A., Campbell, C., et al. (2021). Persistence and photochemical transformation of water soluble constituents from industrial crude oil and natural seep oil in seawater. *Mar. Pollut. Bull.* 165:112049. doi: 10.1016/j.marpolbul.2021.112049

Sørstrøm, S. E. (1985). A note on in-situ fluorescence for detection of oil in water. *Oil Petrochem. Pollut.* 2, 125–132.

Sugiura, K., Ishihara, M., Shimauchi, T., and Harayama, S. (1997). Physicochemical properties and biodegradability of crude oil. *Environ. Sci. Technol.* 31, 45–51.

Toyooka, T., and Ibuki, Y. (2007). DNA damage induced by coexposure to PAHs and light. *Pharmacology* 23, 256–263.

Vaughan, P. P., Wilson, T., Kamerman, R., Hagy, M. E., McKenna, A., Chen, H., et al. (2016). Photochemical changes in water accommodated fractions of MC252 and surrogate oil created during solar exposure as determined by FT-ICR MS. *Mar. Pollut. Bull.* 104, 262–268. doi: 10.1016/j.marpolbul.2016.01.012

Vergeynst, L., Christensen, J. H., Kjeldsen, K. U., Meire, L., Boone, W., Malmquist, L. M. V., et al. (2019). In situ biodegradation, photooxidation and dissolution of petroleum compounds in Arctic seawater and sea ice. *Water Res.* 148, 459–468. doi: 10.1016/j.watres.2018.10.066

Viggor, S., Juhanson, J., Jõesaar, M., Mitt, M., Truu, J., Vedler, E., et al. (2013). Dynamic changes in the structure of microbial communities in Baltic Sea coastal seawater microcosms modified by crude oil, shale oil or diesel fuel. *Microbiol. Res.* 168, 415–427.

Wozniak, A. S., Prem, P. M., Obeid, W., Waggoner, D. C., Quigg, A., Xu, C., et al. (2019). Rapid degradation of oil in mesocosm simulations of Marine oil snow events. *Environ. Sci. Technol.* 53, 3441–3450. doi: 10.1021/acs.est.8b06532

Yan, J., Wang, L., Fu, P. P., and Yu, H. (2004). Photomutagenicity of 16 polycyclic aromatic hydrocarbons from the US EPA priority pollutant list. *Mutat. Res.* 557, 99–108. doi: 10.1016/j.mrgentox.2003.10.004

Yang, T., Nigro, L. M., Gutierrez, T. D., D'Ambrosio, L., Joye, S. B., Highsmith, R., et al. (2016). Pulsed blooms and persistent oil-degrading bacterial populations in the water column during and after the Deepwater Horizon blowout. *Deep-Sea Res. II: Top. Stud. Oceanogr.* 129, 282–291. doi: 10.1016/j.dsr2.2014.01.014

Ziervogel, K., D'souza, N., Sweet, J., Yan, B., and Passow, U. (2014). Natural oil slicks fuel surface water microbial activities in the northern Gulf of Mexico. *Front. Microbiol.* 5:188. doi: 10.3389/fmicb.2014.00188

frontiers | Frontiers in Ecology and Evolution

TYPE Original Research
PUBLISHED 12 April 2023
DOI 10.3389/fevo.2023.1143377

OPEN ACCESS

EDITED BY
Frank S. Gilliam,
University of West Florida, United States

REVIEWED BY
Daria Martynova,
Zoological Institute (RAS), Russia
Rachel Louise Coppock,
Plymouth Marine Laboratory, United Kingdom

*CORRESPONDENCE
Amy N. S. Siuda
✉ siudaan@eckerd.edu
Shannon Gowans
✉ gowanss@eckerd.edu

SPECIALTY SECTION
This article was submitted to Biogeography and Macroecology, a section of the journal Frontiers in Ecology and Evolution

RECEIVED 12 January 2023
ACCEPTED 22 March 2023
PUBLISHED 12 April 2023

CITATION
Fibbe MC, Carroll D, Gowans S and Siuda ANS (2023) Ingestion of microplastics by copepods in Tampa Bay Estuary, FL.
Front. Ecol. Evol. 11:1143377.
doi: 10.3389/fevo.2023.1143377

Ingestion of microplastics by copepods in Tampa Bay Estuary, FL

Mary Claire Fibbe[1], Delphine Carroll[1], Shannon Gowans[2]* and Amy N. S. Siuda[1]*

[1]Marine Science Discipline, Eckerd College, St. Petersburg, FL, United States, [2]Marine Science and Biology Disciplines, Eckerd College, St. Petersburg, FL, United States

Microplastics have been recognized as an emerging contaminant. Copepods are abundant primary consumers in marine food webs. Interactions between copepods and microplastics can lead to negative health effects to the individual and may have implications for populations and ecosystems through biomagnification. Laboratory and field studies have observed various species of zooplankton ingesting microplastics, however, this is the first study to observe microplastic-copepod interactions in Tampa Bay. Over 2 years (November 2017-January 2020), 14 sampling cruises were conducted with seven stations throughout Tampa Bay. At each station copepods were collected by towing a 200 μm mesh ring net (0.5 m diameter) for 3 min. 1,000 individual *Acartia tonsa* copepods were picked from each sample and digested to release gut contents. Gut contents were stained in a Nile Red solution and then visualized using epifluorescent microscopy, quantified, photographed and sized using image analysis. In Tampa Bay, *A. tonsa* consumed fragments over fibers, ranging from 0.018 to 0.642 mm, with an average particle size of 0.076 mm. An overall average of 15.38 particles were ingested per 1,000 copepods, or 6.48 particles m^{-3} when normalized for environmental copepod concentrations. While significant differences were detected between stations and months, no clear spatial (from head to mouth of estuary) or temporal (between wet and dry seasons) trends in ingestion rate or ingested particle size were evident. These results show that *A. tonsa* ingested microplastics throughout Tampa Bay. These robust baseline data, for a copepod species that dominates estuarine zooplankton communities around the world, set the stage for valuable comparisons between estuaries with different physical mechanisms and levels of anthropogenic impact, allowing for exploration of how the environmental conditions impact ecological interactions.

KEYWORDS

microplastics, zooplankton, copepod, field ingestion rates, Tampa Bay, estuary

1. Introduction

Microplastics are small fibers, fragments or granules of plastic, 0.001–5 mm in diameter (reviewed in GESAMP, 2019). Primary microplastics are small beads and fibers, specifically manufactured for use in various products, as well as pellets known as "nurdles," which are used in plastic manufacturing (Ellison, 2007; GESAMP, 2019). Secondary microplastics derive from macroplastics that have broken into smaller pieces through processes of

thermal degradation, photo-oxidative degradation from UV exposure, and *via* mechanical degradation from stressors such as abrasion and impact from waves, rocks, sand and ocean currents (Andrady, 2015; GESAMP, 2019). Hence, it is estimated that the concentration of microplastics in the marine environment is negatively correlated with microplastic size, as the proportion of smaller particles increases relative to the number of larger plastics fragmenting (Cózar et al., 2014; Enders et al., 2015; GESAMP, 2019). Based on increasing production and consumption of plastics, projections indicate that up to 53 million metric tonnes of plastic per year may enter the ocean from land by 2030 (Borrelle et al., 2020). Several studies using environmental data and modeling have estimated that between 7,000–93,000 tons or 1.7–4.85 trillion microplastic particles are present in surface waters of the world's oceans (Cózar et al., 2014; Eriksen et al., 2014; van Sebille et al., 2015; Lebreton et al., 2018), with greater concentrations near continents as opposed to offshore (Tonhua et al., 2020).

With the widespread abundance of plastics in the ocean, there is growing concern for the threats they may pose to marine organisms and ecosystems. Microplastics can transport invasive species (reviewed in García-Gómez et al., 2021) and cause intestinal blockage, pseudo-satiation or even starvation when ingested (reviewed in Egbeocha et al., 2018). Plastics also contain harmful toxins, originating from the manufacturing process, or sorbed hydrophobic toxins from the environment (Engler, 2012; reviewed in Crawford and Quinn, 2017; reviewed in Gallo et al., 2018). Studies have found that if ingested, microplastics and associated toxins can lead to a number of negative reproductive, growth, health, and behavioral impacts (Derriak, 2002; Rochman et al., 2013, 2014; Lönnstedt and Eklöv, 2016; Coppock et al., 2019; Bucci et al., 2020). In the marine environment, an array of animals ingest microplastics, including fishes (Davison and Asch, 2011), seabirds (Van Franeker, 2011), bivalves (Phuong et al., 2018), marine turtles (Duncan et al., 2018), marine mammals (Nelms et al., 2019; Ortega-Borchardt et al., 2023), and zooplankton (reviewed in Botterell et al., 2019). Ecological effects of plastic pollution in the marine environment are less clear and not always detected (Bucci et al., 2020).

The transfer of microplastics from zooplankton to secondary consumers has been observed in laboratory studies (Farrell and Nelson, 2013; Setälä et al., 2014; Athey et al., 2020; Costa et al., 2020; Van Colen et al., 2020; Domínguez-López et al., 2022; Kim et al., 2022), raising concern that plastics and associated toxins have the potential for biomagnification, moving up through trophic levels and accumulating in top consumers. Microscopic plankton represent a potential entry point of microplastics at the base of the food web (Botterell et al., 2019) and may act as bioindicators for overall health of aquatic ecosystems (Hemraj et al., 2016; Araujo et al., 2017). Copepods serve as a vital link between primary producers and higher trophic levels throughout the ocean (Vroom et al., 2017; reviewed in Mauchline, 1998). Investigating copepod interactions with microplastics will not only increase our understanding of the impact of plastics on zooplankton but will also shed light on the potential for zooplankton to serve as vectors of plastic transfer through marine food webs. While investigating grazing rates and size-selection, using microplastics particles as inert "prey," several early laboratory experiments unintentionally demonstrated that copepods ingest microplastics under certain conditions (Burns, 1968; Frost, 1972; Wilson, 1973). More recent laboratory experiments have found that exposure to high concentrations of microplastics can lead to changes in copepod feeding behavior and prey selection (Cole et al., 2013, 2014, 2019; Coppock et al., 2019; Koski et al., 2021), reproductive output (Cole et al., 2014), molting cycles (Cole et al., 2019), lipid production (Cole et al., 2019), and fecal pellet sinking rates (Coppock et al., 2019).

There has been limited research, however, on ingestion of microplastics by copepods in the field. Ingestion rates (particles per copepod) have been estimated for large oceanic copepod species in northern Pacific (Desforges et al., 2015), Arctic (Howell, 2019; Botterell et al., 2022), and Black Sea (Aytan et al., 2022) offshore waters. Despite differences in prey size spectra as function of copepod size and feeding strategy, ingestion rate estimates have also been made for mixed copepod assemblages in coastal waters of the South China Sea (Sun et al., 2017; Amin et al., 2020), Gulf of Thailand (Buathong et al., 2020; Taha et al., 2021), Andaman Sea (Goswami et al., 2020), and western Indian Ocean (Kosore et al., 2018). Notably, few observations have been made of microplastic ingestion by copepods in estuaries, where high biological productivity and high surface microplastic concentrations, resulting from the semi-enclosed shape and proximity to river discharge and anthropogenic activities (GESAMP, 2019), facilitate such interactions. Microplastic ingestion rate estimates were generated from small sample sizes collected over a series of days for copepod assemblages in Malaysia (Taha et al., 2021) and the southeastern United States (Payton et al., 2020), as well as for dominant copepod species in the mid-Atlantic United States (Sipps et al., 2022). In contrast, periodic sampling over the course of many months accounted for seasonal variability in tropical rainfall when measuring microplastic ingestion by copepod assemblages from estuaries in India (Rashid et al., 2022) and China (Zheng et al., 2021).

This study aims to expand understanding of microplastic-copepod interactions by comprehensively characterizing the ingestion of environmental microplastics by a cosmopolitan estuarine calanoid copepod. Tampa Bay is located in the transition zone between subtropical and temperate climates along Florida's west-central coast. Spanning a surface area of 1,036 km^2, it is the largest open-water estuary in Florida. A watershed of approximately 5,700 km^2 feeds into Tampa Bay, including four major rivers and numerous smaller tributaries (Cicchetti and Greening, 2011). However, non-point source stormwater runoff appears to be the greatest input of freshwater to the Bay (Zhu et al., 2015). Pinellas County, to the west, is the most densely populated county in Florida[1] and the Bay supports high levels of tourism, fishing and boating. Additionally, Tampa Bay is the only deep water cargo port on Florida's west coast and the largest cargo port in Florida.[2] This collection of features suggests that Tampa Bay may be especially prone to plastic accumulation; McEachern et al. (2019) estimated an average of 940 particles m^{-3} in Tampa Bay surface waters. Here, we report on the quantities, sizes and types (e.g., fragment or fiber) of microplastic ingested by *Acartia tonsa* over the course of 2 years in Tampa Bay, providing a substantial baseline

1 www.edr.state.fl.us

2 porttb.com

for comparison to future studies in both developed and pristine estuaries.

2. Materials and methods

From November 2017 through January 2020 copepod samples were collected bi-monthly (14 cruises total) at seven stations in Tampa Bay, FL, USA (**Figure 1**). All stations, except for Boca Ciega Bay, were co-located with established Environmental Protection Commission of Hillsborough County (EPC-HC) water quality monitoring sites and selected to represent sub-regions of the Bay with different flushing times and physical mechanisms (e.g., tidal excursion, river influx, and winds). Because Tampa Bay is long and the four major rivers enter on the eastern side, residence times increase from mouth to head (south to north) and east to west (Zhu et al., 2015). Many tidal inlets between barrier islands keep the Boca Ciega Bay region well-flushed with a short residence time (Zhu et al., 2015). Skyway, Pinellas Point, and MacDill Air Force Base stations follow a south to north axis through the open mid-Bay region. The two heads of the Bay differ greatly in residence time. Hillsborough Bay residence time is shorter (100–120 days) due to freshwater input from the Hillsborough and Alafia Rivers, whereas Old Tampa Bay residence time is longest (120–200 days) due to its location in the northwest and the multiple causeways that restrict flow (Zhu et al., 2015). The Egmont Key station sits at the transition between Tampa Bay and open shelf waters.

Copepods were collected using a Sea-Gear Corporation (Florida, USA) model 9000 conical ring net (0.5 m diameter, 200 μm mesh) towed horizontally while submerged just below the surface for 3 min at approximately 1.5 knots. Tow distance was calculated based on straight line distance between beginning and ending GPS coordinates and tow volume was estimated from tow distance and area of the plankton net mouth. Each zooplankton sample was immediately concentrated on a 200 μm mesh sieve and preserved with ethanol to halt ingestion or egestion of microplastic particles.

In the lab, each sample was concentrated on a 200 μm mesh sieve and resuspended in a known volume of Milli-Q water to determine biovolume. From each sample, 1,000 copepods, with full guts and of the dominant species, were individually selected using a glass Pasteur pipet. Each copepod was passed through several Milli-Q water rinses and examined under a dissecting microscope with bright-field, white light to confirm there were no externally adhered microplastic particles. Copepods were transferred in batches of 500 individuals to 2 mL microcentrifuge tubes for an initial room temperature decomposition period of 14 days. Subsequently, the batches were dried for approximately 24 h in a covered heating block set to 60°C. Microcentrifuge tube caps were closed but not firmly sealed to allow for evaporation during the drying step. An enzymatic digestion protocol adapted from Cole et al. (2014), with a ratio of 500 μg mL^{-1} proteinase-K to 0.2 g dry-weight of sample, was used to break apart exoskeletons and release gut content from copepods into solution. For the contents in each tube, 750 μL homogenizing solution (0.25 L stock homogenizing solution consisting of 15.77 g Tris-HCL, 4.38 g EDTA, 1.53 g NaCl, and 1.26 g SDS, with 15 mL of homogenizing solution being 40 mM Tris-HCL, 60 mM EDTA, 105 mM NaCl and 1% SDS) were added. Sample tubes were then vortexed for at least 30 sec and incubated for 1–2 h at 60°C. 40 μL of proteinase-K solution was added and samples were incubated for at least 6–8 h with periodic vortexing. 250 μL of 5M $NaClO_4$ were added and samples were vortexed for several minutes before incubating at 60°C for 24 hrs.

Nile Red [9-diethylamino-5H-benzo(a) phenoxazine-5-one], a selectively fluorescent dye that binds to lipids (Maes et al., 2017; Shim et al., 2017), was used to stain copepod gut content in preparation for visual identification of microplastics. Preliminary protocol testing with plastics of known composition indicated that plastics glowed brightly red, orange, yellow or green, depending on composition, and chitin or cellulose material fluoresced a faint red. It is important to note that the staining pattern may cause semi-synthetic or regenerated cellulosic fibers to be overlooked and the presence of manufacturing dyes can negatively impact the ability of Nile Red to stain some plastic particles (Stanton et al., 2019). Therefore, the quantification of microplastics using this method may represent an underestimation of particles present in a sample.

Digested copepod batches were stained with Nile Red for 30 min in clean and covered glass beakers containing a ratio of 20 mL Milli-Q water to 4 mL Nile Red stock solution (5 mg Nile Red powder dissolved in 1 L acetone). Each batch was then transferred to a 47 mm diameter, 5 μm pore size black polycarbonate filter using vacuum filtration and stored in a clean petri dish with lid. To eliminate contamination, cotton clothing or lab coats were worn at all times and samples and reagent solutions were kept covered while handling. Wet filters left exposed in a variety of locations around the lab for 24 h did not accumulate microplastic particles.

A dissecting microscope equipped with a digital camera and Stereo Microscope Fluorescence Adapter system (NightSea, Lexington, MA, USA) was used to quantify microplastic particles. Sample filters were exposed to cyan light (excitation wavelength: 490–515 nm) and viewed through an orange emission filter (550 nm long pass). Similar to reports by others (Erni-Cassola et al., 2017; Nalbone et al., 2021), brightly glowing microplastic particles clearly contrasted with the faint red of stained copepod exoskeleton fragments remaining after digestion (**Figure 2**). Before imaging a particle and adding its photo to the archive, each particle was also examined at higher magnification under bright-field, white light and physically manipulated with a metal probe to assess hardness. Microplastic particles were categorized as fragments or fibers. ImageJ (Schneider et al., 2012) was used to measure the length of the longest axis.

In addition to directly measured microplastic particle length and number of ingested particles per 1,000 copepods, the number of ingested particles per m^3 was estimated to account for differences in mesozooplankton concentration between samples. Based on observations made while picking copepods for digestion, a conversion of 1 mL biovolume to 1,000 individuals was used to estimate the total number of individuals in each tow. The calculation also assumed that each copepod contained at most a single ingested microplastic particle. As none of these direct-measurement and estimated datasets were normally distributed, single-factor Kruskal–Wallis tests were used to assess differences between groups (e.g., stations, months, and seasons) and Dunn Method for Joint Ranking tests were used to make pairwise comparisons. All data analyses were performed in JMP Version 16 (SAS Institute Inc., Cary, NC, USA).

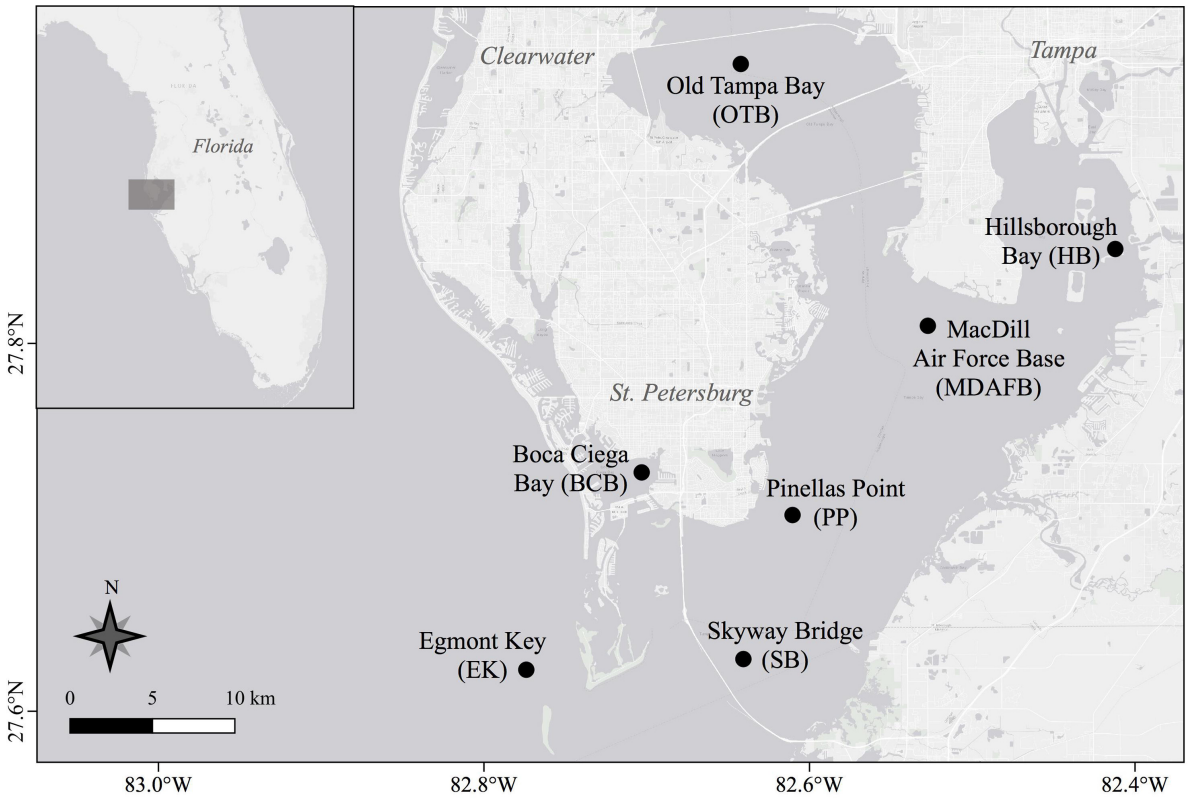

FIGURE 1
Sampling locations in Tampa Bay, Florida, USA. Station map was created using QGIS software (QGIS 3.4.14-Madeira).

3. Result

A total of 1,507 ingested microplastic particles were collected from 97,500 copepods. *A. tonsa* dominated mesozooplankton communities and accounted for all 1,000 copepods picked from samples at all stations, except one–the May 2018 sample from Egmont Key, where 500 copepods representing multiple species were picked in the absence of abundant *A. tonsa*. Most ingested microplastic particles were fragments (96.88%); the remainder of ingested particles were fibers, which were most commonly ingested at the Skyway Bridge and Egmont Key stations. The mean size of all ingested microplastic particles was 0.076 mm (SE ± 0.001; Figure 3). Fragment length ranged from 0.018 to 0.351 mm (mean = 0.072 mm; SE ± 0.001), whereas fiber length ranged from 0.019 to 0.642 mm (mean = 0.202 mm; SE ± 0.022). Significant differences in ingested particle size were detected between sampling stations (H = 22.105, 6 d.f., p = 0.0012; Figure 4A) and months (H = 58.903, 5 d.f., $p < 0.0001$; Figure 4B). Pairwise comparisons indicated that ingested particle size was significantly smaller at the Boca Ciega Bay station than at the Pinellas Point (p = 0.0106), Old Tampa Bay (p = 0.0275) and Hillsborough Bay stations (p = 0.0359). Ingested particle size was significantly smaller during May and November compared with January (May: p = 0.0039; Nov.: <0.0001), March (May: p = 0.0124; Nov.: $p < 0.0001$) and September (May/Nov.: $p < 0.0001$) as well as during July compared with September (p = 0.0153). All other comparisons between stations and months resulted in no significant differences.

The average number of ingested microplastic particles per 1,000 copepods was 15.38 (SE ± 0.85), with a mode of 11 microplastic particles per 1,000 copepods. The Hillsborough Bay sample from May 2018 contained 55 ingested microplastic particles per 1,000 copepods, the maximum observed in this study. The minimum was 4 ingested microplastic particles per 1,000 copepods in the January 2018 MacDill Air Force Base and September 2018 Old Tampa Bay samples. There were no significant differences in the number of microplastic particles ingested per 1,000 copepods between stations (H = 3.214, 6 d.f., p = 0.7815; Figure 5A). However, the number of ingested microplastic particles per 1,000 copepods was significantly lower during the dry season (August to June) compared with the wet season (May to July; H = 4.868, 1 d.f., p = 0.0274). Specifically, the number of ingested particles per 1,000 copepods was lower during September compared with May (p = 0.0274; Figure 5B); no other pairwise comparisons between months were significantly different.

Variable wind and tidal current speed and direction resulted in tow volumes ranging from 7.27 to 83.64 m^3 (mean = 31.81 m^3; SE ± 1.42). Mesozooplankton biovolume per tow ranged from 1.2 to 76 mL (mean = 12.73 mL; SE ± 1.42) after removing one sample with abundant diatoms that skewed the measurement. There was no relationship between tow volume and mesozooplankton biovolume; tow volumes were close to the mean at the maximum and minimum biovolume stations. The estimated number of microplastic particles ingested per m^3 was not significantly different between stations (H = 1.853, 6 d.f., p = 0.9327; Figure 6A) or sampling months (H = 7.742, 5 d.f., p = 0.1710; Figure 6B).

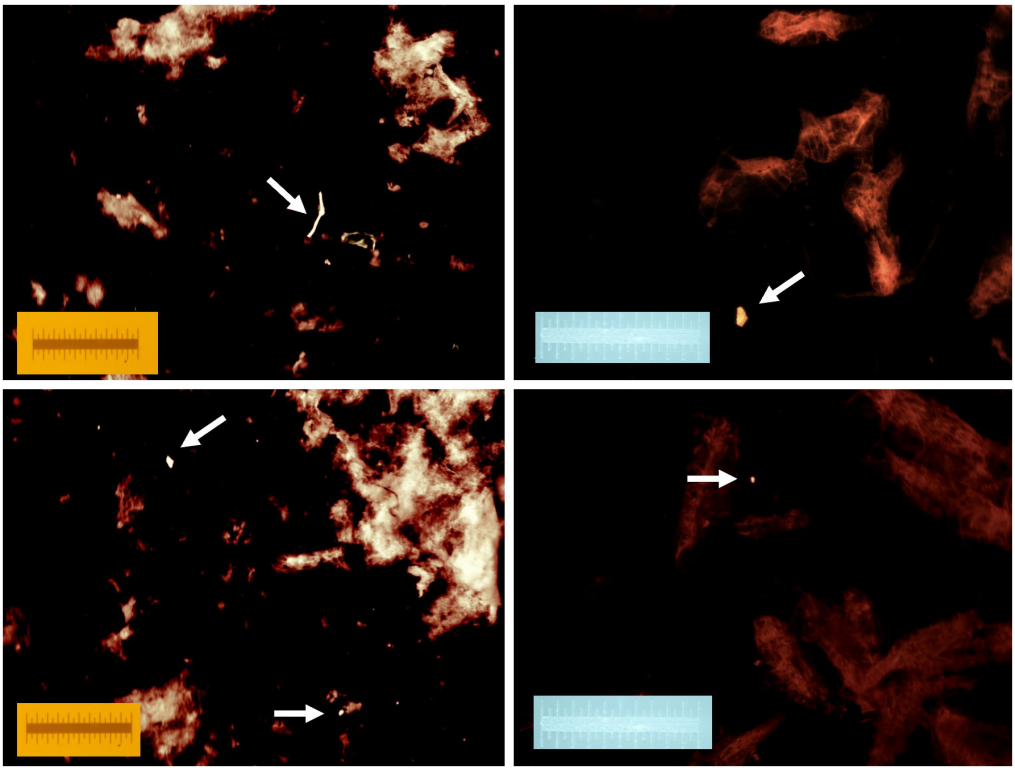

FIGURE 2
Four separate examples of fluorescent microplastics released during copepod digestion. Samples were stained with Nile red following digestion and photographed with a cyan light (490–515 nm) through an orange long pass filter (550 nm). Each image includes a 1 mm scale.

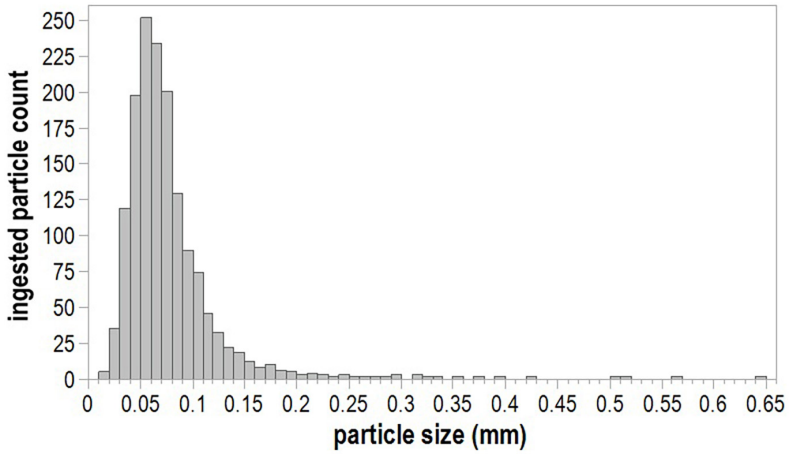

FIGURE 3
Size distribution of ingested microplastics.

However, fewer particles were ingested per m^3 during the dry as compared to the wet season ($H = 6.429$, 1 d.f., $p = 0.0112$).

4. Discussion

A. tonsa copepods in Tampa Bay primarily ingested microplastic fragments. Fibers accounted for <4% of ingested particles, despite having been reported as the most common microplastic type in surface waters of the Bay (McEachern et al., 2019). This pattern of dominant fibers in seawater samples with dominant fragments in concurrent copepod samples has been observed by others (Amin et al., 2020; Aytan et al., 2022) and while fibers were abundantly present in seawater of the Fram Strait, copepods ingested only fragments (Botterell et al., 2022). Overall, however, ingestion of greater proportions of fibers to fragments has been more frequently reported. Kosore et al. (2018) and Taha et al. (2021) found that fibers were dominant in both

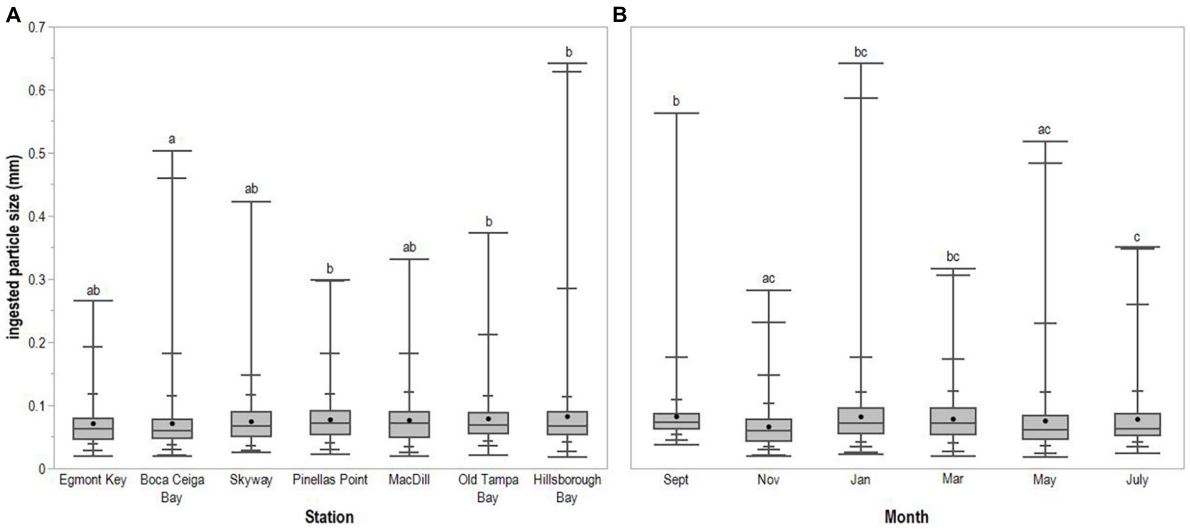

FIGURE 4
Ingested microplastic particle size (mm) across **(A)** sampling stations and **(B)** months. Horizontal line spanning box indicates median, while point indicates mean. Whiskers indicate maximum and minimum values, with intermediate quantiles marked. Letters identify statistically significant differences between stations or months.

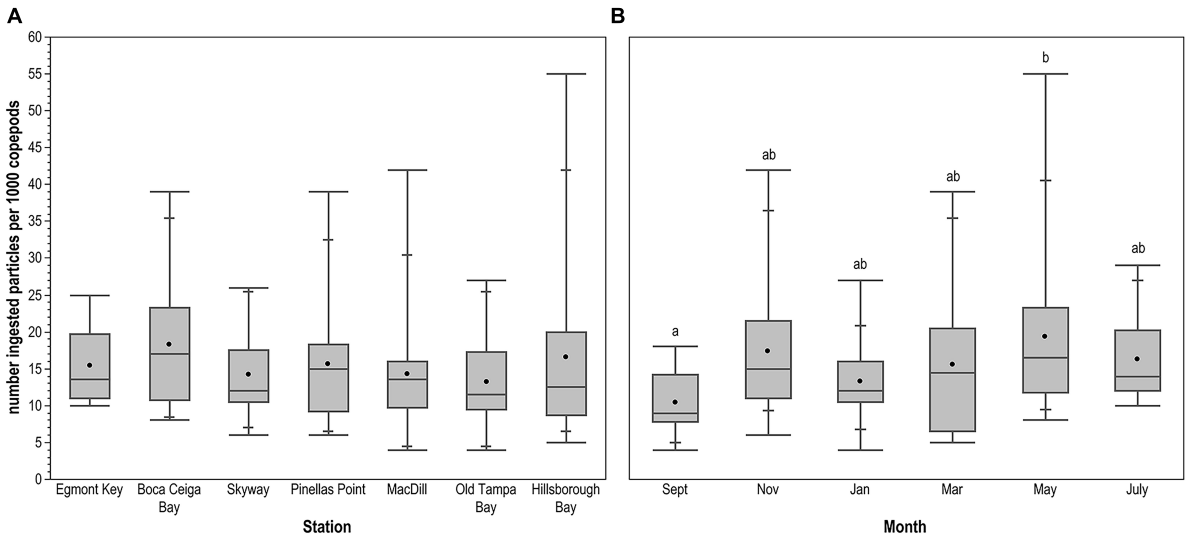

FIGURE 5
Number of ingested microplastic particles per 1,000 copepods across **(A)** sampling stations and **(B)** months. Horizontal line spanning box indicates median, while point indicates mean. Whiskers indicate maximum and minimum values, with intermediate quantiles marked. Letters identify statistically significant differences between months; there were no significant differences between stations.

seawater and copepod samples. Similarly, a greater proportion of microplastic fibers to fragments were ingested by copepods in the other published field studies (Sun et al., 2017; Buathong et al., 2020; Payton et al., 2020; Zheng et al., 2021; Rashid et al., 2022). Amin et al. (2020) suggested that if zooplankton were not preserved immediately after collection, fragments could pass through the digestive system more easily than fibers, leading to reporting of elevated fiber to fragment ingestion ratios. Yet, most methods in the aforementioned studies include a preservation step. Furthermore, *A. tonsa* selected for nylon fibers over polystyrene beads in a laboratory setting (Borrelle et al., 2020). In this particular case, the nylon fibers were smaller than the polystyrene beads, possibly making the fibers more easily ingested. In the field, fibers tend to be larger/longer than fragments (Aytan et al., 2022; Botterell et al., 2022), with lengths that can exceed ingestion capacities. The shape of ingested microplastic appears to be limited both by particle size and availability in the surrounding water. Thus, Desforges et al. (2015) found that a single large copepod species switched from more frequently ingesting fragments at offshore sites to only ingesting fibers at coastal sites, and given the mismatch in shape and size of fibers to the typical estuarine copepod diet of phytoplankton and microzooplankton, more frequent ingestion of fragments by *A. tonsa* was expected.

The average size of particles ingested by *A. tonsa* was comparable to that of their natural phytoplankton prey (0.002–0.106 mm or 2–5% of prosome length; Berggreen et al., 1988),

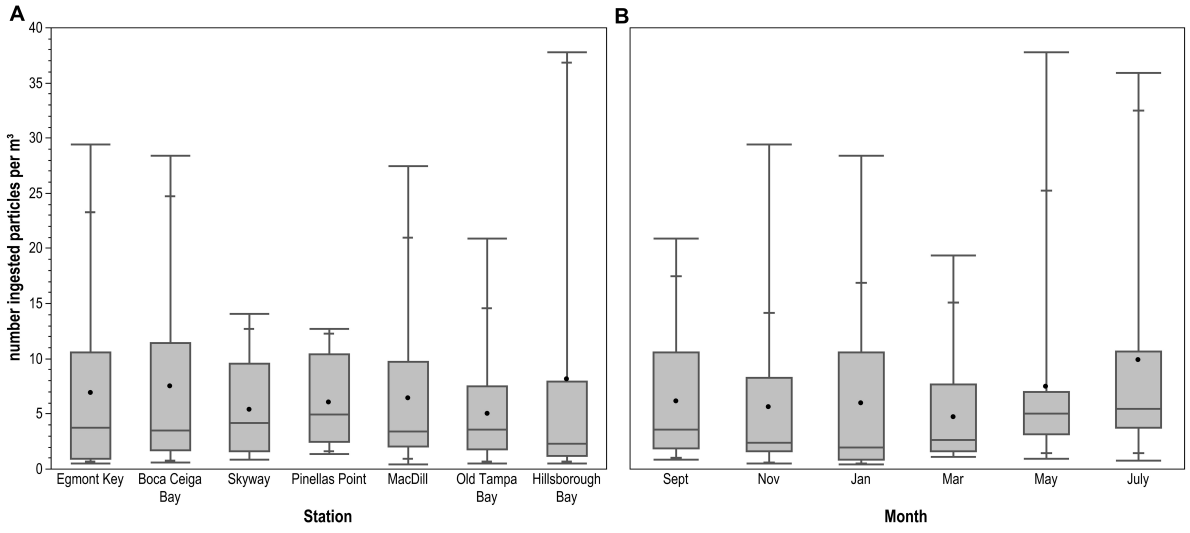

FIGURE 6
Number of ingested microplastic particles per m^3 across **(A)** sampling stations and **(B)** months. Horizontal line spanning box indicates median, while point indicates mean. Whiskers indicate maximum and minimum values, with intermediate quantiles marked. There were no statistically significant differences between stations or months.

as well as to estimates for microplastic ingestion by *A. tonsa* in the Hudson-Raritan Estuary, USA (Sipps et al., 2022) and for the closely related *A. clausi* in the Black Sea (Aytan et al., 2022). These three estimates, however, were smaller than estimates reported for copepods in most other field studies. Ingested particle size clearly scales with copepod size (Hansen et al., 1994). Aytan et al. (2022) observed *Calanus euxinus*, a species of copepod larger than *A. tonsa*, ingesting microplastic particles that were 1.8 times the size of those ingested by *A. tonsa* in Tampa Bay. The largest microplastics (2.485 mm) ingested by copepods were found during a study conducted in Jiaozhou Bay, Yellow Sea (Zheng et al., 2021). Although the copepod species was not reported, the authors indicated that typical prey size for the dominant copepods was approximately 0.5 mm. While the maximum recorded fragment (0.351 mm) and fiber (0.642 mm) lengths ingested by copepods in Tampa Bay were exceptional, Buathong et al. (2020) also measured large particles ingested by calanoid copepods of similar size to *A. tonsa* and Davis (1977) reported an observation of *A. longiremus* (1.16 mm) ingesting a larval Chaetognatha (approx. 2.6 mm), making the prey 2.23 times longer than the predator. Desforges et al. (2015) also suggested that fibers are not always elongated and could be folded into a ball, effectively decreasing the overall size and facilitating ingestion. Alternatively, a few large particles may have remained adhered to exoskeletons even through the extensive rinsing process and been measured along with the ingested particles released during enzymatic digestion. Nevertheless, due to the variety of individual species examined and/or the grouping of copepods into mixed assemblages for ingestion estimates, it is difficult to make further comparisons between studies and assess any potential environmental impacts on copepod-microplastic interactions.

In Tampa Bay, the size of particles ingested by *A. tonsa* exhibited some spatial and temporal variability, but did not show a clear trend. The size of the particles ingested was significantly smaller in Boca Ciega Bay than Pinellas Point, Old Tampa Bay and Hillsborough Bay. This could be caused by slower circulation in Pinellas Point, Old Tampa Bay and Hillsborough Bay (Weisberg and Zheng, 2006) and retention of buoyant microplastic particles from riverine inputs to these areas, whereas water in Boca Ciega Bay exchanges more frequently with the open Gulf of Mexico. Nevertheless, all ingested particles were still within the size range of food particles preferred by *A. tonsa* (Berggreen et al., 1988). Ingested particle size distribution in Hudson-Raritan Estuary was also significantly different based on location (Sipps et al., 2022). However, no clear pattern was observed or viable explanation offered in either of these studies. Temporally, the particle size ingested by *A. tonsa* was significantly smaller in May and November compared to January, March and September. Studies in Fram Strait (Botterell et al., 2022) and Hudson-Raritan Estuary (Sipps et al., 2022) also detected temporal variability that was difficult to explain, while other studies reported no significant differences between the size of ingested particles and season (Zheng et al., 2021; Rashid et al., 2022). Future work could explore the potential relationship between the size of seasonally available phytoplankton and the size of microplastic ingested as well as seasonal variation in microplastic sizes in surface waters.

The overall average microplastic ingestion rate by *A. tonsa* in Tampa Bay was 0.015 particles per individual, which was lower than estimates from estuarine studies conducted in the Hudson-Raritan Estuary, USA (0.56 particles per individual; Sipps et al., 2022), Kochi backwaters, India (0.41 particles per individual; Rashid et al., 2022), and Jiaozhou Bay, China (0.21 particles per individual; Zheng et al., 2021), but on par with estimates from studies in Terengganu Estuary, Malaysia (0.02 particles per individual; Taha et al., 2021) and Charleston Harbor, USA (0.009 particles per individual; Payton et al., 2020). Prey ingestion rates vary by copepod species, as well as prey concentration and nutritional quality (reviewed in Mauchline, 1998). For example, without the presence of infochemicals or biofilms on microplastic particles copepods could be deterred from ingesting microplastics

(Vroom et al., 2017; Borrelle et al., 2020). The differences in ingestion rates between studies could also result from differences in proximity to large industrial areas or large populations and likely greater microplastic loads. Similar to Hudson-Raritan Estuary, calanoid copepods ingested 0.45 particles per individual near an industrial complex in Chonburi Province, Thailand (Buathong et al., 2020). However, other studies have observed that the amount of microplastics present in the water does not correlate with the ingestion rate (Amin et al., 2020; Taha et al., 2021). Moreover, the ingestion rate in the present study was lower than estimates for some offshore environments (Desforges et al., 2015; Sun et al., 2017; Botterell et al., 2022). Ingestion rates could also be affected by the current strength and flux of water in and out of the sampling location. Rashid et al. (2022) observed that ingestion rates for calanoid copepods increased during the pre-monsoon season in the Kochi backwaters of India, when Barrage shutters are closed restricting the flow of water into the estuary. Alternatively, Sipps et al. (2022) found that ingestion rate in the Hudson-Raritan Estuary was lowest in July when the river flow was slow. Compared to other estuaries, Tampa Bay has low river input and long residence time (Zhu et al., 2015).

The ingestion rate of *A. tonsa* showed no significant differences between stations in Tampa Bay. Similar to the present study, there was no spatial pattern to ingestion rates in Terengganu coastal waters and estuary (Amin et al., 2020; Taha et al., 2021), Black Sea (Aytan et al., 2022), Fram Strait (Botterell et al., 2022), northeast Pacific Ocean (Desforges et al., 2015), and South China Sea (Sun et al., 2017). For some, the lack of significance was attributed to a small sample size and a small number of particles ingested by zooplankton (Desforges et al., 2015; Botterell et al., 2022). On the other hand, Zheng et al. (2021) observed significantly greater ingestion rates in the estuary than farther from the coast and attributed this pattern to proximity of estuarine sampling sites to a major river carrying effluent from a large wastewater treatment facility. In contrast, freshwater flow, likely the greatest source of microplastics, into Tampa Bay is dominated by non-point source stormwater runoff (Zhu et al., 2015). Seasonally, in Tampa Bay, there was a significantly lower number of microplastic particles ingested during the dry season (around September) compared to the wet season (around May). This could be attributed to the amount of run-off from the surrounding coastline during the wet season. McEachern et al. (2019) observed that months with increased precipitation levels correlate with increased microplastic concentration in surface waters of Tampa Bay. Regardless of whether or not there is a correlation between microplastic concentrations in surface waters and ingestion rates, freshwater runoff can foster phytoplankton growth (Corcoran et al., 2017), which in turn could increase copepod suspension feeding activity and ingestion of microplastics suspended in the bloom. While other studies also detected significant seasonal differences in ingestion rates, there were no consistent patterns across studies.

In Tampa Bay, the average microplastic ingestion rate normalized for copepod concentration was 6.48 particles m^{-3} and there were no significant differences between stations or sampling months. McEachern et al. (2019) provides the only estimate of microplastic concentration for comparison in Tampa Bay waters, 940 particles m^{-3}. Of note, this microplastic concentration is over twice the average concentration of copepods collected during the present study (440 copepods per m^{-3}). Based on the present results, copepods in Tampa Bay may be ingesting 0.7% of the available microplastics each hour, assuming that is a viable gut passage time (Kiørboe and Tiselius, 1987; Tirelli and Mayzaud, 2005). Few environmental microplastic ingestion studies normalize for zooplankton concentration (Sun et al., 2017; Amin et al., 2020; Taha et al., 2021; Sipps et al., 2022). Our estimate of normalized ingestion rates and our subsequent extrapolation of proportional ingestion impact on microplastic concentration in Tampa Bay were approximately on the same order of magnitude as those for other studies. However, 10 times greater estimates were reported for the Hudson-Raritan Estuary. Future ingestion studies should also consider accounting for zooplankton concentration in their analyses, as this type of calculation is more directly applied to understanding the degree of environmental impact.

In addition to being the most abundant metazoans in the ocean, calanoid copepods can exhibit higher environmental microplastic ingestion rates than other zooplankton (Sun et al., 2017; Amin et al., 2020; Buathong et al., 2020). Microplastic ingestion can have negative effects on copepod populations *via* decreased egg production and survival (Cole et al., 2014; Shore et al., 2021). In turn, population level impacts on copepods could lead to adverse effects further up the food web. However, trophic transfer of microplastics from lower trophic levels to higher trophic levels have only been observed in laboratory experiments. A recent study even demonstrated that *A. tonsa*, specifically, can serve as a vector for microplastic transmission to seahorses, which then retain the microplastic particles and could lead to obstructions in the gastro-intestinal tract (Domínguez-López et al., 2022). Similarly, microplastics in copepod fecal pellets could be transferred to benthic organisms in shallow coastal waters that rely on sinking pellets as an important component of their diet, thus redistributing plastic from the surface to the benthos. However, the presence of microplastics in fecal pellets may decrease their sinking rates (Cole et al., 2016; Coppock et al., 2019; Wieczorek et al., 2019; Shore et al., 2021). Shore et al. (2021) also found that copepods egest smaller and fewer pellets when exposed to high concentrations of microplastics; together these factors could reduce the potential for concentrated redistribution of microplastics from surface to benthos.

5. Conclusion

This study is the first characterization of microplastic-plankton interactions in Tampa Bay Estuary. The microplastic ingestion rate by *A. tonsa* was spatially consistent but temporal differences seem to be driven by rainy/dry seasons. However, no trends were evident once the data were normalized for copepod concentrations in the environment. The size of microplastic ingested varied spatially and temporally without a consistent pattern, however, the size of particles ingested was consistent with the prey size spectra for *A. tonsa*. Additionally, *A. tonsa* ingested significantly more fragments than fibers, and further research is needed to understand the selective behavior of *A. tonsa* in the presence of fragments and fibers. With a focus on *A. tonsa*, a species that dominates estuarine zooplankton communities around the world, this study provides a useful baseline for comparison. Additional data on the same species from estuaries with different physical mechanisms and levels of anthropogenic impact will prove useful in teasing apart the role of

the environment in these interactions. Finally, future studies should further investigate the potential for and impacts of trophic transfer of microplastics across multiple trophic levels.

Data availability statement

The raw data supporting the conclusions of this article will be made available by the authors, without undue reservation.

Author contributions

ANSS and SG directed the research and oversaw the project. ANSS conceived of the research. MCF and DC conducted the sample collection and processing. All authors contributed to the data analysis and writing of the manuscript.

Funding

This work was provided by two grants from the Tampa Bay Environmental Restoration Fund to ANSS and SG. Additional support was provided by Eckerd College's Ford Apprentice Scholars Program (DC and ANSS) and Natural Sciences Summer Research Program (ANSS and SG).

Acknowledgments

We thank the many undergraduate student interns on the Microplastics in Tampa Bay Project at Eckerd College for assisting with sample collection. We particularly thank Karsen Henwood for sustained assistance with sample processing.

Conflict of interest

The authors declare that the research was conducted in the absence of any commercial or financial relationships that could be construed as a potential conflict of interest.

Publisher's note

References

Amin, R. M., Sohami, E. S., Anuar, S. T., and Bachok, Z. (2020). Microplastic ingestion by zooplankton in Terengganu coastal waters, southern South China Sea. *Mar. Pollut. Bull.* 150:110616. doi: 10.1016/j.marpolbul.2019.110616

Andrady, A. (2015). "Persistence of Plastic Litter in the Oceans," in *Marine anthropogenic litter*, eds M. Bergmann, L. Gutow, and M. Klages (Cham: Springer International Publishing), 57–72. doi: 10.1007/978-3-319-16510-3_3

Araujo, A. V., Dias, C. O., and Bonecker, S. L. C. (2017). Differences in the structure of copepod assemblages in four tropical estuaries: Importance of pollution and the estuary hydrodynamics. *Mar. Pollut. Bull.* 115, 412–420. doi: 10.1016/j.marpolbul.2016.12.047

Athey, S. N., Albotra, S. D., Gordon, C. A., Monteleone, B., Seaton, P., Andrady, A. L., et al. (2020). Trophic transfer of microplastics in an estuarine food chain and the effects of a sorbed legacy pollutant. *Limnol. Oceanogr. Lett.* 5, 154–162. doi: 10.1002/lol2.10130

Aytan, U., Esensoy, F. B., and Senturk, Y. (2022). Microplastic ingestion and egestion by copepods in the Black Sea. *Sci. Total Environ.* 806:150921. doi: 10.1016/j.scitotenv.2021.150921

Berggreen, U., Hansen, B., and Kiørboe, T. (1988). Food size spectra, ingestion and growth of the copepod *Acartia tonsa* during development: Implications for determination of copepod production. *Mar. Biol.* 99, 341–352. doi: 10.1007/BF02112126

Borrelle, S. B., Ringma, J., Law, K. L., Monnahan, C. C., Lebreton, L., McGivern, A., et al. (2020). Predicted growth in plastic waste exceeds efforts to mitigate plastic pollution. *Science* 369, 1515–1518. doi: 10.1126/science.aba3656

Botterell, Z. L. R., Beaumont, N., Dorrington, T., Steinke, M., Thompson, R., and Lindeque, P. K. (2019). Bioavailability and effects of microplastics on marine zooplankton: A review. *Environ. Pollut.* 245, 98–110. doi: 10.1016/j.envpol.2018.10.065

Botterell, Z. L. R., Bergmann, M., Hildebrandt, N., Krumpen, T., Steinke, M., Thompson, R. C., et al. (2022). Microplastic ingestion in zooplankton from the Fram Strait in the Arctic. *Sci. Total Environ.* 831:154886. doi: 10.1016/j.scitotenv.2022.154886

Buathong, D., Sriwisait, P., Pnengsakun, S., Chamchoy, C., Mue-suae, O., Phoaduang, S., et al. (2020). Accumulation of microplastics in zooplankton from Chonburi Province, the Upper Gulf of Thailand. *RIST* 3, 1–12.

Bucci, K., Tulio, M., and Rochman, C. M. (2020). What is known and unknown about the effects of plastic pollution: A meta-analysis and systematic review. *Ecol. App.* 30:e02044. doi: 10.1002/eap.2044

Burns, C. W. (1968). The relationship between body size of filter-feeding *Cladocera* and the maximum size of particle ingested. *Limnol. Oceanogr.* 13, 675–678. doi: 10.4319/lo.1968.13.4.0675

Cicchetti, G., and Greening, H. (2011). Estuarine biotope mosaics and habitat management goals: An application in Tampa Bay, FL, USA. *Estuar. Coasts* 34, 1278–1292. doi: 10.1007/s12237-011-9408-4

Cole, M., Coppock, R., Lindeque, P. K., Altin, D., Reed, S., Pond, D. W., et al. (2019). Effects of nylon microplastic on feeding, lipid accumulation, and molting in a coldwater copepod. *Environ. Sci. Technol.* 53, 7075–7082. doi: 10.1021/acs.est.9b01853

Cole, M., Lindeque, P., Fileman, E., Halsband, C., Goodhead, R., Moger, J., et al. (2013). Microplastic ingestion by zooplankton. *Environ. Sci. Technol.* 47, 6646–6655. doi: 10.1021/es400663f

Cole, M., Lindeque, P. K., Fileman, E., Clark, J., Lewis, C., Halsband, C., et al. (2016). Microplastics alter the properties and sinking rates of zooplankton faecal pellets. *Environ. Sci. Technol.* 50, 3239–3246. doi: 10.1021/acs.est.5b05905

Cole, M., Webb, H., Lindeque, P. K., Fileman, E. S., Halsband, C., and Galloway, T. S. (2014). Isolation of microplastics in biota-rich seawater samples and marine organisms. *Sci. Rep.* 4:4528. doi: 10.1038/srep04528

Coppock, R., Galloway, T. S., Cole, M., Fileman, E. S., Queirós, A. M., and Lindeque, P. K. (2019). Microplastics alter feeding selectivity and fecal density in the copepod, *Calanus helgolandicus*. *Sci. Total Environ.* 687, 780–789. doi: 10.1016/j.scitotenv.2019.06.009

Corcoran, A. A., Wolny, J., Leone, E., Ivey, J., and Murasko, S. (2017). Drivers of phytoplankton dynamics in old Tampa Bay, FL (USA), a subestuary lagging in ecosystem recovery. *Estuar. Coast Shelf Sci.* 185, 130–140. doi: 10.1016/j.ecss.2016.11.009

Costa, E., Piazza, V., Lavorano, S., Faimali, M., Garaventa, F., and Gambardella, C. (2020). Trophic transfer of microplastics from copepods to jellyfish in the marine environment. *Front. Environ. Sci.* 8:571732. doi: 10.3389/fenvs.2020.571732

Cózar, A., Echevarría, F., González-Gordillo, J. I., Irigoien, X., Úbeda, B., Hernández-León, S., et al. (2014). Plastic debris in the open ocean. *PNAS* 11, 10239–10244. doi: 10.1073/pnas.1314705111

Crawford, C. B., and Quinn, B. (2017). *Microplastics pollutants*. Amsterdam: Elsevier Inc.

Davis, C. C. (1977). Sagitta as food for *Acartia*. *Astarte* 10, 1–3.

Davison, P., and Asch, R. G. (2011). Plastic ingestion by mesopelagic fishes in the North Pacific Subtropical Gyre. *Mar. Ecol. Prog. Ser.* 432, 172–180. doi: 10.3354/meps09142

Derriak, J. G. B. (2002). The pollution of the marine environment by plastic debris: A review. *Mar. Pollut. Bull.* 44, 842–852. doi: 10.1016/S0025-326X(02)00220-5

Desforges, J. W., Galbraith, M., and Ross, P. S. (2015). Ingestion of microplastics by zooplankton in the Northeast Pacific Ocean. *Arch. Environ. Contam. Toxicol.* 69, 320–330. doi: 10.1007/s00244-015-0172-5

Domínguez-López, M., Bellas, J., Sánchez-Ruiloba, L., Planas, M., and Hernández-Urcera, J. (2022). First evidence of ingestion and retention of microplastics in seahorses (*Hippocampus reidi*) using copepods (*Acartia tonsa*) as transfer vectors. *Sci. Tot. Env.* 818:151688. doi: 10.1016/j.scitotenv.2021.151688

Duncan, E., Broderick, A. C., Fuller, W. J., Galloway, T. S., Godfrey, M. H., Hamann, M., et al. (2018). Microplastic ingestion ubiquitous in marine turtles. *Glob. Chang. Biol.* 25, 744–752. doi: 10.1111/gcb.14519

Egbeocha, C. O., Malek, S., Emenike, C. U., and Milow, P. (2018). Feasting on microplastics: Ingestion by and effects on marine organisms. *Aquat. Biol.* 27, 93–106. doi: 10.3354/ab00701

Ellison, K. (2007). The trouble with nurdles. *Front. Ecol. Environ.* 5:396. doi: 10.1890/1540-9295(2007)5[396:TTWN]2.0.CO;2

Enders, K., Lenz, R., Stedmon, C. A., and Nielsen, T. G. (2015). Abundance, size and polymer composition of marine microplastics ≥10 μm in the Atlantic Ocean and their modeled vertical distribution. *Mar. Pollut. Bull.* 100, 70–81. doi: 10.1016/j.marpolbul.2015.09.027

Engler, R. E. (2012). The complex interaction between marine debris and toxic chemicals in the ocean. *Environ. Sci. Technol.* 46, 12302–12315. doi: 10.1021/es3027105

Eriksen, M., Lebreton, L. C. M., Carson, H. S., Thiel, M., Moore, C. J., Borerro, J. C., et al. (2014). Plastic pollution in the world's oceans: More than 5 trillion plastic pieces weighing over 250,000 tons afloat at sea. *PLoS One* 9:e111913. doi: 10.1371/journal.pone.0111913

Erni-Cassola, G., Gibson, M. I, Thompson, R. C., and Christie-Oleza, J. A. (2017). Lost, but found with Nile Red: A novel method for detecting and quantifying small microplastics (1 mm to 20 μm) in environmental samples. *Environ. Sci. Technol.* 51, 13641–13648. doi: 10.1021/acs.est.7b04512

Farrell, P., and Nelson, K. (2013). Trophic level transfer of microplastic: *Mytilus edulis* (L.) to *Carcinus maenas* (L.). *Environ. Pollut.* 177, 1–3. doi: 10.1016/j.envpol.2013.01.046

Frost, B. W. (1972). Effects of size and concentration of food particles on the feeding behavior of the marine planktonic copepod *Calanus pacificus*. *Limnol. Oceanogr.* 17, 805–815. doi: 10.4319/lo.1972.17.6.0805

Gallo, F., Fossi, C., Weber, R., Santillo, D., Sousa, J., Ingram, I., et al. (2018). Marine litter plastics and microplastics and their toxic chemicals components: The need for urgent preventive measures. *Environ. Sci. Eur.* 30:13. doi: 10.1186/s12302-018-0139-z

García-Gómez, J. C., Garrigós, M., and Garrigós, J. (2021). Plastic as a vector of dispersion for marine species with invasive potential. A review. *Front. Ecol. Evol.* 9:629756. doi: 10.3389/fevo.2021.629756

GESAMP (2019). "Guidelines for the monitoring and assessment of plastic litter and microplastics in the ocean," in *GESAMP joint group of experts on the scientific aspects of marine environmental*, eds P. Kershaw, A. Turra, and F. Galani (Nairobi: United Nations Environment Programme (UNEP)).

Goswami, P., Vinithkumar, N. V., and Dharani, G. (2020). First evidence of microplastics bioaccumulation by marine organisms in the Port Blair Bay, Andaman Islands. *Mar. Pollut. Bull.* 155:111163. doi: 10.1016/j.marpolbul.2020.111163

Hansen, B., Bjornsen, P. K., and Hansen, P. J. (1994). The size ratio between planktonic predators and their prey. *Limnol. Oceanogr.* 39, 395–403. doi: 10.4319/lo.1994.39.2.0395

Hemraj, D. A., Hossain, M. A., Ye, Q., Qin, J. G., and Leterme, S. C. (2016). Plankton bioindicators of environmental conditions in coastal lagoons. *Estuar. Coast Shelf Sci.* 184, 102–114. doi: 10.1016/j.ecss.2016.10.045

Howell, L. M. (2019). *Microplastic pollution in the Arctic Ocean: Assessing ingestion and potential health effects in Calanus and Neocalanus copepods*. Ph.D thesis. Burnaby, BC: Simon Fraser University.

Kim, L., Cui, R., Kwak, J. I., and An, Y.-J. (2022). Sub-acute exposure to nanoplastics via two-chain trophic transfer: From brine shrimp *Artemia franciscana* to small yellow croaker *Larimichthys polyactis*. *Mar. Pollut. Bull.* 175:113314. doi: 10.1016/j.marpolbul.2021.113314

Kiørboe, T., and Tiselius, P. T. (1987). Gut clearance and pigment destruction in a herbivorous copepod, *Acartia tonsa*, and the determination of in situ grazing rates. *J. Plankton Res.* 9, 525–534. doi: 10.1093/plankt/9.3.525

Koski, M., Søndergaard, J., Christensen, A. M., and Nielsen, T. G. (2021). Effect of environmentally relevant concentrations of potentially toxic microplastic on coastal copepods. *Aquat. Toxicol.* 230:105713. doi: 10.1016/j.aquatox.2020.105713

Kosore, C., Ojwang, L., Maghanga, J., Kamau, J., Kimeli, A., Omukoto, J., et al. (2018). Occurrence and ingestion of microplastics by zooplankton in Kenya's marine environment: First documented evidence. *Afr. J. Mar. Sci.* 40, 225–234. doi: 10.2989/1814232X.2018.1492969

Lebreton, L., Slat, B., Ferrari, F., Sainte-Rose, B., Aitken, J., Marthouse, R., et al. (2018). Evidence that the Great Pacific Garbage Patch is rapidly accumulating plastic. *Sci. Rep.* 8:4666. doi: 10.1038/s41598-018-22939-w

Lönnstedt, O. M., and Eklöv, P. (2016). Environmentally relevant concentrations of microplastic particles influence larval fish ecology. *Science* 352, 1213–1216. doi: 10.1126/science.aad8828

Maes, T., Jessop, R., Wellner, N., Haupt, K., and Mayes, A. G. (2017). A rapid-screening approach to detect and quantify microplastics based on fluorescent tagging with Nile Red. *Sci. Rep.* 7:44501. doi: 10.1038/srep44501

Mauchline, J. (ed.) (1998). *The biology of calanoid copepods*. London: Academic Press, 170.

McEachern, K., Alegria, H., Kalagher, A. L., Hansen, C., Morrison, S., and Hastings, D. (2019). Microplastic in Tampa Bay, Florida: Abundance and variability in estuarine waters and sediments. *Mar. Pollut. Bull.* 432, 173–180. doi: 10.1016/j.marpolbul.2019.07.068

Nalbone, L., Panebianco, A., Giarratana, F., and Russell, M. (2021). Nile Red staining for detecting microplastics in biota: Preliminary evidence. *Mar. Pollut. Bull.* 172:112888. doi: 10.1016/j.marpolbul.2021.112888

Nelms, S. E., Barnett, J., Brownlow, A., Davison, N. J., Deaville, R., Galloway, T. S., et al. (2019). Microplastics in marine mammals stranded around the British coast: Ubiquitous but transitory? *Sci. Rep.* 9:1075. doi: 10.1038/s41598-018-37428-3

Ortega-Borchardt, J. A., Ramírez-Alvarez, N., Rios Mendoza, L. M., Gallo-Reynoso, J. P., Barba-Acuna, I. D., García-Hernandez, J., et al. (2023). Detection of microplastic particles in scats from different colonies of California sea lions (*Zalophus californianus*) in the Gulf of California, Mexico: A preliminary study. *Mar. Pollut. Bull.* 186:114433. doi: 10.1016/j.marpolbul.2022.114433

Payton, T. G., Beckingham, B. A., and Dustan, P. (2020). Microplastic exposure to zooplankton at tidal fronts in Charleston Harbor, SC USA. *Estuar. Coast Shelf Sci.* 232:106510. doi: 10.1016/j.ecss.2019.106510

Phuong, N. N., Poirier, L., Pham, Q. T., Lagarde, F., and Zalouk-Vergnoux, A. (2018). Factors influencing the microplastic contamination of bivalves from the French Atlantic coast: Location, season and/or mode of life? *Mar. Pollut. Bull.* 129, 664–674. doi: 10.1016/j.marpolbul.2017.10.054

Rashid, C. P., Jyothibabu, R., Arunpandi, N., Santhikrishnan, S., Vidhya, V., Sarath, S., et al. (2022). Microplastics in copepods reflects the manmade flow restrictions in the Kochi backwaters, along the southwest coast of India. *Mar. Pollut. Bull.* 177:113529. doi: 10.1016/j.marpolbul.2022.113529

Rochman, C. M., Hentschel, B. T., and Teh, S. J. (2014). Long-term sorption of metals is similar among plastic types: Implications for plastic debris in aquatic environments. *PLoS One* 9:e85433. doi: 10.1371/journal.pone.0085433

Rochman, C. M., Hoh, E., Kurobe, T., and Teh, S. J. (2013). Ingested plastic transfers hazardous chemicals to fish and induces hepatic stress. *Sci. Rep.* 3:3263. doi: 10.1038/srep03263

Schneider, C. A., Rasband, W. S., and Eliceiri, K. W. (2012). NIH Image to ImageJ: 25 years of image analysis. *Nat. Methods* 9, 671–675. doi: 10.1038/nmeth.2089

Setälä, O., Fleming-Lehtinen, V., and Lehtiniemi, M. (2014). Ingestion and transfer of microplastics in the planktonic food web. *Environ. Pollut.* 185, 77–83. doi: 10.1016/j.envpol.2013.10.013

Shim, W. J., Hong, S. H., and Eo, S. E. (2017). Identification methods in microplastic analysis: A review. *Anal. Methods* 9, 1384–1391. doi: 10.1039/C6AY02558G

Shore, E. A., deMayo, J. A., and Pespeni, M. H. (2021). Microplastics reduce net population growth and fecal pellet sinking rates for the marine copepod, *Acartia tonsa*. *Environ. Pollut.* 284:117379. doi: 10.1016/j.envpol.2021.117379

Sipps, K., Arbuckle-Keil, G., Chant, R., Fahrenfeld, N., Garzio, L., Walsh, K., et al. (2022). Pervasive occurrence of microplastics in Hudson-Raritan estuary zooplankton. *Sci. Total Environ.* 817:152812. doi: 10.1016/j.scitotenv.2021.152812

Stanton, T., Johnson, M., Nathanail, P., Gomes, R. L., Needham, T., and Burson, A. (2019). Exploring the efficacy of Nile Red in microplastic quantification: A costaining approach. *Environ. Sci. Tech. Lett.* 6, 606–611. doi: 10.1021/acs.estlett.9b00499

Sun, X., Li, Q., Zhu, M., Liang, J., Zheng, S., and Zhao, Y. (2017). Ingestion of microplastics by natural zooplankton groups in the northern South China Sea. *Mar. Pollut. Bull.* 115, 217–224. doi: 10.1016/j.marpolbul.2016.12.004

Taha, Z. D., Amin, R. M., Anuar, S. T., Nasser, A. A. A., and Sohaimi, E. S. (2021). Microplastics in seawater and zooplankton: A case study from Terengganu estuary and offshore waters, Malaysia. *Sci. Total Environ.* 786:147466. doi: 10.1016/j.scitotenv.2021.147466

Tirelli, V., and Mayzaud, P. (2005). Relationship between functional response and gut transit time in the calanoid copepod *Acartia clausi*: Role of food quantity and quality. *J. Plankton Res.* 27, 557–568. doi: 10.1093/plankt/fbi031

Tonhua, T., Gutekunst, S. B., and Biastoch, A. (2020). A near-synoptic survey of ocean microplastic concentration along an around-the-world sailing race. *PLoS One* 15:e0243203. doi: 10.1371/journal.pone.0243203

Van Colen, C., Vanhove, B., Diem, A., and Moens, T. (2020). Does microplastic ingestion by zooplankton affect predator-prey interactions? An experimental study on larviphagy. *Environ. Pollut.* 256:113479. doi: 10.1016/j.envpol.2019.113479

Van Franeker, J. A. (2011). Reshape and relocate: Seabirds as transformers and transporters of microplastics. *NOAA Tech. Memo.* 38, 278–280.

van Sebille, E., Wilcox, C., Lebreton, L., Maximenko, N., Hardesty, B. D., Van Franeker, J. A., et al. (2015). A global inventory of small floating plastic debris. *Environ. Res. Lett.* 10:124006. doi: 10.1088/1748-9326/10/12/124006

Vroom, R. J. E., Koelmans, A. A., Besseling, E., and Halsband, C. (2017). Aging of microplastics promotes their ingestion by marine zooplankton. *Environ. Pollut.* 231, 987–996. doi: 10.1016/j.envpol.2017.08.088

Weisberg, R. H., and Zheng, L. (2006). Circulation of Tampa Bay driven by buoyancy, tides, and winds, as simulated using a finite volume coastal ocean model. *J. Geophys. Res.* 111:C01005. doi: 10.1029/2005JC003067

Wieczorek, A. M., Croot, P. L., Lombard, F., Sheahan, J. N., and Doyle, T. K. (2019). Microplastic ingestion by gelatinous zooplankton may lower efficiency of the biological pump. *Environ. Sci. Technol.* 53, 5387–5395. doi: 10.1021/acs.est.8b07174

Wilson, D. S. (1973). Food size selection among copepods. *Ecology* 54, 909–914. doi: 10.2307/1935688

Zheng, S., Zhao, Y., Liu, T., Liang, J., Zhu, M., and Sun, X. (2021). Seasonal characteristics of microplastics ingested by copepods in Jiaozhou Bay, the Yellow Sea. *Sci. Total Environ.* 776:145936. doi: 10.1016/j.scitotenv.2021.145936

Zhu, J., Weisberg, R. H., Zheng, L., and Han, S. (2015). On the flushing of Tampa Bay. *Estuar. Coasts* 38, 118–131. doi: 10.1007/s12237-014-9793-6

frontiers | Frontiers in Ecology and Evolution

TYPE Original Research
PUBLISHED 12 April 2023
DOI 10.3389/fevo.2023.1143310

OPEN ACCESS

EDITED BY
Michael C. Murrell,
University of West Florida,
United States

REVIEWED BY
Francesco Tiralongo,
University of Catania,
Italy
Elizabeth E. Hieb,
Dauphin Island Sea Lab,
United States

*CORRESPONDENCE
Shannon Gowans
✉ gowanss@eckerd.edu
Amy N. S. Siuda
✉ siudaan@eckerd.edu

SPECIALTY SECTION
This article was submitted to Biogeography and Macroecology, a section of the journal Frontiers in Ecology and Evolution

RECEIVED 12 January 2023
ACCEPTED 22 February 2023
PUBLISHED 12 April 2023

CITATION
Gowans S and Siuda ANS (2023) Microplastics in large marine herbivores: Florida manatees (*Trichechus manatus latirostris)* in Tampa Bay. *Front. Ecol. Evol.* 11:1143310. doi: 10.3389/fevo.2023.1143310

Microplastics in large marine herbivores: Florida manatees (*Trichechus manatus latirostris)* in Tampa Bay

Shannon Gowans[1]* and Amy N. S. Siuda[2]*

[1]Marine Science and Biology, Eckerd College, St. Petersburg, FL, United States, [2]Marine Science, Eckerd College, St. Petersburg, FL, United States

Although there is growing concern about ingestion of microplastics by marine organisms, little research has been conducted on marine herbivores. This is the first study to document microplastic ingestion within the family Sirenia. Subsamples were collected from five locations in the gastrointestinal tracts (GI) of 26 dead manatees (*Trichechus manatus latirostris*) from Tampa Bay, Florida. During gross necropsies, macroplastic pieces were found in seven individuals (26.9%). Careful visual examination of the subsampled portions of the GI contents indicated that 19 individuals (73.1%) contained plastic particles. As five individuals had both macro and microplastic pieces, the overall frequency of occurrence of plastic ingestion was 76.9%. Due to the large volume of cellulose-rich ingested material, it was not feasible to analyze the entire gut contents, nor was it feasible to conduct chemical or enzymatic digestion; therefore, it is very likely that many microplastic pieces were not detected. Despite these technical challenges, it is clear that manatees in Tampa Bay are routinely consuming microplastics in addition to larger plastic pieces. Currently, nothing is known about the physiological effects of microplastic ingestion in sirenians, however environmental plastics could be concentrated by manatees through ingestion and the subsequent production of microplastics-laden feces.

KEYWORDS

manatee, microplastic, seagrass, estuary, ingestion

Introduction

The amount of plastic pollution in marine systems is concerning due to the potential for severe repercussions on humans and wildlife. Around 700 marine species have been documented to have encountered marine debris and 92% of those encounters were with plastic debris (Gall and Thompson, 2015). Plastics threaten marine life through physical interactions such as entanglement, ingestion, acting as a vector for invasive organisms and diseases, and by transporting and leaching toxic substances (Gall and Thompson, 2015; Saliu et al., 2019; Bucci et al., 2020). Early concerns focused on larger pieces of plastic clearly visible to the naked eye (e.g., Laist, 1987), but increasingly the plastic pollution crisis is focusing on microplastics (defined as plastic smaller than 5 mm; Arthur et al., 2009) which are ubiquitous throughout the marine environment and can be ingested by even the smallest of marine organisms (Fibbe et al., 2023).

Marine mammals are vulnerable to entanglement and ingestion of macroplastics (e.g., Simmonds, 2012; Baulch and Perry, 2014; Butterworth, 2016). Microplastics have been found

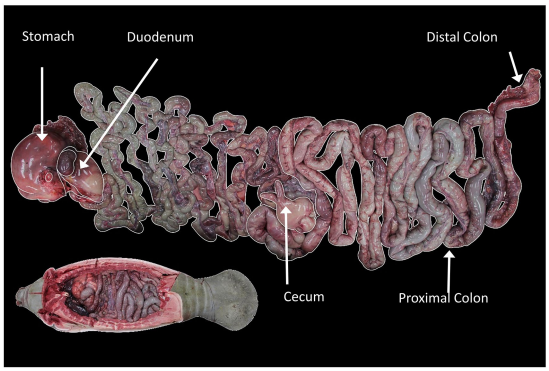

FIGURE 1
Location of sampling sites in the GI tract of the manatee. The lower inset image shows GI tract inside the manatee carcass in anatomical orientation, while the larger image shows the tract layed out. Image credit: Florida Fish and Wildlife Conservation Commission.

in the gastrointestinal (GI) tract or scat of a variety of cetaceans and pinnipeds (see Zantis et al., 2021 for a review). Florida manatees (*Trichechus manatus latirostris*) have been known to ingest a variety of macroplastics including fishing line and plastic bags (Beck and Barros, 1991; Adimey et al., 2014; Reinert et al., 2017) as have Antillean manatees (*Trichechus manatus manatus*; Attademo et al., 2015) and Amazonian manatees (*Trichechus inunguis*; Guterres-Pazin et al., 2012).

Sirenian diets differ greatly from those of other marine mammals as they forage on vegetation, therefore the routes and impact of plastic ingestion may also differ. Detection of microplastics in manatees is especially challenging due to the large quantities of cellulose-rich food they consume. Manatees have long gut passage time (6–9 days; Larkin et al., 2007), large GI tract (tract and contents weighing upwards of 100 kg; Reynolds and Rommel, 1996) and a 500 kg manatee is estimated to consume 4 to 9% of their body weight daily depending on food type and season (Bengtson, 1983; Worthy and Worthy, 2014).

Manatees routinely forage in seagrass beds (Reich and Worthy, 2006) where there is increasing evidence that microplastics are trapped and retained. Microplastic concentrations in sediments from seagrass beds were higher than in sediments from surrounding non-vegetated areas (Huang et al., 2020; Jones et al., 2020; Plee and Pomory, 2020) or higher than in the surrounding seawater (Tahir et al., 2019; Kreitsberg et al., 2021), although some study sites did not see enrichment (e.g., Cozzolino et al., 2020; Unsworth et al., 2021; Boshoff et al., 2023). In some cases, there was variability between different locations within a single study, some showing enrichment of microplastics while other nearby sites did not (Huang et al., 2021). However, all studies found relatively high levels of microplastics in the sediments of seagrass beds. Cozzolino et al. (2020) also found macroplastic (particles >5 mm) concentrations were elevated in seagrass habitats in comparison to nearby unvegetated sites. Additionally, microplastics have been found adhering to seagrass blades or their epibonent algae (Goss et al., 2018; Datu et al., 2019; Cozzolino et al., 2020; Jones et al., 2020; Seng et al., 2020; Sawalman et al., 2021). Seagrass associated benthic invertebrates (Tahir et al., 2019; Jones et al., 2020; Plee and Pomory, 2020; Sawalman et al., 2021), fish (Baalkhuyur et al., 2018; Sbrana et al., 2020; Cabansag et al., 2021) and turtles (Caron et al., 2018; Duncan et al., 2019) have also ingested microplastics.

Given the ability of seagrass beds to trap microplastics and the large volume of seagrasses that manatees consume, it is likely that manatees ingest microplastics, however this has not been previously investigated. The Florida manatee, a subspecies of the West Indian manatee, is native to the southeastern United States, mainly coastal Florida. The subspecies is listed as threatened by the US Fish and Wildlife Service[1] and endangered by the IUCN.[2] Continued threats (Runge et al., 2017) and several recent (Landsberg et al., 2022) and ongoing unusual mortality events[3] indicate that this species is still at risk. This is the first study of microplastic ingestion by any sirenian species.

Materials and methods

Manatee sample collection

In Florida, manatee carcasses are reported by the public to a state-managed wildlife hotline, and regional biologists respond to collect carcass information. A portion of the carcasses are transported to the Marine Mammal Pathobiology Laboratory, located in St. Petersburg, Florida and operated by Florida Fish and Wildlife Conservation Commission's Fish and Wildlife Research Institute, where they are examined according to standardized procedures (Bonde et al., 1983). As a part of a larger project to investigate microplastics in Tampa Bay, we collected samples from the GI tract of manatee carcasses found dead in the Tampa Bay estuary. We excluded all manatees that did not have an intact external body to avoid contamination of the gut contents by external microplastics. Manatees were assigned an age class based on total length: adult >265 cm; juvenile 235–265 cm and calf <235 cm (which includes young animals capable of foraging on their own; Runge et al., 2017).

Approximately 500 mL of GI tract contents were collected from each of five gut segments: stomach, duodenum, cecum, proximal colon and distal colon (Figure 1). Samples were stored in (~700 mL) whirl packs during the necropsy and were frozen at −20°C until processed.

Sample processing

A wide variety of approaches have been used to separate microplastics from the surrounding gut contents. Dissection and visual observation is the simplest approach, but limits the lower size particle that can be detected and, because it typically is a slow process, leads to a higher risk of contamination during processing (Dehaut et al., 2019). Chemical digestion is often used and certain protocols have been proposed as monitoring standards, such as the use of

1 https://www.federalregister.gov/documents/2017/04/05/2017-06657/endangered-and-threatened-wildlife-and-plants-reclassification-of-the-west-indian-manatee-from

2 https://www.iucnredlist.org/species/22106/9359881

3 https://mission.cmaquarium.org/app/uploads/2021/05/Sirenews-73-April2021-update.pdf

HNO3:HClO4 in a 4:1 ratio by ICES (2015). Enzymatic digestions are time-consuming and expensive (Dehaut et al., 2019), while acidic digestions frequently degrade or alter the plastic particles (Enders et al., 2017). Bases such as KOH may be less likely to alter the plastics, but are corrosive and must be used with caution (Dehaut et al., 2019). Separating microplastics from the guts of marine grazers which consume vascular plants can be especially problematic as cellulose remains resistant to many digestion processes (Hurley et al., 2018) and can be difficult to differentiate from microplastic particles (Egea-Corbacho et al., 2022). Hence, a combination of visual separation and fluorescent staining was used in the present study.

To eliminate contamination, cotton clothing or lab coats were worn at all times, samples and reagent solutions were kept covered except for brief periods while handling. After thawing samples, wet weights were collected. Gut contents were initially diluted at a ratio of 1 l water per 100 g of gut content sample. Tap water was used as we were only looking for microplastic pieces ~1 mm or larger. Diluted samples were initially hand stirred and then placed on a stir plate and mechanically stirred for 1 h. The samples were left to settle for 24 h. The entire sample was sieved through a 212 µm sieve and then rinsed with a pressure hose to separate plastics and vegetation from sand. To prevent the degradation of plastics and to conduct the analysis in an efficient and cost effective manner, the GI contents were visually examined by systematically sweeping through the sieved GI contents using stainless steel forceps and spatulas. Potential plastic pieces were collected and removed from the sample. The remaining GI contents were placed in a drying oven at 50°C for 3–5 days and then dry weights were recorded. A similar process was used for Asian elephants (Katlam et al., 2022). All plastic pieces identified from sub-samples collected from the GI tract were missed during the gross necropsy which relied on manual palpitation or visual identification.

Plastic particle identification and imaging

Potential plastics were individually stained with Nile Red (9-diethylamino-5H-benzo[a] phenoxazine-5-one) stock solution (5 mg Nile Red powder dissolved in 1 l acetone) (adapted from Maes et al., 2017) for 30 min and then individually placed in petri dishes to dry and for storage. Dried plastics were imaged using a dissecting microscope equipped with a digital camera and Stereo Microscope Fluorescence Adapter system (NightSea, Lexington, MA). Samples were exposed to cyan light (excitation wavelength: 490–515 nm) and viewed through an orange emission filter (550 nm longpass). Plastics were categorized as micro or macroplastics, as well as fragments, sheets or fibers. Monofilament lines, typically from fishing gear, were recorded as fibers as they can break down into smaller fibers (Wright et al., 2021), but they are additionally listed as monofilament lines in Supplementary Table S1. ImageJ (Schneider et al., 2012) was used to determine the length of the longest axis and area.

Statistical analysis

To investigate if the concentration of microplastics varied between the different sections of the GI tract, we calculated the number of plastic particles per gram of both wet and dry weight of material examined for each sampled location in each manatee. A Shapiro–Wilk test was used to test for normality in the distribution of the data and a nonparametric Kruskal-Wallis test was used to compare the distribution of the plastic particles between the different segments of the GI tract. All data analysis was performed in JMP (SAS Institute, NC, United States).

Results

Between December 2017 and March 2020, 26 manatee carcasses recovered from Tampa Bay were sampled for plastics (see Supplementary Table S1 for details on each individual). There were 16 adults, 7 juveniles and 3 calves; 12 females and 14 males; all of the calves had GI tracts filled with vegetation. During gross necropsy, macroplastics were detected in 26.9% of the individuals (7/26). Most carcasses (81%; 21/26) had full GI tracts, with large quantities of vegetation present throughout the tract. While cause of death varied for these manatees, plastic ingestion was not a direct cause of death, although GI lesions of one (MNW18003) were consistent with having previously passed a foreign body.

A total of 12 pieces of macroplastic were found during gross necropsy ($\bar{x}$ = 0.46, S.E. = 0.19 per individual); 48 plastic pieces were found in the selected sub-samples ($\bar{x}$ = 1.86 S.E. = 0.33 per individual); for a total of 60 plastic pieces ($\bar{x}$ =2.31, S.E. = 0.41 per individual). Plastic pieces ranged in linear measurement from 0.02 mm to 14.9 mm, including eight plastic fibers which were larger than 5 mm, which is the generally accepted definition of microplastics. Fibers were the most common type of microplastics identified in manatees (Table 1; Figure 2), including 11 pieces which were clearly visible as monofilament fishing line. Five of the eight larger plastic fibers were monofilament fishing line. Fragments were typically small particles with an irregular oval shape, while sheets were relatively uncommon, but did include small portions of plastic bags.

We were able to subsample from all five locations in the GI tract for 24 individuals, however individual MNW18009 did not have any ingesta in either the stomach or duodenum, and individual MNW19038 did not have any digesta in the cecum. Plastic pieces were detected in the sub-sampled portion of the GI tract of 73.1% of the individuals (19/26) and when combined with the macroplastics found during gross necropsies, 76.9% (20/26 individuals) contained

TABLE 1 Summary of plastic pieces collected from sub-sampled GI tract from 26 Florida manatees collected in Tampa Bay, Florida.

	Fragment	Fibers	Sheet
N (all) *Restricted to pieces < 5 mm*	16	27 *19*	5
Average Length mm (S.E) (all) *Restricted to pieces < 5 mm*	0.46 ± 0.12	3.94 ± 0.77 *1.85 ± 0.35*	1.75 ± 0.69
Range of Length (mm)	0.08 to 1.82	0.04 to 14.9	0.76 to 4.40
Average Area (S.E) (mm^2)	0.17 ± 0.09	–	1.83 ± 0.87
Range of Area (mm^2)	0.08 to 1.13	–	0.22 to 5.05
Predominant Color	Black	Black	Black and Clear

at least 1 piece of plastic in their GI tract. In carcasses with both types of plastics, the macro- and microplastics came from different items for most individuals (5/6; see Supplementary Table S1). Ingestion of plastics varied between the sexes (10/14–71% males and 10/12–83% females had ingested plastic) and age classes (12/16–75% adults, 457–71% juveniles and 3/3–100% calves had ingested plastic); however, small sample sizes prevented further analysis. Plastic was found in the GI tracts of manatees that had been feeding recently (16/22) as well as those with relatively empty GI tracts (3/4 individuals).

Microplastic pieces were found throughout the GI tract; 6 in the stomach (13%), 5 in the duodenum (10%), 8 in the cecum (19%), 10 in the proximal colon (25%) and 16 in the distal colon (33%). Concentrations of plastics per gram of GI subsample examined varied between the different sections (Table 2). The concentrations of the particles were not normally distributed (Shapiro-Wilks $W = 0.433$, $p < 0.0001$ wet; $W = 0.363$, $p < 0.0001$) and the distribution of particles between the different segments of the GI tract were not significantly different from each other ($\chi = 0.4371$, df = 4, $p = 0.9793$ wet; $\chi = 1.9237$, df = 4, $p = 0.7498$ dry).

Discussion

Overall it is clear that manatees in Tampa Bay routinely ingested plastic during our study period, as 76.5% of individuals sampled contained plastic in their GI tract. Although ingestion of plastic is rarely the leading cause of death in manatees, it can be a contributing factor in some mortalities (Beck and Barros, 1991; Reinert et al., 2017). While this is the first study to investigate microplastic ingestion by manatees, necropsies routinely examine the gastrointestinal tract for marine debris, much of which is plastic. Beck and Barros (1991) found 14.4% of manatees examined between 1978 and 1986 had ingested debris. Between 1993 and 2012, 9.7% of all manatee carcasses (598/6561) contained marine debris, however in just the last five years of the study (2008–2012) 19.7% of the carcasses contained marine debris (Reinert et al., 2017). While our study only examined 26 animals, 26.9% of the carcasses examined contained marine debris, all of which was plastic. Differences in detection rate during gross necropsy, for example increased awareness by prosectors, may also explain part of the increase over the years.

As all the manatees in this study were collected in Tampa Bay, it is possible that manatees in our samples were exposed to higher levels of plastic contamination as the Gulf of Mexico has been recorded to have some of the highest microplastic concentrations reported (Shruti et al., 2021). However, the previous study that included manatees from across Florida did not suggest that Tampa Bay was a hot spot for debris ingestion by manatees (Reinert et al., 2017) nor were concentrations of microplastics in Tampa Bay particularly high (McEachern et al., 2019).

In addition to the seven manatees which contained macroplastic detected during gross necropsies, our study documented an additional 13 manatees containing plastics in their GI tract; and six manatees contained plastics identified by both methods. This suggests that gross necropsy procedures do not identify all plastic pieces ingested by manatees, previous rates of plastic ingestion by manatees underrepresent the high proportion of individuals with plastic in their GI tract and manatees may be routinely ingesting many different plastics. Careful examination of the plastic pieces found in these six manatees, suggests that most of these manatees had ingested several different plastic items. For example, during the necropsy of manatee MNW18132 the Marine Mammal Pathology lab identified a piece of clear string in the colon, while we identified part of a black plastic bag in the distal colon. In contrast, MNW20012 had a large piece of clear monofilament line in its distal colon (found during the necropsy) as well as a smaller piece of monofilament line which could have broken down from the larger piece. At this point, it is not possible to determine if manatee digestive processes including grinding in the mouth are contributing to the further breakdown of plastics, as has been suggested in other organisms (Pérez-Guevara et al., 2021).

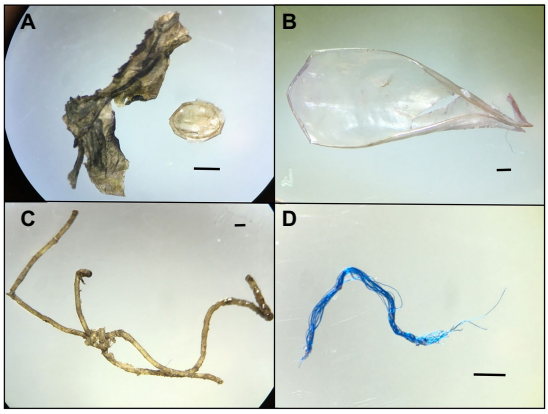

FIGURE 2
Microscopic images of representative plastics of different shapes collected from the GI tract of manatees **(A)** Fragment, two different particles, **(B)** Sheet, **(C)** Monofilament Line Fiber and **(D)** Fiber. Scale bar=1mm.

TABLE 2 Concentration of microplastic pieces throughout the GI tract.

Sample	*n*		Range (Number of pieces/gm)		Mean±standard error (Number of pieces /gm)	
	Dry	Wet	Dry	Wet	Dry	Wet
Stomach	23	23	0–0.0036	0–0.039	0.00061 ± 0.00021	0.0050 ± 0.0021
Duodenum	23	23	0–0.0038	0–0.035	0.00062 ± 0.0002	0.0046 ± 0.0021
Caecum	22	23	0–0.012	0–0.23	0.0011 ± 0.00059	0.015 ± 0.010
Proximal Colon	23	25	0–0.013	0–0.15	0.00095 ± 0.00058	0.012 ± 0.00065
Distal Colon	24	25	0–0.0039	0–0.042	0.00065 ± 0.00023	0.0096 ± 0.0029

Monofilament fishing line, including recreational fishing gear, was the most common macroplastic ingested by manatees (Beck and Barros, 1991; Reinert et al., 2017) and entanglement and ingestion of fishing gear including monofilament line were the most common form of fisheries interactions in manatees (Adimey et al., 2014). Monofilament fishing line was also the most common type of plastic found during necropsies (9/12 pieces; 75%) and during the microplastic detection process (11/48 pieces; 23%). Thus, fishing gear continues to pose a threat to manatees in Florida.

Plastic pieces >1 mm may have been present in at least some of the six individuals in our study in which we did not detect plastic, as we only sub-sampled a small portion of the entire GI contents. Examining a greater proportion of the GI tract would more accurately reflect ingestion rates; however, this process is very labor intensive. Better methods to digest cellulose would be helpful. Hurley et al. (2018) and Egea-Corbacho et al. (2022) have some suggestions but these methods are likely still too complicated, toxic and expensive to deal with the large quantities of cellulose-rich food manatees ingest.

Studies on microplastic ingestion by fish suggest that sample sizes below 10 are unreliable for frequency of observation of microplastic ingestion, especially when relying only on visual detection of plastic particles from gut contents (Markic et al., 2020). This suggests that our sample of 26 individuals, while still small, likely resulted in useful representation of the frequency of observation of microplastic ingestion by manatees in Tampa Bay, however our sample size prevented detailed analysis of other factors such as age, sex or cause of death. A review of microplastic ingestion by marine fishes indicated that about one-third of all individual fish (regardless of species) had ingested plastic, and on average, each fish contained about two plastic pieces (Markic et al., 2020). In our study, a much greater proportion of individuals contained plastic in their GI tract and although we estimated 2.3 plastic pieces per manatee, this is likely an underestimate as we only sub-sampled a small portion of the GI tract. If we had been able to use chemical digestion, filtration and microscopic identification as suggested by Savoca et al. (2021), we would likely have identified many more plastic pieces.

While it is challenging to calculate plastic ingestion rates for manatees, we can calculate a rough ingestion rate based on plastic pieces found in manatee stomachs as this region represents the least processed material. A 500 kg manatee consumes approximately 35 kg of vegetation per day (assuming manatees consume 7% of their body weight per day; Bengtson, 1983; Worthy and Worthy, 2014). Therefore, if we scale the average concentration of 5 plastic pieces/kg wet material examined (Table 2) up to 35 kg of ingested material, it suggests that manatees may be ingesting upwards of 175 microplastic pieces per day. The physiological implications of this ingestion rate are currently unknown for manatees; however, work on several species of sea turtles indicated that greater amounts of plastic ingestion lead to higher risks of mortality (Wilcox et al., 2018).

Plastic ingestion by marine herbivores has not been well studied, and of the herbivores studied, most are fish grazing on algae. Marine herbivorous fish likely ingest plastic particles adhered to vegetation (Cardozo-Ferreira et al., 2021) and have lower rates of plastic ingestion than fish with other foraging strategies (Savoca et al., 2021). Benthic foragers also have relatively high rates of plastic ingestion (Savoca et al., 2021). Manatees in Tampa Bay predominately forage on seagrass, but also often contain sand, shells and benthic invertebrates in their GI tract (Reich and Worthy, 2006) and thus their plastic ingestion rates may be more similar to benthic foragers than marine herbivores.

While there was no clear indication of a concentration of microplastic pieces through the GI tract (Table 2), manatees concentrate forage materials between the stomach and fecal matter which suggests that manatees have the potential to concentrate environmental plastic in their feces. Microplastics in fecal matter is an emerging field of study, with examination of concentrations as well as the potential ecological implications of microplastic-laden feces (Pérez-Guevara et al., 2021). Fecal matter is clearly a vector of microplastics throughout the environment and the role of coprophagy in further transfer of microplastics in the food web deserves further attention (see Pérez-Guevara et al., 2021 for a review).

Conclusion

While it is challenging to identify microplastic pieces from the GI tracts of large herbivores such as manatees, it is clear from this study that manatees are ingesting microplastic in Tampa Bay and likely at fairly high rates. It is likely that all sirenian species are exposed to environmental microplastics which can be ingested while foraging. Further work is needed to assess the potential physiological impacts of microplastic consumption by sirenians as well as the role marine herbivores may play in concentrating environmental plastics into feces for trophic transfer up the food web.

Data availability statement

The original contributions presented in the study are included in the article/Supplementary material, further inquiries can be directed to the corresponding authors.

Ethics statement

Ethical review and approval was not required for the animal study because this research involved diseased animals, not killed for this study. Gross necropsies were conducted by the Florida Fish and Wildlife, Marine Mammal Pathobiology Laboratory and were conducted by authorized personnel in accordance with section 6 of the Endangered Species Act [implementing regulations 50 CFR 17.21(c) and 50 CFR 17.31(b)] and section 109(h) of the Marine Mammal Protection Act (implementing regulation 50 CFR 18.22). The authors were only involved in analysis of the gut content material provided by the Marine Mammal Pathobiology Laboratory.

Author contributions

SG and ANSS directed the research and oversaw the project. SG developed the laboratory methods and drafted the manuscript. All authors contributed to the article and approved the submitted version.

Funding

This work was funded through two grants to SG and ANSS from the Tampa Bay Environmental Restoration Fund and additional grant from the Eckerd College Natural Sciences Summer Research Program.

Acknowledgments

The authors would like to thank Martine de Wit for sample collection and feedback on an early version of the manuscript as well as everyone else at the Florida Fish and Wildlife Marine Mammal Pathobiology Lab for their assistance with the manatee necropsies and procuring our samples. Marine Mammal Protection Act and Endangered Species Permits were not required as materials from within the GI tract are not considered to be a part of the animal. Eckerd College students Sabrina Sorace, Shane Field and Shannon Day were instrumental in setting up the protocols to detect microplastics and for their efforts in identifying microplastic particles in manatee guts.

Conflict of interest

The authors declare that the research was conducted in the absence of any commercial or financial relationships that could be construed as a potential conflict of interest.

Publisher's note

Supplementary material

The Supplementary material for this article can be found online at: https://www.frontiersin.org/articles/10.3389/fevo.2023.1143310/full#supplementary-material

References

Adimey, N. M., Hudak, C. A., Powell, J. R., Bassos-Hull, K., Foley, A., Farmer, N. A., et al. (2014). Fishery gear interactions from stranded bottlenose dolphins, Florida manatees and sea turtles in Florida, USA. *Mar. Poll. Bull.* 81, 103–115. doi: 10.1016/j.marpolbul.2014.02.008

Arthur, C., Baker, J., and Bamford, H. E. (2009). *Proceedings of the International Research Workshop on the Occurrence, Effects and Fate of Microplastic Marine Debris*. University of Washington Tacoma, Tacoma, WA, Unites States.

Attademo, F. L. N., Balensiefer, D. C., da Bôaviagem Freire, A. C., de Sousa, G. P., da Cunha, F. A. G. C., and de Oliveira Luna, F. (2015). Debris ingestion by the Antillean manatee (*Trichechus manatus manatus*). *Mar. Poll. Bull.* 101, 284–287. doi: 10.1016/j.marpolbul.2015.09.040

Baalkhuyur, F. M., Dohaish, E. J. A. B., Elhalwagy, M. E., Alikunhi, N. M., AlSuwailem, A. M., Røstad, A., et al. (2018). Microplastic in the gastrointestinal tract of fishes along the Saudi Arabian Red Sea coast. *Mar. Poll. Bull.* 131, 407–415. doi: 10.1016/j.marpolbul.2018.04.040

Baulch, S., and Perry, C. (2014). Evaluating the impacts of marine debris on cetaceans. *Mar. Poll. Bull.* 80, 210–221. doi: 10.1016/j.marpolbul.2013.12.050

Beck, C. A., and Barros, N. B. (1991). The impact of debris on the Florida manatee. *Mar. Pollut. Bull.* 22, 508–510. doi: 10.1016/0025-326X(91)90406-I

Bengtson, J. L. (1983). Estimating food consumption of free-ranging manatees in Florida. *J. Wildlife Manage.* 47, 1186–1192. doi: 10.2307/3808190

Bonde, R. K., O'Shea, T. J., and Beck, C. A. (1983). *Manual of Procedures for the Salvage and Necropsy of Carcasses of the West Indian Manatee (Trichechus manatus)*. Springfield, VA: National Technical Information Service.

Boshoff, B. J., Robinson, T. B., and von der Heyden, S. (2023). The role of seagrass meadows in the accumulation of microplastics: insights from a south African estuary. *Mar. Poll. Bull.* 186:114403. doi: 10.1016/j.marpolbul.2022.114403

Bucci, K., Tulio, M., and Rochman, C. M. (2020). What is known and unknown about the effects of plastic pollution: A meta-analysis and systematic review. *Ecol. Appl.* 30:e02044. doi: 10.1002/eap.2044

Butterworth, A. (2016). A review of the welfare impact on pinnipeds of plastic marine debris. *Front. Mar. Sci.* 3:00149. doi: 10.3389/fmars.2016.00149

Cabansag, J. B. P., Olimberio, R. B., and Villanobos, Z. M. T. (2021). Microplastics in some fish species and their environs in eastern Visayas. *Philippines. Mar. Poll. Bull.* 167:112312. doi: 10.1016/j.marpolbul.2021.112312

Cardozo-Ferreira, G. C., Calazans, T. L., Benevides, L. J., Luiz, O. J., Ferreira, C. E., and Joyeux, J. C. (2021). Ecological traits influencing anthropogenic debris ingestion by herbivorous reef fishes. *Front. Mar. Sci.* 8:717435. doi: 10.3389/fmars.2021.717435

Caron, A. G., Thomas, C. R., Berry, K. L., Motti, C. A., Ariel, E., and Brodie, J. E. (2018). Validation of an optimised protocol for quantification of microplastics in heterogenous samples: a case study using green turtle chyme. *MethodsX* 5, 812–823. doi: 10.1016/j.mex.2018.07.009

Cozzolino, L., Nicastro, K. R., Zardi, G. I., and Carmen, B. (2020). Species-specific plastic accumulation in the sediment and canopy of coastal vegetated habitats. *Sci. Total Environ.* 723:138018. doi: 10.1016/j.scitotenv.2020.138018

Datu, S. S., Supriadi, S., and Tahir, A. (2019). Microplastic in Cymodocea rotundata seagrass blades. *IJEAB.* 4, 1758–1761. doi: 10.22161/ijeab.46.21

Dehaut, A., Hermabessiere, L., and Duflos, G. (2019). Current frontiers and recommendations for the study of microplastics in seafood. *TRAC* 116, 346–359. doi: 10.1016/j.trac.2018.11.011

Duncan, E. M., Broderick, A. C., Fuller, W. J., Galloway, T. S., Godfrey, M. H., Hamann, M., et al. (2019). Microplastic ingestion ubiquitous in marine turtles. *Glob. Chang. Biol.* 25, 744–752. doi: 10.1111/gcb.14519

Egea-Corbacho, A., Martín-García, A. P., Franco, A. A., Albendín, G., Arellano, J. M., Rodríguez, R., et al. (2022). A method to remove cellulose from rich organic samples to analyse microplastics. *J. Clean. Prod.* 334:130248. doi: 10.1016/j.jclepro.2021.130248

Enders, K., Lenz, R., Beer, S., and Stedmon, C. A. (2017). Extraction of microplastic from biota: recommended acidic digestion destroys common plastic polymers. *ICES J. Mar. Sci.* 74, 326–331. doi: 10.1093/icesjms/fsw173

Fibbe, M. C., Carroll, D., Gowans, S., and Siuda, A. N. S. (2023). Ingestion of microplastics by copepods in Tampa Bay Estuary, FL. *Front. Ecol. Evol.* 11:1143377. doi: 10.3389/fevo.2023.1143377

Gall, S. C., and Thompson, R. C. (2015). The impact of debris on marine life. *Mar. Poll. Bull.* 92, 170–179. doi: 10.1016/j.marpolbul.2014.12.041

Goss, H., Jaskiel, J., and Rotjan, R. (2018). *Thalassia testudinum* as a potential vector for incorporating microplastics into benthic marine food webs. *Mar. Poll. Bull.* 135, 1085–1089. doi: 10.1016/j.marpolbul.2018.08.024

Guterres-Pazin, M. G., Rosas, F. C. W., and Marmontel, M. (2012). Short Note: Ingestion of Invertebrates, Seeds, and Plastic by the Amazonian Manatee (Trichechus inunguis) (Mammalia, Sirenia). *Aqua. Mammal.* 38, 322–324. doi: 10.1578/AM.38.3.2012.322

Huang, Y., Xiao, X., Effiong, K., Xu, C., Su, Z., Hu, J., et al. (2021). New insights into the microplastic enrichment in the blue carbon ecosystem: evidence from seagrass meadows and mangrove forests in coastal South China Sea. *Environ. Sci. Technol.* 55, 4804–4812. doi: 10.1021/acs.est.0c07289

Huang, Y., Xiao, X., Xu, C., Perianen, Y. D., Hu, J., and Holmer, M. (2020). Seagrass beds acting as a trap of microplastics-emerging hotspot in the coastal region? *Environ. Pollut.* 257:113450. doi: 10.1016/j.envpol.2019.113450

Hurley, R. R., Lusher, A. L., Olsen, M., and Nizzetto, L. (2018). Validation of a method for extracting microplastics from complex, organic-rich, environmental matrices. Ea. *Environ. Sci. Technol.* 52, 7409–7417. doi: 10.1021/acs.est.8b01517

ICES (2015). "ICES special request advice Northeast Atlantic and Arctic Ocean" in OSPAR request on development of a common monitoring protocol for plastic particles

in fish stomachs and selected shellfish on the basis of existing fish disease surveys. ICES Advice 2015, Book 1 (June), 1–6.

Jones, K. L., Hartl, M. G., Bell, M. C., and Capper, A. (2020). Microplastic accumulation in a Zostera marina L. bed at Deerness sound, Orkney, Scotland. *Mar. Poll. Bull.*:152:110883. doi: 10.1016/j.marpolbul.2020.110883

Katlam, G., Prasad, S., Pande, A., and Ramchiary, N. (2022). Plastic ingestion in Asian elephants in the forested landscapes of Uttarakhand. *India. J. Nat. Conserv.* 68:126196. doi: 10.1016/j.jnc.2022.126196

Kreitsberg, R., Raudna-Kristoffersen, M., Heinlaan, M., Ward, R., Visnapuu, M., Kisand, V., et al. (2021). Seagrass beds reveal high abundance of microplastic in sediments: a case study in the Baltic Sea. *Mar. Poll. Bull.* 168:112417. doi: 10.1016/j.marpolbul.2021.112417

Laist, D. W. (1987). Overview of the biological effects of lost and discarded plastic debris in the marine environment. *Mar. Poll. Bull.* 18, 319–326. doi: 10.1016/S0025-326X(87)80019-X

Landsberg, J. H., Tabuchi, M., Rotstein, D. S., Subramaniam, K., Rodrigues, T., Waltzek, T. B., et al. (2022). Novel lethal Clostridial infection in Florida manatees (*Trichechus manatus latirostris*): cause of the 2013 unusual mortality event in the Indian River lagoon. *Front. Mar. Sci.* 9:195. doi: 10.3389/fmars.2022.841857

Larkin, I. L., Fowler, V. F., and Reep, R. L. (2007). Digesta passage rates in the Florida manatee (*Trichechus manatus latirostris*). *Zoo Biol.* 26, 503–515. doi: 10.1002/zoo.20150

Maes, T., Jessop, R., Wellner, N., Haupt, K., and Mayes, A. G. (2017). A rapid-screening approach to detect and quantify microplastics based on fluorescent tagging with Nile red. *Sci. Rep.* 7, 1–10. doi: 10.1038/srep44501

Markic, A., Gaertner, J. C., Gaertner-Mazouni, N., and Koelmans, A. A. (2020). Plastic ingestion by marine fish in the wild. *Crit. Rev. Environ. Sci. Technol.* 50, 657–697. doi: 10.1080/10643389.2019.1631990

McEachern, K., Alegria, H., Kalagher, A. L., Hansen, C., Morrison, S., and Hastings, D. (2019). Microplastics in Tampa Bay, Florida: abundance and variability in estuarine waters and sediments. *Mar. Poll. Bull.* 148, 97–106. doi: 10.1016/j.marpolbul.2019.07.068

Pérez-Guevara, F., Kutralam-Muniasamy, G., and Shruti, V. C. (2021). Critical review on microplastics in fecal matter: research progress, analytical methods and future outlook. *Sci.Total Environ.* 778:146395. doi: 10.1016/j.scitotenv.2021.146395

Plee, T. A., and Pomory, C. M. (2020). Microplastics in sandy environments in the Florida keys and the panhandle of Florida, and the ingestion by sea cucumbers (Echinodermata: Holothuroidea) and sand dollars (Echinodermata: Echinoidea). *Mar. Poll. Bull.* 158:111437. doi: 10.1016/j.marpolbul.2020.111437

Reich, K. J., and Worthy, G. A. (2006). An isotopic assessment of the feeding habits of free-ranging manatees. *Mar. Ecol. Prog.* 322, 303–309. doi: 10.3354/meps322303

Reinert, T. R., Spellman, A. C., and Bassett, B. L. (2017). Entanglement in and ingestion of fishing gear and other marine debris by Florida manatees, 1993 to 2012. *Endanger. Species Res.* 32, 415–427. doi: 10.3354/esr00816

Reynolds, J. E. III, and Rommel, S. A. (1996). Structure and function of the gastrointestinal tract of the Florida manatee, *Trichechus manatus latirostris*. *Anat. Rec.* 245, 539–558. doi: 10.1002/(SICI)1097-0185(199607)245:3<539::AID-AR11>3.0.CO;2-Q

Runge, M. C., Sanders-Reed, C. A., Langtimm, C. A., Hostetler, J. A., Martin, J., Deutsch, C. J., et al. (2017). *Status and Threats Analysis for the Florida Manatee (Trichechus manatus latirostris) 2016*. Scientific Investigation Report 2017–5030. Reston: VA. United.States Geological Survey.

Saliu, F., Montano, S., Leoni, B., Lasagni, M., and Galli, P. (2019). Microplastics as a threat to coral reef environments: detection of phthalate esters in neuston and scleractinian corals from the Faafu atoll, Maldives. *Mar. Poll. Bull.* 142, 234–241. doi: 10.1016/j.marpolbul.2019.03.043

Savoca, M. S., McInturf, A. G., and Hazen, E. L. (2021). Plastic ingestion by marine fish is widespread and increasing. *Glob. Chang. Biol.* 27, 2188–2199. doi: 10.1111/gcb.15533

Sawalman, R., Werorilangi, S., Ukkas, M., Mashoreng, S., Yasir, I., and Tahir, A. (2021). Microplastic abundance in sea urchins (*Diadema setosum*) from seagrass beds of Barranglompo Island, Makassar, Indonesia. *IOP Conf. Ser. Earth Environ. Sci.* 763:012057. doi: 10.1088/1755-1315/763/1/012057

Sbrana, A., Valente, T., Scacco, U., Bianchi, J., Silvestri, C., Palazzo, L., et al. (2020). Spatial variability and influence of biological parameters on microplastic ingestion by Boops boops (L.) along the Italian coasts (Western Mediterranean Sea). *Environ. Pollut.* 263:114429. doi: 10.1016/j.envpol.2020.114429

Schneider, C. A., Rasband, W. S., and Eliceiri, K. W. (2012). NIH image to ImageJ: 25 years of image analysis. *Nat. Methods* 9, 671–675. doi: 10.1038/nmeth.2089

Seng, N., Lai, S., Fong, J., Saleh, M. F., Cheng, C., Cheok, Z. Y., et al. (2020). Early evidence of microplastics on seagrass and macroalgae. *Mar. Freshw. Res.* 71, 922–928. doi: 10.1071/MF19177

Shruti, V. C., Pérez-Guevara, F., and Kutralam-Muniasamy, G. (2021). The current state of microplastic pollution in the world's largest gulf and its future directions. *Environ. Pollut.* 291:118142. doi: 10.1016/j.envpol.2021.118142

Simmonds, M. P. (2012). Cetaceans and marine debris: the great unknown. *J. Mar. Biol.* 2012, 1–8. doi: 10.1155/2012/684279

Tahir, A., Samawi, M. F., Sari, K., Hidayat, R., Nimzet, R., Wicaksono, E. A., et al. (2019). Studies on microplastic contamination in seagrass beds at Spermonde archipelago of Makassar Strait, Indonesia. *JPCS* 1341:022008. doi: 10.1088/1742-6596/1341/2/022008

Unsworth, R. K., Higgs, A., Walter, B., Cullen-Unsworth, L. C., Inman, I., and Jones, B. L. (2021). Canopy accumulation: are seagrass meadows a sink of microplastics? *Oceans* 2, 162–178. doi: 10.3390/oceans2010010

Wilcox, C., Puckridge, M., Schuyler, Q. A., Townsend, K., and Hardesty, B. D. (2018). A quantitative analysis linking sea turtle mortality and plastic debris ingestion. *Sci. Rep.* 8, 1–11. doi: 10.1038/s41598-018-30038-z

Worthy, G. A., and Worthy, T. A. (2014). Digestive efficiencies of ex situ and in situ west Indian manatees (*Trichechus manatus latirostris*). *Physiol. Biochem. Zool.* 87, 77–91. doi: 10.1086/673545

Wright, L. S., Napper, I. E., and Thompson, R. C. (2021). Potential microplastic release from beached fishing gear in Great Britain's region of highest fishing litter density. *Mar. Poll. Bull.* 173:113115. doi: 10.1016/j.marpolbul.2021.113115

Zantis, L. J., Carroll, E. L., Nelms, S. E., and Bosker, T. (2021). Marine mammals and microplastics: a systematic review and call for standardisation. *Environ. Pollut.* 269:116142. doi: 10.1016/j.envpol.2020.116142

frontiers | Frontiers in Ecology and Evolution

TYPE Original Research
PUBLISHED 12 May 2023
DOI 10.3389/fevo.2023.1127679

OPEN ACCESS

EDITED BY
Frank S. Gilliam,
University of West Florida, United States

REVIEWED BY
Hussein J. Shareef,
University of Basrah, Iraq
Ramtin Ravanfar,
University of Florida, United States

*CORRESPONDENCE
Amir Ali Khoddamzadeh
✉ akhoddam@fiu.edu

RECEIVED 19 December 2022
ACCEPTED 12 April 2023
PUBLISHED 12 May 2023

CITATION
Khoddamzadeh AA, Flores J, Griffith MP and Souza Costa BN (2023) Saltwater intrusion ecophysiological effects on *Pseudophoenix sargentii*, *Roystonea regia*, *Sabal palmetto* "Lisa," and *Thrinax radiata* in South Florida. *Front. Ecol. Evol.* 11:1127679. doi: 10.3389/fevo.2023.1127679

Saltwater intrusion ecophysiological effects on *Pseudophoenix sargentii*, *Roystonea regia*, *Sabal palmetto* "Lisa," and *Thrinax radiata* in South Florida

Amir Ali Khoddamzadeh[1]*, Jason Flores[1], M. Patrick Griffith[2] and Bárbara Nogueira Souza Costa[1]

[1]Department of Earth and Environment, Institute of Environment, Florida International University, Miami, FL, United States, [2]Montgomery Botanical Center, Coral Gables, FL, United States

Climate change will alter natural areas on a global scale within the next century, especially in low-lying coastal areas where sea-level rise is predicted to severely degrade or destroy many ecosystems. As sea-level rise continues, it is expected that salinity due to saltwater intrusion will impact soil health and agricultural production, this is of even greater importance in areas such as South Florida where the surface and groundwater resources are hydrologically connected due to the shallow and highly permeable limestone soils. The chlorophyll concentrations in leaf tissue were chosen as the primary health indicator to assess whether this is a valuable factor to consider for plant health risk assessment and whether optical sensor technology such as the SPAD and NDVI, are valuable tools when understanding the impact seawater encroachment has on plant nitrogen uptake. Therefore, the aim of this study was to evaluate the effects of salt concentrations on plant growth and health of four palm species. The treatments were from pure reverse osmosis water, Fresh water, brackish water, seawater and hypersaline water (0, 0.5, 5, 10, 15, 25, and 50ppt). Control treatment that received reverse osmosis filtrated water with a salinity concentration of 0ppt had the highest health-indicator averages compared to treatment 50ppt. As the salinity increased, all health indicators gradually declined or remained rather constant and declined as they approached the greater salinity concentrations. The growth parameters and chlorophyll content were reduced over time, particularly at higher salt concentrations for all palm species studied. The chlorophyll content by SPAD and the normalized difference vegetation index (NDVI) can be used as health indicators of the palm species studied, as it was observed in this study a decline in the chlorophyll content as there was an increase in salt concentrations. It is important to emphasize that leaf chlorosis and subsequent decline of palm species were observed in the treatment with higher salt concentration, thus highlighting the importance of chlorophyll content as an indicator of plant health. The species *Roystonea regia* was very susceptible to salinity, and the palm *Sabal palmetto* is more susceptible to salinity than the *Thrinax radiata* and *Pseudophoenix sargentii* palms.

KEYWORDS

Arecaceae, palms, saline stress, chlorophyll content, NDVI

1. Introduction

Climate change will alter natural areas on a global scale within the next century, especially in low-lying coastal areas where sea-level rise is predicted to severely degrade or destroy many ecosystems (Braun de Torrez et al., 2021). Climate change and variability contribute to increased warmer conditions, increased frequency of heavy rain that accounts for an increasing proportion of total rainfall, extreme weather characterized by spatially variable cycles of drought and wetness, increased frequency of tropical storms/hurricanes, increased frequency of storm surges, and accelerated rate of sea-level rise (SLR). As SLR continues, it is expected that salinity due to saltwater intrusion (SWI) will impact soil health and agricultural production, this is of even greater importance in areas such as South Florida where the surface and groundwater resources are hydrologically connected due to the shallow and highly permeable limestone soils (Bayabil et al., 2021). South Florida is home to a diversity of palms (Arecaceae) with 9 native species and many more represented in cultivation for commercial production (Broschat and Black, 2021).

Native palms provide structural integrity and resources for the ecosystems they inhabit, and non-native palms are not only emblematic of the tropics, but generators of novel self-containing ecosystems (Fehr et al., 2020). Montgomery Botanical Center is a nonprofit botanical garden and research institution located in the city of Coral Gables, Florida, just south of Miami. As a coastal landsite hosting an outdoors living collection of nationally accredited palms and cycads that is recognized as vulnerable to sea level-rise and "King Tide" events, we chose to design an *ex situ* experiment based on observations and inferences from this site (Griffith et al., 2017). The coastal location of the botanic garden results in frequent inundation from encroaching oceanwater coming from coastal mangrove forest in the Southeastern section of the property. Previous studies have investigated the effects of saltwater on palms, focusing primarily on the commercially and economically valuable *Phoenix dactylifera* (Yaish and Kumar, 2015). Specific to South Florida, the Cabbage palm (*Sabal palmetto*) has been the subject of many salinity trials (Perry and Williams, 1996).

The relative "greenness" of a leaf can serve as a proxy for chlorophyll concentration and leaf nitrogen levels. This is the very correlation that remote sensing and vegetation indices technologies exploit (Inman et al., 2005). Nitrogen is known to affect plant health indicators such as leaf size, weight, overall plant size, and transpiration rates (Basyouni and Dunn, 2013). The soil plant analysis development (SPAD) sensor is a diagnostic tool used to estimate the nitrogen status of crop foliage in an efficient and non-destructive manner (Sim et al., 2015). Normalized difference vegetation index (NDVI) has been proven to be a useful tool in gaining insights into photosynthetic efficiency, productivity, and yield (Inman et al., 2005).

Thereby, chlorophyll concentrations in leaf tissue were chosen as the primary health indicator to assess whether this is a valuable factor to consider for plant health risk assessment and whether optical sensor technology such as the SPAD and NDVI, are valuable tools when understanding the impact seawater encroachment has on plant nitrogen uptake. SPAD and NDVI sensors offer an insight into the uptake of macronutrients and if any known environmental changes have affected the plant's ability to produce favorable or desirable amounts of chlorophyll. In the context of this experiment optical sensors were utilized to determine any changes in Nitrogen-plant utilization in the presence of saltwater. Thus, assessing the correlation between leaf tissue chlorophyll concentration and saltwater intrusion presents an opportunity for new technology adoption for concerns regarding plants and salinity exposure. Therefore, the aim of this study was to evaluate the effects of salt concentrations on plant growth and plant health of four palm species.

2. Materials and methods

2.1. Plant material

Four-year-old palm saplings were used for the species *Pseudophoenix sargentii*, *Roystonea regi*a, and *Thrinax radiata* collected from Montgomery Botanic Center. Saplings were transplanted from 25.4 cm nursery pots to 35.56 cm nursery pots using a potting soil blend that consists of 25% Canadian peat, 40% pine bark, 25% perlite, and 10% coarse sand. Three-year-old palms were used for the species *S. palmetto* "Lisa." This group of palms had not outgrown their original nursery pots of 15.25 cm, and therefore were not transplanted. A low-rate dosage of 14-4-14 Nutricote slow-release fertilizer was administered to all palms a month prior to the experiment. This was done to rule out the possibility of nutrient deficiencies and to achieve uniformity across each plant. A total of 140 palms were involved in this study, 35 of each species. *P. sargentii* and *S. palmetto* "Lisa" were donated by Montgomery Botanical Center and the remaining species were purchased at a local South Florida plant nursery.

2.2. Growth conditions

The plants were grown in the Montgomery Botanical Center. The site for the *ex situ* experiment was exposed to plenty of sunlight with Southern exposure. Along the edges of the site some neighboring trees cast little shade during early parts of the day, but plants were shuffled in random blocks to address this. With no shade cloth these palms were exposed to all possible rainfall which was accounted for as an analogous for natural freshwater recharge as would occur in the area. A ratio of 45:7 was recorded for rainfall days. Throughout the trial a total of 38.88 cm (15.31 inch) of rainwater was documented. This was accounted for as natural freshwater buffering also occurs in natural settings. Data was recorded during the months of January through June, which had average temperatures of 26.6°C or 79.88°F, which is favorable conditions for these palm species. Palms were arranged in no particular order in the study site and were shuffled in random order twice throughout the study in order to rule out environmental differences such as sunlight exposure, rainwater, and proximity to other elements.

2.3. Treatments and analysis

Treatments were formulated using commercially available aquarium salts in order to closely mimic seawater and retain elements naturally found in the water encroaching coastal and vulnerable landsites. Salinity concentrations were measured using a commercially available refractometer that measures concentrations in ppt. Using reverse osmosis water as the base for the solution, this ensured no unwanted factors impacting results coming from tap water treatments and residues.

Treatments of saltwater were administered uniformly on the same date with a frequency of once every 7 days including with rainfall. Root zones were saturated with solution until leachate was observed at the bottom of the pots. This was administered over a period of 6 months beginning in January 2021 and ending in June 2021. Pure reverse osmosis water was used for the control. So, the treatments were 0 ppt which served as the control, 0.5, 5, 10, 15, 25, and 50 ppt. Fresh water represented by the concentration 0.5 ppt. Brackish water was represented by concentrations 5, 10, and 15 ppt. Seawater was represented by the concentration 25 ppt. Hypersaline water was represented by 50 ppt. The waters used for the treatments were collected from the lakes around the Montgomery Center, salt was not added to the waters used, but the amount of salt in each of them was measured. Plant health parameters consisting of plant height (cm), leaf count (unit), SPAD sensor readings, and Normalized Difference Vegetation Index—NDVI sensor readings were collected uniformly once per month. The Konica Minolta Chlorophyll meter SPAD-502 and the Trimble Greenseeker handheld crop sensor were used to record chlorophyll readings for all treatment and palm species. Three readings were taken from each plant per sensor and averaged out.

2.4. Experimental design and statistics

The experiment was established in a completely randomized design with seven treatments replicated 5 times with single pot replications (one plant in each pot), totaling 20 plants per species. Data were subjected to analysis of variance (ANOVA) and the means compared by Tukey's test ($p \leq 0.05$) using the SISVAR statistical program (Ferreira, 2011).

3. Results

In this study two factors were studied, salt concentrations and evaluation periods represented by days after treatment (DAT). For some plant growth and health parameters there was no interaction between these factors and therefore they were evaluated separately, for all palm species used in this study.

The treatment 0 ppt of salt increased leaf numbers (4.33) compared to 0.5 and 5 ppt (3.87, and 3.80), respectively in of *P. sargentii*. The salt concentrations (25 and 50 ppt) provided an increased number of leaves (4.27 and 4.23) of *P. sargentii* plants, respectively then 5 ppt treatment (3.80). Greater plant height of *P. sargentii* was observed in the treatment control (0 ppt; 152.44), compared to (5, 15, 25, and 50 ppt) treatments (119.65, 138.47, 130.18, 122.19, and 106.31), respectively. The 0.5 ppt treatment provided an increase plant height (141.94) of *P. sargentii* compared to (5, 25, and 50 ppt) treatments (119.65, 122.19, and 106.31), respectively, and the 10 ppt provided treatment an increase plant height (138.47) than (5 ppt—119.65 and 50 ppt—106.31) treatments. However, the (0, 0.5, and 5 ppt) treatments provided an increase for NDVI values (0.81, 0.81, and 0.80), correspondingly than (25 ppt—0.75 and 50 ppt—0.72) treatments, and the 10 and 15 ppt treatments provided an increase for NDVI values (0.79 and 0.78), subsequently compared to 50 ppt treatment (0.72; Table 1).

Greater leaf number of *P. sargentii* was observed at 150 DAT (4.37) compared to 60 DAT (3.94) and 90 DAT (3.91). For plant height an increase was observed in this characteristic at 90 DAT (137.01), 120 DAT (137.01), and 150 DAT (139.14) than 0, 30, and 60 DAT (118.91, 122.29, and 126.64), correspondingly. Greater NDVI values of *P. sargentii* was observed at 30, 60, 90, 120 and 150 DAT (0.79, 0.79, 0.79, 0.80 and 0.78), respectively than 0 DAT (0.73; Table 2).

There was significantly interaction ($p \leq 0.05$) between salt concentrations and evaluation periods represented by days after treatment (DAT) for SPAD values of *P. sargentii* plants. The 0 ppt treatment provided increase in SPAD values at 90 DAT (90.24; Table 3).

Control (0 ppt) treatment provided an increase in plant height (133.68) of *R. regia* plants compared to (0.5, 10, and 25 ppt) treatments (118.88, 120.55, and 114.69), respectively (Table 4).

No significant differences ($p \leq 0.05$) were observed for plant height of *R. regia* at 0, 30 and 60 DAT (Table 5). It is important to note that *R. regia* is a salinity susceptible palm specie because the plants exposed to 25 and 50 ppt treatments died, so we do not have data for the 90, 120, and 150 DAT for this species. Therefore, to homogenize we evaluated all treatments only at 0, 30, and 60 DAT.

There was significantly interaction ($p \leq 0.05$) between salt concentrations and evaluation periods represented by days after treatment (DAT) for leaves number, SPAD and NDVI values of *R. regia*. The 50 ppt treatment provided a decreased leaves number (1.40), SPAD (29.96) and NDVI values (0.31) at 60 DAT compared to other treatments (Table 6).

The (10 ppt—52.03 and 25 ppt—50.43) treatments provided an increase SPAD values of leaves of *T. radiata* plants compared to 50 ppt treatment (43.60). However, the (0, 0.5, 5, 10, 15, and 25 ppt) treatments

TABLE 1 Leaf number, plant height, and normalized difference vegetation index values (NDVI) of *Pseudophoenix sargentii* plants grown in saline conditions.

Salt concentrations (ppt)	Leaf number	Plant height (cm)	NDVI
0	4.33 a	152.44 a	0.81 a
0.5	3.87 bc	141.94 ab	0.81 a
5	3.80 c	119.65 de	0.80 a
10	4.03 abc	138.47 abc	0.79 ab
15	4.13 abc	130.18 bcd	0.78 ab
25	4.27 ab	122.19 cde	0.75 bc
50	4.23 ab	106.31 e	0.72 c

Means followed by the same letter within columns are not significantly different by Tukey's test ($p \leq 0.05$).

TABLE 2 Leaf number, plant height and normalized difference vegetation index values (NDVI) of *Pseudophoenix sargentii* plants at 0, 30, 60, 90, 120 and 150days after treatment.

Days after treatment (DAT)	Leaf number	Plant height (cm)	NDVI
0	4.09 ab	118.91 c	0.73 b
30	4.14 ab	122.29 bc	0.79 a
60	3.94 b	126.64 b	0.79 a
90	3.91 b	137.01 a	0.79 a
120	4.11 ab	137.01 a	0.80 a
150	4.37 a	139.14 a	0.78 a

Means followed by the same letter within columns are not significantly different by Tukey's test ($p \leq 0.05$).

TABLE 3 SPAD values of *Pseudophoenix sargentii* plants grown in saline conditions at 0, 30, 60, 90,120, and 150days after treatment.

Salt concentrations (ppt)	Days after treatment (DAT)					
	0	30	60	90	120	150
	SPAD					
0	58.78 aB	65.18 abB	59.80 aB	90.24 aA	66.10 abB	63.84 aB
0.5	53.38 aB	58.66 abB	63.20 aAB	77.92 abA	69.18 aAB	65.32 aAB
5	56.16 aA	55.60 bA	56.22 aA	61.42 bcA	63.30 abA	65.44 aA
10	56.34 aB	74.74 aA	65.20 aAB	62.60 bcAB	63.74 abAB	63.72 aAB
15	48.40 aA	57.32 abA	53.20 aA	57.36 cA	50.30 bA	55.46 aA
25	50.60 aA	58.72 abA	56.68 aA	57.56 cA	57.30 abA	63.06 aA
50	47.34 aA	60.24 abA	50.92 aA	55.24 cA	54.88 abA	57.08 aA

Means followed by the same letter lower case in the columns (salt concentrations) and upper case in the rows (DAF) are not significantly different by Tukey's test ($p \leq 0.05$).

TABLE 4 Plant height of *Roystonea regia* grown in saline conditions.

Salt concentrations (ppt)	Plant height (cm)
0	133.68 a
0.5	118.88 b
5	121.63 ab
10	120.55 b
15	127.06 ab
25	114.69 b
50	125.42 ab

Means followed by the same letter within columns are not significantly different by Tukey's test ($p \leq 0.05$).

TABLE 5 Plant height of *Roystonea regia* at 0, 30, and 60days after treatment.

Days after treatment (DAT)	Plant height (cm)
0	122.69 a
30	122.46 a
60	124.24 a

Means followed by the same letter within columns are not significantly different by Tukey's test ($p \leq 0.05$).

provided an increase for NDVI values (0.86, 0.86, 0.85, 0.86, 0.85, and 0.84), correspondingly than 50 ppt treatment (0.78; Table 7).

Greater SPAD values of *T. radiata* was observed at 90 DAT (51.22), and 120 DAT (50.87) compared to 0 DAT (45.45). For NDVI values an increase was observed in this characteristic at 30 DAT (0.88) than 0, 90, 120 and 150 DAT (0.83, 0.83, 0.84, and 0.81), respectively (Table 8).

There was significantly interaction ($p \leq 0.05$) between salt concentrations and evaluation periods represented by days after treatment (DAT) for leaves number and plant height of *T. radiata* plants. The 50 ppt treatment provided a decreased leaves number at 150 DAT (4.40) compared to other treatments. However, it is important to note that the plant height increase was observed in the 0 ppt treatment at 90, 120 and 150 DAT (107.70, 115.00, and 119.40), subsequently (Table 9).

The 0.5 ppt treatment provided an increase plant height (31.64) of *S. palmetto* plants compared to (0, 5, 10, 15, 25, and 50 ppt) treatments (27.40, 27.19, 26.95, 21.99, 21.55, and 20.44), appropriately. However, the (0 ppt—27.40, 5 ppt—27.19, and 10 ppt—26.95) treatments

TABLE 6 Leaves number, SPAD values, and normalized difference vegetation index values (NDVI) of *Roystonea regia* plants grown in saline conditions at 0, 30, and 60days after treatment.

Salt concentrations (ppt)	Days after treatment (DAT)		
	0	30	60
	Leaves number		
0	3.60 aA	3.60 aA	4.20 aA
0.5	3.40 aA	3.60 aA	4.00 abA
5	3.60 aA	3.60 aA	3.80 abA
10	3.60 aA	3.60 aA	3.00 bA
15	3.80 aA	3.80 aA	3.20 abA
25	3.60 aA	3.60 aA	3.40 abA
50	3.00 aA	2.40 bA	1.40 cB
	SPAD		
0	50.10 aA	48.60aA	54.16 aA
0.5	45.48 aA	53.82 aA	48.90 aA
5	44.04 aA	42.44 aA	49.22 aA
10	43.98 aA	45.60 aA	48.92 aA
15	50.12 aA	44.32 aA	45.52 aA
25	50.50 aA	50.24 aA	47.32 aA
50	44.24 aA	46.58 aA	29.96 bB
	NDVI		
0	0.83 aA	0.86 aA	0.81aA
0.5	0.76 aA	0.81 aA	0.82 aA
5	0.78 aA	0.78 aA	0.74 aA
10	0.81 aA	0.75 aA	0.73 aA
15	0.80 aA	0.80 aA	0.84 aA
25	0.79 aA	0.83 aA	0.81 aA
50	0.82 aA	0.80 aA	0.31 bB

Means followed by the same letter lower case in the columns (salt concentrations) and upper case in the rows (DAF) are not significantly different by Tukey's test ($p \leq 0.05$).

provided an increase plant height of *S. palmetto* plants than (15 ppt—21.99, 25 ppt—21.55, and 50 ppt—20.44; Table 10).

No significant differences ($p \leq 0.05$) were observed for plant height of *S. palmetto* at 0, 30, 60, 90, 120, and 150 DAT (Table 11).

There was significantly interaction ($p \leq 0.05$) between salt concentrations and evaluation periods represented by days after treatment (DAT) for leaves number, SPAD and NDVI values of *S. palmetto* plants. The 50 ppt treatment provided a decreased leaves number at 90 DAT (1.80), and 120 DAT (1.80), for SPAD values at 120 DAT (22.82), and 150 DAT (19.22), and for NDVI at 90 DAT (0.32), 120 DAT (0.32), and 150 DAT (0.26) compared to other treatments (Table 12).

In order to verify which palm species was more resistant to saline conditions in this study, the interaction was performed between the factors salt concentrations and palm species, so that there was a significant interaction ($p \leq 0.05$) between the factors studied salt concentrations and palm species (Table 13).

In general, with the increase in the salt concentration, there was a decrease in the values to growth parameters and chlorophyll content for all species. The 50 ppt treatment for the palm *S. palmetto* provided a decreased leaves number (2.20), plant height (15.20), SPAD (19.22) and NDVI (0.26) at 150 DAT compared to the other palm species (Table 13). Therefore, the palm *S. palmetto* is more susceptible to high salt concentrations than the *T. radiata* and *P. sargentii* palms.

In response to increasing exposure to high concentrations of salinity in simulated seawater, palm health indicators follow a declining trend. Lower concentrations of salinity also lead health indicators to decline, but with less magnitude. Over the six-month period that data was collected from the *ex situ* trial, it became visible that the hypersaline treatments (50 ppt) were negatively affecting the palms at a much faster rate. Chlorosis and leaf tissue burn became visible in just 3 months, with some palms completely declining the following month. By the end of the trial a total of 8 palms out of the 140 reached complete decline. Five *R. regia*, one *T. radiata*, and two *S. palmetto* "Lisa" all belonging to treatment that received the hypersaline solution with a salt concentration of 50 ppt. Control treatment that received reverse osmosis filtrated water with a salinity concentration of 0 ppt had

TABLE 7 SPAD values, and normalized difference vegetation index values (NDVI) of *Thrinax radiata* plants grown in saline conditions.

Salt concentrations (ppt)	SPAD	NDVI
0	48.41 ab	0.86 a
0.5	49.52 ab	0.86 a
5	48.05 ab	0.85 a
10	52.03 a	0.86 a
15	49.41 ab	0.85 a
25	50.43 a	0.84 a
50	43.60 b	0.78 b

Means followed by the same letter within columns are not significantly different by Tukey's test ($p \leq 0.05$).

TABLE 8 SPAD values, and normalized difference vegetation index values (NDVI) of *Thrinax radiata* plants at 0, 30, 60, 90,120, and 150days after treatment.

Days after treatment (DAT)	SPAD	NDVI
0	45.45 b	0.83 c
30	47.95 ab	0.88 a
60	47.16 ab	0.87 ab
90	51.22 a	0.83 c
120	50.87 a	0.84 bc
150	50.01 ab	0.81 c

Means followed by the same letter within columns are not significantly different by Tukey's test ($p \leq 0.05$).

TABLE 9 Leaf number, and Plant height of *Thrinax radiata* plants grown in saline conditions at 0, 30, 60, 90,120, and 150days after treatment.

Salt concentrations (ppt)	Days after treatment (DAT)					
	0	30	60	90	120	150
	Leaf number (unit)					
0	8.40 aB	8.60 aAB	9.00 aAB	8.60 abAB	9.20 aAB	10.20 aA
0.5	7.40 abB	7.40 abB	7.60 abcAB	8.40 abABC	9.20 aAB	10.00 aA
5	8.20 abA	8.20 aA	8.40 abA	9.00 aA	8.80 abA	9.80 aA
10	7.40 abC	7.40 abC	8.20 abBC	9.20 aAB	9.60 aAB	10.00 aA
15	8.20 abA	8.00 aA	8.20 abA	8.40 abA	8.20 abA	8.60 aA
25	7.40 abA	7.40 abA	7.00 bcA	7.00 bcA	7.00 bcA	6.40 bA
50	6.40 bA	6.00 bAB	5.80 cAB	5.40 cAB	6.00 cAB	4.40 cB
Plant height (cm)						
0	65.50 aC	71.80 aC	83.36 aB	107.70 aA	115.00 aA	119.40 aA
0.5	70.80 aD	76.80 aCD	82.80 abBCD	88.39 bABC	93.60 bcAB	96.40 bA
5	69.00 aB	73.60 aB	79.76 abB	95.96 bA	98.92 bA	103.60 bA
10	71.60 aB	74.20 aB	78.74 abB	93.47 bA	99.40 bA	106.00 bA
15	69.70 aD	72.80 aCD	76.20 bBCD	83.82 bABC	88.20 bcAB	95.20 bcA
25	67.50 aD	70.00 aCD	70.61 bABC	82.80 bA	83.20 cA	82.40 cAB
50	69.50 aA	71.40 aA	76.20 abA	67.98 cA	67.50 dA	67.73 dA

Means followed by the same letter lower case in the columns (salt concentrations) and upper case in the rows (DAF) are not significantly different by Tukey's test ($p \leq 0.05$).

the highest health-indicator averages compared to treatment 50 ppt. As the salinity increased, all health indicators gradually declined or remained rather constant and declined as they approached the greater salinity concentrations. At the end of the study, the effects of increased salinity concentration became very apparent simply by observing the palms, this can be appreciated in Figure 1 as it shows *S. palmetto* "Lisa" grow in saline conditions at 150 days after treatment, each treatment in ascending order from left to right (Figure 1). Pure reverse osmosis water was used for the control. So, the treatments were 0 ppt which served as the control. Fresh water represented by the concentration 0.5 ppt. Brackish water was represented by concentrations 5, 10, and 15 ppt. Seawater was represented by the concentration 25 ppt. Hypersaline water was represented by 50 ppt.

TABLE 10 Plant height of *Sabal palmetto* grown in saline conditions.

Salt concentrations (ppt)	Plant height (cm)
0	27.40 b
0.5	31.64 a
5	27.19 b
10	26.95 b
15	21.99 c
25	21.55 c
50	20.44 c

Means followed by the same letter within columns are not significantly different by Tukey's test ($p \leq 0.05$).

TABLE 11 Plant height of *Sabal palmetto* at 0, 30, 60, 90,120, and 150days after treatment.

Days after treatment (DAT)	Plant height (cm)
0	24.97 a
30	26.65 a
60	26.16 a
90	24.75 a
120	24.75 a
150	24.57 a

Means followed by the same letter within columns are not significantly different by Tukey's test ($p \leq 0.05$).

TABLE 12 Leaves number, SPAD values, and normalized difference vegetation index values (NDVI) of *Sabal palmetto* plants grown in saline conditions at 0, 30, 60, 90,120, and 150days after treatment.

Salt concentrations (ppt)	Days after treatment (DAT)					
	0	30	60	90	120	150
	Leaves number					
0	6.80 aC	7.00 aC	8.20 aBC	9.20 aAB	9.00 aAB	10.20 aA
0.5	6.40 aC	6.40 aC	7.20 abBC	8.00 abABC	8.60 abAB	9.60 aA
5	6.20 aB	6.40 aB	6.40 abB	7.60 abAB	7.60 abAB	8.60 abA
10	6.40 aA	6.40 aA	6.60 abA	6.40 bcA	6.80 bcA	7.40 bA
15	5.20 aA	5.40 aA	5.60 bcA	4.60 cA	5.20 bdA	5.00 cA
25	5.20 aA	5.20 aA	5.40 bcA	4.40 cAB	4.20 dAB	3.20 cdB
50	7.00 aA	6.40 aA	4.20 cB	1.80 dC	1.80 eC	2.20 dC
	SPAD					
0	47.58 aA	48.46 aA	46.50 aA	49.06 aA	47.12 aA	47.32 aA
0.5	50.72 aA	47.42 aA	53.26 aA	49.76 aA	52.44 aA	54.32 aA
5	51.34 aA	50.44 aA	50.68 aA	50.98 aA	46.62 aA	51.30 aA
10	52.36 aA	54.02 aA	54.14 aA	52.78 aA	47.58 aA	50.70 aA
15	49.26 aA	49.92 aA	50.66 aA	49.06 aA	49.22 aA	50.12 aA
25	47.92 aAB	57.32 aA	48.00 aAB	53.52 aAB	45.48 aAB	43.42 aB
50	49.10 aA	45.30 aA	42.66 aA	41.54 aA	22.82 bB	19.22 bB
	NDVI					
0	0.52 aBC	0.65 aAB	0.48 aC	0.60 aABC	0.65 aAB	0.71 aA
0.5	0.49 aBCD	0.59 aABC	0.45 abD	0.48 aCD	0.63 abAB	0.67 aA
5	0.54 aAB	0.63 aAB	0.49 aB	0.57 aAB	0.60 abcAB	0.67 aA
10	0.44 aBC	0.65 aA	0.36 abcC	0.55 aAB	0.50 bcB	0.51 bAB
15	0.50 aAB	0.63 aA	0.40 abcB	0.59 aA	0.53 abcAB	0.51 bAB
25	0.50 aAB	0.64 aA	0.30 bcC	0.48 aB	0.48 cB	0.44 bBC
50	0.52 aA	0.60 aA	0.26 cB	0.32 bB	0.32 dB	0.26 cB

Means followed by the same letter lower case in the columns (salt concentrations) and upper case in the rows (DAT) are not significantly different by Tukey's test ($p \leq 0.05$).

TABLE 13 Leaf number, plant height, SPAD values, and normalized difference vegetation index values (NDVI) of palm species grown in saline conditions at 150days after treatment.

Salt concentrations (ppt)	Palm species		
	Thrinax radiata	*Sabal palmetto*	*Pseudophoenix sargentii*
	Leaves number		
0	10.20 aA	10.20 aA	4.80 aB
0.5	10.00 aA	9.60 aA	4.40 aB
5	9.80 aA	8.60 abA	4.40 aB
10	10.00 aA	7.40 bB	4.40 aC
15	8.60 aA	5.00 cB	4.40 aB
25	6.40 bA	3.20 cdB	4.40 aB
50	4.40 bA	2.20 dB	3.80 aAB
	Plant Height (cm)		
0	119.40 aA	26.60 aB	171.80 aA
0.5	96.40 abA	35.40 aC	151.80 abB
5	103.60 abB	25.80 aC	129.60 bcA
10	106.00 abB	29.40 aC	144.60 bA
15	95.20 abB	20.80 aC	136.00 bcA
25	82.40 bcB	18.80 aC	127.80 bcA
50	67.74 cB	15.20 aC	112.40 cA
	SPAD		
0	49.16 aB	47.32 aB	63.84 aA
0.5	47.28 aB	54.32 aAB	65.32 aA
5	50.38 aB	51.30 aB	65.44 aA
10	57.20 aAB	50.70 aB	63.72 aA
15	51.68 aA	50.12 aA	55.46 aA
25	47.82 aB	43.42 aB	63.06 aA
50	46.56 aA	19.22 bB	54.08 aA
	NDVI		
0	0.84 abA	0.71 aB	0.83 aA
0.5	0.84 aA	0.67 aB	0.83 aA
5	0.83 abA	0.67 aB	0.83 aA
10	0.83 abA	0.51 bB	0.78 abA
15	0.81 abA	0.51 bB	0.79 abA
25	0.79 abA	0.44 bB	0.72 bA
50	0.74 bA	0.26 cB	0.71 bA

Means followed by the same letter lower case in the columns (salt concentrations) and upper case in the rows (palm species) are not significantly different by Tukey's test ($p \leq 0.05$).

4. Discussion

This study examines the ecophysiological effects of palms native to South Florida facing pressures from climate change such as sea level rise. A major consequence affecting plants with sea level rise is saltwater intrusion. Increased exposure to saltwater over time for established palms appears to have less of an effect on their longevity when compared to seedlings or saplings. Plant health decline can be measured and observed in as little as 6 months with the salinity gradient present in this study. This was documented across the four palm species found in this trial, suggesting the possibility of many palm seedlings and saplings not overcoming a similar salinity gradient in vulnerable landsites.

Ecophysiological data is necessary to interpret and model proper responses to seawater encroachment. The data gathered and visible evidence suggest that chlorophyll tissue concentration and plant health declines as exposure to high concentrations of salinity prolongs. It is expected that as chronic exposure to brackish, oceanwater, and hypersaline concentration of salinity continues, plant health will decline appreciably. The data also suggests that extended exposure to lower concentrations of salinity also negatively impacts plant health, but over an extended period. Within the six-month time frame of this

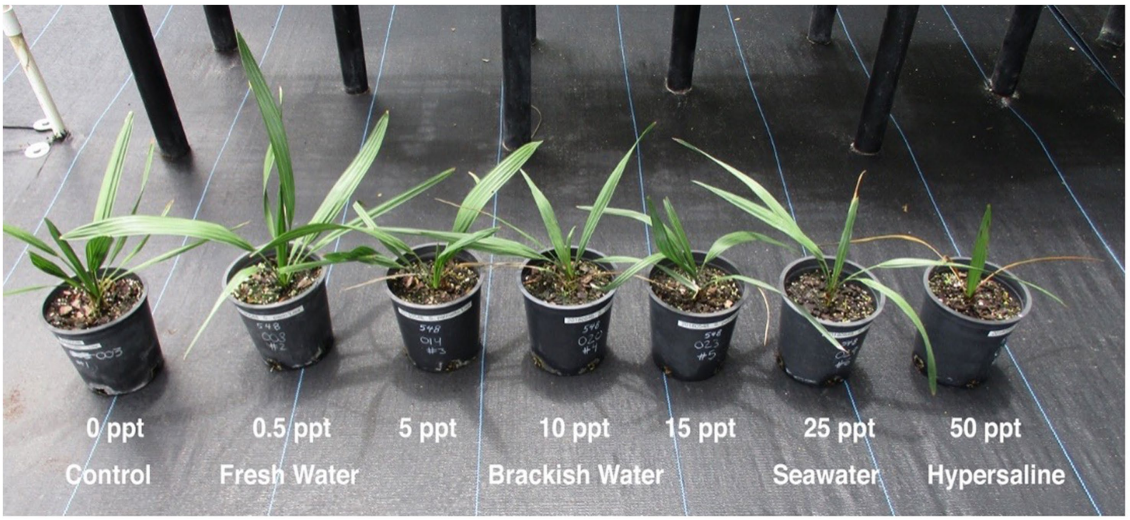

FIGURE 1
S. palmetto 'Lisa' grown in saline conditions at 150 days after treatment, each treatment in ascending order from left to right.

trial, chlorosis and leaf burn became apparent and was documented. In comparison to the control which received irrigation with complete absence of salinity, all plants treated with any amount of salinity scored lower in health indicators. This occurred quickly withing a 6-month period. If this translates to habitats, then it could suggest that saplings and seedlings would have a very tough time establishing themselves into the vegetative state.

Other authors also observed negative effects of salinity on the growth of some plants, corroborating the results found in this study, such as Nascimento et al. (2019) observed saline stress reduces the levels of the photosynthetic pigments and affects adversely the growth, causing reductions in plant height, stem diameter, leaf area and number of leaves of the cotton cultivars. Oliveira et al. (2018) observed that increasing salinity in water (CEa) levels significantly affected the initial growth and gas exchange of cotton cultivars, both at 15 and 30 DAT. Ait-El-Mokhtar et al. (2022) concluded that salt stress induced significant adverse effects on growth, physiological and biochemical attributes of date palm plants. Yu et al. (2021) observed that the plant growth and vigorousness of *Hibiscus rosa-sinensis* and *Mandevilla splendens* grown in nursery crops in south Florida were significantly limited when the salinity concentrations increased. The same authors highlight the need to monitor the salinity levels and prepare groundwater salinity mitigation plans under the projected increases in sea level and the resulting increases in the frequency and severity of saltwater intrusion in south Florida.

The plants, when cultivated under soil with salinity or irrigated with water saline, have their growth compromised due to the osmotic effect, which reduces the water absorption by the plant and/or as a function of the specific effect of the ions that cause functional disorders and damages, especially in leaves, thus affecting plant metabolism (Nobre et al., 2013). Thus, salinity can be considered as one of the abiotic stresses that most limits plant growth (Pedrotti et al., 2015). Biochemical and physiological processes are triggered in plants submitted to saline stress, which consequently interfere with their growth, stomatal behavior, and photosynthetic capacity (Nunkaewa et al., 2014), due to the osmotic effects of the salts and the specific characteristics of Na^+ and Cl^- (Graciano et al., 2011). Qiu et al. (2014) reported that saline stress, specifically, promotes the inhibition of the chlorophyllase enzyme, which results in a reduction in the levels of chlorophyll and its precursor, 5-aminolevulinate.

Despite continuous weekly exposure to irrigation containing more salinity than is ideal, most palms across genera and species continued to show signs of growth and development. All plants increased in average height, leaf count, and chlorophyll, when compared to baseline data (0 DAT). However, there was a decline in health markers the closer the experiment came to the 6-month mark. This can only lead to the conclusion that prolonging exposure would lead to eventual decline of most if not all plants, given sufficient time and continued salt exposure, mainly those exposed to the highest concentrations.

Furthermore, it is important to point out that the specie *R. regia* was very susceptible to salinity, as the plants exposed to the treatments of 25 and 50 ppt died at 90 days after treatment, and the palm *S. palmetto* is more susceptible to salinity than the *T. radiata* and *P. sargentii* palms.

This data is important in driving forward informed decision-making and proper technology adoption for conservation horticulture, horticultural production, landscaping, and botanic gardens in South Florida. As anthropogenic activities continue to alter natural systems, the consequences of sea-level rise and saltwater intrusion should be anticipated for and responded to in an informed and data-driven approach.

5. Conclusion

The growth parameters and chlorophyll content are reduced over time, particularly at higher salt concentrations for all palm species studied. The chlorophyll content by SPAD and the normalized difference vegetation index (NDVI) can be used as health indicators of the palm species studied, as it was observed in this study a decline in the chlorophyll content as there was an increase in salt concentrations. It is important to emphasize that leaf chlorosis and subsequent decline of palm species were observed in the treatment with higher salt concentration, thus highlighting the importance of chlorophyll content as an indicator of plant health. The specie *R. regia*

was very susceptible to salinity, and the palm *S. palmetto* is more susceptible to salinity than the *T. radiata* and *P. sargentii* palms.

Data availability statement

The raw data supporting the conclusions of this article will be made available by the authors, without undue reservation.

Author contributions

AK and MG: conceptualization, supervision, and project administration. JF: methodology. BS: software and formal analysis. JF: investigation. BS and JF: writing—original draft preparation. AK, MG, and BS: writing—review and editing. AK: funding acquisition. All authors contributed to the article and approved the submitted version.

Funding

Funding for this project was provided by the Hispanic Serving Institutions Higher Education Grants Program 2016-38422-25549 from the USDA National Institute of Food and Agriculture.

Acknowledgments

We would like to thank Montgomery Botanical Center (MBC) for providing palm seedlings, materials, and space. In addition to MBC's greenhouse manager, Vickie Murphy and Xavier Gratacos, Superintendent for facilitating resources and support throughout the experiment.

Conflict of interest

The authors declare that the research was conducted in the absence of any commercial or financial relationships that could be construed as a potential conflict of interest.

Publisher's note

All claims expressed in this article are solely those of the authors and do not necessarily represent those of their affiliated organizations, or those of the publisher, the editors and the reviewers. Any product that may be evaluated in this article, or claim that may be made by its manufacturer, is not guaranteed or endorsed by the publisher.

References

Ait-El-Mokhtar, M., Fakhech, A., Ben-Laouane, R., Anli, M., Boutasknit, A., Ait-Rahou, Y., et al. (2022). Compost as an eco-friendly alternative to mitigate salt-induced effects on growth, nutritional, physiological and biochemical responses of date palm. *Int. J. Recycl. Org. Waste Agric.* 11, 85–100. doi: 10.30486/IJROWA.2021.1927528.1233

Basyouni, R., and Dunn, B. (2013). Use of reflectance sensors to monitor plant nitrogen status in horticultural plants. Oklahoma Cooperative Extension ServiceHLA-6719, 1–4. Available at: https://extension.okstate.edu/fact-sheets/print-publications/hla/use-of-optical-sensors-to-monitor-plant-nitrogen-status-in-horticultural-plants-hla-6719.pdf

Bayabil, H. K., Li, Y., Tong, Z., and Gao, B. (2021). Potential management practices of saltwater intrusion impacts on soil health and water quality: a review. *J. Water Clim. Change.* 12, 1327–1343. doi: 10.2166/wcc.2020.013

Braun de Torrez, E. C., Frock, C. F., Boone, W. W., Sovie, A. R., and McCleery, R. A. (2021). Seasick: why value ecosystems severely threatened by sea-level rise? *Estuar. Coasts* 44, 899–910. doi: 10.1007/s12237-020-00850-w

Broschat, T. K., and Black, R. J. (2021). Ornamental palms for South Florida. Enh21/EP009:Ornamental Palms for South Florida. University of Florida. Available at: https://edis.ifas.ufl.edu/publication/EP009

Fehr, V., Buitenwerf, R., and Svenning, J. (2020). Non-native palms (Arecaceae) as generators of novel ecosystems: a global assessment. *Divers. Distrib.* 26, 1523–1538. doi: 10.1111/ddi.13150

Ferreira, D. F. (2011). Sisvar: a computer statistical analysis system. *Cienc. Agrotec.* 35, 1039–1042. doi: 10.1590/S1413-70542011000600001

Graciano, E. S. A., Rejane, J. M. C., Nogueira, R. J. M. C., Lima, D. R. M., Pacheco, C. M., and Santos, S. R. C. (2011). Crescimento e capacidade fotossintética da cultivar de amendoim BR 1 sob condições de salinidade. *Rev. Bras. Eng. Agric. Ambient.* 15, 794–800. doi: 10.1590/S1415-43662011000800005

Griffith, M. P., Barber, G., Lima, J. T., Barros, M., Calonje, C., Noblick, L. R., et al. (2017). Plant collection "half life:" can botanic gardens weather the climate? *Curator.* 60, 395–410. doi: 10.1111/cura.12229

Inman, D., Khosla, R., and Mayfield, T. (2005). On the go active remote sensing for efficient crop nitrogen management. *Sens. Rev.* 25, 209–214. doi: 10.1108/02602280510606499

Nascimento, E. C. S., do Nascimento, R., da Silva, A. A. R., de Castro Bezerra, C. V., Batista, M. C., de Sá Almeida Veloso, L. L., et al. (2019). Growth and photosynthetic pigments of cotton cultivars irrigated with saline water. *Agric. Sci.* 10, 81–91. doi: 10.4236/as.2019.101007

Nobre, R. G., Lima, G. S., Gheyi, H. R., Lourenço, G. S., and Soares, L. A. A. (2013). Emergência, Crescimento e produção da mamoneira sob estresse salino e adubação nitrogenada. *Rev. Cienc. Agron.* 44, 76–85. doi: 10.1590/S1806-66902013000100010

Nunkaewa, T., Kantachote, D., Kanzaki, H., Nitoda, T., and Ritchie, R. J. (2014). Effects of 5-aminolevulinic acid (ALA)-containing supernatants from selected *Rhodopseudomonas palustris* on rice growth under NaCl stress, with mediating effects on chlorophyll, photosynthetic electron transport and antioxidative enzymes. *Electron. J. Biotechnol.* 17, 19–26. doi: 10.1016/j.ejbt.2013.12.004

Oliveira, H., do Nascimento, R., Silva, S., Cardoso, J. A. F., Guimarães, R. F. B., and Nascimento, E. C. S. (2018). Initial growth and gas exchanges of plants of colored cotton submitted to saline stress. *Agric. Sci.* 9, 1652–1663. doi: 10.4236/as.2018.912115

Pedrotti, A., Chagas, R. M., Ramos, V. C., Prata, A. P. M., Lucas, A. A. T., and Santos, P. B. (2015). Causas e consequências do processo de salinização dos solos. Rev. Eletr. Gest. *Educ. Tecnol. Amb.* 19, 1308–1324. doi: 10.5902/2236117016544

Perry, L., and Williams, K. (1996). Effects of salinity and flooding on seedlings of cabbage palm (*Sabal palmetto*). *Oecologia* 105, 428–434. doi: 10.1007/BF00330004

Qiu, Z. B., Guo, J., Jhu, A. J., Zhang, L., and Zhang, M. M. (2014). Exogenous Jasmonic acid can enhance tolerance of wheat seedlings to salt stress. *Ecotoxicol. Environ. Saf.* 104, 202–208. doi: 10.1016/j.ecoenv.2014.03.014

Sim, C. C., Zaharah, A. R., Tan, M. S., and Goh, K. J. (2015). Rapid determination of leaf chlorophyll concentration, photosynthetic activity and NK concentration of *Elaiesguineensis* via correlated SPAD-502 chlorophyll index. *Asian J. Agric. Res.* 9, 132–138. doi: 10.3923/ajar.2015.132.138

Yaish, M. W., and Kumar, P. P. (2015). Salt tolerance research in date palm tree (*Phoenix dactylifera* L.), past, present, and future perspectives. *Front. Plant Sci.* 6:348. doi: 10.3389/fpls.2015.00348

Yu, X., Her, Y., Chang, A., Song, J.-H., Campoverde, E. V., and Schaffer, B. (2021). Assessing the effects of irrigation water salinity on TwoOrnamental crops by RemoteSpectral imaging. *Agronomy* 11:375. doi: 10.3390/agronomy11020375

frontiers | Frontiers in Ecology and Evolution

TYPE Original Research
PUBLISHED 24 May 2023
DOI 10.3389/fevo.2023.1144778

OPEN ACCESS

EDITED BY
Albertus J. Smit,
University of the Western Cape, South Africa

REVIEWED BY
S. Lan Smith,
Japan Agency for Marine-Earth Science and Technology (JAMSTEC), Japan
Patricia M. Glibert,
University of Maryland, College Park, United States

*CORRESPONDENCE
Elise S. Morrison
✉ elise.morrison@essie.ufl.edu

SPECIALTY SECTION
This article was submitted to Biogeography and Macroecology, a section of the journal Frontiers in Ecology and Evolution

RECEIVED 15 January 2023
ACCEPTED 24 March 2023
PUBLISHED 24 May 2023

CITATION
Morrison ES, Phlips E, Badylak S, Chappel AR, Altieri AH, Osborne TZ, Tomasko D, Beck MW and Sherwood E (2023) The response of Tampa Bay to a legacy mining nutrient release in the year following the event. *Front. Ecol. Evol.* 11:1144778. doi: 10.3389/fevo.2023.1144778

The response of Tampa Bay to a legacy mining nutrient release in the year following the event

Elise S. Morrison[1]*, Edward Phlips[2], Susan Badylak[2], Amanda R. Chappel[1], Andrew H. Altieri[1], Todd Z. Osborne[3], David Tomasko[4], Marcus W. Beck[5] and Edward Sherwood[5]

[1]Department of Environmental Engineering Sciences, Engineering School of Sustainable Infrastructure and Environment, University of Florida, Gainesville, FL, United States, [2]School of Forest, Fisheries, and Geomatics Sciences, Institute of Food and Agricultural Sciences, University of Florida, Gainesville, FL, United States, [3]The Whitney Laboratory for Marine Bioscience, University of Florida, St. Augustine, FL, United States, [4]Sarasota Bay Estuary Program, Sarasota, FL, United States, [5]Tampa Bay Estuary Program, St. Petersburg, FL, United States

Introduction: Cultural eutrophication threatens numerous ecological and economical resources of Florida's coastal ecosystems, such as beaches, mangroves, and seagrasses. In April 2021, an infrastructure failure at the retired Piney Point phosphorus mining retention reservoir garnered national attention, as 814 million liters of nutrient rich water were released into Tampa Bay, Florida over 10 days. The release of nitrogen and phosphorus-rich water into Tampa Bay – a region that had been known as a restoration success story since the 1990s – has highlighted the potential for unexpected challenges for coastal nutrient management.

Methods: For a year after the release, we sampled bi-weekly at four sites to monitor changes in nutrients, stable isotopes, and phytoplankton communities, complemented with continuous monitoring by multiparameter sondes. Our data complement the synthesis efforts of regional partners, the Tampa Bay and Sarasota Bay Estuary Programs, to better understand the effects of anthropogenic nutrients on estuarine health.

Results: Phytoplankton community structure indicated an initial diatom bloom that dissipated by the end of April 2021. In the summer, the bay was dominated by *Karenia brevis*, with conditions improving into the fall. To determine if there was a unique carbon (C) and nitrogen (N) signature of the discharge water, stable isotope values of carbon ($\delta^{13}C$) and nitrogen ($\delta^{15}N$) were analyzed in suspended particulate material (SPM). The $\delta^{15}N$ values of the discharge SPM were –17.88‰ $\pm$ 0.76, which is exceptionally low and was unique relative to other nutrient sources in the region. In May and early June of 2021, all sites exhibited a decline in the $\delta^{15}N$ values of SPM, suggesting that discharged N was incorporated into SPM after the event. The occurrence of very low $\delta^{15}N$ values at the reference site, on the Gulf Coast outside of the Bay, indicates that some of the discharge was transported outside of Tampa Bay.

Discussion: This work illustrates the need for comprehensive nutrient management strategies to assess and manage the full range of consequences associated with anthropogenic nutrient inputs into coastal ecosystems. Ongoing and anticipated impacts of climate change – such as increasing tropical storm intensity, temperatures, rainfall, and sea level rise – will exacerbate this need.

KEYWORDS

phosphogypsum, stable isotopes, phytoplankton, harmful algal bloom, carbon, nitrogen, Piney Point

1. Introduction

Cultural eutrophication and climate change are two of the most important threats to the health and sustainability of coastal ecosystems around the world (Nixon, 1995; Hoegh-Guldberg and Bruno, 2010; Doney et al., 2012). From an algal perspective, cultural eutrophication has elevated the potential for harmful algal blooms (HABs; Cloern, 2001; Paerl et al., 2006; Heisler et al., 2008; Glibert, 2020; Gobler, 2020). Current trends in climatic conditions are exacerbating the challenges associated with eutrophication due to increases in temperature, changes in rainfall patterns, and increases in the intensity of tropical storms (Webster et al., 2005; Oneil et al., 2012; Wetz and Yoskowitz, 2013; Glibert et al., 2014; Griffith and Gobler, 2020; Phlips et al., 2020). One of the potential mechanisms for the combined impacts of eutrophication and climate change is the disruption of engineered structures associated with water treatment and retention (Lehner et al., 2011; Beusen et al., 2015; Grill et al., 2015; Maavara et al., 2015). Accidental or unavoidable discharges from compromised infrastructure can expose surrounding aquatic environments to excessive nutrient, algal and pollutant loads that negatively affect water quality, including elevated risks for HABs (Sin et al., 2013; Phlips et al., 2020; Herren et al., 2021; Metcalf et al., 2021). In this study, we examined an emergency release of water from a retired phosphorus mining reservoir into Tampa Bay, Florida and evaluated changes in water quality and algal populations in the Bay a year after the event.

Tampa Bay was designated as an impaired coastal waterbody in the 1980s, in part because of widespread losses of seagrasses. Subsequent restoration efforts and targeted nutrient management strategies resulted in successful restoration of seagrass habitats by the end of the century (Yates et al., 2011; Greening et al., 2014; Sherwood et al., 2017; Tomasko et al., 2018; Beck et al., 2019; DeAngelis et al., 2020; Tomasko et al., 2020). Despite these successes, nutrient management is an ongoing challenge due to increased development, reclaimed water usage, and septic and industrial activities adjacent to the Bay. Recently, higher shallow water temperatures and relatively high, sustained hydrologic inputs potentially linked to climate change drivers may also be confounding nutrient management efforts (Tampa Bay Nitrogen Management Consortium (TBNMC), 2022). During the 2016–2022 period, significant seagrass coverage was lost according to aerial photography estimates (>25% decline from 2016 peak coverage, or > 11,000 acres of seagrass coverage loss; SWFWMD, unpublished data). In addition to this recent bay-wide and regional seagrass loss, water quality declines in the northern portion of the bay (Old Tampa Bay) have occurred, and unexpected events, such as periodic releases of industrial process water, have caused further management challenges (Tampa Bay Estuary Program, 2022).

In late March 2021, an impaired liner at a decommissioned fertilizer facility (Piney Point) prompted the emergency release of 814 million liters of process water mixed with dredge water into the Bay, from March 30th to April 9th, 2021 (Nelson et al., 2021; Beck et al., 2022). The discharge water was high in inorganic nutrients, specifically ammonium and orthophosphate, prompting concerns that this pulse of nutrients might result in increased primary productivity, including phytoplankton, macroalgae and HABs, with adverse effects to seagrass meadows and other coastal habitats. Initial analyses soon after the event determined that there was a localized diatom bloom, and that the excess nutrients within the bay may have exacerbated the development of a red tide (*Karenia brevis*) bloom that was transported into the Bay (Beck et al., 2022).

While the initial effects of the discharge have been reported, the long-term effects on water quality and phytoplankton community structure have not yet been investigated. Here, we further investigate the fate of nutrients released from Piney Point and characterize the water quality conditions and phytoplankton community composition for the year following the event. We hypothesized that the initial pulse of inorganic nutrients was readily utilized by phytoplankton communities. This likely led to internal cycling of Piney Point-derived nutrients within the Bay, although other mechanisms, such as the deposition of nutrients into bay sediments and transport of nutrients outside of the bay were also likely important mechanisms influencing the fate of nutrients discharged from the facility. To evaluate this hypothesis, we monitored changes in water column nutrients, *in situ* water quality parameters, stable isotopes of carbon (C) and nitrogen (N) in suspended particulate material (SPM), chlorophyll *a* concentrations, and phytoplankton community structure over the course of a year after the event.

Our year-long monitoring campaign confirmed there was an initial diatom bloom adjacent to the location of the discharge that dissipated by the end of April 2021, as previously described in Beck et al. (2022), and revealed that elevated diatom biomass was more extensive than previously recognized as it extended to back bay regions. During the summer, the site adjacent to Piney Point had high *K. brevis* biomass (3 mg C L^{-1}), which then declined into the fall. We found that the stable isotope values of C and N ($\delta^{13}C$ and $\delta^{15}N$) of the discharge water SPM were-15.23‰ ± 0.53 and-17.88‰ ± 0.76, respectively. A $\delta^{15}N$ value of-17.88‰ is exceptionally low and was unique relative to other nutrient sources in the region, likely due to isotopic fractionation associated with ammonium assimilation within the reservoir. In May and early June of 2021, all sites in the discharge region exhibited a sharp decline in the $\delta^{15}N$ values of SPM, suggesting that discharge N was incorporated into SPM after the event, which may have been driven either by phytoplankton uptake of N and/or N sorption onto particulate material in the bay. This was further supported by concomitant declines in C:N values. After mid-June 2021, $\delta^{15}N$ values generally returned to April 2021 values. This study found that phytoplankton communities and water quality were altered by the Piney Point event and that these dynamics can be influenced by tropical storms, highlighting the synergistic effects between disruptions of engineered structures and periodic events such as storms, which are predicted to increase in intensity due to climate change (Webster et al., 2005; Wetz and Yoskowitz, 2013).

2. Methods

2.1. Site description

Four sites were selected in consultation with the Tampa Bay Estuary Program (TBEP) and the University of South Florida's Tampa Bay Coastal Ocean model (Chen et al., 2018, 2019). The sites included: one site proximal to Piney Point Creek, which is connected to the Piney Point facility *via* drainage canals (hereafter referred to as Piney Point), two back bay regions that were located south of the discharge location and forecast to have longer residence times (Bishop Harbor and Joe Bay), and one reference site outside of the Bay (St. Joseph Sound; Figure 1). All sites were located adjacent to TBEP seagrass monitoring transects (Beck et al., 2022) and had depths that varied with the tidal cycle, but generally ranged from 1–3 m. One of the back

bay regions (Bishop Harbor) was the site of previous releases from the Piney Point facility (Garrett et al., 2011; Switzer et al., 2011), and the reference site was outside of the Bay, at a relatively pristine location with healthy seagrass meadows (Tomasko et al., 2020). For this event, emergency releases were conveyed directly into Tampa Bay in the vicinity of Port Manatee from March 30th to April 9th 2021, while an uncontrolled discharge to Piney Point creek occurred from March 30th to April 3rd, 2021 (Florida Department of Environmental Protection, 2021; Figure 1).

Water samples were collected on a bi-weekly basis from April 2021 until April 2022. At each site, water samples were collected from surface to near bottom (to avoid collection of bottom material) on a near bi-weekly basis using a depth-integrated pole sampling method (Phlips et al., 2010) to minimize any bias from water column stratification. Water samples were collected for total and dissolved nutrients, suspended particulate material (SPM), chlorophyll *a*, and phytoplankton community analyses, as described below. In addition to bi-weekly water samples, a discharge water sample was collected on April 7th, 2021, and processed as described for other water samples.

FIGURE 1
(A) Location of the Piney Point facility and study sites within and outside Tampa Bay. **(B)** Lower bay sites and their location in relationship to Piney Point and the discharge locations. Discharges occurred at Port Manatee from March 31st to April 9th, and at Piney Point Creek until April 3rd. Sites are marked with yellow points, locations of interest are marked with red points.

An additional sample collection was conducted in October 2021 at the southern holding pond where the initial liner tear occurred to evaluate seasonal changes in reservoir characteristics and efforts to employ innovative treatment technologies within the remaining wastewater held at the facility following the emergency release. All samples were transported on ice and either refrigerated or frozen until analyzed.

2.2. Chlorophyll *a* and phytoplankton analyses

Water samples were collected and filtered for chlorophyll *a* analysis in the field. Phytoplankton were filtered onto 0.7-µm Whatman glass fiber filter and stored in a dark container at −20°C. Chlorophyll *a* was solvent extracted (Sartory and Grobbelaar, 1984) and measured spectrophotometrically according to Standard Methods (American Public Health Association, 2005).

Integrated, whole water samples were preserved on-site with Lugol's solution (American Public Health Association, 2005) and analyzed microscopically for phytoplankton abundance and species composition. General phytoplankton abundance and composition were determined using the Utermöhl method (Utermohl, 1958), as described in Badylak et al. (2014). Samples preserved in Lugol's were settled in 19 mm diameter cylindrical chambers. Phytoplankton cells were identified and counted at 400× and 100× with a Leica phase contrast inverted microscope. At 400×, a minimum of 100 cells of a single taxon and 5 grids were counted. If 100 cells were not counted by 30 grids, up to a maximum of 100 grids were counted until 100 cells of a single taxon were reached. At 100×, a total bottom count was completed for taxa >30 µm in size.

Picocyanobacteria abundances were determined using a Zeiss Axio compound microscope, using green and blue light excitation (Fahnenstiel and Carrick, 1992; Phlips et al., 1999). Samples were preserved with buffered glutaraldehyde. Subsamples of water were filtered onto 0.2 µm Nucleopore filters and mounted between a microscope slide and cover slip with immersion oil and picoplankton counted at 1000x magnification.

Count data were converted to phytoplankton biovolume, using the closest geometric shape method (Smayda, 1978; Sun and Liu, 2003). Phytoplankton C values (as mg C L^{-1}) were estimated by applying conversion factors for different taxonomic groups to biovolume estimates (expressed as $10^6 \mu m^3 mL^{-1}$): i.e., 0.065 × biovolume of diatoms, 0.22 x biovolume for cyanobacteria, and 0.16 × biovolume for dinoflagellates or other taxa (Strathmann, 1967; Ahlgren, 1983; Sicko-Goad et al., 1984; Verity et al., 1992; Work et al., 2005).

2.3. *In situ* measurements

A YSI EXO2 multiparameter sonde was deployed at each of the four study sites on April 16th, 2021, soon after the discharge ceased on April 9th. Deployment depth ranged from 1–3 m, depending on the site. Sondes continuously measured salinity, optical dissolved oxygen (DO), *in situ* chlorophyll, phycoerythrin (PE), fluorescent dissolved organic matter (fDOM), specific conductivity, temperature, pH, total dissolved solids, turbidity, and total suspended solids every 10 min. The average value for each day is reported here. Sondes were

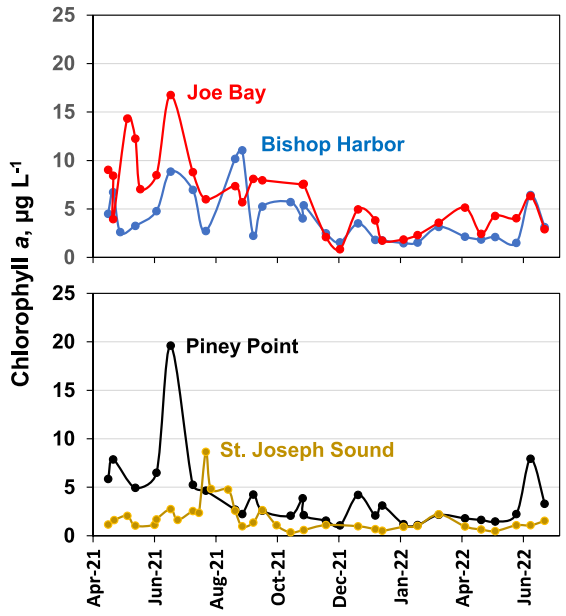

FIGURE 2
Chlorophyll *a* concentrations (μgL^{-1}) at the three lower bay sampling sites (i.e., Bishop Harbor, Joe Bay, and Piney Point), and reference site (i.e., St. Joseph Sound).

inspected on a bi-weekly basis, with maintenance and calibration occurring every ~3 weeks, or sooner if needed, according to the manufacturer's instructions. Data were downloaded from sondes during bi-weekly sampling trips using KorEXO software. Data from April 16th, 2021 to May 5th, 2022 were aggregated and cleaned for this study using R version 4.1 (R Core Development Team, 2008). Values that were out of sensor range were flagged and removed from the dataset prior to analysis. For all parameters, approximately 1% or less of the values were out of range, except for *in situ* chlorophyll where 9.8% of the values were out of range.

2.4. Dissolved and particulate samples

Water samples collected for total phosphorus (TP) and total Kjeldahl nitrogen (TKN) were acidified to a pH of 2 in the field prior to analysis and analyzed within 28 days according to EPA Method 365.1 and 353.2, respectively. Water samples for ammonium-N (NH_4-N) and nitrate + nitrite (NO_x) analyses were 0.2 μm filtered and acidified to a pH of 2 in the field and analyzed within 28 days according to EPA Method 350.1. Water samples for total orthophosphate (orthoP) were not acidified and were analyzed within 48 h according to EPA Method 365.1. All nutrient analyses were certified and conducted at the University of Florida's Analytical Research Laboratory, a National Environmental Laboratory Accreditation Program (NELAP) certified facility. Values below the minimum detection limit were set to NA prior to analysis.

Suspended particulate material was collected on pre-combusted, pre-weighed glass fiber filters (GF/F), frozen and then freeze dried. Filters were then placed into tin capsules for elemental (total carbon (TC) and total nitrogen (TN)) and stable isotope ($\delta^{13}C$, $\delta^{15}N$) analysis. Elemental and stable isotope analyses were conducted at the University of Florida's Stable Isotope Laboratory, using a Carlo Erba 1500 CN elemental analyzer coupled to a Thermo Electron DeltaV Advantage isotope ratio mass spectrometer (Carlo Erba/ThermoFisher Scientific™, Waltham, MA, United States). Stable isotope ratios are reported for $\delta^{13}C$ and $\delta^{15}N$ in standard delta notation (‰) relative to Vienna Pee Dee Belemnite (VPDB) and atmospheric N_2 standards, respectively. Total carbon and TN are reported on a percent mass basis. The C:N ratio is reported as the mass ratio, i.e., weight %TC ÷ weight %TN.

2.5. Data analysis

Data analysis was conducted in R version 4.1 (R Core Development Team, 2008). Grab sample values (i.e., chlorophyll *a*, phytoplankton, elemental analysis and isotope values) were averaged by location and month, while *in situ* sonde measurements were averaged by location and day. Trends in these values were then examined to elucidate the timing of maximum and minimum values relative to the emergency release and Tropical Storm Elsa, as well as variation between sites and relative to published values. Analysis scripts are available at the following GitHub repository.[1]

3. Results

3.1. Chlorophyll *a* concentrations and total phytoplankton biomass

Chlorophyll *a* concentrations were used as one of the indicators of phytoplankton biomass. Overall temporal trends in chlorophyll *a* concentrations were similar at the three lower bay sampling sites, with concentrations mostly over 5 μg L^{-1} from April through August 2021 (Figure 2), exceeding an annual average lower bay management target of 4.6 μg L^{-1} (Tampa Bay Estuary Program, 2022). Peaks in chlorophyll *a* during the latter period of April–August reached values up to 20 μg L^{-1} at Piney Point. After summer, chlorophyll *a* declined to below 5 μg L^{-1} through the end of the study period, with a few exceptions. By contrast, chlorophyll *a* concentrations at the St. Joseph Sound reference site were consistently below 3 μg L^{-1} except for moderately elevated concentrations in July and August of 2021, coincident to red tide blooms that extended along the Southwest Florida coast during this time. Lower Tampa Bay values exceeded the 2006 to 2020 long-term median chlorophyll *a* value of lower Tampa Bay, which was 3.1 μg L^{-1} (min 2.3 μg L^{-1}, max 3.5 μg L^{-1}; Beck et al., 2022), but values of the reference site were similar to the long-term median value of the Lower Tampa Bay (3.1 μg L^{-1}).

On April 7th, 2021, emergency release water was dominated by a spherical single-celled green alga (Chlorophyta). Cell density of the green alga was 3.4 × 10^8 cells L^{-1}, and biomass was 2.34 mg C L^{-1}, almost an order of magnitude higher than the mean biomass for the study period in the Piney Point nearshore basin which was 0.36 mg C L^{-1}. The discharge sample also contained several other species of

1 https://github.com/elisemorrison/PineyPoint2021

nanophytoplankton, but the biomass contributions of these taxa were minor, i.e., < 0.02 mg C L^{-1}.

The time-series of total phytoplankton biomass for the three lower bay sampling sites (i.e., Piney Point, Bishop Harbor, and Joe Bay) from April 9th, 2021, through May 2022 exhibited similar temporal patterns, with elevated levels in the late Spring of 2021, with peaks near, or over, 1.5 mg C L^{-1} (Figure 3). In mid-summer, biomass levels declined, and remained near, or below, 0.5 mg C L^{-1} through the end of the study period in May 2022. The reference site in St. Joseph Sound had modestly elevated total biomass in June and July, with peaks near 0.5 mg C L^{-1}, then remained below 0.3 mg C L^{-1} for the rest of the study period. Mean total phytoplankton biomass values for the study period were similar across the three lower bay sampling sites, while the reference site exhibited the lowest value – although statistically it could not be differentiated from the Bishop Harbor or Piney Point sites (Table 1).

3.2. Phytoplankton composition

The initial peaks in phytoplankton biomass at the Bishop Harbor, Joe Bay and Piney Point sites in May 2021 were dominated by diatoms (Figure 3). Three diatom taxa, *Leptocylindrus minimus*, *Leptocylindrus danicus*, and *Cerataulina pelagica,* dominated the initial peak period in terms of biomass (Table 2). The subsequent major peak in biomass at the Piney Point site in June was dominated by the toxic dinoflagellate *Karenia brevis* and reached 3 mg C L^{-1}. The more modest peaks in biomass at St. Joseph Sound in May and June of 2022 were dominated by dinoflagellates, including *K. brevis* in June. After July 2022, the Bishop Harbor, Joe Bay, and Piney Point sites showed variability in dominant taxa, with periods of supremacy by all four major phytoplankton groups, i.e., dinoflagellates, diatoms, cyanobacteria (primarily picocyanobacteria), and "other" taxa (most prominently nanophytoplankton, such as cryptophytes; Figure 3; Table 2).

Over the study period, mean biomass of diatoms were higher than dinoflagellates, cyanobacteria and "other" taxa at Bishop Harbor and Joe Bay (Table 1). At Piney Point, mean dinoflagellate and diatom biomass was higher than cyanobacteria and "other" taxa. At St. Joseph Sound, there were no significant differences in mean biomass of the four phytoplankton groups. In terms of regional differences within each phytoplankton group, mean dinoflagellate and cyanobacteria biomass levels across all the sites were not significantly different, despite the high mean value of dinoflagellates at the Piney Point site (Table 1). The apparent anomalously high annual mean at Piney Point reflects the effect of exceptionally high biomass of *K. brevis* in June on the mean. Joe Bay had a significantly higher mean diatom biomass than at St. Joseph Sound. For "other" taxa, Joe Bay had the highest mean biomass and St. Joseph Sound had the lowest mean biomass.

To examine more specific differences in taxonomic composition at the reference and lower study sites, a comparison was made of the individual taxa that accounted for the top 10% of biomass observations in the two regions, which roughly represented the Top-50 taxa observations at the St. Joseph Sound (reference site), and the Top-150 taxa observations for the combined results from the Bishop Harbor, Joe Bay and Piney Point sites (lower bay sites; Table 2). There were several key similarities, including the strong representation of cyanobacteria on both lists, and many similarities in the list of dinoflagellate species, including the prominence of the HAB species *Karlodinium veneficum* and *K. brevis*. These similarities fall in line with the lack of significant differences between sites for mean values of cyanobacteria and dinoflagellates biomass over the study period (Table 1). By contrast, for diatoms, there was a wider range of species and higher biomass values for the lower bay sites than the reference site (Table 2). The Top-150 list for the lower bay sites was led by spherical picoplanktonic cyanobacteria, other undefined small nanoplanktonic eukaryotes and the euryhaline cosmopolitan diatom species *Skeletonema costatum, L. danicus* and *Rhizosolenia setigera*, in terms of frequency on the list (Table 2). In terms of highest biomass observations, the dinoflagellate *K. brevis*, and the diatoms *L. minimus*, *L. danicus*, *Guinardia delicatula, Skeletonema costatum*, and *C. pelagica* led the Top-150 list, with peak biomass values greater than 0.40 mg C L^{-1}.

The Top-50 list for the St. Joseph Sound reference site was led by spherical picoplanktonic cyanobacteria, other undefined small nanoplanktonic eukaryotes, and the dinoflagellate *Karlodinium veneficum*, in terms of frequency on the list (Table 2). for the three primary sampling sites. In terms of highest biomass observations in the Top-50 list for the St. Joseph Sound reference site, only *K. brevis* had a peak value similar to that encountered in the Top-150 list, i.e., 0.25 mg C L^{-1}.

Another feature of the Top-50 and Top-150 lists of highest biomass observations was the presence of known HAB species, most of which are potential producers of toxins (Lassus et al., 2015; Table 2). The largest number of HAB species for both lists were dinoflagellates. *K. veneficum, K. brevis*, *Takayama* sp. and *Akashiwo sanguinea* were near the top of both lists in terms of HAB species. *K. brevis* had the highest peak biomass for HAB species in both lists, with a peak of 2.71 mg C L^{-1} (i.e., 3.9 million cells L^{-1}) on the Top-150 list, which represents a major bloom. The potentially toxic filamentous nitrogen-fixing cyanobacterium *Trichodesmium erythraeum* and pennate diatom *Pseudo-nitzschia* sp. were on both lists. *Karenia brevis* was the only HAB species that reached major levels of concern in terms of harmful impact during this study period.

3.3. Total and dissolved nutrients

On April 6th, 2021, the water discharged from the facility was dominated by inorganic nutrients, namely ammonium-N (210 mg L^{-1}) and orthophosphate (140 mg L^{-1}), with NO_x concentrations of 0.004 mg L^{-1} (Supplementary Table 1; Beck et al., 2022). All sites exhibited their greatest orthoP values in April 2021, with lower orthoP concentrations seen at sites further from the discharge site at that time (Supplementary Tables 1, 2). OrthoP values were greater in April 2021 when compared to April 2022 for all sites. All sites also exhibited their highest average total P values in April 2021 and had lower TP values in April 2022 when compared to April 2021, except for the reference site St. Joseph Sound. St. Joseph Sound had slightly lower total P values in April 2021 (11.38 µg L^{-1}) when compared to April 2022 (13.71 µg L^{-1}). For all sites, ammonium-N was highest in the first 5 months after the event, and in January 2022 with concentrations peaking in June and July of 2021 and in January 2022. Average monthly ammonium-N values in the lower Tampa Bay sites were from 0.14 mg L^{-1} (Piney Point and Bishop Harbor) to 0.17 mg L^{-1} (Joe Bay). Generally, NO_x was not detectable at our sites (Supplementary Tables 1, 2).

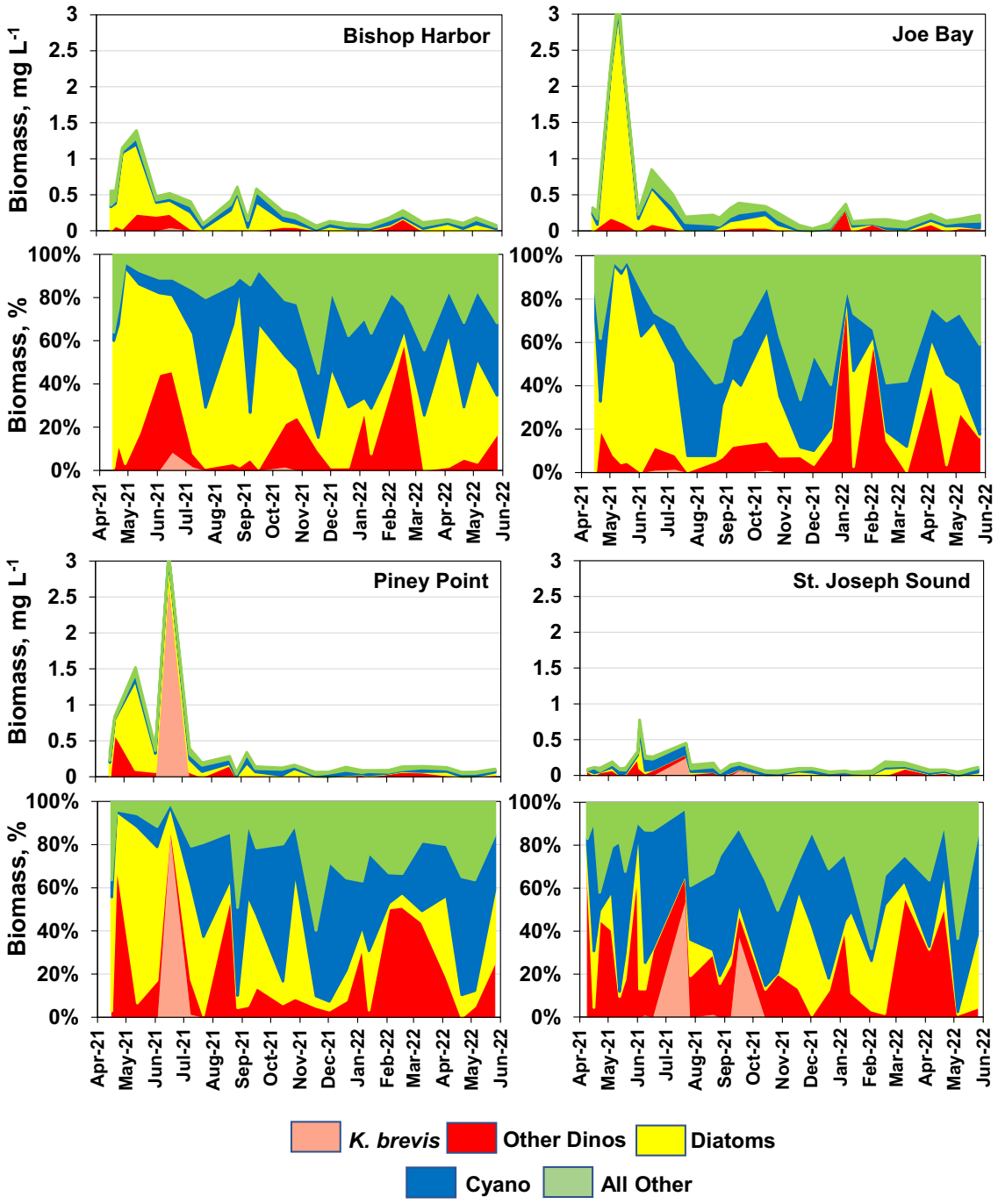

FIGURE 3
Time series of phytoplankton biomass (mg carbon L^{-1}) for the four core sites, i.e., Bishop Harbor, Joe Bay, Piney Point, and St. Joseph Sound (reference site). Time series are divided into four phytoplankton groups, dinoflagellates (red), diatoms (yellow), cyanobacteria (blue), and all "other" taxa (green). Bottom panels for each site show relative (%) contribution of each group to total biomass.

3.4. *In situ* measurements

For *in situ* measurements, there were distinct differences between the study sites. Salinity was consistently higher at the reference site, St. Joseph Sound (lowest 27.04 psu in mid-February 2022 and highest in early June 2021 34.96 psu) relative to the lower bay sites (0.66 to 34.94 psu). Salinity was highest at the beginning of the study period (Figure 4A), particularly for Piney Point and Bishop Harbor, which are further into the Bay. Joe Bay (closer to the mouth of Tampa Bay), and St. Joseph Sound (reference site) had increases in salinity through May and June 2021, then a decline in salinity in June and July 2021. Joe Bay's salinity was lowest in mid-August 2021 (24.70 psu), and greatest in mid-June 2021 (34.94 psu). Piney Point's salinity was lowest in early July 2021 (16.98 psu), likely due to Tropical storm Elsa, and greatest in early June 2021 (33.13 psu). Bishop Harbor's salinity dipped in October 2021 to 0.66 psu, and its highest salinity was at the end of May 2021 (34.47 psu; Figure 4A).

TABLE 1 Mean biomass of four groups of phytoplankton (i.e., dinoflagellates, diatoms, cyanobacteria and all "other" taxa) at the four sampling sites (i.e., Bishop Harbor, Joe Bay, Piney Point and St. Joseph Sound) over the entire study period.

Phytoplankton	Mean Biomass, μg carbon L^{-1}			
Group	Bishop Harbor	Joe Bay	Piney Point	St. Joseph Sound
Dinoflagellates	0.050 b	0.055 b	0.168 a	0.048 a
	(0.015)	*(0.014)*	*(0.113)*	*(0.013)*
	A	A	A	A
Diatoms	0.192 a	0.329 a	0.115 a	0.035 a
	(0.054)	*(0.143)*	*(0.050)*	*(0.018)*
	AB	A	AB	B
Cyanobacteria	0.050 b	0.048 b	0.044 b	0.045 a
	(0.005)	*(0.005)*	*(0.005)*	*(0.008)*
	A	A	A	A
Other Taxa	0.054 b	0.085 b	0.039 b	0.030 a
	(0.008)	*(0.010)*	*(0.005)*	*(0.003)*
	B	A	BC	C
Total	0.347	0.516	0.366	0.159
	(0.065)	(0.153)	(0.131)	(0.027)
	AB	A	AB	B

Standard errors are shown in parentheses. The results of Duncan multiple range tests are shown as letters associated with the mean values. Capital letters relate to statistical differences between mean values for a phytoplankton group at each of the four sampling sites. A comparison of mean values for total phytoplankton biomass at the four sampling sites is shown at the bottom of the Table. Lower case letters relate to differences in mean values for the four phytoplankton groups at each site. Mean values with the same letter designation are not significantly different.

Dissolved oxygen (DO) was greatest at the reference site, St. Joseph Sound, and at Piney Point, while DO was lower in the back bay sites (Figure 4B). DO values tended to be lowest in mid- to late summer of 2021 and were highest from December 2021 to February 2022. All sites exhibited a slight decline in DO into the summer, and experienced increases in DO starting in October 2021, with a peak in DO in early 2022. The lowest daily mean DO at Bishop Harbor was at the end of September 2021 (1.52 mg L^{-1}) and greatest in early February 2022 (8.98 mg L^{-1}). The lowest DO at Joe Bay was in mid-June (3.45 mg L^{-1}) and highest in December 2021 (8.63 mg L^{-1}). The lowest DO at Piney Point was at the end of June (4.64 mg L^{-1}) and greatest in early July 2021 (10.27 mg L^{-1}; Figure 4B), at the time of peak *K. brevis* blooms in the Bay. The lowest DO at the reference site St. Joseph Sound was at the end of September 2021 (4.06 mg L^{-1}) and greatest in February 2022 (9.90 mg L^{-1}).

In situ chlorophyll was consistently higher when compared to extracted chlorophyll *a* (described above), and was greatest at Joe Bay and Piney Point, both of which exhibited an increase in June and July 2021. In general, sites exhibited the greatest *in situ* chlorophyll values in mid-summer 2021, during the period of peak *K. brevis* blooms, and lowest values in the late fall and winter (Figure 4C). At Bishop Harbor, *in situ* chlorophyll was greatest in early September 2021 (24.99 μg L^{-1}), and lowest in late December 2021 (0.59 μg L^{-1}). At Joe Bay, the greatest *in situ* chlorophyll values were in late June 2021 (36.96 μg L^{-1}), and the lowest values were in early December 2021 (0.95 μg L^{-1}). At the Piney Point site, the greatest *in situ* chlorophyll was in early July 2021 (30.21 μg L^{-1}), and the lowest values were in mid-December 2021 (2.55 μg L^{-1}). At St. Joseph Sound, the greatest *in situ* chlorophyll values were in mid-July 2021 (24.4 μg L^{-1}), and the lowest values were in mid-October 2021 (0.03 μg L^{-1}).

Phycoerythrin (PE) was greatest at Piney Point and Joe Bay, which had spikes in PE in June and July of 2021 (Figure 4D). Similar to *in situ* chlorophyll, PE was greatest in mid-summer 2021, corresponding with *K. brevis* blooms in the region, and lowest in the winter months. At Bishop Harbor, PE was greatest in early September 2021 (15.55 relative fluorescent units [RFU]) and lowest in late November 2021 (0.63 RFU). At Joe Bay, PE was greatest in mid-June 2021 (15.81 RFU) and lowest in early December (0.69 RFU). At Piney Point, PE was greatest in early July (14.74 RFU) and lowest in mid-May (1.32 RFU). At St. Joseph Sound, the greatest PE values were in mid-July (9.74 RFU), and lowest values were in mid-December (0.05 RFU).

Florescent dissolved organic matter (fDOM) was consistently higher in the back bay sites Bishop Harbor and Joe Bay, and lowest in the reference site, St. Joseph Sound. All lower bay sites exhibited an increase in fDOM in late July 2021 (Supplementary Figure 1). At Bishop Harbor the lowest value was early October 2021 (10.97 quinine sulfate units [QSU]) and greatest in mid-August 2021 (54.54 QSU). Joe bay was lowest in March 2022 (0.67 QSU) and highest in late July (42.84 QSU). Piney Point was lowest in mid-April 2022 (15.11 QSU) and greatest in mid-August 2021 (55.84 QSU). St. Joseph Sound was lowest in mid-December 2021 (5.15 QSU) and greatest in mid-October 2021 (22.34 QSU).

Patterns of turbidity varied by region (Supplementary Figure 1). The turbidity at Bishop Harbor was lowest in mid-August 2021 [0.31 formazin nephelometric units (FNU)] and greatest in early September 2021 (22.71 FNU), which coincided with higher *in situ* chlorophyll and PE values. The turbidity at Joe Bay was lowest in late January 2022 (0.70 FNU) and greatest in mid-September 2021 (42.59 FNU). Piney Point had the lowest turbidity in mid-August 2021 (0.41 FNU) and greatest in late November 2021 (68.12 FNU). St. Joseph Sound had the lowest turbidity in mid-October 2021 (0.29 FNU) and greatest in mid-July 2021 (82.76 FNU).

3.5. Suspended particulate material

The discharge water SPM had an exceptionally depleted $\delta^{15}N$ value of −17.88‰ ± 0.76, and a $\delta^{13}C$ value of −15.23‰ ± 0.53. Stable isotope values were determined with a precision of 0.05‰ and 0.09‰ for $\delta^{15}N$ and $\delta^{13}C$, respectively. The total nitrogen (TN) of the discharge water SPM was 2.8% ± 0.1, and total carbon (TC) was 11.9% ± 0.5, with a C:N ratio of 4.3 ± 0.2. The SPM of the reservoir water in October had similarly low $\delta^{15}N$ and $\delta^{13}C$ values as the discharge water from April, −19.15‰ ± 0.05 and −13.44 ‰ ± 0.03, respectively. Differences between the SPM from April discharge and October reservoir samples are likely due to the fact that on-site treatment technologies were being employed at the site since April 2021.

The greatest particulate TC values (2.88–3.77%) were seen in April 2021 for three of the four sites and then declined over the course of the study period (Figure 5A). The only exception was Piney Point, which

10.3389/fevo.2023.1144778

TABLE 2 List of Top-50 individual biomass observations for individual taxa over the study period at the reference site, St. Joseph Sound (top panel), and Top-150 for the combined record for the three lower bay sites, i.e., Bishop Harbor, Joe Bay, and Piney Point (bottom panel).

Reference site – St. Joseph Sound				
		Frequency	Biomass range	Max. #Cells
Species	Group	Top-50	Carbon mg L^{-1}	10^3 cells L^{-1}
Cryptophyte spp.	Cryptophytes	3	0.02–0.03	3,537
Spherical picocyanobacteria spp.	Cyanobacteria	15	0.03–0.16	894,902
Synechococcus spp.		2	0.02–0.04	116,726
*Trichodesmium erythraeum**		1	0.05	5
Leptocylindrus danicus	Diatoms	3	0.04–0.08	362
Chaetoceros sp.		2	0.04–0.13	2,181
Amphora/Entomoneis sp.		2	0.02–0.11	907
Chaetoceros wighamii		1	0.09	15,600
Pseudo-nitzschia sp.*		1	0.04	3,265
Thalassionema bacillare		1	0.02	181
*Karlodinium veneficum**	Dinoflagellates	5	0.02–0.16	635
*Karenia brevis**		2	0.07–0.25	355
*Akashiwo sanguinea**		2	0.03–0.06	8
Takayama sp.*		1	0.06	181
Protoperidinium brevipes		1	0.06	91
Gyrodinium pingue		1	0.03	91
*Prorocentrum texanum**		1	0.03	9
*Prorocentrum minimum**		1	0.02	91
Nanoplankton spp. (2 µ–5 µ) (UD)	Nanophytoplankton	5	0.02–0.05	15,238
		Biomass range in top-50: 0.02–0.25		
Primary sites – Bishop Harbor, Joe Bay, and Piney Point				
		Frequency	Biomass range	Max. #Cells
Species	Group	Top-150	Carbon mg L^{-1}	10^3 cells L^{-1}
Cryptophyte spp.	Cryptophytes	3	0.04–0.05	5,351
Spherical picocyanobacteria	Cyanobacteria	32	0.05–0.16	894,902
*Trichodesmium erythraeum**		1	0.05	5
Rhizosolenia setigera	Diatoms	9	0.06–0.12	2,902
Skeletonema costatum		7	0.19–0.42	29,568
Leptocylindrus danicus		7	0.08–0.73	3,325
Chaetoceros sp.		5	0.05–0.06	3,627
Dactyliosolen fragilissimus		4	0.08–0.36	3,265
Cerataulina pelagica		4	0.07–0.42	2,358
Guinardia delicatula		4	0.05–0.61	1995
Leptocylindrus minimus		3	1.05–1.95	132,393
Amphora/Entomoneis sp.		3	0.06–0.11	907
Pennate diatom sp.		3	0.05–0.07	12,879
Bellerochea horologicalis		2	0.04–0.05	9
Coscinodiscus sp.		1	0.14	2
Chaetoceros wighamii		1	0.09	15,600
Cyclotella choctawhatcheana		1	0.08	28,117
Thalassionema bacillare		1	0.08	605
Chaetoceros costatus		1	0.07	726
Grammatophora marina		1	0.07	181
Rhabdonema adriaticum		1	0.07	11
Chaetoceros danicus		1	0.05	605
Pseudo-nitzschia sp.*		1	0.04	3,265

(Continued)

TABLE 2 (Continued)

Primary sites – Bishop Harbor, Joe Bay, and Piney Point				
		Frequency	Biomass range	Max. #Cells
Species	Group	Top-150	Carbon mg L^{-1}	10^3 cells L^{-1}
*Karlodinium veneficum**	Dinoflagellates	17	0.05–0.19	726
*Karenia brevis**		4	0.04–2.71	3,847
Takayama sp.*		4	0.06–0.07	302
*Karenia mikimoto**		2	0.10–0.11	181
*Prorocentrum rhathymum**		2	0.06–0.34	94
*Akashiwo sanguinea**		2	0.06–0.27	31
Gymnoid sp.		2	0.06–0.09	2,720
Peridinium quinquecorne		1	0.2	181
*Prorocentrum texanum**		1	0.1	29
Protoperidinium brevipes		1	0.06	91
Nanoplankton spp. (2 µ–5 µ) (UD)	Nanophytoplankton	18	0.05–0.20	64,088
		Biomass range in top-150: 0.04–2.72		

Frequency of occurrence on the "Top" lists for each taxon are shown, along with the range of biomass values for the observations on the list, and the highest cell density observed for taxa on the lists. Taxa* with an asterisk are species on the IOC Harmful Algal Bloom list (Lundholm et al., 2009 onwards). "UD" indicates observations without a specific species identification.

exhibited its highest TC values (2.4% ± 1.3) in June 2021 coinciding with the *K. brevis* bloom in the bay and had its second highest TC in April 2021 (average 1.8% ± 0.5; max 2.6%), concurrent with the release from the Piney Point facility. The lowest TC values at Bishop Harbor and St. Joseph Sound site were seen in mid-July 2021 (0.2 ± 0.02%). A similar trend was seen in TN values, where Bishop Harbor and Joe Bay exhibited their greatest TN values in April 2021 (0.3–0.46%) Piney Point had its greatest particulate TN value in June 2021 (0.32% ± 0.10; Figure 5B). After early July 2021, sites exhibited a decline in particulate TN, with the exception of St. Joseph Sound, which exhibited an increase in particulate TN in August 2021, followed by a decline.

Over the study period, the lower Tampa Bay sites showed similar trends in C:N values, with all sites exhibiting a higher C:N value in April 2021, with a subsequent decline in C:N to a value of ~5 in June 2021 (Figure 5C). After June 2021, C:N values of the bay sites increased and then stabilized from July 2021 to April 2022. Patterns in C:N were slightly different at the reference site, St. Joseph Sound, which also had high C:N values in April 2021, and a subsequent decrease in June 2021. However, in July 2021 there was a decline in C:N at St. Joseph Sound, likely driven by an influx of N derived from the surrounding watershed in association with Tropical Storm Elsa's passing. Values then quickly increased and plateaued, until another decline in C:N was seen in January 2022 at St. Joseph Sound. The lower Tampa Bay sites also exhibited a slight decrease in C:N at this time, but to lesser degrees.

All sites exhibited similar trends from April to December 2021 for $\delta^{15}N$ in SPM (Figure 6A). Specifically, $\delta^{15}N$ values declined in all regions in May 2021, with values as low as −11.4‰ at Bishop Harbor, and −10.8‰ ± 0.02 at Piney Point, while the lowest average values at the reference site, St. Joseph Sound (−8.75‰ ± 10.8). and Joe Bay (−4.28‰ ± 7.7), were seen in June 2021. The decline in $\delta^{15}N$ values may be related to mixing and/or uptake of N from the Piney Point discharge since the SPM $\delta^{15}N$ value of the Piney Point discharge in April 2021 was −17.88‰ ± 0.76. Additionally, the Bishop Harbor and St. Joseph Sound sites had an increase in $\delta^{15}N$ values in January 2022, which coincided with a drop in C:N values, possibly driven by terrestrial inputs of N, or remineralization by macroalgae in the region.

In April 2021, $\delta^{13}C$ values were consistently low at all sites ranging from −26.1 ± 3.3 at St. Joseph Sound to −22.6‰ ± 0.9 at Joe Bay. An increase in $\delta^{13}C$ values was seen in May 2021 (Figure 6B), possibly driven by C input from SPM within the Piney Point discharge, which had $\delta^{13}C$ values ranging from −14.01 to −15.82‰.

4. Discussion

4.1. Initial phytoplankton response to the discharge

Temporal trends in phytoplankton composition and biomass offer insights into possible effects of the 2021 Piney Point discharge event on Tampa Bay proper. Chlorophyll *a* concentrations in the 3 months following the discharge period were significantly higher than the same period in the following year at all three Bay sites proximal to the source of the discharge (i.e., Bishop Harbor, Joe Bay, and Piney Point). At the reference site, St. Joseph Sound, outside of Tampa Bay proper, there was no major elevation of chlorophyll *a* concentrations during the 3 months directly after the discharge period, followed by moderately elevated concentrations in July and August of 2021, coincident with red tide blooms that extended along the Southwest Florida coast during this time. During the 3 months following the discharge, peak chlorophyll *a* values at our Tampa Bay sites fell within a range associated with meso-eutrophic coastal regions, i.e., > 10–20 µg L^{-1} (Hagy III et al., 2022). The latter chlorophyll levels (~20 µg L^{-1}) are common in the northeast region of upper Tampa Bay, which is subject to autochthonous HAB events, including blooms of the toxic dinoflagellate *Pyrodinium bahamense*, but are rare in the outer regions of the bay (Badylak et al., 2007). As such, the chlorophyll *a* values seen in the three months following

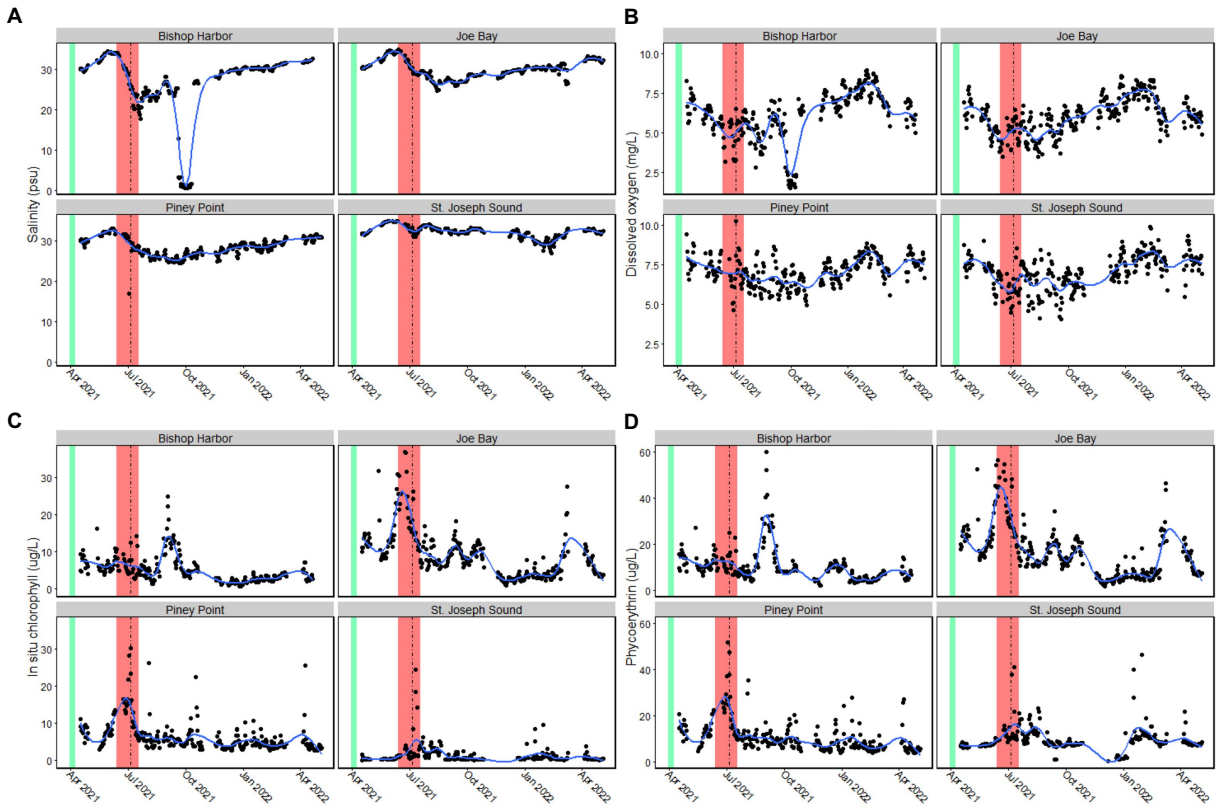

FIGURE 4
In situ measurements for daily means of **(A)** salinity (psu), **(B)** dissolved oxygen (mgL^{-1}), **(C)** *in situ* chlorophyll (μgL^{-1}), and **(D)** phycoerythrin (relative fluorescence units, RFU) over the course of the study. The Piney Point event (March 30th – April 9th, 2021) is denoted by the green line, the period with maximum (> 10^5 cells L^{-1}) *Karenia brevis* cell counts (Beck et al., 2022) is shown in the red box, and the date of tropical storm Elsa (July 5th, 2021) is shown with the vertical dashed black line. The smoothing line was generated using local polynomial regression fitting with a span of 0.175.

the discharge exceeded the long-term median and range of chlorophyll *a* values in lower Tampa Bay from 2006 to 2020, which was 3.1 μg L^{-1} and 2.3–3.5 μg L^{-1} (Beck et al., 2022), and exceeded the annual average lower bay management target of 4.6 μg L^{-1} (Tampa Bay Estuary Program, 2022). High chlorophyll *a* levels are encountered along the southwest coast of Florida during red tides of the toxic dinoflagellate *Karenia brevis* (Heil et al., 2014; Milbrandt et al., 2021; Phlips et al., 2023), which periodically intrude into Tampa Bay, as observed in this study (Beck et al., 2022).

Peaks in phytoplankton biomass observed at the lower bay sampling sites in the 2 months following the Piney Point discharge event were dominated by euryhaline diatom species (Eppley, 1977; Brand, 1984; Balzano et al., 2011; Karthik et al., 2017), most prominently *Leptocylindrus minimus*, *Leptocylindrus danicus*, and *Cerataulina pelagica*. The three species are commonly found in estuaries around the world (Reynolds, 2006), and in Florida (Badylak and Phlips, 2004; Quinlan and Phlips, 2007; Hart et al., 2015), including Tampa Bay (Badylak et al., 2007). The euryhaline characteristic of these species makes them competitive in estuaries like Tampa Bay, in which salinities can range from mesohaline (i.e., 5–18 psu) to euhaline (i.e., >30 psu), as observed in the three lower bay sites in this study. The three diatom species are also known to have high maximum growth rates, i.e., >1.5 dbl. day^{-1} (Stolte and Garcés, 2006; Ajani et al., 2016). The high growth rates allow such species to take advantage of pulses of nutrients (Litchman et al., 2007; Cermeño et al., 2011; Karthik et al., 2017; Anderson et al., 2022), such as those observed with the Piney Point discharge, compared to many bloom-forming dinoflagellates encountered in coastal ecosystems in Florida (Phlips et al., 2006, 2011) which have maximum growth rates less than 1 dbl. day^{-1} (Stolte and Garcés, 2006; Matsubara et al., 2007). This is particularly true during cooler months of the year in Florida when water temperatures fall within 20–25°C, which is well within the optimal temperature range for growth of these diatom species, as opposed to other regionally important bloom-forming cyanobacteria and dinoflagellate species which have growth temperature optima between 25 and 35°C (Phlips and Mitsui, 1982; Montagnes and Franklin, 2001; Phlips et al., 2006; Anderson and Rynearson, 2020). Another factor that can enhance the success of diatom taxa with spines, a characteristic of the three aforementioned species, is lower grazing loss rates (Irigoien et al., 2005). While most diatoms are not viewed as serious HAB species, with the noted exception of toxin-producing species of *Pseudo-nitzschia* (Lassus et al., 2015), major blooms of *Leptocylindrus* and *Cerataulina* have been implicated in mortalities, or other health issues, in fish and shellfish populations, in relationship to physical damage, production of congestive muscilage, or generation of hypoxic conditions (Taylor et al., 1985; Buschmann et al., 2006; Ianora et al., 2008; Martin and LeGresley, 2014). These observations highlight the importance of including these types of taxa in monitoring and management plans for impacted ecosystems such as Tampa Bay.

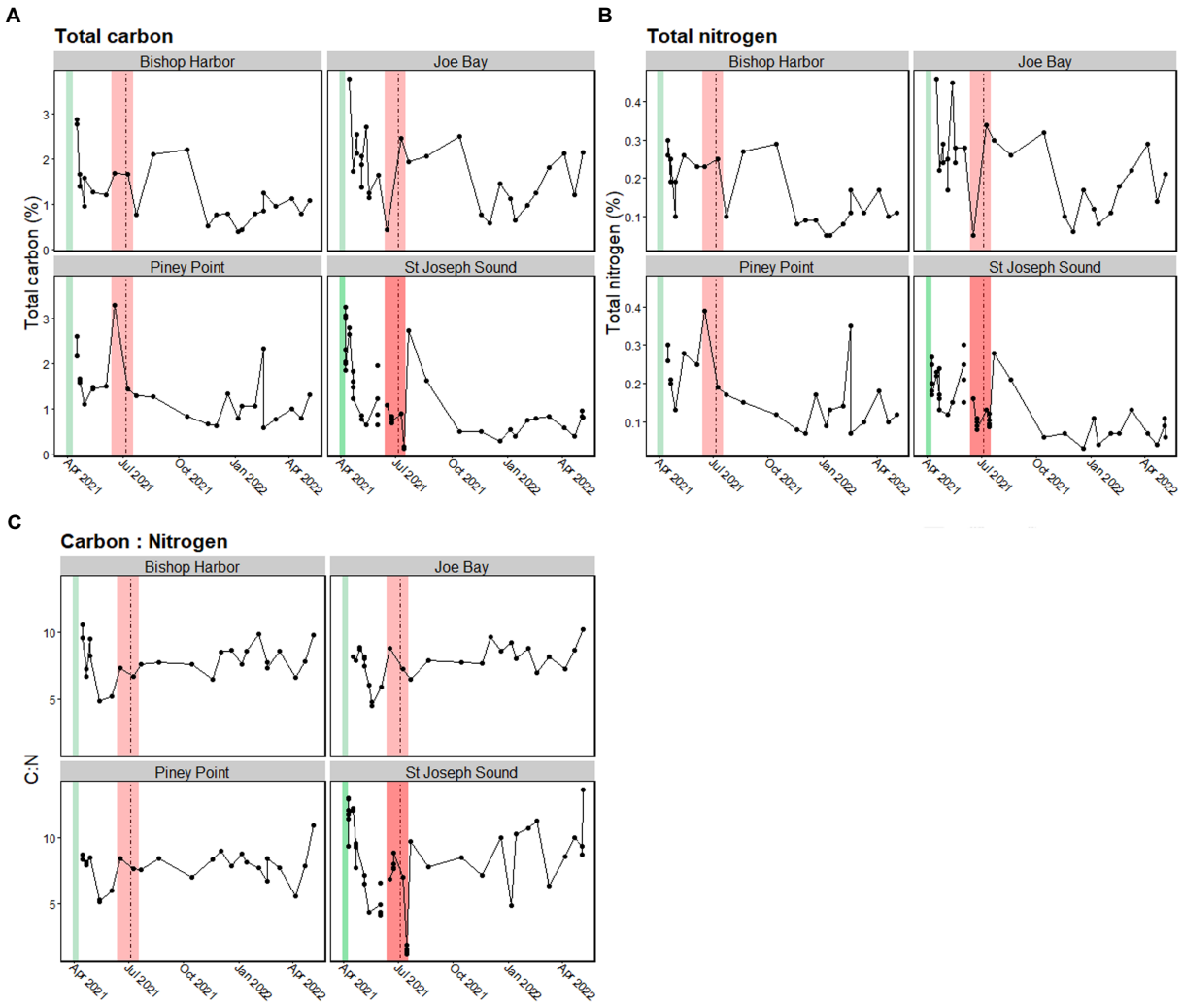

FIGURE 5
Bulk measures for suspended particulate material (SPM) for each location over the study period. Values for **(A)** total suspended particulate carbon, **(B)** total suspended particulate nitrogen, and **(C)** Carbon to Nitrogen (C:N) ratios are presented for each site. The Piney Point event (March 30th – April 9th, 2021) is denoted by the green line, the period with maximum (> 10^5 cells L^{-1}) *Karenia brevis* cell counts (Beck et al., 2022) is shown in the red box, and the date of tropical storm Elsa (July 5th, 2021) is shown with the vertical dashed black line. The smoothing line was generated using local polynomial regression fitting with a span of 0.175.

4.2. Karenia brevis *bloom dynamics post-discharge*

Another noteworthy aspect of the post Piney Point discharge period were peak biomass observations of the toxic red tide dinoflagellate, *K. brevis* at the Piney Point site in June 2021. *Karenia brevis* was also observed at Bishop Harbor and St. Joseph Sound during the same general time period, at lower biomass levels. This corroborates with Beck et al. (2022), who reported high concentrations of *K. brevis* in lower and middle Tampa Bay for the weeks of June 13th to July 18th, 2021. During the *K. brevis* bloom, there was an increase in extracted and *in situ* chlorophyll, as well as *in situ* measurements of PE. The peak biomass value for *K. brevis* observed at Piney Point was 2.71 mg C L^{-1} (i.e., 3.85 million cells L^{-1}), which ranks it as a major bloom of concern to the health of the estuary - including the potential for animal mortalities, development of anoxia, and human health issues (Kirkpatrick et al., 2004; Fleming et al., 2005; Landsberg et al., 2009; Heil and Muni-Morgan, 2021). During this period, extensive fish kills were also reported in Middle and Lower Tampa Bay (Beck et al., 2022; Florida Fish and Wildlife Conservation Commission, 2022).

K. brevis is a HAB species whose blooms initiate on the west Florida Shelf from upwelling events and are then advected to the nearshore through wind and currents, where they negatively affect coastal communities, particularly on the southwest coast of Florida between Tampa Bay and the Caloosahatchee Basin (Heil et al., 2014; Weisberg et al., 2019). The source of *K. brevis* at our study sites was likely the Gulf of Mexico, brought inshore by winds and current, and was facilitated by high salinities and available nutrients in the bay at that time, since *K. brevis* is known to be somewhat intolerant of low salinities (i.e., <20 psu; Steidinger, 2009; Beck et al., 2022). *K. brevis* blooms are a common feature along the west coast of Florida (Steidinger, 2009; Vargo, 2009; Heil et al., 2014), and typically originate offshore on the coastal shelf, and then are introduced to coastal estuaries through prevailing nearshore circulation patterns (Weisberg

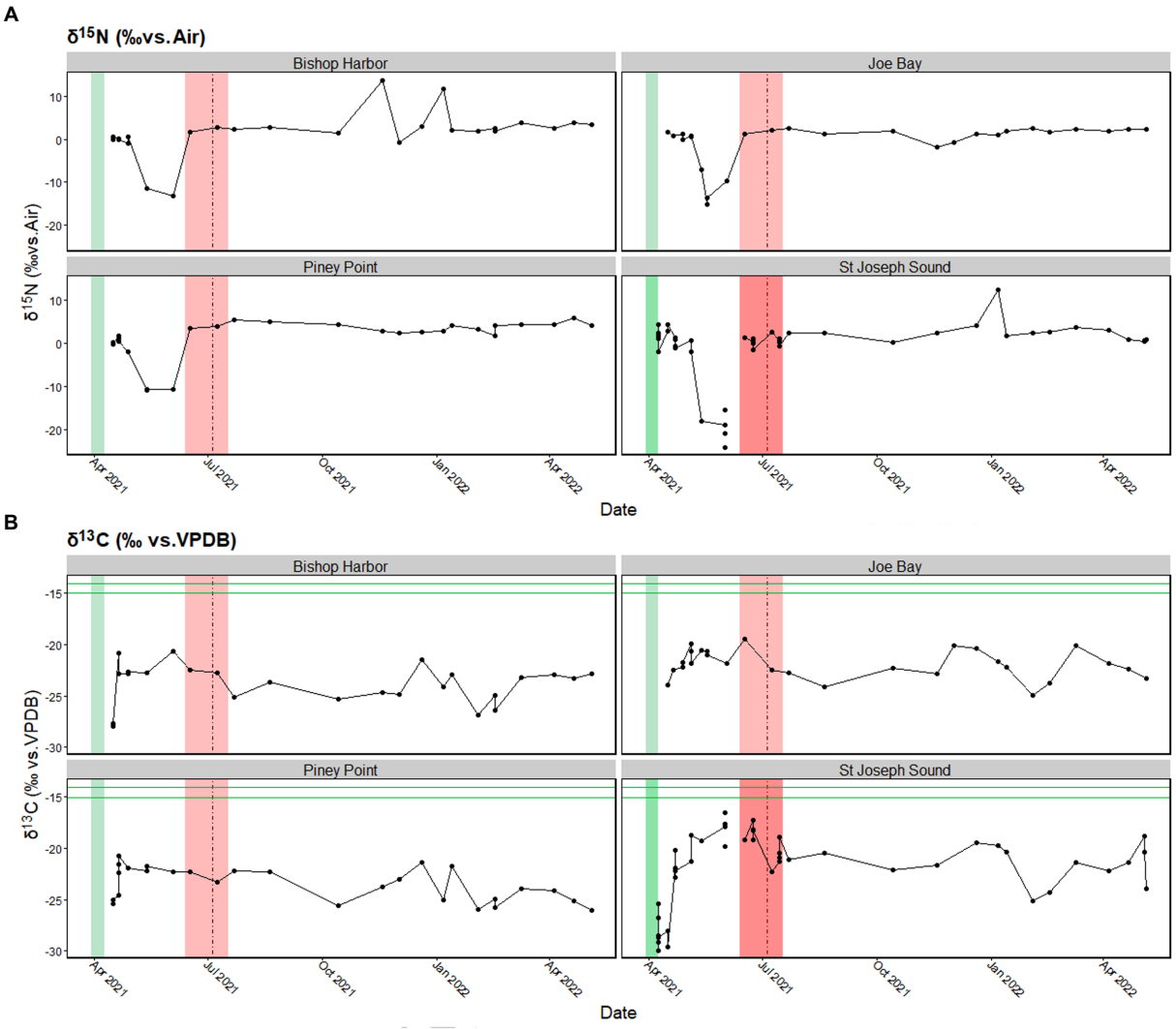

FIGURE 6
Stable isotope values for **(A)** nitrogen and **(B)** carbon in suspended particulate material (SPM). Values from the Piney Point discharge are shown with the horizontal green line. The Piney Point event (March 30th – April 9th, 2021) is denoted by the green line, the period with maximum (>10^5 cells L^{-1}) *Karenia brevis* cell counts (Beck et al., 2022) is shown in the red box, and the date of tropical storm Elsa (July 5th, 2021) is shown with the vertical dashed black line.

et al., 2019). High nutrient discharge from the Piney Point reservoir was suspected to contribute to the high biomass of *K. brevis* observed in the Piney Point region in June and July. Once *K. brevis* reaches the nearshore, terrestrial nutrient sources may influence bloom conditions, and several recent studies have observed positive relationships between elevated nutrient concentrations in discharges from local coastal watersheds and the intensity of red tide events (Medina et al., 2020, 2022; Phlips et al., 2023). However, further research is needed to define whether the high *K. brevis* biomass was associated with autochthonous production in the region, or allochthonous introduction of *K. brevis* from Tampa Bay, although evidence suggests both occurred during this event.

4.3. Suspended particulate material

Stable isotopes of N have been utilized in Tampa Bay and other coastal ecosystems to evaluate contributions from N sources and investigate N cycling, and our investigation of particulate $\delta^{13}C$ and $\delta^{15}N$ values revealed that Piney Point discharge had a unique SPM source signature. The discharge water SPM had an exceptionally low $\delta^{15}N$ value of −17.88‰ ± 0.76 ($n = 5$), and a $\delta^{13}C$ value of −15.23‰ ± 0.53 ($n = 5$). A $\delta^{15}N$ value of −17.88‰ is unusually low and is considerably lower than values reported for inorganic fertilizers, which can be as low as ~ −10‰ (Bateman and Kelly, 2007). In Tampa Bay, particulate and dissolved N stable isotopes have been used to identify N sources in stormwater runoff (Jani et al., 2020), constrain nutrient sources for *K. brevis* blooms (Havens, 2004), and asses N sources within the Gulf of Mexico (Knapp et al., 2021), and our unusually low value makes the $\delta^{15}N$ value of Piney Point SPM unique, and much more depleted, relative to other nutrient sources in the region. Local rainfall nitrate (NO_3^-) values range from −4.42 to 5.69‰, stormwater runoff $\delta^{15}N$-NO_3^- values range from −9.72 to 8.06‰, particulate organic N values range from −1.99 to 6.27‰, and local vegetation sources range from −1.70 to −0.83 ‰ (*Quercus virginia* leaves), 1.55 to 1.60‰ (*Quercus virginia* acorns), and −1.93 to 0.68‰ (*Stenotaphrum secundatum* grass clippings; Jani et al., 2020). Additionally, the Piney Point SPM $\delta^{15}N$ values are much lower than those reported for particulate N in the Gulf

of Mexico (1.6–5.0‰; Knapp et al., 2021). The only available published study that reported exceptionally low $\delta^{15}N$ values comparable to ours was a study of seagrass meadows of *Halodule uninervis* in Qatar, which documented $\delta^{15}N$ values as low as ~ −12.4‰, which was attributed to undefined but localized sediment processes (Walton et al., 2016).

This unusual $\delta^{15}N$ value is likely due to the unique characteristics of the reservoir and the water discharged from it. The discharge water was not pure diammonium phosphate, but rather a combination of waste derived from the production of diammonium phosphate, seawater from dredging operations, and rainwater, which have created unique conditions within the reservoir since it was partially filled in 2011 (Beck et al., 2022). Thus, the SPM collected from the reservoir contained particulate material that included phytoplankton and other microorganisms that were growing in the reservoir water, and as such, should not be expected to have $\delta^{15}N$ values that exactly resemble ammonium (NH_4^+) fertilizer. Given the novel growth conditions presented at the reservoir, it is likely that the highly depleted values seen in the discharge water in April 2021 (−17.88‰ ± 0.76), and in the reservoir water in October 2021 (−19.15‰ ± 0.05), were driven by isotope fractionation associated with ammonium transport and assimilation within the reservoir. Differences between the April and October $\delta^{15}N$ and nutrient values are likely from on-site treatment technologies used since April 2021 to reduce total P and total N within the reservoir.

Stable isotope values of $\delta^{15}N$ can be influenced by various isotopic fractionation pathways which we suggest explains the extreme $\delta^{15}N$ values we observed. Many phytoplankton and other microorganisms preferentially utilize NH_4^+ rather than NO_3^-. When ammonium is transported and assimilated by phytoplankton or other microorganisms, isotopic fractionation can occur when they preferentially utilize the light (^{14}N) isotope and leave the heavy ^{15}N isotope behind. This process can be concentration dependent, and when the ammonium concentration is higher, organisms discriminate more against the heavy isotope (^{15}N) and take up more of the lighter (^{14}N) isotope. This transport and assimilation of ^{14}N into their biomass decreases the relative proportion of ^{15}N in their biomass, and subsequently results in lower $\delta^{15}N$ values of the SPM ($\delta^{15}N_{SPM}$). We hypothesize that, under the extremely high (~210 mg L^{-1}) ammonium concentrations in the Piney Point reservoir, this isotope fractionation occurred to such an extent that it resulted in extremely low $\delta^{15}N$ values observed in the SPM of the reservoir.

While no laboratory studies to date have explored isotopic fractionation associated with ammonium concentrations as high as those in the study reservoir, Liu et al. (2015) reported the occurrence of concentration dependent isotopic fractionation when *Chlorella vulgaris* F1068 was grown in media with 4, 10 and 50 mg L^{-1} ammonium. *C. vulgaris* F1068 is a member of the division Chlorophyta, which was also the division of the dominant alga identified in the Piney Point reservoir. While the maximum *C. vulgaris* F1068 growth rate was seen at 4 mg L^{-1}, this species is capable of tolerating high (50 mg L^{-1}) concentrations of ammonium (Liu et al., 2015). While Liu et al. (2015) did not quantify the isotope enrichment factor (ε; a measure of isotopic discrimination against heavier isotopes) at 50 mg L^{-1}, they found an ε of −2.37‰ when *C. vulgaris* was grown at 10 mg L^{-1} ammonium, and that there was greater discrimination against the heavy isotope when *C. vulgaris* was grown under higher ammonium concentrations (Liu et al., 2015). Concentration dependent isotopic fractionation is not solely limited to members of Chlorophyta, as another laboratory study found that ε values of the diatom *Skeletonema* significantly decreased from −7.8‰ to −27.2‰ when grown on increasing concentrations of ammonium, indicating that when ammonium concentrations are higher, ^{14}N is incorporated faster than ^{15}N, thereby depleting (lowering) the $\delta^{15}N$ value of the phytoplankton and SPM (Pennock et al., 1996).

Anomalously low SPM $\delta^{15}N$ values seen at our study sites in May and June of 2021 suggest that there was incorporation of highly depleted Piney Point discharge into particulate material in the region. Previous work in Tampa Bay has suggested that *K. brevis* utilizes sources with low $\delta^{15}N$ values (Havens, 2004), however, the low SPM $\delta^{15}N$ values occurred prior to the dates of the peak *K. brevis* bloom, suggesting that the NH_4^+ from the discharge water was either (1) taken up by fast growing diatoms in May/June and incorporated into phytoplankton biomass/SPM; or (2) NH_4^+ may have been utilized during the early stage of the bloom, as initially low *K. brevis* cell counts were seen in lower Tampa Bay as early as the week of April 18th, 2021. However, we do not have sufficient evidence to explicitly evaluate these two scenarios.

The discharge water had a $\delta^{13}C$ value of −15.23‰ ± 0.53, which is within the range of bacteria or C4 terrestrial organic matter (Lamb et al., 2006). All sites exhibited a increase in $\delta^{13}C$ values concomitant with the decrease in $\delta^{15}N$ values, suggesting that C derived from the Piney Point discharge was also incorporated into SPM at the same time that $\delta^{15}N$ and C:N values declined. Interestingly, while phytoplankton biomass was lower overall at the reference site, St. Joseph Sound, the same trends in SPM stable isotope values were seen in the reference site. This may be an indication of the export of discharge C and N into regions outside of the bay, which is supported by initial findings from Liu et al. (2021) that showed the discharge was gradually flushed out of the bay and into adjacent coastal waters (Liu et al., 2021). The persistence of highly depleted SPM $\delta^{15}N$ values approximately 50 km from the discharge site is unexpected, but other regions distant to the discharge site, such as upper Sarasota Bay were also likely affected by the discharged waters (Tomasko, 2023). Additionally, we found that the reference site had elevated orthoP values in April 2021 relative to April 2022, suggesting that orthoP from the discharge was also transported to the reference site.

It must be emphasized that while the stable isotope values reported here indicate a transport of discharge outside of the bay, we did not observe large, associated shifts in chlorophyll values and phytoplankton community structure at the reference site, suggesting that, even if the SPM at the reference site reflects N contributions from the Piney Point discharge, these values may not have had adverse ecological effects at this location on the phytoplankton community. However, it should be noted that the released nutrients may have had other fates such as uptake into macroalgae and seagrasses, as well as deposition into bay sediments, both of which may have important implications for the long-term health of the Bay. For example, macroalgae blooms have contributed to seagrass losses throughout the Bay, which have been ongoing since before Piney Point. After Piney Point, *Ulva* was abundant in Hillsborough Bay and *Dapis* was abundant in most of the Bay (Tomasko, 2023), which may adversely affect seagrass meadows. Deposition into Bay sediments may also be an important mechanism by which nutrients from the discharge may have been removed from the water column and stored in the sediments. This legacy nutrient source may have implications for future water quality, as sedimentary resuspension, and fluxes of inorganic nutrients from sediments can provide an important source of nutrients to primary producers,

including phytoplankton and HABs (Dixon et al., 2014). Further investigation into macroalgae and seagrass stable isotope values and sedimentary records from the study area will provide a more complete picture of nutrient effects on the ecosystem.

4.4. Tropical storms and export of piney point discharge to surrounding areas

In addition to capturing some of the effects of the Piney Point discharge on Tampa Bay's phytoplankton communities and particulate material, we also detected a signal of Tropical Storm Elsa on the water quality of different regions within the Bay. The passage of tropical storm Elsa through the Tampa Bay area (July 5th, 2021) resulted in approximately 8–18 cm of rain delivered to the west coast of Florida (Cangialosi et al., 2022), and increased stream flows of the Anclote River and Little Manatee River which are tributaries to our study area (USGS, 2021a,b). The maximum stream flow reported for the Anclote river (USGS monitoring location 02310000), near the reference site St. Joseph Sound, was 954 $ft^3\ s^{-1}$ on July 10th, 2021, compared to 5.05 $ft^3\ s^{-1}$ during pre-storm conditions on July 1st, 2021 (USGS, 2021a), and the maximum stream flow reported for the Little Manatee River (USGS monitoring location 02300500), closest to the lower Tampa Bay sites, was 1,510 $ft^3\ s^{-1}$ on July 8th compared to 43.1 $ft^3\ s^{-1}$ during pre-storm conditions on June 28th, indicating that there were considerable increases in stream flow rates associated with this storm event.

The increased rainfall and streamflow into the study sites was associated with lower salinities, particularly at the lower bay sites. A decrease in fDOM, extracted and *in situ* chlorophyll, as well as PE were seen at the lower Tampa Bay sites, likely due to dilution of terrestrial DOM, in the case of fDOM, and possibly due to flushing of phytoplankton from the bay, in the case of chlorophyll and PE. The effects of Tropical Storm Elsa also likely influenced particulate TC values, as the lowest TC values (0.2 ± 0.02%) at Bishop Harbor and St. Joseph Sound site were seen immediately following the storm and likely driven by a dilution effect from freshwater inflows. We also observed a decline in C:N values at these sites, likely driven by an influx of N derived from the surrounding watershed associated with the storm. Past work in the region found that after some storm events, the concentration of all forms of N decreased, which was attributed to a dilution effect followed by a slight increase in TN concentrations after rainfall ceased (Jani et al., 2020). This was seen in 3 out of 4 sites in this study following the passage of Tropical Storm Elsa, where particulate N values exhibited an initial decrease after the storm, followed by a slight increase at Bishop Harbor and St. Joseph Sound sites, highlighting the important role that tropical storms play in influencing nutrient fluxes from terrestrial systems.

In addition, the occurrence of tropical storms and hurricanes can have interactive effects with built infrastructure, potentially resulting in increased threats to coastal systems and changes in nutrient regimes. For example, the capacity of the holding reservoirs at Piney Point had decreased due to rain events and tropical storms in the years prior to the event (Beck et al., 2022) increasing the risk of overflow or breaching which likely contributed to the 2021 event. Closure activities at the site are now centered on reducing the accumulation of rainfall within the wastewater reservoir system. As tropical storms and hurricanes are projected to increase in frequency and intensity, events such as the Piney Point 2021 wastewater discharge emphasize the vulnerability of coastal infrastructure and the potential ongoing threats these vulnerable facilities pose to coastal ecosystems.

5. Conclusion

Here we document changes in phytoplankton community composition, water quality, and SPM in the year following the 2021 Piney Point discharge event. Soon after the discharge, elevated diatom biomass was seen in the lower Tampa Bay sites, followed by high biomass of the harmful algae *K. brevis* in the summer of 2021. Nitrogen stable isotope values in SPM were very low in May and June of 2021 and were similar to $\delta^{15}N$ values from the discharge, suggesting that N from the Piney Point discharge was incorporated into SPM in the region. Low $\delta^{15}N$ values were also seen in the SPM samples collected from the reference site, St. Joseph Sound, and higher orthophosphate concentrations were seen at the site in April 2021 versus 2022, further suggesting that some of the Piney Point discharge was exported out of Tampa Bay proper. While the stable isotope values reported here indicate a transport of discharge outside of the bay, chlorophyll values and phytoplankton communities did not exhibit notable shifts at the reference site, suggesting that, even though SPM at the reference site reflects N contributions from the Piney Point discharge, these values may not have had adverse ecological effects at this location, at least from a phytoplankton perspective. While onsite treatment technologies have reduced the N and P concentrations in the reservoir, and have reduced the risk to nearby coastal ecosystems, the Piney Point event highlights the threat that industrial infrastructure failures can cause along Florida's coastlines. In addition, these vulnerabilities should be assessed with other factors, such as estuarine flushing rates, water residence times, climatic factors, and storms and hurricanes, which can also influence the initiation and persistence of HABs and the health of Florida's coastal ecosystems (Phlips et al., 2020; Tomasko et al., 2020). Here, the effects of Tropical Storm Elsa showed changes in water quality in the region, and storms such as Hurricane Ian, which passed through the region in September 2022, may also have interactive effects with the discharge-impacted regions in the Bay. This work underscores the need for comprehensive nutrient management strategies and convergent research to assess and manage the full range of consequences associated with anthropogenic nutrient inputs into coastal ecosystems. Ongoing and anticipated impacts of accelerated climate change – such as increasing tropical storm intensity, temperatures, rainfall, and sea level rise – will amplify this need.

Data availability statement

The datasets presented in this study can be found in online repositories. The names of the repository/repositories and accession number(s) can be found at: https://github.com/elisemorrison/PineyPoint2021

Author contributions

EM: conceptualization, data collection, field sampling, data curation, formal analysis, methodology, writing – original draft, and

writing – review and editing. EP: conceptualization, data curation, formal analysis, methodology, writing – original draft, and writing – review and editing. SB: data curation, formal analysis, methodology, and writing – review and editing. AC and AA: data collection, field sampling, data curation, methodology, and writing – review and editing. TO: data curation and writing – review and editing. DT: data curation and writing – review and editing. MB and ES: writing – review and editing. All authors contributed to the article and approved the submitted version.

Funding

This research was supported by the National Science Foundation (RAPID Award Number 2130675 to EM and EP and Award Number 2019435), and the Ocean Conservancy award to EM, EP, AA and Christine Angelini.

Acknowledgments

The authors would like to thank: Todd Van Natta, Patrick Norby, Charli Pezoldt, and Adam Hymel for their assistance with sampling, sonde maintenance, and data management; Jason Curtis at the UF Stable Isotope Laboratory; Jean Lockwood for assistance with phytoplankton analyses and Leslie Landauer for assistance with chlorophyll analyses; and Megan Sanford for laboratory support and sample preparation.

Conflict of interest

The authors declare that the research was conducted in the absence of any commercial or financial relationships that could be construed as a potential conflict of interest.

Publisher's note

All claims expressed in this article are solely those of the authors and do not necessarily represent those of their affiliated organizations, or those of the publisher, the editors and the reviewers. Any product that may be evaluated in this article, or claim that may be made by its manufacturer, is not guaranteed or endorsed by the publisher.

Supplementary material

The Supplementary material for this article can be found online at: https://www.frontiersin.org/articles/10.3389/fevo.2023.1144778/full#supplementary-material

References

Ahlgren, G. (1983). Comparison of methods for estimation of phytoplankton carbon. *Arch. Hydrobiol.* 98, 489–508.

Ajani, P. A., Armbrecht, L. H., Kersten, O., Kohli, G. S., and Murray, S. A. (2016). Diversity, temporal distribution and physiology of the centric diatom *Leptocylindrus Cleve* (Bacillariophyta) from a southern hemisphere upwelling system. *Diatom Res.* 31, 351–365. doi: 10.1080/0269249X.2016.1260058

American Public Health Association (2005). *Standard methods for the examination of water and wastewater*. Washington, DC, USA: American Public Health Association (APHA).

Anderson, S. I., Franzè, G., Kling, J. D., Wilburn, P., Kremer, C. T., Menden-Deuer, S., et al. (2022). The interactive effects of temperature and nutrients on a spring phytoplankton community. *Limnol. Oceanogr.* 67, 634–645. doi: 10.1002/lno.12023

Anderson, S. I., and Rynearson, T. A. (2020). Variability approaching the thermal limits can drive diatom community dynamics. *Limnol. Oceanogr.* 65, 1961–1973. doi: 10.1002/lno.11430

Badylak, S., and Phlips, E. (2004). Spatial and temporal patterns of phytoplankton composition in subtropical coastal lagoon, the Indian River lagoon, Florida, USA. *J. Plankton Res.* 26, 1229–1247. doi: 10.1093/plankt/fbh114

Badylak, S., Phlips, E. J., Baker, P., Fajans, J., and Boler, R. (2007). Distributions of phytoplankton in Tampa Bay estuary, USA 2002-2003. *Bull. Mar. Sci.* 80, 295–317.

Badylak, S., Phlips, E. J., and Mathews, A. L. (2014). *Akashiwo sanguinea* (Dinophyceae) blooms in a sub-tropical estuary: an alga for all seasons. *Plank. Benthos Res.* 9, 147–155. doi: 10.3800/pbr.9.147

Balzano, S., Sarno, D., and Kooistra, W. H. (2011). Effects of salinity on the growth rate and morphology of ten *Skeletonema* strains. *J. Plankton Res.* 33, 937–945. doi: 10.1093/plankt/fbq150

Bateman, A. S., and Kelly, S. D. (2007). Fertilizer nitrogen isotope signatures. *Isot. Environ. Health Stud.* 43, 237–247. doi: 10.1080/10256010701550732

Beck, M. W., Altieri, A., Angelini, C., Burke, M. C., Chen, J., Chin, D. W., et al. (2022). Initial estuarine response to inorganic nutrient inputs from a legacy mining facility adjacent to Tampa Bay Florida. *Mar. Pollut. Bull.* 178:113598. doi: 10.1016/j.marpolbul.2022.113598

Beck, M. W., Sherwood, E. T., Henkel, J. R., Dorans, K., Ireland, K., and Varela, P. (2019). Assessment of the cumulative effects of restoration activities on water quality in Tampa Bay, Florida. *Estuar. Coasts* 42, 1774–1791. doi: 10.1007/s12237-019-00619-w

Beusen, A., Van Beek, L., Bouwman, A., Mogollón, J., and Middelburg, J. (2015). Coupling global models for hydrology and nutrient loading to simulate nitrogen and phosphorus retention in surface water–description of IMAGE–GNM and analysis of performance. *Geosci. Model Dev.* 8, 4045–4067. doi: 10.5194/gmd-8-4045-2015

Brand, L. E. (1984). The salinity tolerance of forty-six marine phytoplankton isolates. *Estuar. Coast. Shelf Sci.* 18, 543–556. doi: 10.1016/0272-7714(84)90089-1

Buschmann, A. H., Riquelme, V. A., Hernández-González, M. C., Varela, D., Jiménez, J. E., Henríquez, L. A., et al. (2006). A review of the impacts of salmonid farming on marine coastal ecosystems in the Southeast Pacific. *ICES J. Mar. Sci.* 63, 1338–1345. doi: 10.1016/j.icesjms.2006.04.021

Cangialosi, J. P., Delgado, S., and Berg, R. (2022). *National Hurricane Center Tropical Cyclone Report Hurricane Elsa (AL052021)* Miami FL: ELSA.

Cermeño, P., Lee, J.-B., Wyman, K., Schofield, O., and Falkowski, P. G. (2011). Competitive dynamics in two species of marine phytoplankton under non-equilibrium conditions. *Mar. Ecol. Prog. Ser.* 429, 19–28. doi: 10.3354/meps09088

Chen, J., Weisberg, R. H., Liu, Y., and Zheng, L. (2018). The Tampa Bay coastal ocean model performance for hurricane Irma. *Mar. Technol. Soc. J.* 52, 33–42. doi: 10.4031/MTSJ.52.3.6

Chen, J., Weisberg, R. H., Liu, Y., Zheng, L., and Zhu, J. (2019). On the momentum balance of Tampa Bay. *J. Geophys. Res. Oceans* 124, 4492–4510. doi: 10.1029/2018JC014890

Cloern, J. E. (2001). Our evolving conceptual model of the coastal eutrophication problem. *Mar. Ecol. Prog. Ser.* 210, 223–253. doi: 10.3354/meps210223

Deangelis, B. M., Sutton-Grier, A. E., Colden, A., Arkema, K. K., Baillie, C. J., Bennett, R. O., et al. (2020). Social factors key to landscape-scale coastal restoration: lessons learned from three US case studies. *Sustainability* 12:869. doi: 10.3390/su12030869

Dixon, L. K., Murphy, P. J., Becker, N. M., and Charniga, C. M. (2014). The potential role of benthic nutrient flux in support of *Karenia* blooms in West Florida (USA) estuaries and the nearshore Gulf of Mexico. *Harmful Algae* 38, 30–39. doi: 10.1016/j.hal.2014.04.005

Doney, S. C., Ruckelshaus, M., Emmett Duffy, J., Barry, J. P., Chan, F., English, C. A., et al. (2012). Climate change impacts on marine ecosystems. *Annu. Rev. Mar. Sci.* 4, 11–37. doi: 10.1146/annurev-marine-041911-111611

Eppley, R. W. (1977). The growth and culture of diatoms. *Biol. Diatoms* 32:2.

Fahnenstiel, G. L., and Carrick, H. J. (1992). Phototrophic picoplankton in lakes Huron and Michigan: abundance, distribution, composition, and contribution to biomass and production. *Can. J. Fish. Aquat. Sci.* 49, 379–388. doi: 10.1139/f92-043

Fleming, L. E., Kirkpatrick, B., Backer, L. C., Bean, J. A., Wanner, A., Dalpra, D., et al. (2005). Initial evaluation of the effects of aerosolized Florida red tide toxins (brevetoxins) in persons with asthma. *Environ. Health Perspect.* 113, 650–657. doi: 10.1289/ehp.7500

Florida Department of Environmental Protection (2021). Piney point update - April 6, 2021 [online]. Available at: https://protectingfloridatogether.gov/node/285# (Accessed October 1, 2023).

Florida Fish and Wildlife Conservation Commission (2022). Fish kill database search result report [online]. Available at: https://app.myfwc.com/FWRI/FishKillReport/ReportWorkSheet.aspx (Accessed 14 January, 2023).

Garrett, M., Wolny, J., Truby, E., Heil, C., and Kovach, C. (2011). Harmful algal bloom species and phosphate-processing effluent: field and laboratory studies. *Mar. Pollut. Bull.* 62, 596–601. doi: 10.1016/j.marpolbul.2010.11.017

Glibert, P. M. (2020). Harmful algae at the complex nexus of eutrophication and climate change. *Harmful Algae* 91:101583. doi: 10.1016/j.hal.2019.03.001

Glibert, P. M., Icarus Allen, J., Artioli, Y., Beusen, A., Bouwman, L., Harle, J., et al. (2014). Vulnerability of coastal ecosystems to changes in harmful algal bloom distribution in response to climate change: projections based on model analysis. *Glob. Chang. Biol.* 20, 3845–3858. doi: 10.1111/gcb.12662

Gobler, C. J. (2020). Climate change and harmful algal blooms: insights and perspective. *Harmful Algae* 91:101731. doi: 10.1016/j.hal.2019.101731

Greening, H., Janicki, A., Sherwood, E. T., Pribble, R., and Johansson, J. O. R. (2014). Ecosystem responses to long-term nutrient management in an urban estuary: Tampa Bay, Florida, USA. *Estuar. Coast. Shelf Sci.* 151, A1–A16. doi: 10.1016/j.ecss.2014.10.003

Griffith, A. W., and Gobler, C. J. (2020). Harmful algal blooms: a climate change co-stressor in marine and freshwater ecosystems. *Harmful Algae* 91:101590. doi: 10.1016/j.hal.2019.03.008

Grill, G., Lehner, B., Lumsdon, A. E., Macdonald, G. K., Zarfl, C., and Liermann, C. R. (2015). An index-based framework for assessing patterns and trends in river fragmentation and flow regulation by global dams at multiple scales. *Environ. Res. Lett.* 10:015001. doi: 10.1088/1748-9326/10/1/015001

Hagy Iii, J. D., Kreakie, B. J., Pelletier, M. C., Nojavan, F., Kiddon, J. A., and Oczkowski, A. J. (2022). Quantifying coastal ecosystem trophic state at a macroscale using a Bayesian analytical framework. *Ecol. Indic.* 142:109267, –109212. doi: 10.1016/j.ecolind.2022.109267

Hart, J., Phlips, E., Badylak, S., Dix, N., Petrinec, K., Mathews, A., et al. (2015). Phytoplankton biomass and composition in a well-flushed, sub-tropical estuary: the contrasting effects of hydrology, nutrient loads and allochthonous influences. *Mar. Environ. Res.* 112, 9–20. doi: 10.1016/j.marenvres.2015.08.010

Havens, J. A. (2004). *A stable isotopic examination of particulate organic matter during Karenia brevis blooms on the central West Florida shelf: Hints at nitrogen sources in oligotrophic waters*.

Heil, C. A., Dixon, L. K., Hall, E., Garrett, M., Lenes, J. M., Oneil, J. M., et al. (2014). Blooms of *Karenia brevis* (Davis) G. Hansen & Ø. Moestrup on the West Florida shelf: nutrient sources and potential management strategies based on a multi-year regional study. *Harmful Algae* 38, 127–140. doi: 10.1016/j.hal.2014.07.016

Heil, C. A., and Muni-Morgan, A. L. (2021). Florida's harmful algal bloom (HAB) problem: escalating risks to human, environmental and economic health with climate change. *Front. Ecol. Evol.* 9:646080. doi: 10.3389/fevo.2021.646080

Heisler, J., Glibert, P. M., Burkholder, J. M., Anderson, D. M., Cochlan, W., Dennison, W. C., et al. (2008). Eutrophication and harmful algal blooms: a scientific consensus. *Harmful Algae* 8, 3–13. doi: 10.1016/j.hal.2008.08.006

Herren, L., Brewton, R., Wilking, L., Tarnowski, M., Vogel, M., and Lapointe, B. (2021). Septic systems drive nutrient enrichment of groundwaters and eutrophication in the urbanized Indian River lagoon. *Florida. Mar. Pollut. Bull.* 172:112928. doi: 10.1016/j.marpolbul.2021.112928

Hoegh-Guldberg, O., and Bruno, J. F. (2010). The impact of climate change on the world's marine ecosystems. *Science* 328, 1523–1528. doi: 10.1126/science.1189930

Ianora, A., Casotti, R., Bastianini, M., Brunet, C., D'ippolito, G., Acri, F., et al. (2008). Low reproductive success for copepods during a bloom of the non-aldehyde-producing diatom *Cerataulina pelagica* in the North Adriatic Sea. *Mar. Ecol.* 29, 399–410. doi: 10.1111/j.1439-0485.2008.00226.x

Irigoien, X., Flynn, K., and Harris, R. (2005). Phytoplankton blooms: a "loophole" in microzooplankton grazing impact? *J. Plankton Res.* 27, 313–321. doi: 10.1093/plankt/fbi011

Jani, J., Yang, Y.-Y., Lusk, M. G., and Toor, G. S. (2020). Composition of nitrogen in urban residential stormwater runoff: concentrations, loads, and source characterization of nitrate and organic nitrogen. *PLoS One* 15:e0229715. doi: 10.1371/journal.pone.0229715

Karthik, R., Padmavati, G., Elangovan, S. S., and Sachithanandam, V. (2017). Monitoring the diatom bloom of *Leptocylindrus danicus* (Cleve 1889, Bacillariophyceae) in the coastal waters of south Andaman Island. *Indian J. Geo-Mar. Sci.* 46, 958–965. http://nopr.niscpr.res.in/handle/123456789/41662

Kirkpatrick, B., Fleming, L. E., Squicciarini, D., Backer, L. C., Clark, R., Abraham, W., et al. (2004). Literature review of Florida red tide: implications for human health effects. *Harmful Algae* 3, 99–115. doi: 10.1016/j.hal.2003.08.005

Knapp, A. N., Thomas, R. K., Stukel, M. R., Kelly, T. B., Landry, M. R., Selph, K. E., et al. (2021). Constraining the sources of nitrogen fueling export production in the Gulf of Mexico using nitrogen isotope budgets. *J. Plankton Res.* 44, 692–710.

Lamb, A. L., Wilson, G. P., and Leng, M. J. (2006). A review of coastal palaeoclimate and relative sea-level reconstructions using δ13C and C/N ratios in organic material. *Earth Sci. Rev.* 75, 29–57. doi: 10.1016/j.earscirev.2005.10.003

Landsberg, J., Flewelling, L., and Naar, J. (2009). *Karenia brevis* red tides, brevetoxins in the food web, and impacts on natural resources: decadal advancements. *Harmful Algae* 8, 598–607. doi: 10.1016/j.hal.2008.11.010

Lassus, P., Chaumérat, N., Hess, P., and Nézan, E. (2015). Toxic and harmful microalgae of the World Ocean, International Society for the Study of harmful algae and the United Nations ….

Lehner, B., Liermann, C. R., Revenga, C., Vörösmarty, C., Fekete, B., Crouzet, P., et al. (2011). High-resolution mapping of the world's reservoirs and dams for sustainable river-flow management. *Front. Ecol. Environ.* 9, 494–502. doi: 10.1890/100125

Litchman, E., Klausmeier, C. A., Schofield, O. M., and Falkowski, P. G. (2007). The role of functional traits and trade-offs in structuring phytoplankton communities: scaling from cellular to ecosystem level. *Ecol. Lett.* 10, 1170–1181. doi: 10.1111/j.1461-0248.2007.01117.x

Liu, N., Li, F., Ge, F., Tao, N., Zhou, Q., and Wong, M. (2015). Mechanisms of ammonium assimilation by *Chlorella vulgaris* F1068: isotope fractionation and proteomic approaches. *Bioresour. Technol.* 190, 307–314. doi: 10.1016/j.biortech.2015.04.024

Liu, Y., Weisberg, R., Zheng, L., Sun, Y., and Chen, J. Nowcast/forecast of the Tampa Bay, piney point effluent plume: a rapid response AGU fall Meeting Abstracts (2021). OS35B–1036.

Lundholm, N., Churro, C., Fraga, S., Hoppenrath, M., Iwataki, M., Larsen, J., et al. (Eds) (2009 onwards). IOC-UNESCO Taxonomic Reference List of Harmful Micro Algae. Accessed at https://www.marinespecies.org/hab on yyyy-mm-dd. doi: 10.14284/362

Maavara, T., Parsons, C. T., Ridenour, C., Stojanovic, S., Dürr, H. H., Powley, H. R., et al. (2015). Global phosphorus retention by river damming. *Proc. Natl. Acad. Sci. U. S. A.* 112, 15603–15608. doi: 10.1073/pnas.1511797112

Martin, J. L., and Legresley, M. (2014). Phytoplankton monitoring in the Western isles region of the bay of Fundy during 2003–2006, Biological Station: Fisheries and Oceans Canada.

Matsubara, T., Nagasoe, S., Yamasaki, Y., Shikata, T., Shimasaki, Y., Oshima, Y., et al. (2007). Effects of temperature, salinity, and irradiance on the growth of the dinoflagellate *Akashiwo sanguinea*. *J. Exp. Mar. Biol. Ecol.* 342, 226–230. doi: 10.1016/j.jembe.2006.09.013

Medina, M., Huffaker, R., Jawitz, J. W., and Muñoz-Carpena, R. (2020). Seasonal dynamics of terrestrially sourced nitrogen influenced *Karenia brevis* blooms off Florida's southern Gulf Coast. *Harmful Algae* 98:101900. doi: 10.1016/j.hal.2020.101900

Medina, M., Kaplan, D., Milbrandt, E. C., Tomasko, D., Huffaker, R., and Angelini, C. (2022). Nitrogen-enriched discharges from a highly managed watershed intensify red tide (*Karenia brevis*) blooms in Southwest Florida. *Sci. Total Environ.* 827:154149. doi: 10.1016/j.scitotenv.2022.154149

Metcalf, J., Banack, S., Wessel, R., Lester, M., Pim, J., Cassani, J., et al. (2021). Toxin analysis of freshwater cyanobacterial and marine harmful algal blooms on the west coast of Florida and implications for estuarine environments. *Neurotox. Res.* 39, 27–35. doi: 10.1007/s12640-020-00248-3

Milbrandt, E. C., Martignette, A., Thompson, M., Bartleson, R., Phlips, E., Badylak, S., et al. (2021). Geospatial distribution of hypoxia associated with a *Karenia brevis* bloom. *Estuar. Coast. Shelf Sci.* 259:107446. doi: 10.1016/j.ecss.2021.107446

Montagnes, D. J., and Franklin, M. (2001). Effect of temperature on diatom volume, growth rate, and carbon and nitrogen content: reconsidering some paradigms. *Limnol. Oceanogr.* 46, 2008–2018. doi: 10.4319/lo.2001.46.8.2008

Nelson, N. G., Cuchiara, M. L., Hendren, C. O., Jones, J. L., and Marshall, A.-M. (2021). Hazardous spills at retired fertilizer manufacturing plants will continue to occur in the absence of scientific innovation and regulatory enforcement. *Environ. Sci. Technol.* 55, 16267–16269. doi: 10.1021/acs.est.1c05311

Nixon, S. W. (1995). Coastal marine eutrophication: a definition, social causes, and future concerns. *Ophelia* 41, 199–219. doi: 10.1080/00785236.1995.10422044

Oneil, J. M., Davis, T. W., Burford, M. A., and Gobler, C. J. (2012). The rise of harmful cyanobacteria blooms: the potential roles of eutrophication and climate change. *Harmful Algae* 14, 313–334. doi: 10.1016/j.hal.2011.10.027

Paerl, H. W., Valdes, L. M., Peierls, B. L., Adolf, J. E., and Harding, L. J. W. (2006). Anthropogenic and climatic influences on the eutrophication of large estuarine ecosystems. *Limnol. Oceanogr.* 51, 448–462. doi: 10.4319/lo.2006.51.1_part_2.0448

Pennock, J. R., Velinsky, D. J., Ludlam, J. M., Sharp, J. H., and Fogel, M. L. (1996). Isotopic fractionation of ammonium and nitrate during uptake by *Skeletonema costatum*: implications for δ15N dynamics under bloom conditions. *Limnol. Oceanogr.* 41, 451–459. doi: 10.4319/lo.1996.41.3.0451

Phlips, E., Badylak, S., Bledsoe, E., and Cichra, M. (2006). Factors influencing the distribution and abundance of *Pyrodinium bahamense* in coastal ecosystems of Florida. *Mar. Ecol. Prog. Ser.* 322, 99–115. doi: 10.3354/meps322099

Phlips, E. J., Badylak, S., Christman, M. C., and Lasi, M. A. (2010). Climatic trends and temporal patterns of phytoplankton composition, abundance, and succession in the Indian River lagoon, Florida, USA. *Estuar. Coasts* 33, 498–512. doi: 10.1007/s12237-009-9166-8

Phlips, E. J., Badylak, S., Christman, M., Wolny, J., Brame, J., Garland, J., et al. (2011). Scales of temporal and spatial variability in the distribution of harmful algae species in the Indian River lagoon, Florida, USA. *Harmful Algae* 10, 277–290. doi: 10.1016/j.hal.2010.11.001

Phlips, E. J., Badylak, S., and Lynch, T. C. (1999). Blooms of the picoplanktonic cyanobacterium *Synechococcus* in Florida bay, a subtropical inner-shelf lagoon. *Limnol. Oceanogr.* 44, 1166–1175. doi: 10.4319/lo.1999.44.4.1166

Phlips, E., Badylak, S., Matthews, A. L., Milbrandt, E. C. R. M. L., Morrison, E., Nelson, N. G., et al. (2023). Algal blooms in a river-dominated estuary and nearshore region of Florida, USA: the influence of regulated discharges from water control structures on hydrology and nutrient conditions. *Hydrobiologia*. doi: 10.1007/s10750-022-05135-w.

Phlips, E. J., Badylak, S., Nelson, N. G., and Havens, K. E. (2020). Hurricanes, El Niño and harmful algal blooms in two sub-tropical Florida estuaries: direct and indirect impacts. *Sci. Rep.* 10, 1–12. doi: 10.1038/s41598-020-58771-4

Phlips, E., and Mitsui, A. (1982). "Temperature preference and tolerance of aquatic photosynthetic microorganisms [including blue-green algae]," in *CRC handbook of biosolar resources*. eds. A. Mitsui and C. Black (Boca, Florida: CRC Press), 335–361.

Quinlan, E. L., and Phlips, E. J. (2007). Phytoplankton assemblages across the marine to low-salinity transition zone in a Blackwater dominated estuary. *J. Plankton Res.* 29, 401–416. doi: 10.1093/plankt/fbm024

R Core Development Team (2008). *R: A language and environment for statistical computing*. R Foundation for Statistical Computing: Vienna, Austria.

Reynolds, C. S. (2006). *Ecology of Phytoplankton*. Cambridge: Cambridge University Press.

Sartory, D., and Grobbelaar, J. (1984). Extraction of chlorophyll a from freshwater phytoplankton for spectrophotometric analysis. *Hydrobiologia* 114, 177–187. doi: 10.1007/BF00031869

Sherwood, E. T., Greening, H. S., Johansson, J. R., Kaufman, K., and Raulerson, G. E. (2017). Tampa Bay (Florida, USA) documenting seagrass recovery since the 1980's and reviewing the benefits. *Southeast. Geogr.* 57, 294–319. doi: 10.1353/sgo.2017.0026

Sicko-Goad, L. M., Schelske, C. L., and Stoermer, E. F. (1984). Estimation of intracellular carbon and silica content of diatoms from natural assemblages using morphometric techniques 1. *Limnol. Oceanogr.* 29, 1170–1178. doi: 10.4319/lo.1984.29.6.1170

Sin, Y., Hyun, B., Jeong, B., and Soh, H. Y. (2013). Impacts of eutrophic freshwater inputs on water quality and phytoplankton size structure in a temperate estuary altered by a sea dike. *Mar. Environ. Res.* 85, 54–63. doi: 10.1016/j.marenvres.2013.01.001

Smayda, T. J. (1978). "From phytoplankters to biomass". In *Phytoplankton Manual*. ed. A. Sournia (Paris: UNESCO), 273–279.

Steidinger, K. A. (2009). Historical perspective on *Karenia brevis* red tide research in the Gulf of Mexico. *Harmful Algae* 8, 549–561. doi: 10.1016/j.hal.2008.11.009

Stolte, W., and Garcés, E. (2006). "Ecological aspects of harmful algal in situ population growth rates," in *Ecology of harmful algae* (London: Springer).

Strathmann, R. R. (1967). Estimating the organic carbon content of phytoplankton from cell volume or plasma volume 1. *Limnol. Oceanogr.* 12, 411–418. doi: 10.4319/lo.1967.12.3.0411

Sun, J., and Liu, D. (2003). Geometric models for calculating cell biovolume and surface area for phytoplankton. *J. Plankton Res.* 25, 1331–1346. doi: 10.1093/plankt/fbg096

Switzer, T. S., Tyler-Jedlund, A. J., Rogers, K. R., Grier, H., Mcmichael, R. H., and Fox, S. (2011). Response of estuarine nekton to the regulated discharge of treated phosphate-production process water. TR-16. Florida Fish and Wildlife Conservation Commission. Fish and Wildlife Research Institute. Technical Report. St. Petersburg, FL. http://hdl.handle.net/1834/41127

Tampa Bay Estuary Program (2022). State of the bay 2019-2021. Available at: https://tbep.org/estuary/state-of-the-bay/ (Accessed October 1, 2023).

Tampa Bay Nitrogen Management Consortium (TBNMC) (2022). Tampa Bay Reasonable Assurance Compliance Assessment Report. Available at: https://tbep-tech.github.io/tbnmc-compliance-assessment-2022/index.html

Taylor, F., Taylor, N., and Walsby, J. (1985). A bloom of the planktonic diatom, *Cerataulina pelagica*, off the coast of northeastern New Zealand in 1983, and its contribution to an associated mortality of fish and benthic fauna. *Internationale Revue der gesamten Hydrobiologie und Hydrographie* 70, 773–795. doi: 10.1002/iroh.19850700602

Tomasko, D. (2023). Ecological impacts to Sarasota Bay from Piney Point discharges - examining the evidence. *Florida Scientist*.

Tomasko, D., Alderson, M., Burnes, R., Hecker, J., Iadevaia, N., Leverone, J., et al. (2020). The effects of hurricane Irma on seagrass meadows in previously eutrophic estuaries in Southwest Florida (USA). *Mar. Pollut. Bull.* 156:111247. doi: 10.1016/j.marpolbul.2020.111247

Tomasko, D., Alderson, M., Burnes, R., Hecker, J., Leverone, J., Raulerson, G., et al. (2018). Widespread recovery of seagrass coverage in Southwest Florida (USA): temporal and spatial trends and management actions responsible for success. *Mar. Pollut. Bull.* 135, 1128–1137. doi: 10.1016/j.marpolbul.2018.08.049

USGS (2021a). USGS water data Anclote River [online]. Available at: https://waterdata.usgs.gov/monitoring-location/02310000/#parameterCode=00060&startDT=2021-04-01&endDT=2022-05-01 (Accessed November 1, 2023).

USGS (2021b). USGS water data little Manatee River [online] Available at: https://waterdata.usgs.gov/monitoring-location/02300500/#parameterCode=00060&startDT=2021-04-01&endDT=2022-05-01 (Accessed November 1, 2023).

Utermohl, H. (1958). To the perfection of quantitative phytoplankton methodology. *Mitt. Int. Ver. Theor. Angew. Limnol.* 9, 1–38.

Vargo, G. A. (2009). A brief summary of the physiology and ecology of *Karenia brevis* Davis (G. Hansen and Moestrup comb. nov.) red tides on the West Florida shelf and of hypotheses posed for their initiation, growth, maintenance, and termination. *Harmful Algae* 8, 573–584. doi: 10.1016/j.hal.2008.11.002

Verity, P. G., Robertson, C. Y., Tronzo, C. R., Andrews, M. G., Nelson, J. R., and Sieracki, M. E. (1992). Relationships between cell volume and the carbon and nitrogen content of marine photosynthetic nanoplankton. *Limnol. Oceanogr.* 37, 1434–1446. doi: 10.4319/lo.1992.37.7.1434

Walton, M., Al-Maslamani, I., Haddaway, N., Kennedy, H., Castillo, A., Al-Ansari, E., et al. (2016). Extreme 15N depletion in seagrasses. *Estuar. Coasts* 39, 1709–1723. doi: 10.1007/s12237-016-0103-3

Webster, P. J., Holland, G. J., Curry, J. A., and Chang, H.-R. (2005). Changes in tropical cyclone number, duration, and intensity in a warming environment. *Science* 309, 1844–1846. doi: 10.1126/science.1116448

Weisberg, R. H., Liu, Y., Lembke, C., Hu, C., Hubbard, K., and Garrett, M. (2019). The coastal ocean circulation influence on the 2018 West Florida Shelf *K. brevis* red tide bloom. *J. Geophys. Res. Oceans* 124, 2501–2512. doi: 10.1029/2018JC014887

Wetz, M. S., and Yoskowitz, D. W. (2013). An "extreme" future for estuaries? Effects of extreme climatic events on estuarine water quality and ecology. *Mar. Pollut. Bull.* 69, 7–18. doi: 10.1016/j.marpolbul.2013.01.020

Work, K., Havens, K., Sharfstein, B., and East, T. (2005). How important is bacterial carbon to planktonic grazers in a turbid, subtropical lake? *J. Plankton Res.* 27, 357–372. doi: 10.1093/plankt/fbi013

Yates, K., Greening, H., and Morrison, G. (2011). Integrating science and resource management in Tampa Bay, Florida Prepared in partnership with the Tampa Bay Estuary Program.

frontiers | Frontiers in Ecology and Evolution

TYPE Original Research
PUBLISHED 23 June 2023
DOI 10.3389/fevo.2023.1167767

OPEN ACCESS

EDITED BY
Marcus W. Beck,
Tampa Bay Estuary Program, United States

REVIEWED BY
Brandon Jarvis,
United States Environmental Protection Agency (EPA), United States
Lise Montefiore,
North Carolina State University, United States

*CORRESPONDENCE
Amanda C. Croteau
✉ acroteau@uwf.edu

RECEIVED 16 February 2023
ACCEPTED 29 May 2023
PUBLISHED 23 June 2023

CITATION
Croteau AC, Gancel HN, Gebremicael TG, Caffrey JM and Deitch MJ (2023) Implications of changing trends in hydroclimatic and water quality parameters on estuarine habitats in the Gulf Coastal Plain.
Front. Ecol. Evol. 11:1167767.
doi: 10.3389/fevo.2023.1167767

Implications of changing trends in hydroclimatic and water quality parameters on estuarine habitats in the Gulf Coastal Plain

Amanda C. Croteau[1]*, Haley N. Gancel[2], Tesfay G. Gebremicael[3], Jane M. Caffrey[1] and Matthew J. Deitch[3]

[1]Center for Environmental Diagnostics and Bioremediation, University of West Florida, Pensacola, FL, United States, [2]Pensacola and Perdido Bays Estuary Program, Pensacola, FL, United States, [3]IFAS West Florida Research and Education Center, Department of Soil and Water Sciences, University of Florida, Milton, FL, United States

Florida's low elevation and geographic location make it particularly vulnerable to climate change effects such as sea level rise, increased intensity and frequency of storm events, and altered precipitation. Climate change is expected to exacerbate hydrological cycling with potential widespread implications for estuarine habitats that thrive under specific salinity regimes. We used historical data from sites in the eastern Gulf Coastal Plain, USA to examine trends and trend variability of several climatic, hydrologic, and estuarine water quality variables which have implications on seagrass and oyster habitat extent in downstream estuarine environments. We analyzed temperature, precipitation, low-flow and high-flow metrics (including the highest or lowest daily, 7-day average, and 30-day average) for each season annually over the period 1985–2020. We also analyzed estuarine water clarity metrics and salinity within waterbody segments of four estuary systems within the study area. Hydroclimate results showed that temperature increased at most sites. While there was variation in streamflow, the overall trend was declining streamflow. Declining trends were observed in most water clarity metrics, indicating improved clarity, especially in winter. Salinity generally declined across the study area. While overall streamflow decreased, main river stems to the estuaries had increasing trends in maximum streamflow characteristics, likely contributing to the decrease in estuarine salinity across the region. These results indicate that trends in streamflow (both magnitude and timing) in the watershed affect downstream estuarine water quality. These results have important implications on seagrass and oyster restoration and management efforts in the region, indicating that it is important to understand changing climatic and hydrologic conditions and how they may impact the estuarine resources.

KEYWORDS

streamflow, precipitation, temperature, water clarity, salinity, estuary, Seasonal Mann-Kendall analysis, Gulf Coastal Plain

1. Introduction

The Coastal Plain of southeastern North America is ecologically significant due to high biodiversity and endemism (Blaustein, 2008; Noss et al., 2015). Aquatic ecosystems of the Gulf Coastal Plain, including alluvial plains of Florida, Alabama, and Mississippi are particularly ecologically rich (Hamilton et al., 2022). This region is home to diverse communities of fishes

(Warren Jr et al., 2000), amphibians (Walls, 2014), aquatic insects (Markos et al., 2016), and plants (Estill and Cruzan, 2001), more than 2,000 of which are endemic to the region (Noss et al., 2015). Aquatic and adjacent terrestrial ecosystems in the Gulf Coastal Plain also provide a number of ecosystem services that benefit human well-being. Managed forests across the region provide among the highest volumes of timber harvested annually in the world (Fox et al., 2007). Estuarine systems at the base of the Coastal Plain benefit from upstream process, particularly freshwater discharge, which helps maintain suitable environments for many fish, invertebrate, and plant species. Freshwater discharge from upstream catchments supports some of the largest commercial and recreational fisheries in the Gulf of Mexico (Karnauskas et al., 2013), which in turn provide the fishing industry with billions of dollars of revenue each year (Karnauskas et al., 2013; National Marine Fisheries Service, 2016).

Climatic stability is a key factor contributing to biodiversity and endemism, especially in the Gulf Coastal Plain, where topography and relief are low compared to other biodiversity hotspots (Harrison and Noss, 2017). While analysis of rainfall and streamflow trends in other parts of the U.S. illustrate statistically significant declining or increasing trends depending on the season, trends in the Gulf Coastal Plain from a handful of sites have appeared relatively stable over the latter 20th Century (Ficklin et al., 2016; Poshtiri and Pal, 2016). Despite this, recent extremes in precipitation and weather events have raised concerns about long-term aquatic ecosystem and water resource sustainability (Lockette, 2016). Climate change studies have reported regional and global increases in temperature and increases in both frequency and intensity of extreme weather events, which can alter the timing and intensity of freshwater flow to estuaries and coastal areas. Changes to freshwater flow have implications on estuarine function, influencing productivity through nutrient and organic matter availability, and altered salinity regimes that impact habitat and species distributions along the estuarine gradient. Marshall et al. (2021) examined five estuaries in the northwestern Gulf of Mexico and determined that all had decreases in freshwater inflow over the last 40 years. Changes in duration and intensity of freshwater flow regimes can result in shifts to parameters influencing key foundation species within these estuarine systems, such as seagrasses and oysters. Both seagrass and oysters provide critical ecological roles (habitat, food, etc.) in estuarine systems of the northern Gulf of Mexico and numerous ecosystem benefits, such as improved water clarity, shoreline stabilization, and enhancement of fisheries (Congdon et al., 2018; Shepard et al., 2018).

The growth and survival of seagrasses are directly related to both the quantity and quality of light penetrating the water (Dennison et al., 1993). Light penetration is tied directly to water clarity parameters such as color, turbidity, and total suspended solids. In the northern Gulf of Mexico, water transparency has been identified as a primary ecological integrity parameter for seagrass (Congdon et al., 2018). Seagrass species composition, seasonal abundance, and spatial distribution have been linked to salinity patterns (Lirman et al., 2008; Browder et al., 2013; Congdon et al., 2018).

Eastern Oysters (*Crassotrea virginica*) are typically found in salinities of 10–30 ppt, but can tolerate short periods of much lower (as low as 2 ppt) and higher (as high as 40 ppt) salinities (Gunter and Geyer, 1955). Short periods of freshwater inflow can reduce predation, but extended low salinity exposure can reduce spat survival and lead to sedimentation, while periods of high salinity can result in increased predation and disease exposure (Soniat, 1996; Chu and Volety, 1997; La Peyre et al., 2003, 2009, 2013; Volety et al., 2009). Salinity, in particular mean summer salinity, has been identified as the primary indicator of ecological integrity for oysters in the northern Gulf of Mexico (Shepard et al., 2018).

Despite the biodiversity value of the Gulf Coastal Plain of North America, few studies have investigated the dynamics or trends in discharge in this region. The purpose of this paper is to examine trends in several hydroclimatic and associated water quality variables in a portion of the Gulf Coastal Plain biodiversity hotspot—the northwest Florida Panhandle—over the period 1985–2020. Studies focusing on a particular region can help to understand regional relationships and variability among hydrologic variables at a finer level of detail than larger-scale studies in hydrologic trends can provide (e.g., Bawden et al., 2015; Ficklin et al., 2016; Poshtiri and Pal, 2016). Data analysis over a temporal scale of three to four decades can provide important hydrological insights: significant upward or downward trends over a period of three to four decades can allow inferences regarding shifts and deviations in water balance relationships (Ficklin et al., 2016; Wei et al., 2017). Long-term hydroclimatic trends can also help explain shifts in ecological communities: reduced flows over tens of years or less can cause long-term changes in aquatic ecosystem composition (Beche et al., 2006). Understanding shifts in freshwater flow, and associated impacts on salinity and water clarity are important for the long-term management and restoration of both seagrasses and oysters, especially in the context of anticipated impacts from climate change. In this study, we examined trends in precipitation, temperature, and high-and low-streamflow magnitude over the period 1985–2020 across the Gulf Coastal Plain. We also analyzed trends in several water clarity metrics (turbidity, total suspended solids) and salinity in four downstream estuaries: St. Andrews Bay, Choctawhatchee Bay, Pensacola Bay, and Perdido Bay.

2. Materials and methods

2.1. Study area

We examined climatic, hydrologic, and estuarine water quality variables in southern Alabama and northwest Florida, located in the Gulf Coastal Plain of North America (Figure 1). The Gulf Coastal Plain is topographically characterized as flat or hilly with elevations ranging from 0 to 549 m above sea level, and is distinguished from the alluvial deposits of the Mississippi River (United States Army Corps of Engineers, 2010). Precipitation in the eastern Gulf Coastal Plain is bimodal, with high rainfall in winter and summer followed by drier seasons in spring and fall. Stream discharge is typically highest in late winter and early spring, with a slight increase in summer. The lower discharge in summer, relative to rainfall, is likely a result of higher summer evapotranspiration (United States Army Corps of Engineers, 2010). Most streams in this region flow south into one of six estuaries: Apalachicola Bay, St. Andrew Bay, Choctawhatchee Bay, Pensacola Bay, Perdido Bay, and Mobile Bay. In addition to their high ecological (United States Army Corps of Engineers, 2010; Karnauskas et al., 2013) and fisheries value (National Marine Fisheries Service, 2016), the associated beaches of these estuaries are a popular regional tourism destination (Hollis, 2004). The majority of the urban development and population growth has occurred in the southern

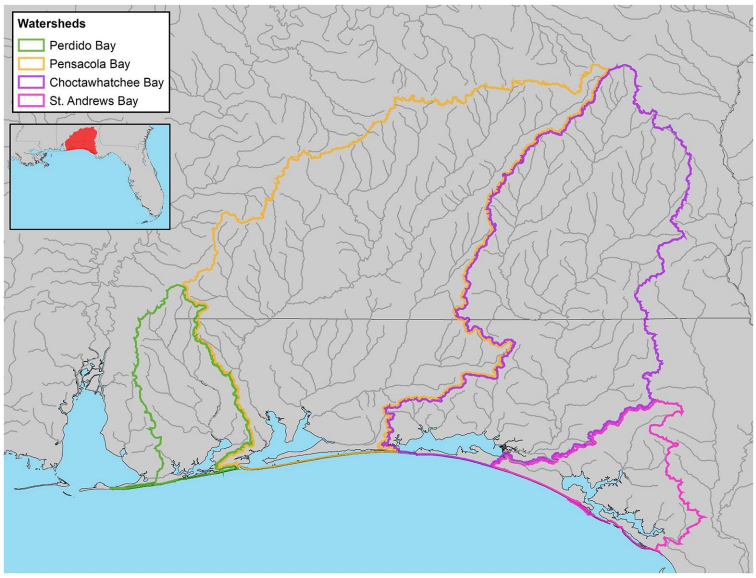

FIGURE 1
Location of study area, indicating the watershed boundary for each estuary: Perdido Bay, Pensacola Bay, Choctawhatchee Bay, and St. Andrew Bay.

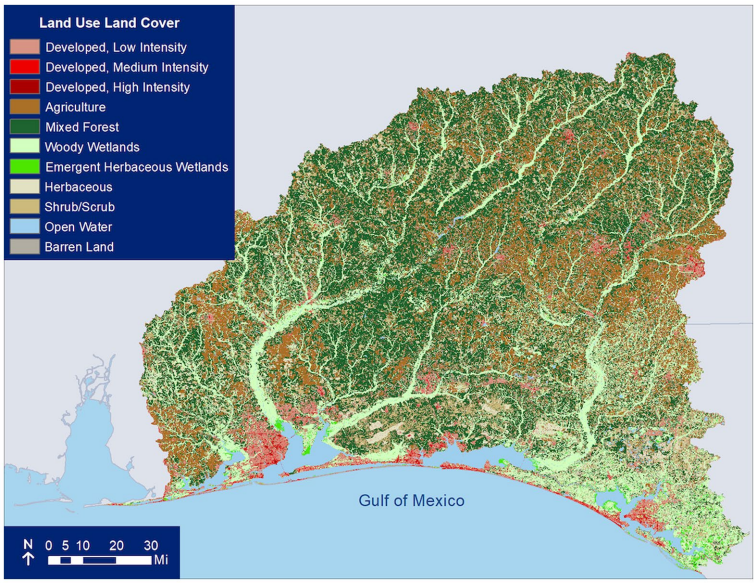

FIGURE 2
Land use and land cover of the study area from 2019. Data source: National Land Cover Database.

portions of the watershed and along the bays (Northwest Florida Water Management District, 2017a,b,c,d; Figure 2).

2.1.1. St. Andrew Bay

The St. Andrew Bay catchment encompasses approximately 3,000 km^2 over six counties and receives inflow from the spring-fed Econfina Creek (from the Gainer Spring group, which has an average discharge of more than 350,000 m^3 per day) through Deer Point Lake Reservoir. Only 12% of the catchment is developed; much of it is held as conservation land including the Econfina Creek Water Management Area. Major habitats in St. Andrew Bay system consist of springs, coastal dune lakes, tidal creeks, marshes, wetlands, estuarine, marine, and terrestrial ecosystems (Northwest Florida Water Management District, 2017a). Major stressors to the St. Andrew Bay include nutrient and bacterial loading from point and non-point sources, low dissolved oxygen, and high chlorophyll levels (Northwest Florida Water Management District, 2017a).

2.1.2. Choctawhatchee Bay

The Choctawhatchee Bay watershed spans approximately 13,800 km^2 across parts of 10 counties in southern Alabama and six counties in northwest Florida. The Pea and Choctawhatchee Rivers are

the primary sources of freshwater delivery to Choctawhatchee Bay. Most of the watershed is forested or agricultural (Le et al., 2015), with most commercial and residential development (including resort communities such as Destin and Seaside) immediately surrounding the bay, owing to the popularity of local beaches and the Gulf of Mexico coastline (Figure 2). A large portion of the catchment in Florida (1,700 km^2) is held by Eglin Air Force Base, with smaller areas held in conservation by the State of Florida, local governments, and non-profits (including the river delta and adjacent areas designated per the Florida Administrative Code as Outstanding Florida Waters). Primary habitats in the bay and watershed are seagrasses, coastal dune lakes, longleaf pine uplands, steephead ravines, and wetlands. The Choctawhatchee River and Bay are also important habitat for many rare and endangered species such as the Gulf Sturgeon, for which the Choctawhatchee River population of over 3,000 adults is second only to the Suwannee River (Wakeford, 2001). Specific stressors include hillslope, channel bank, and road-related erosion from the watershed and nutrient loading, which have negatively impacted seagrasses beds of the region; other reported stressors relating to water quality in Choctawhatchee Bay are heavy metals, bacterial loading, and low dissolved oxygen (Northwest Florida Water Management District, 2017b).

2.1.3. Pensacola Bay

The Pensacola Bay catchment extends from southern Alabama through northwest Florida to the Gulf of Mexico, covering approximately 18,100 km^2, with approximately two-thirds of the catchment located in Alabama. The Escambia, Blackwater, and Yellow Rivers discharge into the Pensacola Bay complex. The Pensacola Bay system is comprised of four main bays (Pensacola, Escambia, Blackwater, and East Bay), several urban bayous, and Santa Rosa Sound. The area surrounding the estuary consists of wetlands, upland forests, agricultural lands, and urban and residential development (Figure 2). Stressors include point and non-point pollution (nutrients and organic compounds) and sedimentation from urban and agricultural development, which have degraded seagrass habitats and sediment quality (Northwest Florida Water Management District, 2017c). The bay has also been impacted from long-term industrial pollution (Northwest Florida Water Management District, 2017c).

2.1.4. Perdido Bay

Perdido Bay serves as the border between Florida and Alabama and the catchment extends from southern Alabama through northwest Florida, covering approximately 2,900 km^2. It receives major freshwater inputs from the Perdido River flowing approximately 110 km. The area surrounding the estuary consists of wetlands, upland forests, agricultural lands, and urban and residential development (Figure 2). System stressors include point and non-point pollution and sedimentation from urban and agricultural development, which have degraded seagrass habitats and sediment quality, and impacts from long-term industrial pollution (Northwest Florida Water Management District, 2017d).

2.2. Data sources

Climate data (daily precipitation and average daily temperature) were obtained through the NOAA National Climatic Data Center (NCDC) Global Historical Climatology Network (National Oceanic and Atmospheric Administration National Climatic Data Center Global Historical Climatology Network, 2022) and Climate Data Online (CDO) Weather-Bureau-Army-Navy dataset (National Oceanic and Atmospheric Administration Climate Data Online, 2022). We performed quality control checks on climate data for omitted values (indicated by no data entered for a date) and erroneous data (indicated by 9,999 or 99.99). Precipitation and temperature values other than those with omitted or error values were presumed accurate after plotting the data to check for other outliers. We only used those sites with a combined data error under 5% for both common data error types during 1985–2020, which resulted in 20 precipitation sites (Alabama $N = 14$, Florida $N = 6$) and 17 temperature sites (Alabama $N = 12$, Florida $N = 5$; Figure 3). Climate variable stations, where precipitation and temperature data were collected were assigned a station code (CV-1 – CV-20).

We identified 13 US Geological Survey (USGS) streamflow gauges (United States Geological Survey National Water Information System, 2022) upstream of the bay systems from St. Andrew Bay to the east and Perdido Bay to the west and north, with at least 30 years of streamflow records between 1985 and 2020 (Figure 3). Gauge stations were assigned a station code (G-1 – G-13). Out of the 13 stations, 10 had complete records and the remaining 4 stations had some missing values (Table 1). Seven of the 13 sites are part of the USGS Hydro-Climatic Data Network (HCDN, intended to indicate streams that are minimally affected by large-scale water management operations), and others are within state forests or other protected areas.

Estuarine water clarity parameters [turbidity and total suspended solids (TSS)] and salinity data were obtained from the US EPA Water Quality Portal (United States Environmental Protection Agency Water Quality Portal, 2022) and Florida Department of Environmental Protection's (DEP) Impaired Waters Rule database. All estuarine parameters were the result of discrete sampling events collected by multiple organizations across our study area and sampling frequency varied by both organization and over the study period. Downloaded data were standardized to sample depth (surface, ≤1 m), comparable analysis methods and units, and then cleaned by removing quality control samples and duplicate entries. Datasets with unknown or non-standard sampling or analysis methods, did not have associated units, or were missing other metadata that prevented standardization were removed. Within each of the four estuarine systems (St. Andrew, Choctawhatchee, Pensacola, and Perdido Bays), parameter metrics were calculated for each unique estuarine segment using the Florida DEP and Alabama Department of Environmental Management waterbody identification (WBID) number, resulting in 9 St. Andrew Bay segments, 19 Choctawhatchee Bay segments, 13 Pensacola Bay segments, and 6 Perdido Bay segments (Figure 4). Estuary segments were assigned a station identification code consisting of a bay code and numerical identifier (SAB-1 – SAB-9, CB-1 – CB-19, PB-1 – PB-9, and PDB-1 – PDB-6).

2.3. Metrics

2.3.1. Climate

We used historical precipitation and temperature records to calculate seasonal median precipitation and maximum temperature. Seasons in the study region are classified as winter (December to February), spring (March to May), summer (June to August), and fall (September to November). To reduce the influence of zeros in the dataset, a 7-day total precipitation was calculated for each day (sum

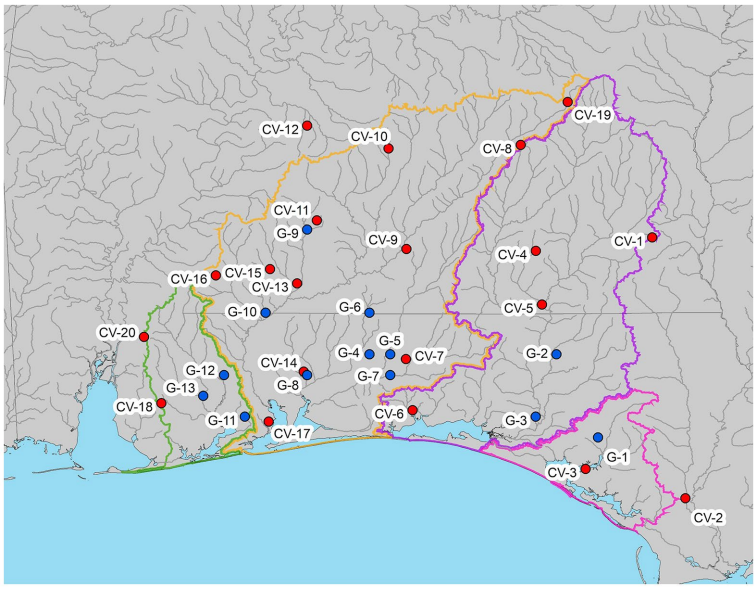

FIGURE 3
Location of climate variable (temperature and precipitation) stations (CV), and USGS streamflow gauge stations (G). Stations with both precipitation and temperature datasets are indicated in red, and stations with only precipitation are indicated in blue.

TABLE 1 Summary characteristics of the hydrological monitoring stations.

Station ID	Location	Lat (deg)	Long (deg)	Basin area (km^2)	Analysis period	Annual flow (m^3/s)	Missing (%)
G-1	Econfina Creek at Bennett	30.4	−85.6	316	1985–2018	170	5.5
G-2	Choctawhatchee River at Caryville	30.8	−85.8	9,060	1985–2020	1,699	0
G-3	Choctawhatchee River at Bruce	30.5	−85.9	6,170	1985–2020	2,265	0
G-4	Shoal River at Crestview	30.7	−86.6	1,230	1985–2020	9,968	0
G-5	Yellow River at Milligan	30.8	−86.6	1,620	1986–2020	510	5.5
G-6	Blackwater River at Bradley	31	−86.7	227	1985–2020	113	0
G-7	Blackwater River at Baker	30.8	−86.7	531	1985–2020	57	10.1
G-8	Big Coldwater Creek at Milton	30.7	−87	614	1985–2020	6,909	10.1
G-9	Murder Creek at Evergreen	31.4	−87	456	1985–2020	85	0
G-10	Escambia River at Century	31	−87.2	9,890	1985–2020	1926	0
G-11	Elevenmile Creek at Pensacola	30.5	−87.3	72	1987–2020	281	0
G-12	Perdido River at Barreneau Park	30.7	−87.4	1,020	1985–2020	255	0
G-13	Styx River at Elsanor	30.6	−87.5	497	1987–2020	3,568	0

that day and six previous days), and the seasonal median value was determined for each season.

2.3.2. Streamflow

Streamflow data were used to develop metrics describing high and low flow magnitudes and their timing each year over the 36-year study period. We used three metrics to examine changes in low-flow magnitude over different timescales: lowest mean daily flow, 7-day low flow (calculated as the average flow for the period with the lowest total discharge over seven consecutive days) and the 30-day low flow (calculated as the average flow for the period with the lowest total discharge over 30 consecutive days). Similarly, we calculated three metrics to examine high-flow trends over different timescales: the highest mean daily flow, 7-day high flow (the average flow over the seven-day period with highest discharge), and the 30-day high flow (the average flow over the 30-day period with highest discharge). This range of time scales was examined because different flow regimes can have differing effects on the downstream aquatic communities. In their analysis of long-term flow data in the US, Poshtiri et al. (2018) found no difference in variability between daily, 7-day, and 30-day minimum flow metrics. We chose to include all variables in our analysis to examine not only positive and negative trends but also differences in timing and magnitude of flows, as increasing or decreasing trends in minimum and maximum daily flows may have less of an impact on estuarine water quality than trends over longer timescales.

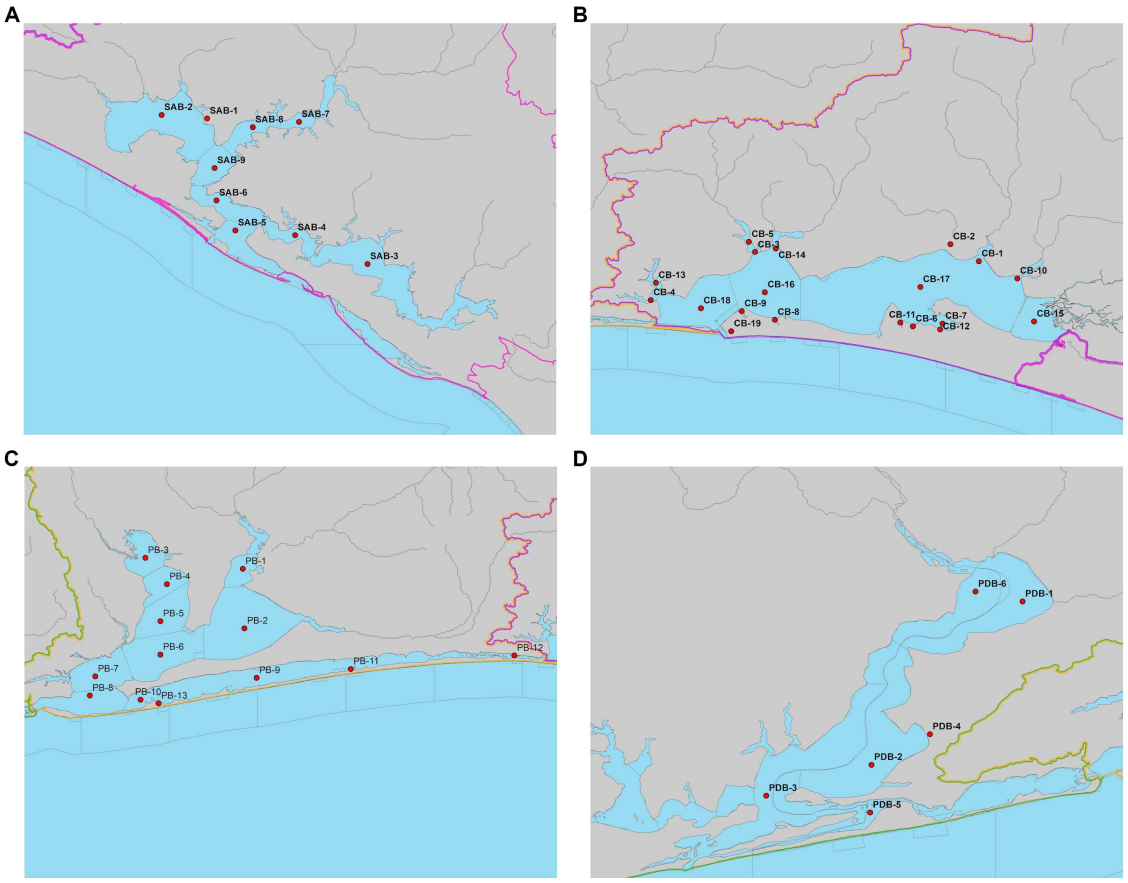

FIGURE 4
Location of estuarine variable stations in **(A)** St. Andrew Bay system, **(B)** Choctawhatchee Bay system, **(C)** Pensacola Bay system, and **(D)** Perdido Bay; gray lines indicate borders among state-designated estuary segments.

2.3.3. Estuarine

To examine downstream impacts of changes in climate and flow regimes, we looked at water quality metrics associated with freshwater discharge with implications for key estuarine habitats (seagrass and oysters): salinity, turbidity, and TSS. Within each of the four estuarine systems (St. Andrew, Choctawhatchee, Pensacola, and Perdido Bays), seasonal means were generated for parameters at each unique estuarine segment. This scale allows for the examination of trends over time and spatial area, not just using annual averages, but within specific seasons that are key to seagrass and oyster growth and recruitment. For example, water clarity declines during the seagrass growing season could lead to reductions in seagrass coverage and inhibit restoration efforts. Similarly, altered salinity regimes can shift community composition of seagrass, expose oysters to increased predation (high salinity), or reduce oyster recruitment and growth (low salinity).

2.4. Statistical analysis

Time-series data for the climatic, streamflow, and estuarine water quality parameters were analyzed with a Seasonal Mann-Kendall trend (Kendall, 1948; Meals et al., 2011) and Sen's slope tests (Sen, 1968; Meals et al., 2011) using the "Trend" package in R (Pohlert, 2020). The Seasonal Mann-Kendall (SMK) trends test evaluates whether there is an upward or downward trend in a time-series dataset by conducting a Mann-Kendall trend for each time unit (i.e., month and season), then combining the results for each unit. For example, only July (for monthly) observations are compared to other July observations and summer (for seasonal) to other summer observations. The SMK test is robust, powerful, and recommended for water quality trend monitoring (Meals et al., 2011). The SMK test determines whether the trend is significant at a given significance level (e.g., at $\alpha = 0.05$ or $\alpha = 0.10$), and an estimate of the trend slope can be calculated using the Sen slope. The Mann-Kendall test is especially useful for examining trends among hydrologic data because it is a non-parametric statistical analysis, and thus does not assume normally distributed data (Helsel and Hirsch, 2002; Yue et al., 2003; Zhang et al., 2011).

In addition to testing whether a data set has a statistically significant upward or downward trend, the Mann-Kendall test also produces a standardized Z statistic which characterizes the consistency of the trend, thus making it a useful metric for comparing the trend "strength" among sites with varying Z values (Modarres and Rodriguez da Silva, 2007; Ficklin et al., 2016). Negative Z statistics correspond to downward trends, and positive values correspond to upward trends. Unlike the SMK test, which only provides a significant positive or negative trend, the non-parametric Sen's slope (Sen, 1968) is a powerful tool to estimate the magnitude of trends in hydroclimatic time-series data (Tabari et al., 2011; Gocic and Trajkovic, 2013; Da Silva et al., 2015; Dawood, 2017).

Estuarine trends were analyzed using the best available continuous datasets. Date ranges (years and included seasons) were selected to maximize temporal coverage. Because seasonal means were calculated, any missing data was considered a gap and not estimated. Trends were considered short-term if the dataset contained 5–9 years of continuous data. Long-term trends were identified through the analysis of 10+ years of continuous data.

3. Results

3.1. Climate trends

3.1.1. Temperature

Significant trends in maximum temperature (Tmax) were observed at 11 of 17 sites (65%) in the study area (Figure 5). Seasonal change in Tmax showed an increasing tendency among most of those sites with significant Tmax trends (82%), with only two Alabama stations (CV-10 Greenville, AL and CV-13 Brewton, AL) displaying a significant declining trend (Figure 5). As indicated by the Sen's slope, the maximum rate of seasonal increase in Tmax ranged from 0.03–0.11°C year^{-1}, while the decreasing stations decreased at a rate of 0.07 and 0.04°C year^{-1}, respectively (Supplementary Table S1).

Within each season, significant trends were observed most often in winter (5 stations), followed by fall (4 stations), spring (3 stations), and summer (2 stations; Supplementary Table S1). In the winter, only increasing trends were observed, indicating that higher maximum winter temperatures are occurring with frequency at 29% of the stations in the study area, and 45% of the stations with an overall significant trend. Crestview, FL (CV-7) was the only station to have a significant trend (increasing) in every season.

3.1.2. Precipitation

Analysis of median precipitation data *via* SMK and Sen's slope tests yielded mixed results. An overall significant trend ($\alpha = 0.05$) in precipitation occurred at 15% (3 of 20) of stations (Figure 5). Two stations in close proximity to one another, Niceville (CV-6) and Crestview, FL (CV-7) had significant increasing trends, while the neighboring station to the west, Milton, FL (CV-14) had a declining trend (Figure 5). One additional station observed an increasing trend for a season, and two had significant declining trends for a single season (Supplementary Table S2). All other stations (14 of 20) had no observed overall or seasonal trends (Supplementary Table S2).

3.1.3. Streamflow

Overall trends in daily minimum, 7-day, and 30-day minimum flows were significant at 31, 15, and 23% of stations, respectively. Most of the locations with significant daily minimum trends (3 of 4) had declining trends (Figure 6), indicating that minimum flows were decreasing across the study period. The station that displayed the most consistent declining trend, Eleven Mile Creek (G-11), had decreasing daily, 7-day, and 30-day minimum flows observed in all seasons (Table S3-5). Two stations had increasing minimum flow trends. Econfina Creek (G-1) had significant increasing trends for all three flow metrics and Yellow River (G-5) had significant increasing 30-day minimum flows (Supplementary Tables S3-S5).

Maximum flow characteristics were more variable. Econfina Creek (G-1) had increasing trends across all maximum flow metrics (Figure 7), with that trend largely being driven by increases in winter (Supplementary Tables S3-S5). Yellow River (G-5) and one of the Choctawhatchee River sites (G-2) also had an increasing winter trend in daily maximum flow. Eleven Mile Creek (G-11) had an overall significant decreasing 30-day maximum flow, which may be driven by decreases in spring as all three flow metrics had significant decreasing trends in the spring (Supplementary Tables S3-S5).

3.2. Estuarine trends

3.2.1. St. Andrew Bay

There were 9 WBIDs with continuous seasonal data for at least one parameter across the study period. TSS had the lowest spatial (2 WBIDs) and temporal (10 years or less) coverage. Neither location had significant trends (Figure 8). Of the 5 waterbody segments with continuous turbidity data, only West Bay (SAB-2) had significant trends (Figure 8). These declining trends were observed in the overall, winter and spring values (Supplementary Table S6).

Salinity trends were less variable. Significant increasing trends in salinity were observed in 55% of WBIDs (Figure 8). All of the stations with significant overall trends, had significant increasing winter trends and half of them had significant increasing spring trends (Table S6). Two WBIDs, St. Andrew Bay (SAB-5) and St. Andrew Bay middle (SAB-6) had decreasing seasonal trends which were observed in the summer and fall, respectively (Supplementary Table S6). Both of these sites had a declining overall trend, but neither of them were significant.

3.2.2. Choctawhatchee Bay

The Choctawhatchee Bay system had 19 WBIDs with continuous seasonal data distributed across the study period. TSS trends were analyzed for 14 WBIDs. Date ranges varied by site with most sites having continuous coverage for some period between 1999 to 2019. Most WBIDs (78%) had significant overall declining trends in TSS (Figure 9). Significant trends by season varied by waterbody, but they were all declining trends. Two WBIDs, Hogtown Bayou East (CB-7) and Lagrange Bayou (CB-10) had significant declining trends across all seasons, and another Rocky Bayou (CB-14) had declining trends across all seasons (Supplementary Table S7). While trends were observed in 4 WBIDs, spring had the fewest significant locations. Turbidity data was more variable. Of the 19 WBIDs, 6 had significant increasing trends and an additional segment had a significant declining trend (Figure 9). When significant seasonal trends were present, they matched the directionality of the corresponding overall trend (Supplementary Table S7).

There were WBIDs in the Choctawhatchee Bay system with significant long-term declining trends in salinity (Figure 9; Supplementary Table S7). Some of these segments showed similar trends in either the summer or fall. Two additional WBIDs had declining trends in the fall. The only bay segment that had a significant positive trend was Choctawhatchee Bay middle (CB-17) in the fall (Supplementary Table S7).

3.2.3. Pensacola Bay

The Pensacola Bay system had 13 WBIDs with continuous seasonal data. TSS coverage was limited to 7 waterbody segments with 10 years or less of continuous data, and only a single WBID, Pensacola Bay middle (PB-7) had a significant short-term increasing trend for its overall and summer values (Figure 10; Supplementary Table S8). Turbidity data was available at 11 waterbody segments. Only two WBIDs, East Bay (PB-2) and Liza Jackson Park in Santa Rosa Sound

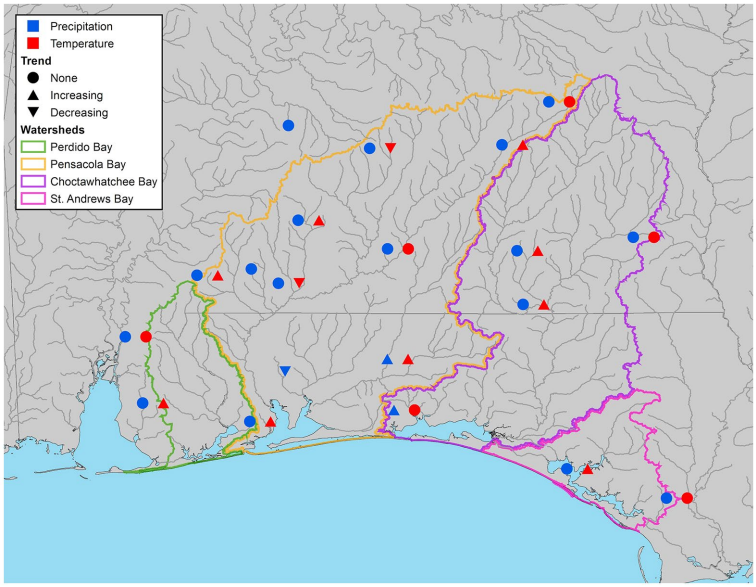

FIGURE 5
Climate stations illustrating significant increasing, decreasing, or no trend (α=0.05) in both precipitation (blue) and maximum temperature (red).

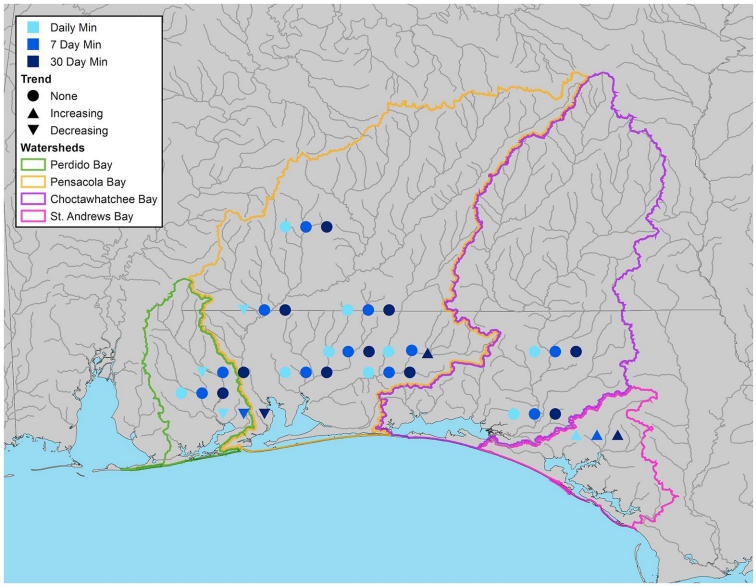

FIGURE 6
Streamflow gauges illustrating significant increasing, decreasing, or no trend (α=0.05) for minimum daily (light blue), 7-day (blue), and 30-day (dark blue) flow.

(PB-12) had significant overall short-term trends, both of which were declining (Figure 10). Declines were also observed in the fall at both East Bay (PB-2) and Pensacola Bay north (PB-6), and in the spring at Pensacola Bay mouth (PB-8; Supplementary Table S8).

Over the study period, only 4 of 13 WBIDs had significant trends in salinity (Figure 10). Of those two had increasing trends, Blackwater Bay south (PB-1) and Escambia Bay south (PB-5) and two had decreasing trends, Pensacola Bay middle (PB-7) and Santa Rosa Sound (PB-9; Supplementary Table S8). The two significant seasonal trends, one positive in spring and one negative in the summer matched the corresponding overall trends (Supplementary Table S8).

3.2.4. Perdido Bay

The Perdido Bay system had the fewest total WBIDs per estuary (6) and suffered from episodic monitoring, thus trends within this system are harder to summarize across the study period. Overall TSS values declined in lower Perdido Bay (PDB-2), but increased in the Intracoastal Waterway (PDB-5; Figure 11). No significant trends in turbidity for overall or seasonal values were observed (Figure 11; Supplementary Table S9). Salinity increased at one station on the Alabama side of the bay (PDB-3) with significant trends observed in overall and fall values (Supplementary Table S9).

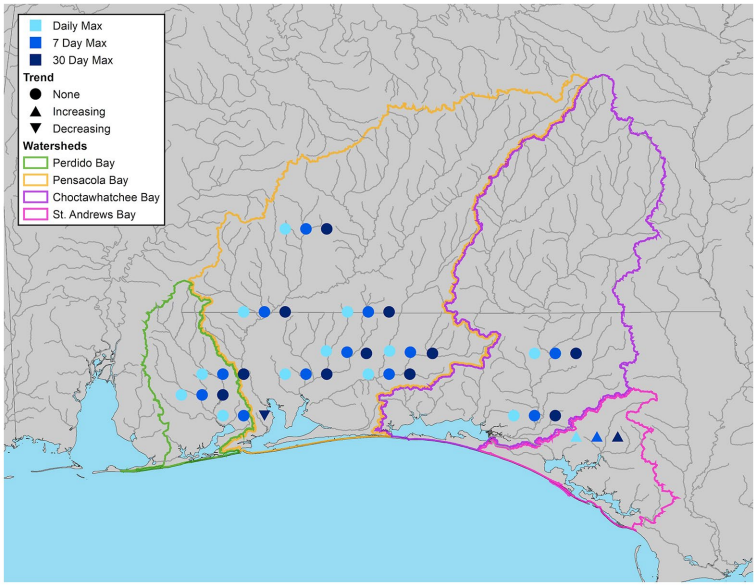

FIGURE 7
Streamflow gauges illustrating significant increasing, decreasing, or no trend (α=0.05) for maximum daily (light blue), 7-day (blue), and 30-day (dark blue) flow.

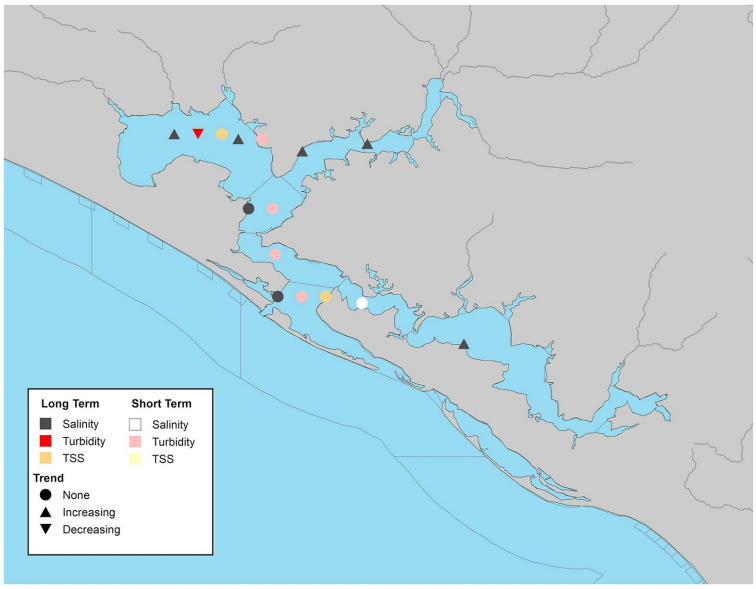

FIGURE 8
Waterbody identification (WBIDs) within St. Andrew Bay system with at least 10years of data, illustrating significant increasing, decreasing, or no trend (α=0.05) with long-term datasets indicated by darker symbols and short-term in lighter symbols for turbidity (red/pink), total suspended solids (orange/yellow), and salinity (dark gray/white).

4. Discussion

4.1. Climate trends

4.1.1. Similarities and differences in trends

The results above highlight the complexity of interactions between climate characteristics and ecologically significant hydrologic variables in streams within the eastern Gulf Coastal Plain. In general, precipitation has not significantly increased or decreased at annual or seasonal scales, suggesting that total rainfall amounts have been the same over the past 36 years. These results mirror similar studies that found precipitation to be relatively stable in the late 20th and early 21st Centuries (Ficklin et al., 2016; Maleski and Martinez, 2017). This is seen despite changes in global multi-annual climate patterns such as El Nino-Southern Oscillation that could result in wetter conditions in summer and fall in El Nino years and drier conditions in La Nina years (Ropelewski and Halpert, 1986; Clark II et al., 2014). Trends in temperature were stronger with maximum temperature increasing at

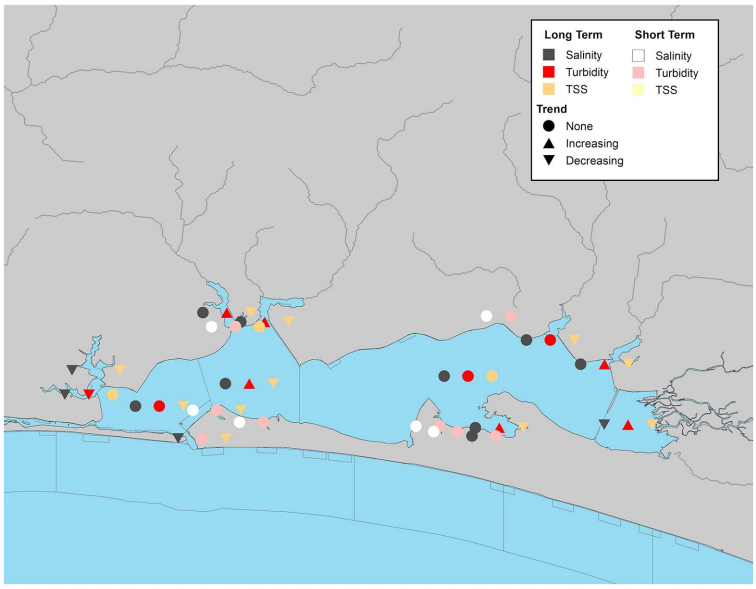

FIGURE 9
Waterbody identification within Choctawhatchee Bay system with at least 10years of data, illustrating significant increasing, decreasing, or no trend (α=0.05) with long-term datasets indicated by darker symbols and short-term in lighter symbols for turbidity (red/pink), total suspended solids (orange/yellow), and salinity (dark gray/white).

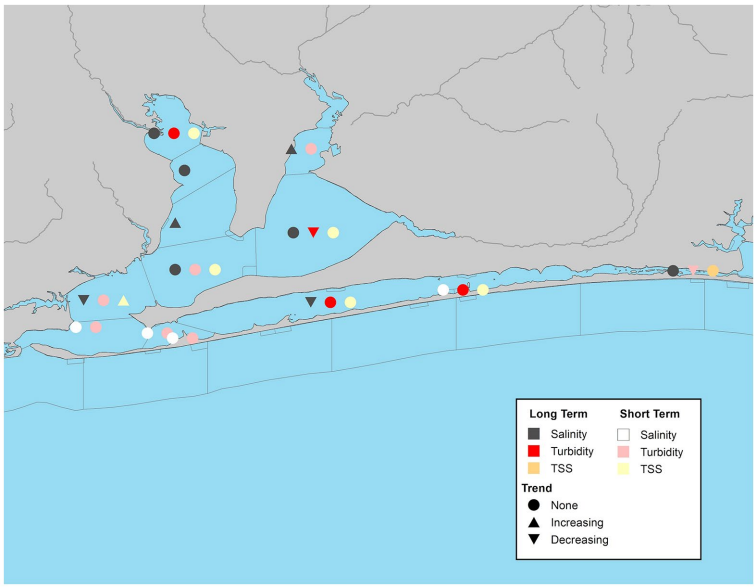

FIGURE 10
Waterbody identification within the Pensacola Bay system with at least 10years of data, illustrating significant increasing, decreasing, or no trend (α=0.05) with long-term datasets indicated by darker symbols and short-term in lighter symbols for turbidity (red/pink), total suspended solids (orange/yellow), and salinity (dark gray/white).

most sites, and especially in winter, but in other seasons as well. This contrasts to other studies of temperature trends within other river basins in the region that found relatively static high temperatures (Maleski and Martinez, 2017). This contrast may be due to differences in the period of analysis in both scale (118 years versus 36 years) and the influence of more contemporary temperature data. Warmer temperatures, especially during winter, can lead to meaningful changes in crop production (Parker and Abatzoglou, 2019), accelerated tree growth in pine forests (Harvey et al., 2020), and expansion of tropical species into subtropical regions (Osland et al., 2021). With forests comprising more than 50% of the project area (Le et al., 2015), increased high temperatures could amplify forest evapotranspiration, resulting in reduced streamflow especially during base flow conditions.

Increased forest evapotranspiration caused by higher temperatures may be a factor in the observed general declines in low-flow characteristics in streams throughout the project area. Significant declining trends were observed in both the Escambia and Perdido Rivers where the majority of their watershed is in upland forests (Figure 2; Northwest Florida Water Management District, 2017c,d). Further, while trends within season were mostly not significant at $\alpha = 0.05$, only Econfina Creek (G-1) did not have a negative tendency across all seasons for daily and 7-day minimum flows. Eleven Mile Creek (G-11) had significant declining trends in all four seasons for all minimum flow metrics. Our results contrast broader, national-scale studies that described few trends among low base flow conditions in the Gulf Coastal Plain (Ficklin et al., 2016), or mixed and weak trends among low-flow conditions based on fewer sites in the region (Rice et al., 2016). The main difference between this study and those previous is related to the temporal resolution of low-flow conditions. Events such as daily, 7-day, and monthly low-flow values represent the driest conditions within each time interval, likely to occur between rain events when air temperature is high, and thus when evapotranspiration may be highest. Such especially low-flow conditions may have the greatest ecological significance because they represent the greatest stress placed on organisms over the time period (Obedzinski et al., 2018; Vander Vorste et al., 2020).

Results of peak flows analysis were less consistent. Only Econfina Creek (G-1) had a significant positive trend across all maximum flow metrics. While not significant, many gauged streams tended to have increasing tendencies in winter and negative tendencies in all other seasons. This tendency is less apparent at the 30-day time-scale indicating that changes to peak flows were not sustained over longer (i.e., monthly) time periods. These results corroborate larger-scale studies of storm flow indicating mixed directionality related to high-flow conditions (Groisman et al., 2004; Ficklin et al., 2016). One of the commonly described hydrologic variations expected in the 21st Century is an increase in variability, and specifically, more frequent and extreme low flow conditions and high flow conditions (Trenberth et al., 2014).

4.1.2. Variations in low flow trends

In addition to illustrating an overall declining trend in low flow among streams in the Gulf Coastal Plain, streamflow data from the region also potentially indicates the role of water management on low-flow conditions in the region. Streamflow at the site with the consistently strongest downward trend among the 13 studied—Eleven Mile Creek near Pensacola—is strongly influenced by water management operations. Eleven Mile Creek received discharge from a local industrial facility through the early 2000s; its discharge location was moved to a constructed wetland in 2012, and from 2012 to 2016, dry-season base flow was reduced by about 50 percent.

The most surprising anomaly in our analysis was that some of the larger river sites, had increasing tendencies in low-flow conditions. This anomaly may also reflect nearby land management and potentially shifts in seasonal climatic dynamics. This sensitivity to land management may be especially relevant in forested land, which is the predominant land cover type in catchments of the Florida Panhandle and southern Alabama (Le et al., 2015), and especially in the lower portions of the Escambia and Choctawhatchee River catchments. In addition to timber harvesting potentially leading to increased low-flow conditions, high-intensity hurricanes that altered forest cover in the 21st Century (Sharma et al., 2021) may also have led to reduced evapotranspiration and elevated low-flow conditions. Because strategic forest management in the Gulf Coastal Plain can lead to greater discharge through reducing evapotranspiration (McLaughlin et al., 2013), managed forests may have the capacity to buffer the effects of climate change on low-flow conditions in small streams

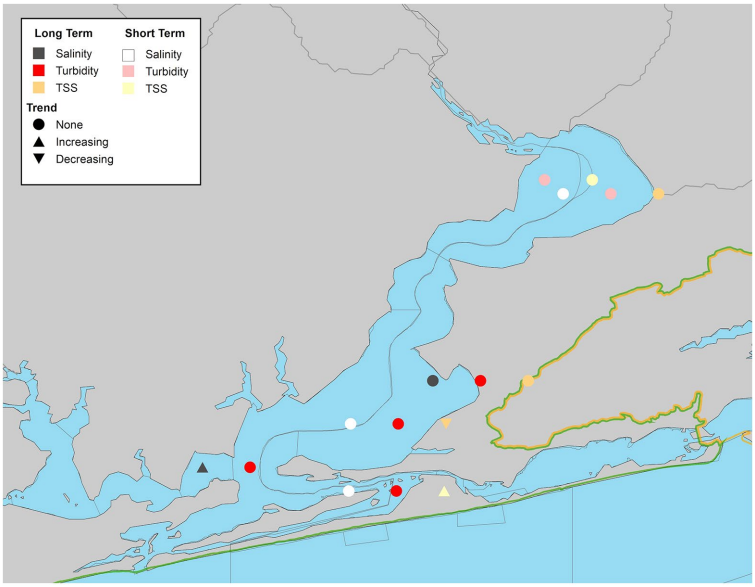

FIGURE 11
Waterbody identification within Perdido Bay system with at least 10years of data, illustrating significant increasing, decreasing, or no trend observed (α=0.05) with long-term datasets indicated by darker symbols and short-term in lighter symbols for turbidity (red/pink), total suspended solids (orange/yellow), and salinity (dark gray/white).

throughout the region. Our results corroborate Rodgers et al. (2020) who found that seasonal streamflow decreased across the southern and southeastern US from 1950 to 2015. In their study, 88% of sites were influenced by factors other than climate variables such as management practices.

4.2. Estuarine response

Estuarine responses to these changes in streamflow and precipitation varied with declines in salinity across most locations in all four estuaries. While Econfina Creek (G-1), the major inflow to St. Andrew Bay had increasing trends in maximum and minimum streamflow, most estuarine locations had increasing trends in salinity. In the other three estuaries, general declining tendencies in maximum and minimum seasonal flow by the major rivers (Choctawhatchee, Escambia, and Perdido) were observed as well as decreases in estuarine salinity at many WBIDs. Other factors such as stormwater runoff or increased heavy rainfall events induced by climate change may be causing system-wide reductions in salinity (Paerl et al., 2006).

Declines in salinity may initially benefit oysters due to reduction in predation (Powell et al., 1996; La Peyre et al., 2009), although extended declines and pulsed freshwater inputs have negative effects on growth and spat and larval survival (Powell et al., 2003; Powers et al., 2017). Long-term declines in salinity can result in complete loss of oyster reefs as larvae and spat are not able to recruit into the population and overtime as hard substrate (mainly from oyster shells) is lost from the system, making it harder to restore oyster populations and their associated ecosystem services (Parker et al., 2013). Additionally, freshwater pulses may also bring in contaminants including microbial pathogens and other pollutants that are a human health risk. In the Pensacola Bay system, declines in water quality due to microbial pathogens have affected oyster aquaculture and wild harvesting, resulting in expansions to the prohibited shellfish harvest areas in recent years (Birch et al., 2021; Florida Department of Agriculture and Consumer Services, 2022).

Submerged aquatic vegetation (SAV) in the oligohaline regions of estuaries may benefit from lower salinity and expand their coverage provided low salinity extends throughout the growing season. In the past, extended drought conditions and higher salinity has led to losses of submerged aquatic vegetation in Pensacola Bay (Lores and Sprecht, 2001). Like oysters, seagrass growth, particularly that of *Thalassia testudinum*, is inhibited by low salinity (Lirman and Cropper, 2003; Kahn and Durako, 2006). Thus, there is a need to understand the drivers of freshening of these estuarine systems.

Surprisingly, declines in salinity did not lead to increasing turbidity and total suspended solids, which can be expected with higher freshwater inputs. Particulates in estuaries may be more affected by deposition and resuspension within the estuary which results in a shorter residence time in the water column than freshwater, leading to lower particulates (TSS and turbidity) and higher water clarity. Another explanation is that pulsed events from the greater maximum streamflow observed in this study may not be captured by monitoring programs in the region, which primarily conduct quarterly sampling. A limitation of this study is the lack of frequent consistent estuarine monitoring, and the resulting mismatch between long-term records for flow and climate variables, and shorter-term estuarine variables. Regardless of the cause of increased water clarity, both oysters and seagrass can benefit from increased clarity.

5. Conclusion

Over the 36-year period 1985–2020, data from stream gauges in the Florida Panhandle and southern Alabama illustrate a decline in low-flow conditions, supporting the general prediction that increased hydrologic variability is likely in the 21st Century. The data do not, however, illustrate the same predominant trend of increased high-flow conditions. The decline in low flow we document above has not occurred in parallel with declining annual rainfall, occurrence of low precipitation, or increase in temperature; rather, our analysis suggests that declining low-flow conditions may be a result of a seasonal shift in the timing of precipitation in the region, with less rainfall during the late summer dry season and increased rainfall during the winter. Declining low-flow conditions may also be attributed to other factors such as changes in land management which can modify the partitioning of rainfall into different hydrological components, alterations in surface runoff due to changing land use, or increases in evapotranspiration. This analysis provides a more thorough exploration of the hydrologic trends in this biologically unique region than other recent studies can provide. For the water quality parameters, declining trends were observed in most water clarity metrics, indicating improved clarity, especially in winter. Salinity generally declined across the study area. Improved water clarity and reduced particulate levels may have a beneficial effect on SAV and oysters, although more research is needed to evaluate the linkage between water quality and habitat quality.

Maintaining the unique ecosystems of the Gulf Coastal Plain will likely be a major challenge for biologists and other resource managers in the coming decades, but it may be possible with thoughtful planning and resource management. Are there techniques in forest management or other management techniques that mitigate declining streamflow trends? Further studies involving correlations with catchment-scale variables such as land cover (and changes in land cover over time) and evapotranspiration may help to indicate land use types where best management practices could be most beneficial for reducing downward streamflow trends. Understanding how coastal and oceanic scale climate changes affect estuarine water quality in this region is also needed. Given the relatively short water quality data sets (compared to climate or streamflow) continued monitoring of these systems is critical. The ecosystems of this region will depend on monitoring, strategic management and targeted research to thrive through the 21st Century.

Data availability statement

Publicly available datasets were analyzed in this study. This data can be found here: National Oceanic and Atmospheric Administration National Climatic Data Center (NOAA NCDC) Global Historical Climatology Network. Available: https://www.ncei.noaa.gov/products/land-based-station/global-historical-climatology-network-daily National Oceanic and Atmospheric Administration Climate Data Online (NOAA CDO). Available: https://www.ncdc.noaa.gov/cdo-web/ United States Environmental Protection Agency Water

Quality Portal (USEPA WQP). Available: https://www.waterqualitydata.us United States Geological Survey National Water Information System (USGS NWIS). Available: https://waterdata.usgs.gov/nwis/sw.

Author contributions

MD and JC received funding that supported this manuscript. MD and AC contributed to conception and design of the study and wrote the first draft of the manuscript. MD, AC, and HG cleaned and organized the data. AC performed the statistical analysis. MD, AC, HG, and JC wrote sections of the discussion and conclusion. All authors contributed to manuscript revision, read, and approved the submitted version.

Funding

Funding support was provided by Florida RESTORE Act Center of Excellence Program grant 4710-1129-00-A.

Acknowledgments

The authors wish to thank the University of West Florida Center for Environmental Diagnostics and Bioremediation and the University of Florida (UF) Institute of Food and Agricultural Sciences (IFAS) Research and the UF IFAS West Florida Research and Education Center for support of this project, as well as two reviewers whose inputs greatly improved the quality of this manuscript.

Conflict of interest

The authors declare that the research was conducted in the absence of any commercial or financial relationships that could be construed as a potential conflict of interest.

Publisher's note

All claims expressed in this article are solely those of the authors and do not necessarily represent those of their affiliated organizations, or those of the publisher, the editors and the reviewers. Any product that may be evaluated in this article, or claim that may be made by its manufacturer, is not guaranteed or endorsed by the publisher.

Supplementary material

The Supplementary material for this article can be found online at: https://www.frontiersin.org/articles/10.3389/fevo.2023.1167767/full#supplementary-material

References

Bawden, A. J., Burn, D. H., and Prowse, T. D. (2015). Recent changes in patterns of western Canadian river flow and association with climatic drivers. *Hydrol. Res.* 46, 551–565. doi: 10.2166/nh.2014.032

Beche, L. A., Mcelravy, E. P., and Resh, V. H. (2006). Long-term seasonal variation in the biological traits of benthic-macroinvertebrates in two Mediterranean-climate streams in California, USA. *Freshwater. Biol.* 51, 56–75. doi: 10.1111/j.1365-2427.2005.01473.x

Birch, A., Brumbaugh, R., DeAngelis, B., Geselbracht, L., Graves, A., Blair, J., et al. (2021). Oyster fisheries and habitat management plan for the Pensacola bay system. *Nature Conserv.* 78. Available at: https://www.ppbep.org/PDFs/PBS_OysterFisheriesHabitatMgtPlan_18May2021_Final_ADA_corrected-11.22.2021.pdf

Blaustein, R. J. (2008). Biodiversity hotspot: the Florida panhandle. *Bioscience* 58, 784–790. doi: 10.1641/B580904

Browder, J. A., Fourqurean, J., Lirman, D., and Nuttle, W. K. (2013). "Benthic habitat: seagrasses. In integrated conceptual ecosystem model development for the Southeast Florida coastal marine ecosystem," in *NOAA technical Memorandum,OAR_AOML_103 and NOS-NCCOS-163*. eds. W. K. Nuttle and P. J. Fletcher (Miami, Florida: National Oceanic and Atmospheric Administration), 84–93.

Chu, F. L. E., and Volety, A. K. (1997). Disease processes of the parasite Perkinsus marinus in eastern oyster *Crassostrea virginica*: minimum dose for infection initiation, and interaction of temperature, salinity, and infective cell dose. *Dis. Aquat. Org.* 28, 61–68. doi: 10.3354/dao028061

Clark, C. II, Nnaji, G., and Huang, W. (2014). Effects of el-niño and la-niña sea surface temperature anomalies on annual precipitations and streamflow discharges in southeastern United States. *J. Coast. Res. SI* 68, 113–120. doi: 10.2112/SI68-015.1

Congdon, V. M., Dunton, K. H., Brenner, J., Goodin, K. L., and Ames, K. W. (2018). "Ecological resilience indicators for seagrass ecosystems," in *Ecological resilience indicators for five northern Gulf of Mexico ecosystems*. eds. K. L. Goodin, D. Faber-Langendoen, J. Brenner, S. T. Allen, R. H. Day, V. M. Congdon. et al. (Arlington, VA: NatureServe), 57.

Da Silva, R. M., Santos, C. A., Moreira, M., Corte-Real, J., Silva, V. C., and Medeiros, I. C. (2015). Rainfall and river flow trends using Mann–Kendall and Sen's slope estimator statistical tests in the Cobres River basin. *Nat. Hazards.* 77, 1205–1221. doi: 10.1007/s11069-015-1644-7

Dawood, M. (2017). Spatio-statistical analysis of temperature fluctuation using Mann–Kendall and Sen's slope approach. *Clim. Dyn.* 48, 783–797. doi: 10.1007/s00382-016-3110-y

Dennison, W. C., Orth, R. J., Morre, K. A., Stevenson, J. C., Carter, V., Kollar, S., et al. (1993). Assessing water quality with submersed aquatic vegetation. *Bioscience* 43, 86–94. doi: 10.2307/1311969

Estill, J. C., and Cruzan, M. B. (2001). Phytogeography of rare plant species endemic to the southeastern United States. *Castanea* 66, 3–23.

Ficklin, D., Robeson, S., and Knouft, J. (2016). Impacts of recent climate change on trends in baseflow and stormflow in United States watersheds. *Geophys. Res. Lett.* 43, 5079–5088. doi: 10.1002/2016GL069121

Florida Department of Agriculture and Consumer Services (2022). Pensacola bay #02: shellfish management information. Available at: https://www.fdacs.gov/Agriculture-Industry/Aquaculture/Shellfish-Harvesting-Area-Classification/Shellfish-Harvesting-Area-Information/Pensacola-Bay-02-Shellfish-Management-Information

Fox, T. R., Jokela, E. J., and Allen, H. L. (2007). The development of pine plantation silviculture in the southern United States. *J. For.* 105, 337–347.

Gocic, M., and Trajkovic, S. (2013). Analysis of changes in meteorological variables using Mann-Kendall and Sen's slope estimator statistical tests in Serbia. *Glob. Planet. Change.* 100, 172–182. doi: 10.1016/j.gloplacha.2012.10.014

Groisman, P., Knight, R., Karl, T., Easterling, D., Sun, B., and Lawrimore, J. (2004). Contemporary changes of the hydrological cycle over the contiguous United States: trends derived from in situ observations. *J. Hydrometeorol.* 5, 64–85. doi: 10.1175/1525-7541

Gunter, G., and Geyer, R. A. (1955).*Studies on fouling organisms of the Northwest Gulf of Mexico*. Port Aransas: University of Texas Marine Science Institute, 38–67.

Hamilton, H., Smyth, R. L., Young, B. E., Howard, T. G., Tracey, C., Breyer, S., et al. (2022). Increasing taxonomic diversity and spatial resolution clarifies opportunities for protecting US imperiled species. *Ecol. Appl.* 32:2534. doi: 10.1002/eap.2534

Harrison, S., and Noss, R. (2017). Endemism hotspots are linked to stable climatic refugia. *Ann. Bot.* 119, 207–214. doi: 10.1093/aob/mcw248

Harvey, J. E., Smiljanić, M., Scharnweber, T., Buras, A., Cedro, A., Cruz-García, R., et al. (2020). Tree growth influenced by warming winter climate and summer moisture availability in northern temperate forests. *Glob. Chang. Biol.* 26, 2505–2518. doi: 10.1111/gcb.14966

Helsel, D.R., and Hirsch, R.M., (2002). *Statistical methods in water resources. Techniques of water resources investigations of the United States geological survey, book 4, hydrologic analysis and investigation*. United States Geological Survey, Washington, DC, USA.

Hollis, T. (2004). *Florida's miracle strip: from redneck Riviera to Emerald Coast.* Jackson Mississippi: Univ Press of Mississippi.

Kahn, A. E., and Durako, M. J. (2006). *Thalassia testudinum* seedling responses to changes in salinity and nitrogen levels. *J. Exp. Mar. Biol. Ecol.* 335, 1–12. doi: 10.1016/j.jembe.2006.02.011

Karnauskas, M., Schirripa, M. J., Kelble, C. R., Cook, G. S., and Craig, J. K. (2013). Ecosystem status report for the Gulf of Mexico. *NOAA Technical Memorandum NMFS-SEFSC* 653:52p.

Kendall, M.G. (1948). *Rank correlation methods*. Griffin, Oxford.

La Peyre, M. K., Eberline, B. S., Soniat, T. S., and La Peyre, J. F. (2013). Differences in extreme low salinity timing and duration differentially affect eastern oyster *Crassostrea virginica* recruitment, size class growth and mortality in Breton sound, LA. *Estuarine Coastal Shelf Sci.* 135, 146–157. doi: 10.1016/j.ecss.2013.10.001

La Peyre, M. K., Gossman, B., and La Peyre, J. F. (2009). Defining optimal freshwater flow for oyster production: effects of freshet rate and magnitude of change and duration on eastern oysters and Perkinsus marinus infection. *Estuar. Coasts* 32, 522–534. doi: 10.1007/s12237-009-9149-9

La Peyre, M. K., Nickens, A. D., Volety, A. K., Tolley, S. G., and La Peyre, J. F. (2003). Environmental significance of freshets in reducing Perkinsus marinus infection in eastern oysters, *Crassostrea virginica*: potential management applications. *Mar. Ecol. Prog. Ser.* 248, 165–176. doi: 10.3354/meps248165

Le, C., Lehrter, J. C., Hu, C., Schaeffer, B., MacIntyre, H., Hagy, J. D., et al. (2015). Relation between inherent optical properties and land use and land cover across Gulf Coast estuaries: Gulf Coast estuaries optical dynamics. *Limnol. Oceanogr.* 60, 920–933. doi: 10.1002/lno.10065

Lirman, D., and Cropper, W. P. (2003). The influence of salinity on seagrass growth, survivorship, and distribution within Biscayne Bay, Florida: field, experimental, and modeling studies. *Estuaries* 26, 131–141. doi: 10.1007/BF02691700

Lirman, D., Deangelo, G., Serafy, J., Hazra, A., Smith, D., and Brown, A. (2008). Geospatial video monitoring of nearshore benthic habitats of western Biscyane Bay (Florida, USA) using the shallow-water positioning system (SWaPS). *J. Coast. Res.* 1, 135–145. doi: 10.2112/04-0428.1

Lockette, T. (2016). *Drought highlights need for water plan, critics say*. Alabama: LexisNexis Academic.Web

Lores, E. M., and Sprecht, D. T. (2001). Drought-induced decline of submerged aquatic vegetation in Escambia Bay, Florida. *Gulf Mexico Sci.* 19:8. doi: 10.18785/goms.1902.08

Maleski, J., and Martinez, C. (2017). Historical trends in precipitation, temperature and drought in the Alabama–Coosa–Tallapoosa and Apalachicola–Chattahoochee–Flint river basins. *Int. J. Climatol.* 37, 583–595. doi: 10.1002/joc.4723

Markos, P. D., Kaller, M. D., and Kelso, W. E. (2016). Channel stability and the structure of coastal stream aquatic insect assemblages. *Fund. Appl. Limnol.* 188, 187–199. doi: 10.1127/fal/2016/0865

Marshall, D. A., La Peyre, M. K., Palmer, T. A., Guillou, G., Sterba-Boatwright, B. D., Pollack, J. B., et al. (2021). Freshwater inflow and responses from estuaries across a climatic gradient: an assessment of northwestern Gulf of Mexico estuaries based on stable isotopes. *Limnol. Oceanogr.* 66, 3568–3581. doi: 10.1002/lno.11899

McLaughlin, D. L., Kaplan, D. A., and Cohen, M. J. (2013). Managing forests for increased regional water yield in the southeastern U.S. coastal plain. *J. Am. Water Resour. Assoc.* 49, 953–965. doi: 10.1111/jawr.12073

Meals, D.W., Spooner, J., Dressing, S.A., and Harcum, J.B. (2011). Statistical analysis for monotonic trends. National Nonpoint Source Montoring Program Tech Notes 6. Available at: https://www.epa.gov/polluted-runoff-nonpoint-source-pollution/nonpoint-source-monitoring-technical-notes

Modarres, R., and Rodriguez da Silva, V. D. P. (2007). Rainfall trends in arid and semi-arid regions of Iran. *J. Arid Environ.* 70, 344–355. doi: 10.1016/j.jaridenv.2006.12.024

National Marine Fisheries Service (2016). *Fisheries economics of the United States, 2014. U.S. Dept. of commerce, NOAA Tech. Memo. NMFS-F/SPO-163*, –237.

National Oceanic and Atmospheric Administration Climate Data Online (2022). Available at: https://www.ncdc.noaa.gov/cdo-web/

National Oceanic and Atmospheric Administration National Climatic Data Center Global Historical Climatology Network (2022). Available at: https://www.ncei.noaa.gov/products/land-based-station/global-historical-climatology-network-daily

Northwest Florida Water Management District (2017a). *St. Andrew bay system surface water information and management plan. Program development series 17–08*. Northwest Florida water Management District, Mariana, FL

Northwest Florida Water Management District (2017b). *Choctawhatchee Bay surface water information and management plan. Program development series 17–05*. Northwest Florida Water Management District, Mariana, FL

Northwest Florida Water Management District (2017c). *Pensacola bay system surface water information and management plan. Program development series 17–06*. Northwest Florida water Management District, Mariana, FL

Northwest Florida Water Management District (2017d). *Perdido River and bay surface water information and management plan. Program development series 17–07*. Northwest Florida Water Management District, Mariana, FL.

Noss, R. F., Platt, W. J., Sorrie, B. A., Weakley, A. S., Means, D. B., Costanza, J., et al. (2015). How global biodiversity hotspots may go unrecognized: lessons from the north American coastal plain. *Divers. Distrib.* 21, 236–244. doi: 10.1111/ddi.12278

Obedzinski, M., Nossaman Pierce, S., Horton, G. E., and Deitch, M. J. (2018). Effects of flow-related variables on oversummer survival of juvenile Coho salmon in intermittent streams. *Trans. Am. Fish. Soc.* 147, 588–605. doi: 10.1002/tafs.10057

Osland, M. J., Stevens, P. W., Lamont, M. M., Brusca, R. C., Hart, K. M., Waddle, J. H., et al. (2021). Tropicalization of temperate ecosystems in North America: the northward range expansion of tropical organisms in response to warming winter temperatures. *Glob. Chang. Biol.* 27, 3009–3034. doi: 10.1111/gcb.15563

Paerl, H. W., Valdes, L. M., Joyner, A. R., Peierls, B. L., Piehler, M. F., Riggs, S. R., et al. (2006). Ecological response to hurricane events in the Pamlico sound system, North Carolina, and implications for assessment and management in a regime of increased frequency. *Estuar. Coasts* 29, 1033–1045. doi: 10.1007/BF02798666

Parker, L. E., and Abatzoglou, J. T. (2019). Warming winters reduce chill accumulation for peach production in the southeastern United States. *Climate* 7:94. doi: 10.3390/cli7080094

Parker, M. L., Arnold, W. S., Geiger, S. P., Gorman, P., and Leone, E. H. (2013). Impacts of freshwater management activities on eastern oyster (*Crassostrea virginica*) density and recruitment: recovery and long-term stability in seven Florida estuaries. *J. Shellfish Res.* 32, 695–708. doi: 10.2983/035.032.0311

Pohlert, T. (2020). Trend. R package version. Available at: https://CRAN.R-project.org/package=trend

Poshtiri, M. P., and Pal, I. (2016). Patterns of hydrological drought indicators in major US River basins. *Clim. Chang.* 134, 549–563. doi: 10.1007/s10584-015-1542-8

Poshtiri, M. P., Towler, E., and Pal, I. (2018). Characterizing and understanding the variability of streamflow drought indicators within the USA. *Hydrol. Sci. J.* 63, 1791–1803. doi: 10.1080/02626667.2018.1534240

Powell, E. N., Klinck, J. M., and Hofmann, E. E. (1996). Modeling diseased oyster populations. II. Triggering mechanisms for Perkinsus marinus epizootics. *J. Shellfish Res.* 15, 141–165.

Powell, E. N., Klinck, J. M., Hofmann, E. E., and McManus, M. A. (2003). Influence of water allocation and freshwater inflow on oyster production: a hydrodynamic–oyster population model for Galveston Bay, Texas, USA. *Environ. Manag.* 31, 100–0121. doi: 10.1007/s00267-002-2695-6

Powers, S. P., Grabowski, J. H., Roman, H., Geggel, A., Rouhani, S., Oehrig, J., et al. (2017). Consequences of large-scale salinity alteration during the Deepwater horizon oil spill on subtidal oyster populations. *Mar. Ecol. Prog. Ser.* 576, 175–187. doi: 10.3354/meps12147

Rice, J. S., Emanuel, R. E., and Vose, J. M. (2016). The influence of watershed characteristics on spatial patterns of trends in annual scale streamflow variability in the continental US. *J. Hydrol.* 2016, 850–860. doi: 10.1016/j.jhydrol.2016.07.006

Rodgers, K., Roland, R., Hoos, A., Crowley-Ornelas, E., and Knight, R. (2020). An analysis of streamflow trends in the southern and southeastern US from 1950-2015. *Water* 12:3345. doi: 10.3390/w12123345

Ropelewski, C. F., and Halpert, M. S. (1986). North American precipitation and temperature patterns associated with the El Niño/south oscillation (ENSO). *Mon. Weather Rev.* 114, 2352–2362. doi: 10.1175/1520-0493(1986)114<2352:NAPATP>2.0.CO;2

Sen, P. K. (1968). Estimates of regression coefficient based on Kendall's tau. *J. Am. Stat. Assoc.* 63, 1379–1389. doi: 10.1080/01621459.1968.10480934

Sharma, A., Ojha, S. K., Dimov, L. D., Vogel, J. G., and Nowak, J. (2021). Long-term effects of catastrophic wind on southern US coastal forests: lessons from a major hurricane. *PLoS One* 16:e0243362. doi: 10.1371/journal.pone.0243362

Shepard, C., Brenner, J., Goodin, K. L., and Ames, K. W. (2018). "Ecological resilience indicators for oyster ecosystems," in *Ecological resilience indicators for five northern Gulf of Mexico ecosystems*. eds. K. L. Goodin, D. Faber-Langendoen, J. Brenner, S. T. Allen, R. H. Day, V. M. Congdon. et al. (Arlington, VA: NatureServe), 40.

Soniat, T. M. (1996). Epizootiology of Perkinsus marinus disease of eastern oysters in the Gulf of Mexico. *Oceanogr. Lit. Rev.* 12:1265.

Tabari, H., Safar, M., Ali, A., Parisa, H., and Kurosh, M. (2011). Trend analysis of reference evapotranspiration in the Western half of Iran. *Agric.* 151, 128–136. doi: 10.1016/j.agrformet.2010.09.009

Trenberth, K. E., Dai, A., van der Schrier, G., Jones, P. D., Barichivich, J., Briffa, K. R., et al. (2014). Global warming and changes in drought. *Nat. Clim. Chang.* 4, 17–22. doi: 10.1038/nclimate2067

United States Army Corps of Engineers (2010). "Regional supplement to the Corps of Engineers Wetland Delineation Manual: Atlantic and gulf coastal plain region (version 2.0)" in *Engineer research development center technical Report-10-20*. eds. J. S. Wakeley, R. W. Lichvar and C. V. Noble (Vicksburg, Mississippi: U.S. Army Engineer Research and Development Center)

United States Environmental Protection Agency Water Quality Portal (2022). Available at: https://www.waterqualitydata.us

United States Geological Survey National Water Information System (2022). Available at: https://waterdata.usgs.gov/nwis/sw

Vander Vorste, R., Obedzinski, M., Nossaman Pierce, S., Carlson, S. M., and Grantham, T. E. (2020). Refuges and ecological traps: extreme drought threatens persistence of an endangered fish in intermittent streams. *Glob. Chang. Biol.* 26, 3834–3845. doi: 10.1111/gcb.15116

Volety, A. K., Savarese, M., Tolley, S. G., Arnold, W. S., Sime, P., Goodman, P., et al. (2009). Eastern oysters *Crassostrea virginica* as an indicator for restoration of Everglades ecosystems. *Ecol. Indic.* 9, S120–S136. doi: 10.1016/j.ecolind.2008.06.005

Wakeford, A., (2001). State of Florida conservation plan for gulf sturgeon. (No FMRI Technical Report TR-8) Florida Fish and Wildlife Conservation Commission.

Walls, S. C. (2014). Identifying monitoring gaps for amphibian populations in a north American biodiversity hotspot, the southeastern USA. *Biodivers. Conserv.* 23, 3341–3357. doi: 10.1007/s10531-014-0782-7

Warren, M. L. Jr., Burr, B. M., Walsh, S. J., Bart, H. L. Jr., Cashner, R. C., Etnier, D. A., et al. (2000). Diversity, distribution, and conservation status of the native freshwater fishes of the southern United States. *Fisheries* 25, 7–31. doi: 10.1577/1548-8446(2000)025<0007:DDACSO>2.0.CO;2

Wei, Q., Sun, C., Wu, G., and Pan, L. (2017). Haihe River discharge to Bohai Bay, North China: trends, climate, and human activities. *Hydrol. Res.* 48, 1058–1070. doi: 10.2166/nh.2016.142

Yue, S., Pilon, P., and Phinney, B. O. B. (2003). Canadian streamflow trend detection: impacts of serial and cross-correlation. *Hydrol. Sci. J.* 48, 51–63. doi: 10.1623/hysj.48.1.51.43478

Zhang, Q., Singh, V. P., Sun, P., Chen, X., Zhang, Z., and Li, J. (2011). Precipitation and streamflow changes in China: changing patterns, causes and implications. *J. Hydrol.* 410, 204–216. doi: 10.1016/j.jhydrol.2011.09.017

Frontiers in
Ecology and Evolution

Ecological and evolutionary research into our natural and anthropogenic world

This multidisciplinary journal covers the spectrum of ecological and evolutionary inquiry. It provides insights into our natural and anthropogenic world, and how it can best be managed.

Discover the latest Research Topics

See more →

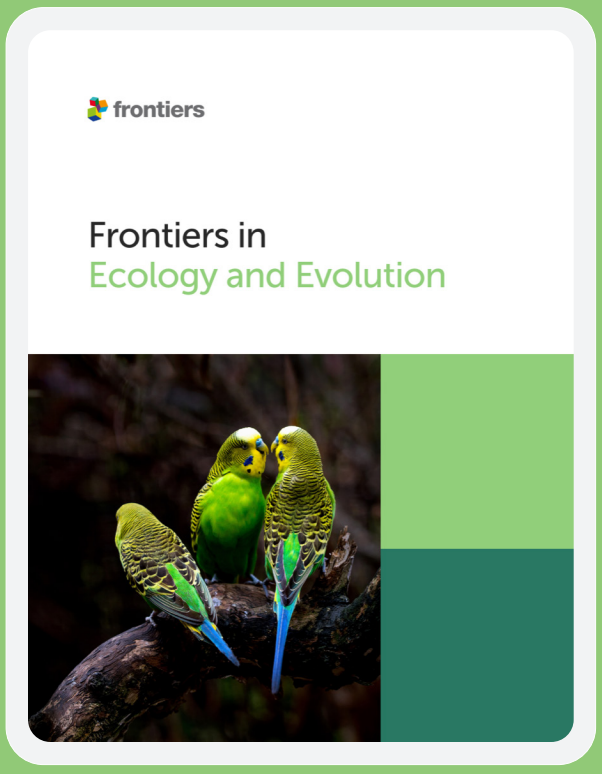

Frontiers

Avenue du Tribunal-Fédéral 34
1005 Lausanne, Switzerland
frontiersin.org

Contact us

+41 (0)21 510 17 00
frontiersin.org/about/contact